DISS. ETH NO. 27782

Characterization of permafrost microbial communities and their response to climate change

A thesis submitted to attain the degree of

DOCTOR OF SCIENCES of ETH ZURICH

(Dr. sc. ETH Zurich)

presented by

Carla Pérez Mon
M.Sc. Evolutionary Biology, Uppsala University

born on 23.11.1989
citizen of Spain

accepted on the recommendation of

Prof. Dr. Mark Alexander Lever
Prof. Dr. Martin Herbert Schroth
Dr. Beat Walter Frey

2021

“I have a dream that the people in power, as well as the media, start treating this [Climate] crisis like the existential emergency it is.”

Greta Thunberg

U.S. Congress, Washington DC, September 18, 2019

Contents

SUMMARY

Mid-latitude alpine permafrost is extensively thawing due to amplified global warming. Thawing-induce conditions of elevated soil temperature and moisture, and a greater availability of soil C and nutrients are predicted to activate the permafrost microbiome. This could alter soil microbial diversity and microbially-mediated soil processes (e.g. heterotrophic respiration) that governs mountain soil-climate feedbacks (e.g. CO_2 fluxes). The alpine permafrost microbiome could be additionally affected by soil freeze-thaw cycles, whose frequency is increasing because the soils are losing the thermal insulation previously provided by the snow. Yet, predictions about the specific changes in the mountain soil microbiome in the future, and their feedbacks to the climate, are precluded by a poor understanding about (1) the physiological features, including C- and N- cycling metabolic functions, of the alpine permafrost microbial communities and (2) their structural and metabolic responses to the climate-driven changes in the soil.

The investigations included in this Dissertation contributed to narrow these two aforementioned knowledge gaps, using the long-term permafrost monitoring summit of Muot da Barba Peider (MBP; 2979 m a.s.l.) in the Swiss Alps as a model ecosystem. In the first research chapter of this Dissertation (Chapter 2) I provided a pioneer detailed picture of the functional gene diversity and metabolic potential of alpine permafrost and active-layer microbiota. Most importantly, the > 1 m deep permafrost metagenomes were enriched in cold-stress genes and genes involved in transcription, and DNA remodeling and repair, which suggest the presence of active microbial cells inhabiting the permafrost. Permafrost metagenomes were also enriched in genes related to cell defense and competition. Permafrost contained a remarkable high diversity of C and N-cycling genes, including genes coding for hydrolytic enzymes that are used by microorganisms to obtain C, nutrients and energy from biopolymers (e.g. lignocellulose). Versatile C-degrading capabilities could facilitate the growth of the microbial cells upon thawing.

In the second and third research chapters of this Dissertation (Chapters 3 and 4), I tested the responses of the MBP permafrost and active-layer microbiomes to soil conditions linked to climate warming. In Chapter 3, I evaluated the impacts of increased freeze-thaw cycle (FTC) frequency on the north- and south-facing active layers microbiomes of MBP, by conducting a

microcosm experiment in which the soils were exposed to weekly and daily (more frequent) FTCs. Using amplicon sequencing I showed that daily and weekly FTCs shift the structure of the prokaryotic (i.e. Bacteria and Archaea) communities in the soils. The more frequent, daily FTCs promoted soil copiotrophic bacterial taxa (e.g. *Noviherbaspirillum*) over oligotrophic groups, whereas soil fungal communities were only minimally affected by freeze-thawing. Both weekly and daily FTCs diminished soil heterotrophic respiration, but this activity was more strongly affected by the weekly freeze-thawing. This suggest that shorter periods of freezing during warmer winters could favor soil CO_2 releases in the future. Similar microbial responses were observed in Swedish mountain north- and south-facing active layers, included in the experiment.

In Chapter 4, I evaluated during three years the *in situ* responses of the MBP permafrost and active-layer microbiomes to a projected warmer climate, where conditions of (1) increased temperatures, (2) a greater availability of C and nutrients and (3) (more) frequent FTCs, co-occur in the soil. To simulate warming, permafrost was transplanted from a depth of 160 cm into active-layer topsoils near the MBP summit, and north-facing active layers were transplanted into the warmer south-facing topsoil. Field-simulated warming led to augmented microbial abundance in the permafrost, mainly owing to the increase in copiotrophic prokaryotic taxa (e.g. *Noviherbaspirillum*) over metabolically restricted bacteria (i.e. Patescibacteria). Mostly ascomycetous sapro-pathotrophic fungi profited from warming, superseding basidiomycetous yeasts. Similar compositional shifts were observed within the MBP north-facing active layer transplanted into the south-facing slope, but to a lesser extent than in the permafrost. The soil microbiota of the permafrost transplanted into topsoils grew on a broader range of C-substrates but it did not show enhanced heterotrophic respiration; likely limited by the soil C deficiency. My observations suggest that, in the absence vegetation, C-depleted permafrost soils, such as the MBP soils, will not contribute to warming with the release of CO_2. In the so rapidly changing mountain landscapes, my investigations enable to better understand the links between the alterations in the soil microbiome and the soil ecosystem functioning (e.g. gas fluxes) in the future, which might ultimately inform soil–climate feedback models at the regional and global scales.

ZUSAMMENFASSUNG

Der alpine Permafrost in den mittleren Breiten taut aufgrund der verstärkten globalen Erwärmung weitgehend auf. Erhöhte Bodentemperatur und -feuchtigkeit sowie eine grössere Verfügbarkeit von Kohlenstoff und Nährstoffen im Boden werden voraussichtlich das Wachstum des Permafrost-Mikrobiom ankurbeln. Als Folge dieser Veränderungen werden die mikrobielle Vielfalt im Boden und die mikrobiell vermittelten Bodenprozesse (z.B. heterotrophe Atmung) beeinflusst, die die Rückkopplungen zwischen Boden und Klima im Gebirge (z.B. CO_2-Flüsse) steuern. Das alpine Permafrost-Mikrobiom wird zusätzlich durch zunehmende Boden-Frost-Tau-Zyklen beeinflusst, weil zukünftiger Schneemangel die Böden weniger stark isolieren. Vorhersagen über mögliche Veränderungen des Bodenmikrobioms im alpinen Raum und deren Rückkopplungen auf das Klima sind aufgrund eines unzureichendes Verständnis (1) der physiologischen Eigenschaften, einschließlich der C- und N-relevanten Umsetzungsprozesse, und (2) der strukturellen und metabolischen Reaktionen auf die klimabedingten Veränderungen im Boden schwierig.

Die Untersuchungen im Rahmen dieser Dissertation trugen dazu bei, diese beiden oben genannten Wissenslücken zu verkleinern. Hierzu diente der Berggipfel oberhalb Pontresina Muot da Barba Peider (MBP; 2979 m ü. M.) in den Schweizer Alpen als Modellökosystem. Im ersten Forschungskapitel dieser Dissertation (Kapitel 2) lieferte ich erstmalig für das zentraleuropäische Hochgebirge ein detailliertes Bild des metabolischen Potentials eines alpinen Permafrost-Mikrobioms. Die unter einem Meter liegenden Permafrost Böden waren mit Genen angereichert, damit lebende Zellen nicht gefrieren und sie so vor Kälte schützen. Ebenfalls waren Gene, die für die Transkription und Reparatur von Zellen verantwortlich sind, im Permafrost erhöht gegenüber der Tauschicht im Oberboden. Im weiteren waren auch Gene im Permafrost vermehrt vorhanden, die lebende Zellen im Permafrost vor konkurrenzierenden Mikroorganismen schützen. Permafrost enthielt eine hohe Vielfalt an Genen, die für C- and N-Prozesse in Böden, einschliesslich Genen, die für hydrolytische Enzyme kodieren, die von Mikroorganismen zur Gewinnung von C, Nährstoffen und Energie aus Biopolymeren (z. B. Lignocellulose) verwendet werden. Vielseitige C-abbauende Enzyme könnten das Wachstum der mikrobiellen Zellen beim Auftauen fördern.

Im zweiten und dritten Forschungskapitel dieser Dissertation (Kapitel 3 und 4) überprüfte ich die Reaktionen des Mikrobioms aus dem Permafrost und der überliegenden Auftauschicht auf die mit der Klimaerwärmung verbundenen veränderten Bodenbedingungen. In Kapitel 3 untersuchte ich die Auswirkungen von unterschiedlichen Gefrier-Tau-Zyklen (i.e. freeze-thaw cycles, FTCs) auf das Bodenmikrobiom der Auftauschicht der Nord- und Südseite des Berggipfels auf dem MBP. Die Böden wurden täglichen (häufigeren) und wöchentlichen FTCs im Labor unter kontrollierten Bedingungen ausgesetzt. Tägliche und wöchentliche FTCs haben die Struktur der prokaryotischen (d.h. Bakterien und Archaeen) Lebensgemeinschaften in den Böden verändert. Tägliche FTCs förderten prokaryotische Taxa (z.B. *Noviherbaspirillum*) mit copiotropher Lebensweise gegenüber langsam wachsenden, oligotrophen Arten, während die Pilzgemeinschaften im Boden nur minimal durch die Gefrier-Tauzyklen beeinflusst wurden. Beide Behandlungen verringerten die heterotrophe Atmung, aber die mikrobielle Aktivität wurde durch wöchentliche Gefrier-Tauzyklen stärker beeinflusst. Diese Untersuchungen zeigen, dass kürzere Frostperioden in zukünftigen, wärmeren Wintern die Bodenatmung begünstigen könnten. Ähnliche Reaktionen wurden in Böden aus dem schwedischen Gebirge beobachtet, die parallel durchgeführt wurden.

In Kapitel 4 habe ich während drei Jahren die *in situ*-Reaktionen des Mikrobioms aus dem Permafrost und der aktiven Tauschicht in MBP auf ein projiziertes wärmeres Klima untersucht, in dem Bedingungen von (1) erhöhten Temperaturen, (2) einer grösseren Verfügbarkeit von C und Nährstoffen und (3) (häufigeren) FTCs im Boden auftreten. Eine Erwärmung wurde simuliert, indem Permafrost aus einer Tiefe von 160 cm in den Oberboden (0 - 15 cm) eingesetzt wurde. Zusätzlich wurde Boden aus der aktiven Tauschicht von der kälteren Nordseite auf die wärmere Südseite des Berggipfels transferiert. Die im Feld simulierte Erwärmung führte zu einer Vergrösserung der mikrobiellen Biomasse im Permafrost, hauptsächlich aufgrund der Zunahme von prokaryotischen Taxa (z.B. *Noviherbaspirillum*) mit einer copiotrophen Ernährungsweise gegenüber langsam wachsenden Bakterien mit eingeschränktem Metabolismus (z.B. Patescibacteria). Vor allem sapro-pathotrophe Pilze aus dem Stamm der Ascomycota profitierten von der Erwärmung und verdrängten kälteadaptierte Hefepilze aus dem Stamm der Basidiomycota. Ähnliche Verschiebungen in der mikrobiellen Zusammensetzung wurden in den Böden beobachtet, die von der Nordseite auf die Südseite transferiert wurden, allerdings weniger ausgeprägt als im Permafrost. Das Permafrost-

Mikrobiom, das in den Oberboden transferiert wurde, konnte ein breiteres Spektrum von C-Substraten ausnutzen, zeigte aber keine erhöhte heterotrophe Atmung, wahrscheinlich begrenzt durch den Mangel an verfügbaren Nährstoffen im Boden. Diese ersten Resultate zeigen, dass C-arme Permafrostböden durch Erwärmung nicht zur erhöhten Freisetzung von CO_2 beitragen. Abschliessend tragen diese Untersuchungen zu einem besseren Verständnis der Zusammenhänge zwischen den Veränderungen des Bodenmikrobioms und der Funktionalität des Bodenökosystems (z. B. Gasflüsse), in einer sich rasch verändernden Gebirgslandschaft bei.

1. CHAPTER 1. General introduction

1.1. Global warming in the alpine permafrost regions

Global warming refers to the worldwide increase in air and sea surface temperatures, mainly caused by the continual emission of greenhouse gases (GHGs), such as CO_2, CH_4 and N_2O, to the atmosphere, owing to human activities involving the burning of fossil fuels (e.g. for heat and electricity production) (IPCC, 2014, 2019). Warming is amplified in polar regions and in mountainous (alpine) regions at lower latitudes, where mean annual air temperatures could increase ≥ 8℃ above pre-industrial (before 1750) levels by 2100 (RCP8.5 scenario) (IPCC, 2014; Overland et al., 2019).

Permafrost is defined as soil that remains at subzero temperatures for two or more consecutive years, and is overlain by seasonally unfrozen soil called *active layer* (Margesin, 2009). Permafrost soils in alpine regions cover an estimated total area of 3.6–5.2 million km^2, most of which is in Asian mountain ranges, with lesser portions in mountain ranges of the European and American continents (Hock et al., 2019) (Fig. 1. A and B). In mid-latitude mountains, permafrost temperatures are currently increasing at a rate of 0.2°C per decade (Biskaborn et al., 2019) (Fig. 1. C). Models predict the thawing of more than 60% (under the RCP8.5 scenario) of the permafrost in the Himalayan-Tibetan Plateau (abbr. Tibet) by 2100 (Hock et al., 2019), and that permafrost may disappear almost entirely from areas with narrow peaks below 3 850 m above sea level (a.s.l.), such as the Alps (Magnin et al., 2017). Permafrost thawing causes slope instability, which results in landslides, rockfalls and infrastructure failures (Noetzli et al., 2003). These warming associated hazards pose severe threats to human inhabitants and have negative socio-economic impacts on human settlements, especially in densely populated mountain areas such as the Alps (IPCC, 2019). Permafrost thawing also affects the chemistry of watersheds, which are crucial sources of potable water (Scapozza et al., 2020; Steingruber et al., 2020) and might promote the dissolution of toxins such as mercury (Schuster et al., 2018). Warming might furthermore activate microbial communities inhabiting alpine permafrost soils, and lead to changes in GHGs feedbacks between permafrost soils and the atmosphere (Nikrad et al., 2016). A more active soil microbiota could also facilitate vegetation growth (Jacoby et al., 2017), thereby accelerating the transformation of the mountain landscapes, which are a cultural heritage (IPCC, 2019).

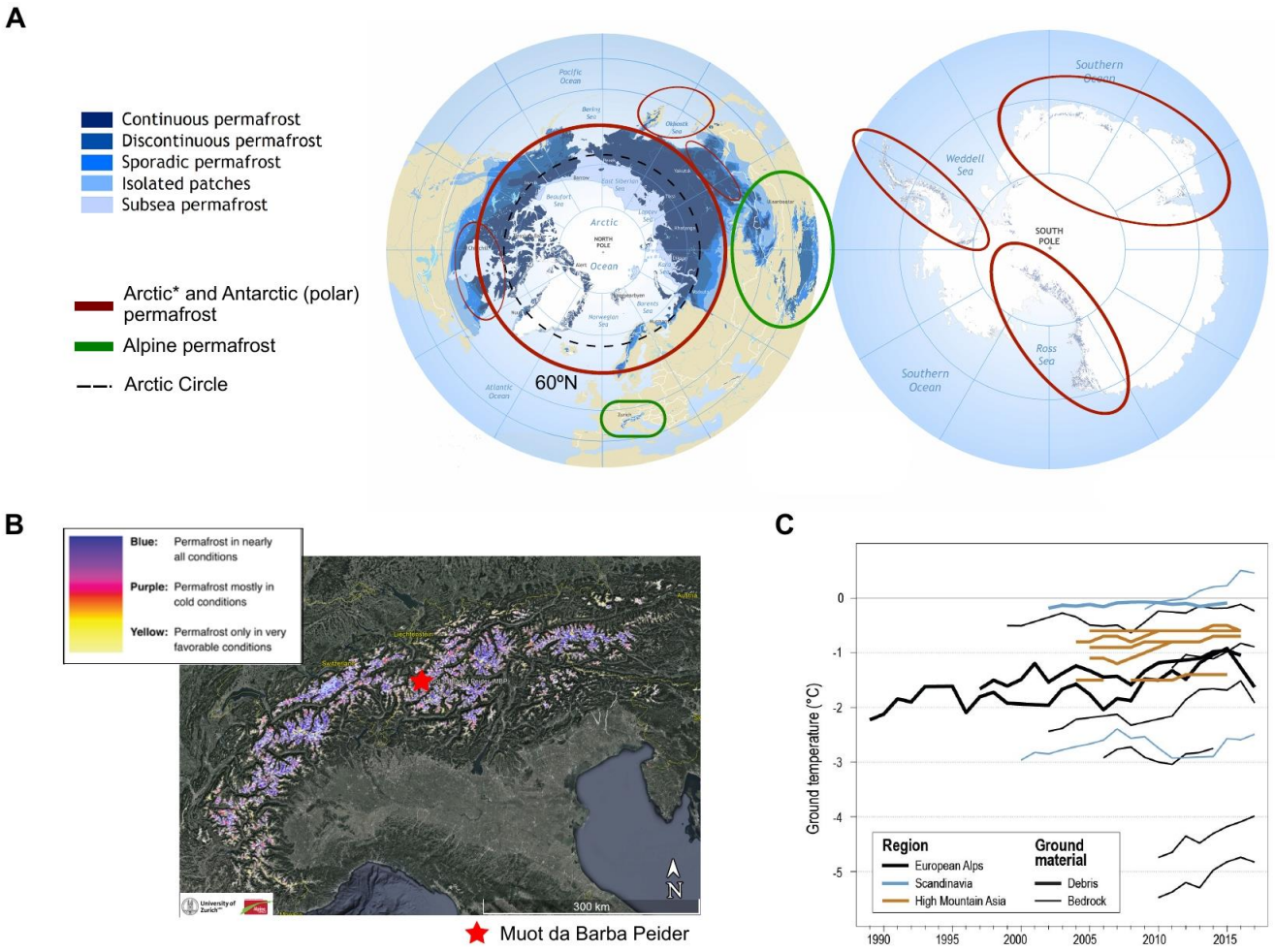

Figure 1. Permafrost distribution in the Northern and Southern hemisphere **(A)** with a close-up overview of the permafrost distribution in the Alps **(B)** and a graphical representation of the current trends of increasing permafrost temperatures (i.e. ground temperatures from 10m-deep boreholes) overtime in alpine permafrost areas, retrieved from Hock et al, 2019 (p. 147) **(C).** The global permafrost distribution map was modified from the map of (Brown et al., 1997), retrieved from the International Permafrost Association (IPA) website (https://ipa.arcticportal.org/). *The red circle defining the permafrost areas in the Northern hemisphere is an approximate representation of the areas comprised in the High-Arctic, Low-Arctic and Sub-Arctic regions, based on the map shown in (Meredith et al., 2019) (p. 211). The permafrost distribution map from the Alps was drawn with the Google Earth software, using the data provided by the Longterm Permafrost Monitoring Network (PermaNET, http://www.permanet-alpinespace.eu/). The active-layer and permafrost soils used for the investigations included in this Dissertation were mainly collected in the summit of Muot da Barba Peider.

1.2. The alpine permafrost habitat and its microbiome

Mid-latitude alpine permafrost soils generally occur at altitudes above 2 500 m a.s.l. (Margesin, 2009). Compared with the permafrost from the polar regions, alpine permafrost is sporadic, relatively warm (0 to -4℃) and exhibits active layers of depths greater than 1 m (Table 1). Similar to Antarctic soils and unlike Arctic permafrost, alpine permafrost soils are dominated by well-drained coarse-grained sediments depleted in soil organic carbon (i.e. global SOC stock of 66 Pg; Bockheim & Munroe, 2014). High-altitude mountain soils are exposed to more precipitation and stronger UV radiation than lowlands in polar regions (Table 1). Furthermore, alpine permafrost regions exhibit shorter snow-covered seasons and larger inter-annual and daily fluctuations of temperatures and incoming solar radiation than polar soils (Barry, 2008; Margesin, 2009). Compared with the better studied densely vegetated soils in the sub-Arctic, vegetation is more scarce in alpine permafrost areas, and largely consists of grasses (e.g. *Poa*) and sedges (*Carex* sp.) (Adamczyk et al., 2019; Germino, 2013).

Table 1. Area, climate characteristics and soil properties in the alpine and polar permafrost regions.

	Alpine	Arctic	Antarctic
Area (km^2)[1]	3.6–5.2 x 10^6	7.2 x 10^6	3.1 x 10^5
AT (°C)	< 0 (except in summer)	< 0 (except in summer)	< 0
MAP (mm)	> 1000	60 to 160	50
Light regime	Diurnal	Seasonal	Seasonal
Permafrost	Sporadic to Continuous	Sporadic to Continuous	Continuous
PT (°C)[2]	0 to -4℃	0 to -15℃	0 to -23℃
Permafrost depth[3] (cm b.g.s)	≥ 120	> 40	> 3
Soil organic carbon[4] (Pg)	66	1000	< 1
Soil Moisture	dry	Waterlogged / dry	dry
Vegetation	Scarcely vegetated or barren	Scarcely to densely vegetated	Scarcely vegetated or barren

The information shown in the table is based on Margesin, 2009 unless specified otherwise. AT: Air Temperature, MAP: Mean Annual Precipitation, PT: Permafrost Temperature. [1]Values reported in Hock et al., 2019 (Alpine), Margesin, 2009 (Arctic) and Obu et al., 2020 (Antarctic). [2]Borehole temperature values reported in Biskaborn 2019 (Alpine and Arctic) and Obu 2020 (Antarctic). [3]Values reported in Peng et al., 2018. [4]Values reported in Bockheim & Munroe, 2014 (Alpine), Mishra et al., 2021 (Arctic) and Claridge et al., 2000 (Antarctic)

Despite being C-poor, alpine permafrost harbor taxonomically diverse and active microbial communities, mostly composed of Bacteria and Fungi (Adamczyk et al., 2019; Hu et al., 2015; Margesin & Collins, 2019). Alpine permafrost layers are particularly enriched in poorly characterized (e.g. Verrucomicrobiota phylum) and uncultured (e.g. Patescibacteria superphylum) bacteria (Aszalos et al., 2020; Frey et al., 2016). Alpine permafrost fungal communities mainly comprise ascomycetous patho-saprotrophs (e.g. *Extremus*) (Schmidt et al., 2012), cold-adapted lichenized fungi (e.g. *Lecanora*) (Nimis et al., 2018) and endemic basidiomycetous yeasts (e.g. *Mrakia*) (Frey et al., 2016; Hassan et al., 2016).

Microbial studies conducted in topsoils from Tibetan grasslands, meadows and steppes at ≥ 4000 m a.s.l have shown the microbially-mediated release of CO_2 (Ding et al., 2016; Pei et al., 2003) and, to a lesser extent, N_2O (Cao et al., 2018; Pei et al., 2003; Pei et al., 2004). Heterotrophic respiration has been reported on permafrost layers of Tibetan soil cores incubated at -5℃ (Chen et al., 2016). In the alpine active-layers, soils are exposed to oxygen and receive fresh inputs of carbon (C) and nitrogen (N) from atmospheric deposition and autotrophic activities, including plant-derived substrates (Adamczyk et al., 2021; Peng et al., 2020; Rime et al., 2016; Schmidt et al., 2008a). Active-layer soil microorganisms exhibit aerobic metabolisms and feed mainly on fresh inputs of organics (Tas et al., 2018; Xue et al., 2020). At permafrost depths of > 1 m below ground surface (b.g.s.) in alpine areas, where the availability of dissolved substrates and oxygen is reduced, it could be that permafrost microorganisms use anaerobic respiratory and fermentative metabolisms (Tas et al., 2018), CO_2-fixation and the processing of inorganic N to cover their energetic and nutritional needs (Guo et al., 2015; Yang et al., 2014). These buried permafrost microbial cells might show specific physiological adaptations, e.g. cell membranes of increased fluidity, and extensive synthesis of cold-shock proteins and intracellular osmolytes, that enable the cells to survive and remain active despite constant freezing of the permafrost, and resulting conditions of desiccation (De Maayer et al., 2014). Permafrost cells have been also posited to be enriched in functions related to cell defense and competition (Coolen & Orsi, 2015; Mackelprang et al., 2017). However, little is still known about the physiologies of alpine soil microorganisms, particularly within permafrost, and the C- and N- cycling microbial functions that modulate GHG exchanges between alpine soils and the atmosphere. A functional characterization of both

permafrost and active layers microbiota is needed as a first step towards predicting the growth and functionality of the alpine soil microbiome in response to global warming.

1.3. The alpine permafrost microbiome undergoing warming

1.3.1. *Microbial responses to permafrost thawing and enhanced vegetation*

Permafrost thawing results in elevated soil moisture and dissolved C and nutrients in soils owing to the release of liquid water and organic materials previously occluded in frozen layers (Chen et al., 2016; Reyes & Lougheed, 2015). Conditions of elevated soil temperatures (Chen et al., 2021; Donhauser et al., 2020; Luláková et al., 2019), and a greater availability of soil C and nutrients (Adamczyk et al., 2021), have been shown to shift the structure (β-diversity) of soil microbiota in Tibetan and central European permafrost and active-layer soils. Prokaryotes (i.e. Bacteria and Archaea) inhabiting the permafrost are often categorized as *oligotrophic* (Frey et al., 2016; Mackelprang et al., 2017), which describes taxa that grow slowly in low-nutrient artificial media (e.g. Verrucomicrobial strains; Sangwan et al., 2005) and are often stress tolerant (Koch, 2001; Lauro et al., 2009). Conversely, copiotrophic prokaryotic taxa grow fast in nutrient rich media, they are metabolically versatile and they are often resilient to environmental changes (Koch, 2001). Upon permafrost thawing, copiotrophic taxa might acclimate quickly to the change in soil temperatures, growing speedily on the increased concentrations of dissolved C and nutrients in the soils (Schostag et al., 2019).

Alpine vegetation is migrating towards higher altitudes, following the increasing air temperatures (Steinbauer et al., 2018). Copiotrophs inhabiting the active-layer alpine soils might benefit from both elevated temperatures (Donhauser et al., 2020) and additional inputs of plant-derived organics from warming-induced increases in vegetation (Adamczyk et al., 2021; Peng et al., 2020). Permafrost and active-layer oligotrophic taxa could be superseded by copiotrophs, which might reduce prokaryotic α-diversity, as observed for Tibetan permafrost soils exposed to warming (Chen et al., 2021). This notwithstanding, the copiotrophy-oligotrophy categorization is conceptual and it has to be interpreted with care, because physiological traits in microorganisms are context-dependent and often vary between close relatives, e.g. individuals belonging to the same genus (Morrissey et al., 2016; Song et al., 2017).

Fungal communities in alpine active-layer and permafrost soils treated to higher temperatures have shown weaker alterations in α- and β-diversity than their prokaryotic counterparts (Feng et al., 2020; Xiong et al., 2014). However, augmented inputs of C and nutrients in alpine permafrost and mineral Arctic soils have been reported to enhance fungal growth, leading to compositional variations within fungal communities and the abundance increase of soil fungi over the prokaryotes (Adamczyk et al., 2020; Adamczyk et al., 2021; Deslippe et al., 2012).

Besides promoting diversity shifts, elevated temperatures and C and nutrient availability in alpine permafrost soils have been shown to stimulate C mineralization activities (Adamczyk et al., 2021; Bao et al., 2016), and lead to augmented soil microbial biomass (Guo et al., 2015). GeoChip-based genetic profiling of Tibetan permafrost incubated for 5 months at 5℃ reported higher rates of CO_2 production in soils, related to greater C-degrading genetic capabilities of soil microorganisms, including enhanced potential for hydrolysis of plant-derived biopolymers (Chen et al., 2021). Likewise, alpine permafrost and active-layer soils amended with labile C and nutrients showed a boost in heterotrophic respiration and broader ranges in using organic C-substrates (Adamczyk et al., 2021).

Enhanced CO_2 emissions from alpine permafrost soils could contribute to the ongoing warming in the mountain regions, even if soil C stocks are small compared to the Arctic (Donhauser & Frey, 2018; Knowles et al., 2019). This would be particularly the case for soils influenced by vegetation, e.g. meadows and grasslands, that contain enough C and nutrients to sustain both microbial growth and high rates of cell metabolic activities in the long-term (Peng et al., 2020). However, in alpine permafrost areas where vegetation is scarce or absent and in which soil C pools are small, e.g. barren soils in the narrow peaks of the Alps, microbial growth and heterotrophic activities might be constrained (Luláková et al., 2019). In these barren soils, warming could lead to greater soil CO_2-fixation, first by stimulating activity of autotrophic microorganisms and secondly by upward migration of plants (Donhauser & Frey, 2018). Enhanced soil CO_2-fixation could outweigh soil CO_2 production and thereby offset warming (Donhauser & Frey, 2018). Quantitative evidence of structural and functional responses of alpine permafrost microbial and plant communities to warming is, however, still insufficient to predict future CO_2 gas fluxes from these mountain regions. This is particularly the case for mountainous permafrost areas outside Tibet, where warming-related microbial data is limited

to laboratory-based incubation experiments of short duration (< 1 year) (Donhauser & Frey, 2018).

1.3.2. *Microbial responses to increased freeze-thaw cycles frequency*

Freeze-thaw cycles (FTCs) refer to cyclic events of soil freezing and thawing that occur when soil temperature transitions from above to below 0℃ and *vice versa* (Wang et al., 2020). Reduced snowfall, associated with a warmer climate, results in poorly insulated active layers that experience more frequent freeze-thaw cycles (Henry, 2008). Repeated freeze-thawing causes cell lysis, which leads to the death of microbial taxa that fail to adjust quickly to environmental changes (Larsen et al., 2002; Schimel & Clein, 1996). The death of the FTCs-sensitive microorganisms results in reduced soil microbial abundance and biomass, and altered microbial β-diversity (Han et al., 2018; Schostag et al., 2019). Furthermore, FTCs breaks soil aggregates (Wang et al., 2012) and organic substrates (Feng et al., 2007), which releases labile C and N sources. An increase in necromass and the FTCs-induced release of labile substrates could facilitate the expansion of copiotrophic prokaryotic taxa (Schostag et al., 2019). Soil microorganisms might switch from the utilization of complex polymeric substrates to the consumption of simpler C sources, as observed in alpine and Arctic topsoils undergoing frequent FTCs (Han et al., 2018; Schimel & Mikan, 2005). Contrary to what has been observed for elevated soil temperatures, repeated FTCs in alpine soils have been shown to reduce soil CO_2 respiration (Han et al., 2018). These reductions in soil respiration have been linked to decreases in soil microbial abundance or to lower rates of microbial activities in soils; likely because the microbial cells slow down their metabolic processes during freezing (Han et al., 2018).

The sensitivity of alpine active-layer soil microbiota to increases in FTC frequency might be influenced by environmental legacy. For instance, repeated FTCs applied to arable topsoils from central Europe caused a > 90% drop in heterotrophic respiration and diminished microbial abundance. Contrastingly, they only minimally affected the microbiota from Himalayan topsoils (> 5000 m a.s.l), which are exposed to frequent FTCs at their location (Stres et al., 2010). Likewise, soils of distinct origin might harbor fungal communities which are more (Feng et al., 2007) or, conversely, less (Sharma et al., 2006) sensitive to freeze-thawing than prokaryotic

communities. FTCs-related microbial studies in permafrost soils are, however, scarce, particularly in alpine regions, and the effects of FTCs on soil fungal communities have been rarely addressed. Yet, it is necessary to understand the influence of increased FTC frequency on alpine soil microbiomes to accurately predict alterations in microbial structure and functions under a warmer climate.

1.4. Main study site and approaches used in this Dissertation to characterize the soil microbiota

1.4.1. *The long-term monitoring permafrost site of "Muot da Barba Peider"*

The active-layer and permafrost soils investigated in this Dissertation were mainly from the summit of "Muot da Barba Peider" (MBP; 2979 m a.s.l., N 46°29.78040' E 009°55.88700'), a mountain located in the upper Engadine valley in eastern Switzerland (Fig. 1. B). MBP summit is a study site of the Swiss Permafrost Monitoring Network (PERMOS; http://www.permos.ch/). PERMOS has installed boreholes in numerous locations in the Alps, including two at MBP, which have been monitoring ground temperatures since 1996.

Permafrost at MBP is found near the summit, below a depth of 150 cm on the north-facing (N) slope (Fig. 2). The south-facing (S) slope of MBP does not have permafrost; thus all soils located there are part of the active layer (Zenklusen Mutter et al., 2010). Mean annual precipitation in the region is ~950 mm (automatic meteorological station of Bernina; www.meteoswiss.admin.ch). The S slope of MBP exhibits a 3℃ warmer climate than the N slope, with less snow, more FTCs, and presence of vegetation (Frey et al., 2016) (Fig. 2). Soils around the summit of MBP consist of coarse-grained materials (67–90% sand content), with low pH < 6 and limited C (< 1%) and N (≤ 0.1%) content (Frey et al., 2016). The bedrock at MBP is gneiss, dominated by quartz and feldspars, from the upper Austroalpine Languard nappe. I use MBP as a model ecosystem for my investigations because its permafrost distribution is well characterized (Haberkorn et al., 2021), its landscape features and soil properties are comparable to other alpine permafrost environments (Böckli, 2013), and the summit is at a relatively close location and accessible.

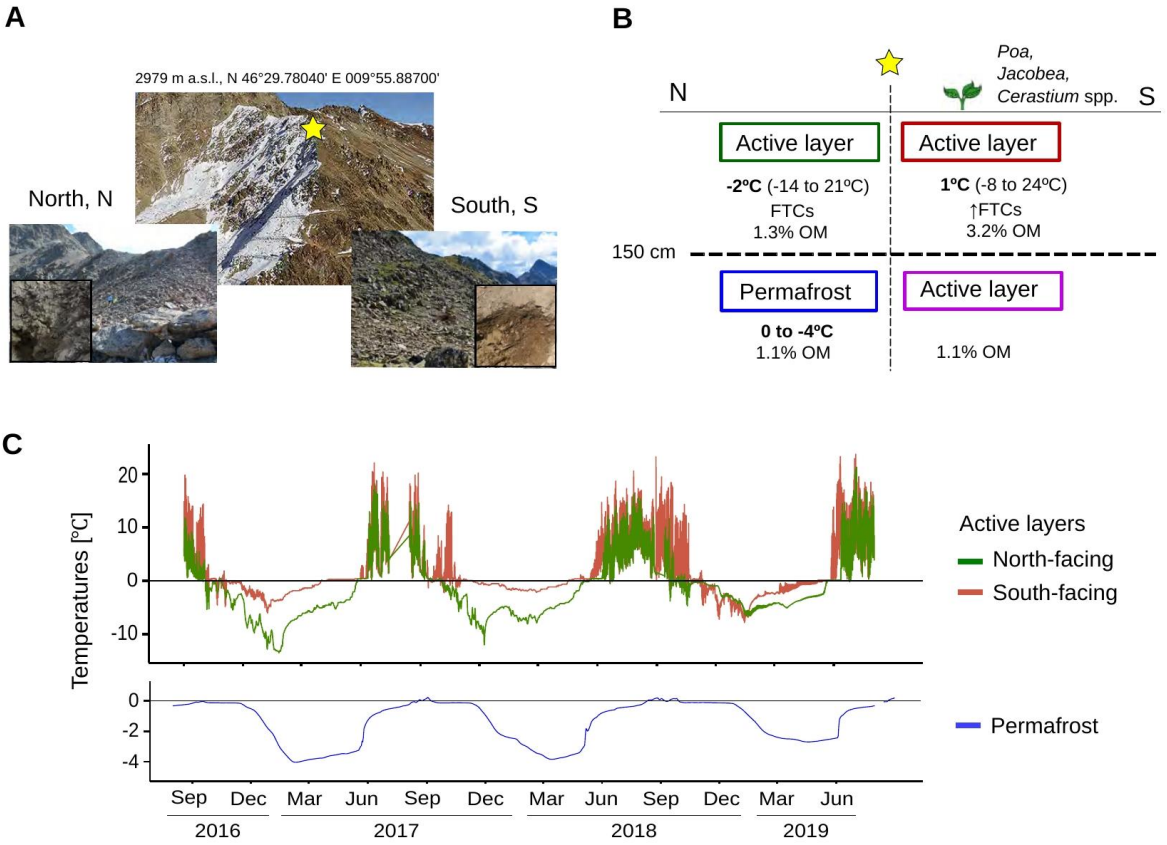

Figure 2. Visualization of Muot da Barba Peider (MBP) **(A)** and overview of the vegetation, organic matter content **(B)** and temperatures **(B** and **C)** of the active-layer and permafrost soils. An aerial view of the MBP summit (yellow star) is shown, with overlapping images of the north-facing and south-facing sampling locations near the summit, and close-up photographs of the active layers. Active-layer temperatures were measured at a depth of 5 cm using M-Log5W-SIMPLE sensors (GeoPrecision GmbH, Ettlingen, Germany). Permafrost temperatures are mean values of the temperatures measured at a depth of 1 and 2m by the PERMOS borehole MBP_0196, 2946 m a.s.l., N 46°29.784' E 009°55.8645 (http://www.permos.ch/data.html). FTCs: freeze–thaw cycles, OM: organic matter. The aerial photograph of MBP was provided by Dr. Marcia Phillips (CERC, Davos).

1.4.2. *Genomic methods used to study soil microbial diversity*

The main insights of this Dissertation are from taxonomic and functional characterizations of soil microbial communities. To identify and quantify taxa in the soils I used an "amplicon sequencing" approach (Fig. 3). In this method, DNA is extracted from soils, and "marker" genomic regions in the DNA, which are highly conserved within species (e.g. the 16S rRNA gene in prokaryotic cells and the ITS2 genomic region in fungi) are amplified by polymerase chain reaction (PCR). Amplicons are then sequenced by high-throughput sequencing (e.g. Illumina technology). *In silico*, the obtained sequences are grouped based on 97% similarity

into Operational Taxonomic Units (OTUs), which represent “species” (Edgar, 2013). OTUs are aligned to taxonomic databases containing representative sequences of all microbial “species” worldwide (e.g. SILVA database for prokaryotes and UNITE database for fungi) (Wang et al., 2007) to identify the taxa present in the soil. Amplicon sequencing overcomes limitations of classical culture-based approaches by detecting both culturable and unculturable microbial taxa at high taxonomic resolution (e.g. genus level). DNA-based sequencing does not, however, reliably inform about active microorganisms or their functions.

To reveal the potential functional characteristics of the soil microbiota I applied a “shotgun metagenomic sequencing” approach (Fig. 3). In this method, DNA extracted from soils is fragmented (shot-gun) into short pieces (e.g. 350 bp) and high-throughput sequenced (Breitwieser et al., 2019). Ideally, the obtained sequences represent the entire genetic content of the soils. *In silico*, sequences with overlapping regions that belong to the same genomic regions are then joined together (assembly), forming larger fragments (> 1.5 Kbp) that are called contigs. Contigs belonging to the same genome, and thus representing a same microorganism, are grouped together (binning) into bins (Breitwieser et al., 2019). Bins that represent draft genomes (with > 50% completeness) can be called MAGs (Metagenome-Assembled Genomes) (Bowers et al., 2017). Shorter reads can then be aligned to contigs or MAGs (Breitwieser et al., 2019) to provide information about the abundance (i.e. coverage) of the different genomic regions within contigs and MAGs.

Gene functions can be predicted within genomic regions of contigs and the MAGs by aligning sequenced genes to protein databases (e.g. EggNOG database) (Breitwieser et al., 2019). Additionally, taxonomic marker genes can be identified in contigs and MAGs, and be aligned to taxonomic databases. Unlike amplicon sequencing, metagenomic approaches enable extensive functional interpretations of microbial taxa (Breitwieser et al., 2019). Metagenomic approaches, however, only inform about potential microbial metabolisms. Ultimately, it is necessary to enrich, and preferably isolate, microorganisms in the laboratory to determine their physiological features with certainty (Lambrechts et al., 2019).

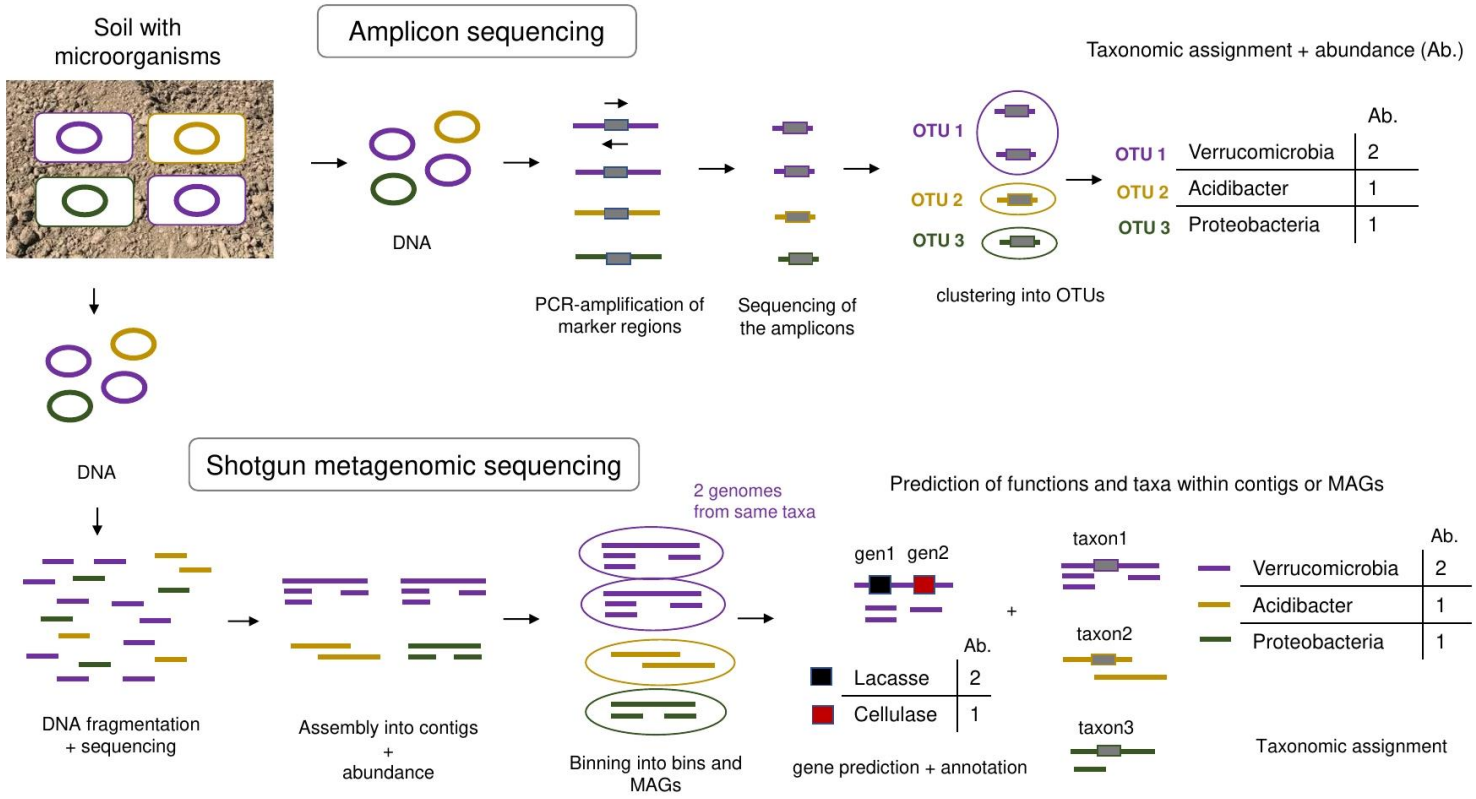

Figure 3. Main steps of the amplicon and shotgun metagenomic sequencing approaches. The DNA of the soil microbiota is extracted. In the amplicon sequencing approach, a marker genomic region, i.e. genomic regions that differ between species, is amplified by PCR. The amplicons are sequenced. Sequences with > 97% similarity are grouped together into Operational Taxonomic Units (OTUs). OTUs are classified taxa by aligning the OTU sequences to taxonomic databases containing representative sequences of worldwide described microbial taxa. The abundance of the taxa in the soils is estimated by counting the number of sequences grouped into the OTUs that are classified to a same taxon. In the shotgun metagenomic sequencing approach, all DNA extracted from the soil is fragmented and sequenced. The sequenced fragments are joined together (assembly) into longer fragments (contigs). The abundance (coverage) of contigs is obtained by aligning all sequences to the contigs. Contigs belonging to a same genome (representing a microbial cell) can be clustered together (binning) into bins (partial genomes) or Metagenome-Assembled Genomes (MAGs; genomes with at least 50% completeness). Functional and taxonomic marker genes are identified within the contigs and MAGs. Annotation of the genes to protein and taxonomic databases reveal the microbial taxa in the soils and their associated functions.

1.5. Research gaps

Our knowledge on the physiological characteristics, including C- and N- cycling metabolic functions, of soil microbiota in alpine soils from permafrost areas is still limited. Specifically, we lack information about the functional genetic potential of soil microbial communities within 1m deep mountain permafrost, which ultimately delimits the range of possible metabolic responses of soil microbiota to thawing. From a biogeochemical perspective, functional gene profiling of alpine permafrost could inform about microbial pathways involved in the transformation of organic materials and minerals in deep soils, whose developmental processes and properties are still poorly known.

In the context of climate change, we still do not thoroughly comprehend how warming-induced conditions of elevated soil temperatures, greater availability of C and nutrients and (more) frequent FTCs will shape the structure of microbial communities in alpine permafrost soils in the future, and how this will in turn modulate microbially-mediated feedbacks between mountain soils and climate (e.g. soil CO_2 sequestration and release). For instance, it is not clear whether warming-associated changes in habitat conditions in alpine permafrost soils will differently affect prokaryotic taxa with copiotrophic or oligotrophic attributes. It is also unclear how climate warming will influence the growth of alpine soil fungal populations relative to their prokaryotic counterparts. Initially, an abundance increase in copiotrophic taxa could lead to a higher release of CO_2 in mountain soils, and thus contribute to global warming. This effect could diminish later on, however, if fungal abundance increases in warmer, nutrient-enriched soils. Fungi generally assimilate C-substrates more efficiently than prokaryotes, thereby producing less CO_2 per unit of C (Kallenbach et al., 2016). We, furthermore, still do not understand the temporal dynamics of soil prokaryotic and fungal populations in a warmer climate. Likewise, the links between climate-driven changes in soil microbial community composition and microbial activities, e.g. C mineralization rates and patterns of organic carbon assimilation, are still poorly resolved. Particularly within the 1m permafrost from temperate mountains, quantitative insights into the structural and functional responses of soil microbiota to *in situ* warming are still lacking.

1.6. Objectives of the thesis and publication output

In this thesis, I advanced the understanding of the microbial ecology of permafrost soils from alpine regions and the impacts of warming on the alpine permafrost microbiome. I used the monitoring site of MBP as a model ecosystem, where I conducted my investigations. I pursued three research objectives, each of them fulfilled in Chapters 2, 3 and 4 of this Dissertation:

Objective of Chapter 2: Evaluate the microbial functional gene diversity and metabolic potential of the alpine permafrost and active layers

Objective of Chapter 3: Analyze the impacts of increased FTC frequency on the structure and functionality of the alpine active-layer soil microbiota.

Objective of Chapter 4: Quantify the structural and functional responses of the alpine permafrost and active-layer microbiomes to *in situ* conditions of warming.

To fulfill the **objective** of **Chapter 2**, I revealed the functional gene profiles of the MBP alpine permafrost and north- and south-facing active layers, using shotgun metagenomics. I **hypothesized** that MBP permafrost: (**2.1**) has a higher proportion of cold-stress genes and genes related to cell defense and competition and (**2.2**) shows distinct C- and N-cycling functions than the active layers. This chapter corresponds to the following publication:

Perez-Mon C., Qi W., Vikram S., Frossard A., Makhalanyane T. P., Cowan D. A. & Frey B. (2021). Shotgun metagenomics reveals distinct functional diversity and metabolic capabilities between 12 000-year-old permafrost and active layers on Muot da Barba Peider (Swiss Alps). Microbial Genomics 7(4). doi: 10.1099/mgen.0.000558

To fulfill the **objective** of **Chapter 3**, I performed a microcosm experiment in which I compared the impacts of repeated FTCs of differing frequency (more frequent daily vs. less frequent weekly FTCs) on prokaryotic and fungal communities from both the north- and south-facing active layers of MBP. In this experiment I also included topsoils collected from the north- and south-facing slopes of a mountain ridge in the Swedish Arctic, which experience less FTCs than the alpine soils at their site of origin. I **hypothesized** that: (**3.1**) more frequent FTCs cause larger alterations in the structure of soil microbial communities, (**3.2**) microbial compositional shifts are coupled to alterations in microbial metabolic functions, and (**3.3**) microbial

communities from soils with a legacy of more FTCs are less sensitive to increased FTC frequency. This chapter has also been published:

Perez-Mon C., Frey B. & Frossard, A. (2020). Functional and structural responses of Arctic and alpine soil prokaryotic and fungal communities under freeze-thaw cycles of different frequencies. Frontiers in Microbiology 11, 982. doi:10.3389/fmicb.2020.00982

To fulfill the objective of **Chapter 4**, I monitored for three years a field experiment which was established in 2016 at the summit of MBP. In this experiment, a projected warmer climate was simulated in the MBP permafrost and active layers, by transplanting (1) permafrost soils from a depth of 160 cm into active-layer topsoils, and (2) north-facing active layers into the warmer south-facing topsoil. I **hypothesized** that *in situ* simulated warming lead to (**4.1**) shifts in soil microbial diversity, due to abundance increases in fungi and copiotrophic prokaryotes relative to oligotrophic prokaryotes, and (**4.2**) enhance microbial turnover of carbon substrates and soil CO_2 effluxes. This chapter correspond to the publication:

Perez-Mon C., Stierli B., Plötze M., Frey B. (2021). Fast and persistent responses of alpine permafrost microbial communities to *in situ* warming. Science of the Total Environment 807, 150720. doi:10.1016/j.scitotenv.2021.150720

In addition of the research work included in this Dissertation, I contributed to several other publications over the course of my PhD:

Luláková P., **Perez-Mon C.**, Šantrůčková H., Ruethi J. & Frey, B. (2019). High-alpine permafrost and active-layer soil microbiomes differ in their response to elevated temperatures. Frontiers in Microbiology 10, 668. doi:10.3389/fmicb.2019.00668

Adamczyk M., **Perez-Mon C.**, Gunz S. & Frey B. (2020). Strong shifts in microbial community structure are associated with increased litter input rather than temperature in High Arctic soils. Soil Biology and Biochemistry 151, 108054. doi:10.1016/j.soilbio.2020.108054

Frey B., Walthert L., **Perez-Mon C.**, Stierli B., Köchli R., Dharmarajah A. & Brunner I. (2021). Deep soil layers of drought-exposed forests harbor poorly known bacterial and fungal communities. Frontiers in Microbiology 12, 1061. doi:10.3389/fmicb.2021.674160

2. CHAPTER 2. Shotgun metagenomics reveals distinct functional diversity and metabolic capabilities between 12 000-year-old permafrost and active layers on Muot da Barba Peider (Swiss Alps)

Authors: **Carla Perez-Mon[1*]**, Weihong Qi[2], Surendra Vikram[3], Aline Frossard[1], Thulani Makhalanyane[3], Don Cowan[3], Beat Frey[1*]

[1]Forest Soils and Biogeochemistry, Swiss Federal Institute for Forest, Snow and Landscape Research WSL, Birmensdorf, Switzerland

[2]Functional Genomics Center of the University of Zurich and the ETH Zurich, Zurich, Switzerland

[3]Centre for Microbial Ecology and Genomics, Department of Biochemistry, Genetics and Microbiology, University of Pretoria, Pretoria, South Africa

∗**Correspondence to:** Beat Frey, Swiss Federal Research Institute WSL, Zürcherstrasse 111, CH-8903 Birmensdorf, Switzerland. Tel: +41-44-739-25-41; E-mail: beat.frey@wsl.ch

Carla Perez-Mon, Swiss Federal Research Institute WSL, Zürcherstrasse 111, CH-8903 Birmensdorf, Switzerland. E-mail: carla.perezmon@wsl.ch

Keywords: alpine, permafrost, warming, soil, microbial communities, metagenomics

2.1. Abstract

The warming-induced thawing of permafrost promotes microbial activity, often resulting in enhanced greenhouse gas emissions. The ability of permafrost microorganisms to survive the *in situ* sub-zero temperatures, their energetic strategies and their metabolic versatility in using soil organic materials determine their growth and functionality upon thawing. Hence, functional characterization of the permafrost microbiome, particularly in the underexplored mid-latitudinal alpine regions, is a crucial first step in predicting its responses to the changing climate, and the consequences for soil–climate feedbacks. In this study, for the first time, the functional

potential and metabolic capabilities of a temperate mountain permafrost microbiome from central Europe has been analyzed by using shotgun metagenomics. Permafrost and active layers from the summit of Muot da Barba Peider (MBP) (Swiss Alps, 2979 m a. s. l.) revealed a strikingly high functional diversity in the permafrost (north-facing soils at a depth of 160 cm). Permafrost metagenomes were enriched in stress-response genes (e.g. cold-shock genes, chaperones), as well as in genes involved in cell defense and competition (e.g. antiviral proteins, antibiotics, motility, nutrient-uptake ABC transporters), compared with active-layer metagenomes. Permafrost also showed a higher potential for the synthesis of carbohydrate-active enzymes, and an overrepresentation of genes involved in fermentation, carbon fixation, denitrification and nitrogen reduction reactions. Collectively, these findings demonstrate the potential capabilities of permafrost microorganisms to thrive in cold and oligotrophic conditions, and highlight their metabolic versatility in carbon and nitrogen cycling. Our study provides a first insight into the high functional gene diversity of the central European mountain permafrost microbiome. Our findings extend the understanding of the microbial ecology of permafrost and represent a baseline for future investigations comparing the functional profiles of permafrost microbial communities at different latitudes.

2.2. Introduction

Global warming is causing extensive thawing of permafrost soils, distributed in the Arctic, Antarctic and mid-latitudinal alpine regions (Biskaborn et al., 2019; Gobiet et al., 2014; Hock et al., 2019). Permafrost thawing increases microbial activity, often leading to enhanced soil greenhouse gas emissions (Chen et al., 2016; Donhauser & Frey, 2018; Genxu et al., 2008; Karhu et al., 2014; Mackelprang et al., 2016; Nikrad et al., 2016; Schuur et al., 2008). Permafrost in polar and alpine regions represents different terrestrial cryoenvironments (Donhauser & Frey, 2018; Margesin, 2009) and harbors diverse microbial communities (Frey et al., 2016; Hu et al., 2015; Jansson & Tas, 2014), whose carbon (C) and nitrogen (N) cycling functions, energetic metabolisms and survival are still not well understood (De Maayer et al., 2014; Mackelprang et al., 2016; Margesin & Collins, 2019; Nikrad et al., 2016). The ability of

permafrost microorganisms to withstand the persistent sub-zero temperatures and their metabolic capabilities together determine their capacity for growth and functionality upon thawing (Bakermans et al., 2012; De Maayer et al., 2014; Mackelprang et al., 2016; Nikrad et al., 2016). Hence, functional characterization of the permafrost microbiome at different latitudes is a crucial first step in predicting its responses to the changing climate, and the consequences for the soil–climate feedbacks.

Functional information about the permafrost microbiome is mostly restricted to Arctic cryoenvironments (Jansson & Hofmockel, 2020; Mackelprang et al., 2016; Margesin & Collins, 2019; Nikrad et al., 2016). Arctic permafrost is usually overlaid by active layers with a depth of < 1 m, and it exhibits temperatures ranging from 0 to below -10°C (Biskaborn et al., 2019; Donhauser & Frey, 2018; Margesin, 2009). The generally high moisture content of Arctic soils lead to suboxic conditions at the permafrost table (Margesin, 2009). Suboxia and the sub-zero temperatures promote the accumulation of poorly-decomposed detritus in the permafrost, resulting in a high soil organic carbon content (i.e. global SOC stock of 977 Pg) (Donhauser & Frey, 2018; Margesin, 2009). In accordance with the suboxic conditions, meta-omic studies have shown that Arctic permafrost contains more genes related to anaerobic respiratory and fermentative metabolism than the overlying active layers (Hultman et al., 2015; Mackelprang et al., 2016; Mueller et al., 2018; Woodcroft et al., 2018; Xue et al., 2020). Permafrost microbiomes also feature a high abundance of carbohydrate-active enzymes (CAZys), which are involved in the decomposition of organic polymers (Leewis et al., 2020; Tas et al., 2018; Woodcroft et al., 2018; Xue et al., 2020). Moreover, permafrost metagenomes are enriched in genes involved in stress responses (e.g. cold-shock genes and chaperones), DNA repair, cell defense (e.g. antiviral proteins) and competition (e.g. antibiotics, motility) (Coolen & Orsi, 2015; De Maayer et al., 2014; Mackelprang et al., 2017; Margesin & Collins, 2019; Van Goethem et al., 2018; Xue et al., 2020; Zhang et al., 2018).

Microbial studies in alpine permafrost regions are mainly in topsoils (i.e. at a depth of 5–10 cm) and they often lack functional information. Whereas the soil microbiome of the Tibetan mountains has been recurrently investigated, other mountain regions, e.g. in central Europe, remain underexplored (Donhauser & Frey, 2018). Mid-latitudinal alpine permafrost is usually located on poorly vegetated steep slopes of mountains above 2500 m a. s. l., and dominated by coarse sediments that favor thermal conduction and the leaching of water and organic materials due to enhanced percolation (Chen et al., 2016; Donhauser & Frey, 2018; Gruber & Haeberli, 2007). In comparison to permafrost in polar regions, alpine permafrost is relatively warm (0 to -2°C), and often found at soil depths > 1m. Furthermore, unlike the Arctic permafrost but similar to the Antarctic soils, alpine permafrost is well-drained and depleted in organic materials (i.e. global SOC stock of 66 Pg) (Donhauser & Frey, 2018; Margesin, 2009).

GeoChip microarray surveys along altitudinal gradients in the Tibetan plateau (3200 to 3800 m a. s. l.) indicated a higher abundance of cold-stress, carbon-fixation and denitrification genes in permafrost-like topsoils at higher altitudes (Guo et al., 2015; Yang et al., 2014), which was associated with decreasing soil temperatures and organic C and N. Reduced inputs of labile C and N from fresh plant residues with increasing soil depths (Fontaine et al., 2007) and the preservation of poorly-decomposed polymeric substrates at sub-zero temperatures (Leewis et al., 2020) might contribute to habitat differences between the active layers and the permafrost. The abiotic differences between these soils might result in soil microbiota of distinct taxonomic composition (Frey et al., 2016) and metabolic features, including a greater genetic potential for the utilization of biopolymers in the permafrost. Furthermore, the large spatial and microenvironmental variability in alpine soils, owing to the extreme climatic heterogeneity of mountain regions (Adamczyk et al., 2019; Haeberli & Gruber, 2009; Liang et al., 2015), might be reflected in soil microbial communities with a particularly high diversity of functional genes.

Here, we analyzed the microbial functional diversity and metabolic potential of an alpine permafrost soil and active layers from central Europe, using shotgun metagenomics. We compared soils at the same depths on two slopes from a well-characterized permafrost site in the Swiss Alps, the mountain summit of Muot da Barba Peider (MBP) (2979 m a. s. l.) (Frey et al., 2016; PERMOS, 2016; Zenklusen Mutter et al., 2010). Permafrost on MBP is found in the north-facing slope below a depth of 150 cm (Frey et al., 2016; PERMOS, 2016; Zenklusen Mutter et al., 2010) and has an estimated age of 12 kyr, whereas soils on the south-facing slope at this depth are part of the active layer (Frey et al., 2016; PERMOS, 2016; Zenklusen Mutter et al., 2010). Like in other mountain systems in the Northern hemisphere, the south-facing topsoils of MBP exhibit higher temperatures and water-holding capacity than the north-facing topsoils, and a greater content of C and N, which together favor microbial life and the growth of plants (Frey et al., 2016). A previous amplicon sequencing study conducted on MPB revealed that the soil microbial communities at different depths of the north- and south-facing slopes exhibit distinct diversities and structures (Frey et al., 2016). In particular, permafrost soils in the north-facing slope were found to harbor a high proportion of metabolically versatile psychrophilic fungi and potentially parasitic bacterial taxa (Frey et al., 2016). Our current study complements this earlier work and uses the same experimental design to analyze the functional gene profiles of the permafrost and the active layers. We first compared the metagenomes of north-facing permafrost soils collected at a depth of 160 cm (N160) with the metagenomes of north-facing active-layer soils collected at a depth of 10 cm (N10). We further explored the metabolic potential of the metagenomes in the south-facing active layers (S10 and S160) in comparison with the north-facing soils (N10 and N160). We hypothesized that, compared with the active layers, MBP permafrost (N160): (1) exhibits a distinct functional gene diversity and structure, (2) has a higher proportion of cold-stress genes and genes related to cell defense and competition, and (3) shows distinct C- and N-cycling genes, including a higher abundance of CAZys. We also hypothesize that (4) south-facing soils exhibit a higher functional diversity than north-facing soils.

2.3. Methods

2.3.1. *Study site and sample collection*

The study was conducted on the summit of Muot da Barba Peider (MBP) (N 46.49634 E 9.93145, 2979 m a. s. l.), located in the upper Engadine valley in eastern Switzerland (Fig. S1). This site is part of the long-term monitoring of permafrost in the Swiss Alps (PERMOS, 2016). Soil temperatures measured at a depth of 5 cm near the summit during three consecutive years (2016 to 2019), showed mean annual values of -2°C (ranging from -14°C to 21°C) in the north-facing slope and 1°C (ranging from -8°C to 24°C) in the south-facing slope. Mean annual precipitation in the region is 1500 mm (Frey et al., 2016). The ground is covered with snow from October/November until May/June (Beniston et al., 2003; Rodder & Kneisel, 2012). The soil around the summit of MBP consists of coarse-grained materials in the uppermost 200 cm and finer-grained materials at greater depths (Zenklusen Mutter et al., 2010). The bedrock is found at 340–500 cm depth and consists of gneiss from the upper Austroalpine Languard nappe. Permafrost exists at 150 cm depth in the north-facing slope of the summit whereas soils on the south-facing slope at this depth are part of the active layer (PERMOS, 2016; Zenklusen Mutter et al., 2010). Soils are acidic and depleted in C (< 1% DW) and N (< 0.1% DW), especially in the north-facing slope (Table S1). Vegetation is scarce, and mostly occurs in the south-facing slope, with sparse observations of the taxa *Poa*, *Cerastium* and *Jacobea* spp. (Frey et al., 2016).

Soil samples were collected as described in detail in (Frey et al., 2016). Briefly, near the summit of MBP, six soil profiles were excavated with shovels down to a depth of 160 cm. Three profiles were excavated in both the north-facing and the south-facing slopes. The distance between the two sites over the mountain ridge was approximately 50 m. The external layer of the profiles, exposed to air, was removed with sterilized (70% ethanol solution) spatulas, to eliminate debris and to prevent cross-contamination from upper soil layers. Bulk soil samples were collected from the pristine portion of the profiles at depths of 10 cm and 160 cm (2 slopes × 2 soil depths × 3 soil profiles = 12 samples in total), using freshly sterilized spatulas. The

collected samples (5 subsamples of ≥ 100 g from each depth and profile) were homogenized in autoclaved bags, and roots were removed when present. Samples were transported in dry ice to the laboratory facilities, where they were immediately stored at -80°C.

2.3.2. *Soil DNA extraction*

Total DNA was extracted from 20 g of stored soil using a combination of the DNeasy PowerMax Soil Kit and the DNeasy PowerSoil Kit (Qiagen, Hilden, Germany). The soils were weighed into PowerMax® Bead Tubes and the DNA extraction steps for (1) soil homogenization and cell lysis, and (2) removal of non-DNA materials from the lysates were completed using the PowerMax Kit. The lysates were loaded into the spin columns of the PowerSoil kit, where the (3) DNA molecules bound into the silica membrane. The last extraction steps for the (4) washing and elution of the bounded DNA (in 100 µl of elution buffer) were performed using the PowerSoil Kit.

All DNA extraction steps of the two kits were conducted according to the manufacturer's instructions. To enhance cell lysis, an extra step was added to the PowerMax kit procedures. After weighing the soils into the PowerMax® Bead tubes and adding the PowerBead and the C1-SDS solutions, the tubes were vortexed (Vortex-genie 2, Scientific Industries Inc., New York, USA) for 15 minutes at the maximum speed of 3200 rpm. Then, the tubes were heated for 15 minutes at 65℃ in a shaking water bath. The combination of the two extraction kits complemented with the additional heating step yielded enough DNA (> 0.1 ng μl^{-1}) for sequencing. To eliminate foreign DNA and prevent microbial contaminations, working bench surfaces and non-autoclavable materials were cleaned with 5% sodium hypochlorite and 70% ethanol solutions, prior to the extractions. Negative controls (extraction buffer without soil) were included in the DNA extractions.

2.3.3. *Shotgun sequencing*

Library preparation using NEB Next ultra DNA Prep Kit (Illumina Inc., San Diego, California, USA) and shotgun sequencing of the eluted DNA samples were performed at the Genome Quebec Innovation Centre at McGill University (Montreal, Canada), using the HiSeq 2500 system (2 × 125 bp; Illumina Inc.). The twelve metagenomes were from the four soil habitats (each with three replicates): active-layer soils collected at a depth of 10 cm in the north-facing (N10) and south-facing (S10) slopes, and soils collected at a depth of 160 cm in the north-facing (N160; permafrost) and south-facing (S160; active layer) slopes.

2.3.4. *Assembly and functional annotation of assembled contigs*

Pre-processing of metagenomic reads, assembly of reads into contigs, contig binning, and functional and phylogenetic annotation of contigs and bins were achieved using a customized pipeline. Briefly, raw reads were quality checked using FastQC (https://www.bioinformatics.babraham.ac.uk/projects/fastqc/). They were quality filtered and trimmed (i.e. pre-processed reads) using Trimmomatic v0.36 (Q=20, minimum read length = 40) (Bolger et al., 2014). Pre-processed read pairs and singletons were assembled into contigs (> 200 bp) by iteratively building *de Bruijn* graphs using *k*-mers of increasing size with the *de novo* assembler MEGAHIT v1.1.3 (–k-min 27 –k-step 10) (Li et al., 2015).

Protein-coding sequences contained in the assembled contigs were predicted with MetaGeneMark v3.38 (Zhu et al., 2010). To uncover the potential metabolic capabilities of the soil metagenomes, protein-coding genes were assigned to functions (i.e. functional genes). About 50% of the predicted genes (4 706 835) were assigned to general metabolic and cellular functions through EggNOG v4.5, which classifies the genes to clusters of orthologous groups (COGs) of proteins and organizes the COGs into general functional categories (Huerta-Cepas et al., 2016). Annotation to EggNOG v4.5 was performed using the eggnog-mapper v1.0.3 with DIAMOND search mode against all protein sequences (Huerta-Cepas et al., 2017). The

annotations obtained with EggNOG were compared with COG annotations obtained through the curated MD5nr database (Wilke et al., 2012), in which 0.2% of the genes (16 245) were assigned to functions. About 1% (98 331) of the protein-coding genes were assigned to CAZys using the CAZy database (release of July 2017) (Cantarel et al., 2009). About 0.2% of the genes (15 326) were assigned to N-cycling families using the NCycDB database. Annotations against the MD5nr, CAZy and NCycDB (Tu et al., 2019) databases were performed using SWORD v1.0.3 (Vaser et al., 2016) (-v 10^{-5}) (Anwar et al., 2019).

2.3.5. *Abundance quantification of protein-coding genes*

Pre-processed read pairs from each of the samples were mapped to the assembled contigs, using the BWA aligner v0.7.15 (bwa-mem) (Li, 2013). Mapping of the reads to the assembled protein-coding gene sequences to obtain gene abundances was done using the function *featureCounts* from the package Subread v1.5.1 (-minOverlap 10, Q=10, -primary) (Liao et al., 2014).

2.3.6. *Metagenome binning and phylogenetic annotation of genome bins*

Contigs were binned with Metabat v2.12.1 (Kang et al., 2015), which iteratively clusters contigs into bins, based on similarities in abundance and tetranucleotide composition between pairs of contigs. Contig abundance was calculated with the *-jgi_summarize_bam_contig_depths* function, based on the bwa mem mapping of the pre-processed read pairs described in the previous section. Only contigs larger than 1500 bp and with a read depth > 1 were included in the binning. Bins were assessed for quality (i.e. completion, contamination and strain heterogeneity) with CheckM v1.0.11 (Parks et al., 2015). Bins with > 90% completion and < 5% contamination, presumably high-quality draft metagenome-assembled genomes (Bowers et al., 2017), were phylogenetically classified using the same program. The *-ssu_finder* function in CheckM was applied to identify SSU rRNA sequences in the contigs within the bins (16S for prokaryotes and 18S for eukaryotes). These sequences were taxonomically annotated

via the SINA online aligner v1.2.11 (Pruesse et al., 2012) against the SILVA database (release 132)(Quast et al., 2013).

2.3.7. *Data analyses*

Statistical analyses were completed using the open-source software R v3.6.0 (R Core Team, 2017) and graphical representations of results were created with the R package *ggplot2* (Wickham, 2016), unless specified otherwise. A significance level (*p*) of 0.05 was applied in all analyses. Protein-coding genes for which the sum of the reads over all soil samples was < 10 were excluded from the analyses to lower the false discovery rate caused by stochasticity between samples.

Differences in protein-coding gene richness and Shannon diversity between the soil habitats were assessed with Welch's t-tests followed by Games-Howell post-hoc tests, after verifying that residuals were normally distributed but that variance of the response variable differed between the groups. Differences in functional structure between the soils were assessed by computing Bray-Curtis dissimilarity matrices based on read abundance of the protein-coding genes normalized to transcripts-per-million (TPM) (Abrams et al., 2019). Bray-Curtis dissimilarities between samples were visualized with principal coordinate analyses (PCoAs) (*vegan* R package; (Oksanen et al., 2019)). The statistical significance of observed differences was assessed with permutational analyses of variance (PERMANOVA, 10^5 permutations, Monte Carlo approximated *p* value) using PRIMER v7 (Clarke & Gorley, 2015). Multivariate homogeneity of group dispersions was checked prior to the PERMANOVAs, also with PRIMER v7, to ensure that detected significant differences were associated with the tested factors and not with differences in the within-group variabilities.

To evaluate the dissimilarities in metabolic capabilities between the four soil habitats, we identified the functional genes -annotated against EggNOG, MD5nr, CAZy and NCycDB databases- that were differentially abundant between the soils using pairwise DESeq2

analyses (Love et al., 2014). For all pairwise comparisons median-of-ratio normalization was applied to account for differences in sequencing depth among samples. *p* values were adjusted for multiple testing using the Benjamini–Hochberg method with a false discovery rate threshold of 5%.

2.4. Results

2.4.1. *Protein-coding genes diversity*

Whole-metagenome sequencing of the twelve soil metagenomes (N10, N160, S10, S160) generated an average of 40 to 45 million high-quality reads per soil (Table 1). Megahit assembly of reads into contigs produced a total of 6 627 330 contigs of 713 bp on average, ranging from 200 to 939 240 bp and with a N50 value of 761 bp. A total of 9 837 348 different protein-coding genes were predicted from the assembled contigs. Gene quantification of the contigs associated with the different soil habitats revealed that soil metagenomes contained in average 51–58% protein-coding sequences, except for the S160 soils, where values reached up to 77% (Table 1).

Soil metagenomes differed in their functional diversity and structure (Fig. 1, Fig. S2). Richness and Shannon's diversity of the predicted protein-coding genes were highest for the N160 soils and lowest for the S160 soils (Fig. 1). N160 (permafrost) soils significantly ($p < 0.05$; PERMANOVA) differed from the S160 soils (active layer) in their protein-coding gene structures (Fig. 1, Table S2). Interestingly, the N10 and N160 soils clustered closely together ($p > 0.05$), indicating an overall similar composition of protein-coding genes.

Table 1. Total number of sequences and percentage of protein-coding genes and contigs assigned to taxa for the soils of different origins. Mean ± SD (n=3).

	N10			N160			S10			S160		
Raw reads [10^6]	41	±	4	46	±	8	46	±	3	46	±	4
HQ reads [10^6]	39	±	3	45	±	8	45	±	3	45	±	3
Reads mapped to contigs [%]	54	±	7	58	±	1	54	±	7	80	±	2
Reads mapped to CDS genes[1] [%]	51	±	8	58	±	1	55	±	6	77	±	0
Taxonomically assigned contigs[2] [%]	99.6	±	0.1	99.3	±	0.3	99.8	±	0.2	99.7	±	0.1
Archaea [%]	0.6	±	0.4	0.3	±	0.1	0.4	±	0.1	0.8	±	0.2
Bacteria [%]	87.1	±	8.2	97.7	±	0.6	93.9	±	6.7	98.4	±	0.6
Eukarya [%]	11.9	±	8.6	1.3	±	0.4	5.4	±	6.6	0.5	±	0.6

[1]CDS genes: protein-coding genes, [2]From a total of 823 contigs > 1500 bp in which SSU regions > 300 bp were identified. N: north-facing, S: south-facing, 160: at a depth of 160 cm, 10: at a depth of 10 cm.

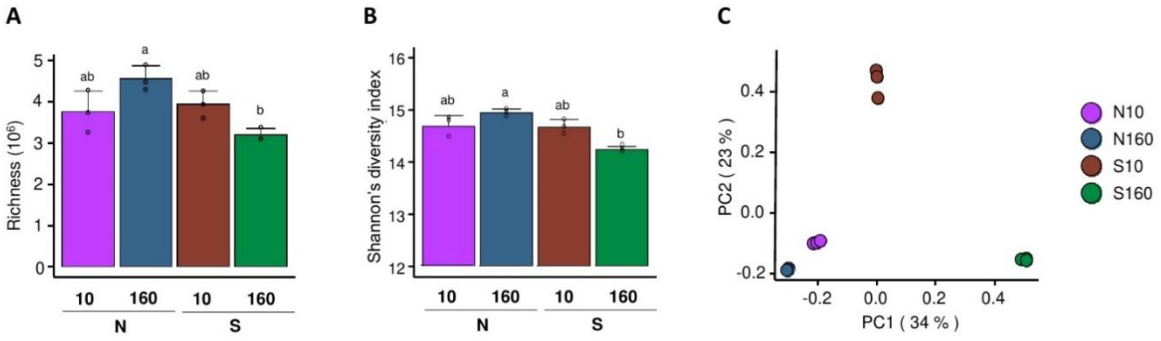

Figure 1. Functional diversity and structure of protein-coding genes for the different soil habitats. **A**. Number of different protein-coding genes (i.e. richness). **B**. Shannon's diversity index based on read abundance normalized to transcripts-per-million (TPM). Barplots depict the mean ± SD of the diversity values for the soil groups, whereas open dots represent the diversity values of the individual soils. C. Principal coordinate analyses (PCoAs) computed on Bray-Curtis dissimilarities based on TPM normalized abundances of the protein-coding genes. Only protein-coding genes for which the sum of the reads over all soil samples was ≥ 10 are included. N: north-facing, S: south-facing, 10: at a depth of 10 cm, 160: at a depth of 160 cm.

2.4.2. *Overall metabolic capabilities of the soil metagenomes*

DESeq2 analyses of protein-coding genes assigned to functions (i.e. functional genes) enabled to uncover differences in potential metabolic capabilities between the soil metagenomes. N160 (permafrost) metagenomes showed a higher diversity (richness and Shannon's diversity index, Table S3, Fig. S3) and a higher abundance of genes ($\log_2$ fold

change > 0) assigned to different COGs (EggNOG and MD5nr databases) than the N10 and the S160 metagenomes (Fig. 2A, Table S4). Differentially abundant COGs were distributed across all functional categories, suggesting that differences in potential metabolic capabilities between the soil habitats comprise a broad range of intracellular and extracellular processes (Fig. 2, Table S5). Permafrost metagenomes contained a higher proportion of: genes coding for cold-shock proteins and chaperones, involved in stress responses; restriction nucleases and CRISPRs proteins involved in cell defense; and antibiotics, flagellar proteins and ABC transporters related to competition (Fig. 2B, Table S5). Genes involved in chromatin remodeling and transcription regulation processes, including DNA repair, were also overrepresented in the permafrost soils (Fig. 2B), whereas only few sporulation genes were detected across all the soils (Table S5). Proteins involved in anaerobic and aerobic respiratory metabolism were also overrepresented in the permafrost metagenomes. These included transporters of metals and inorganic anions, N and S reductases, [NiFe]-hydrogenases, and catalases and oxidoreductases from the aerobic respiratory chain (Fig. 2B, Table S5).

Permafrost soils showed a higher abundance of genes involved in fermentative processes (e.g. those coding for phosphoketolase, and alcohol and L-lactate dehydrogenases) than the N10 soils and, to a lesser extent, the S160 soils (Fig. 2B, Table S5). Genes coding for key enzymes involved in anaerobic C fixation (pyruvate:ferredoxin oxidoreductase and citrate lyases) were also enriched in the permafrost metagenomes relative to those from the active layers.

Differences in COG diversity (Table S3, Fig. S3) and abundance were apparent between the N10 and S10 soils (Fig. 2, Tables S4 and S5). Overall, S10 soils exhibited a higher abundance of COGs involved in all analyzed cellular and extracellular processes than the north-facing soils. S10 vs. S160 comparisons also showed a higher abundance of COGs in the S10 soils (data not shown).

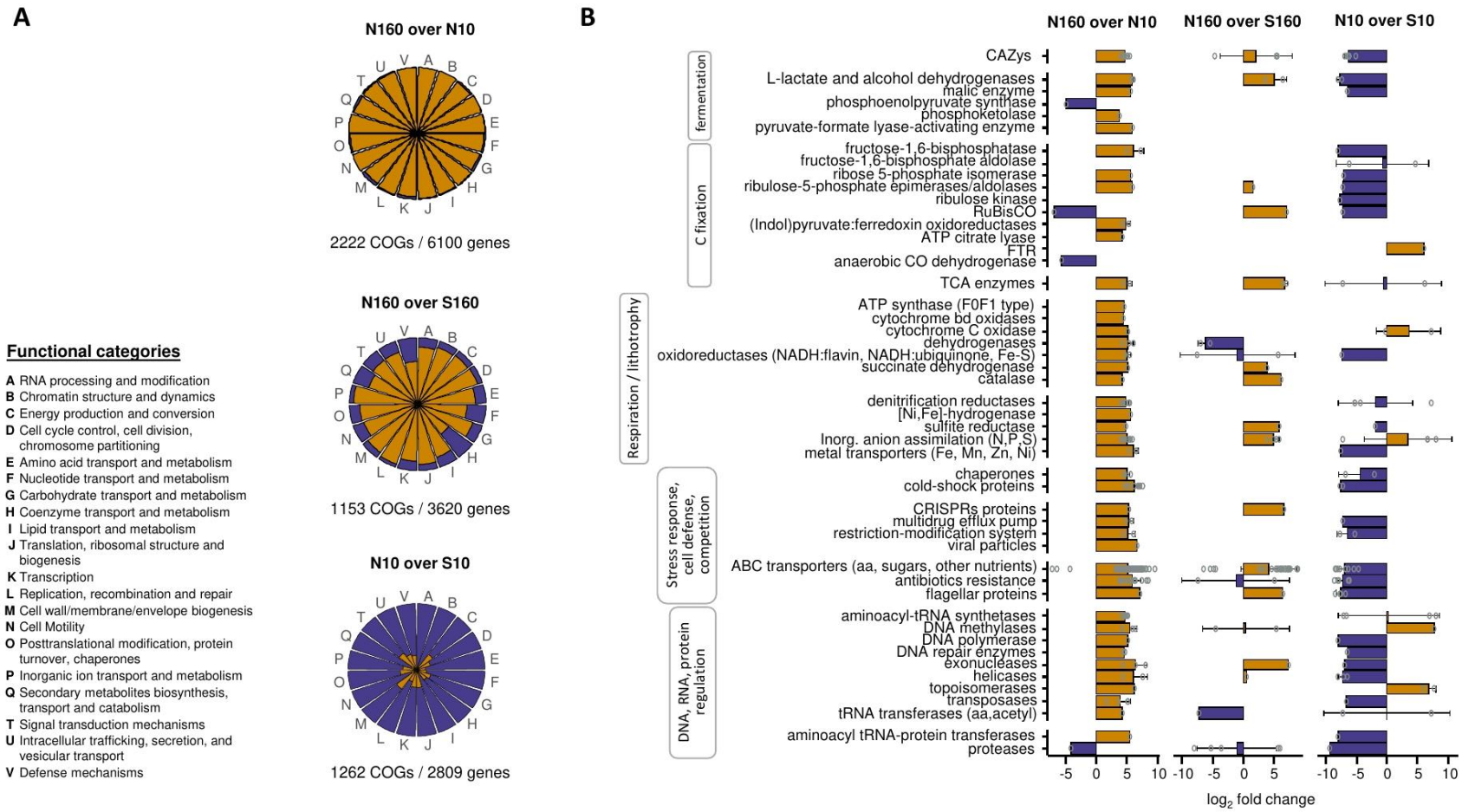

Figure 2. Overall functional differences between the different soil habitats. **A**. Relative abundance of overrepresented COGs (orange) and underrepresented COGs (violet) distributed across COG functional categories, for the comparisons between north-facing permafrost and active-layer soils (N160 over N10), between north-facing permafrost and south-facing active-layer soils at a depth of 160 cm (N160 over S160), and between north-facing and south-facing active-layer soils at a depth of 10 cm (N10 over S10). The log2 fold change (lfc) value "N160 over N10" is the log2 of (gene abundance of N160 / gene abundance of N10). The same stands for "N160 over S160" and "N10 over S10". For each pairwise comparison, highly differentially abundant genes ($p < 0.01$) among the 80% most abundant genes assigned to COGs were selected. The represented COGs are those in which all selected genes were overrepresented (lfc > 0) or underrepresented (lfc < 0). Values below the pie charts indicate the total number of different COGs and genes included in the representations. **B**. Log2 fold change in selected differentially abundant COGs assigned to proteins associated with C cycling and relevant metabolic and cellular processes for the compared soil habitats. COGs were assigned to proteins using the EggNOG database and annotations were curated with the non-redundant MD5nr database. Barplots depict the mean ± SD of the lfc values for the protein groups, whereas open dots represent the lfc values of the individual COG genes. A list of all selected genes with their relative abundance, their COG classification and the assigned functions is provided in Table S5. RuBisCO: Ribulose-1,5-bisphosphate carboxylase, FTR: formylmethanofuran:tetrahydromethanopterin formyltransferase.

2.4.3. *Carbohydrate-active enzymes genes*

The most abundant CAZy genes (CAZy database) across all MBP soils coded for glycosyl transferases, followed by glycoside hydrolases, carbohydrate-binding modules, carbohydrate esterases, auxiliary activity enzymes and polysaccharide lyases (Table S3). N160 soils had a higher diversity (Table S3, Fig. S4) and a higher abundance of genes coding for different CAZys (i.e. families and individual proteins) than the N10 and S160 soils (Fig. 3, Tables S4 and S6). Overrepresented CAZys in the permafrost soils included peroxidases (AA1 to AA10), pectate lyases (PL families), and cellulases (GH families), which are involved in the decomposition of complex plant components (i.e. lignocellulose and pectin) (Fig. 3, Table S6). Permafrost metagenomes were also enriched in CAZys involved in the use of labile substrates (i.e. starch) (Fig. 3). These included genes coding for pullulanases, α-amylases and α-glucosidases within the GH13 families (Fig. 3, Table S6). CAZys involved in chitin depolymerization (e.g. β-N-acetylhexosaminidases) were also overrepresented in the permafrost.

The diversity of CAZy genes was similar in the active layers from the north- and south-facing slopes (N10 over S10) (Table S3, Fig. S4). The S10 soils showed a higher abundance of CAZys involved in the depolymerization of hemicellulose (e.g. xylanases) and labile starch (e.g. α-glucosidases) than the N10 soils (Fig. 3, Table S6).

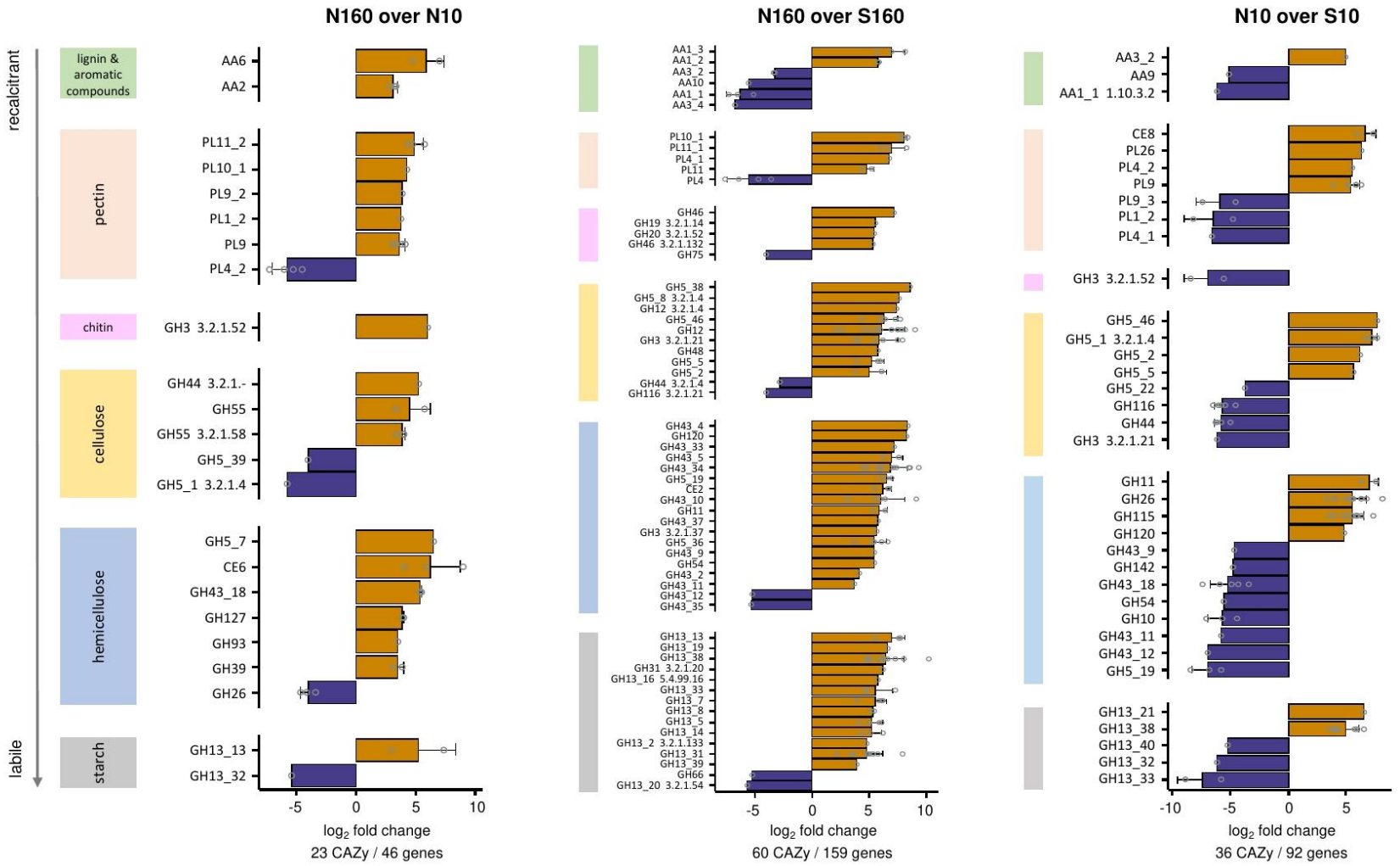

Figure 3. Differences in CAZy abundance between the different soil habitats. Pairwise comparisons were conducted between north-facing permafrost and active-layer soils (N160 over N10), between north-facing permafrost and south-facing active-layer soils at a depth of 160 cm (N160 over S160), and between north-facing and south-facing active-layer soils at a depth of 10 cm (N10 over S10). The $\log_2$ fold change (lfc) value "N160 over N10" is the $\log_2$ of (gene abundance of N160 / gene abundance of N10). The same stands for "N160 over S160" and "N10 over S10". For each pairwise comparison, differentially abundant genes ($p < 0.05$) that were among the 80% most abundant genes assigned to CAZys were selected. The represented CAZys are those in which all selected genes were overrepresented (lfc > 0) or underrepresented (lfc < 0). CAZy families and proteins were linked to specific substrates based on their decomposing activities. Only families associated with a unique decomposing activity or mostly with a specific decomposing activity (the same activity was described for at least 50% of all characterized enzymes in families with a total of ≤ 3 enzymes, http://www.cazy.org/ browser) are represented. CBM families are not shown. Barplots depict the mean ± SD of the lfc values for the CAZy families, whereas open dots represent the lfc values of the individual genes. Values below the bar graphs indicate the total number of CAZys and genes included in the representation. A list of all selected genes with their relative abundance, CAZy classification and associated enzymatic activity is provided in Table S6.

2.4.4. *N-cycling genes*

N160 soils exhibited a higher diversity (Table S3, Fig. S5) and a higher abundance of N-cycling families (NCycDB database) involved in denitrification, dissimilatory nitrogen reduction (DNR) (e.g. *nor*, *nir* and *nar* genes) and assimilatory nitrogen reduction (ANR) (e.g. *nas* genes) than the N10 and S160 soils (Fig. 4, Table S7). Conversely, nitrification genes (e.g. *amo*) were less abundant in the permafrost than in the other soils. Comparisons between topsoils (N10 over S10) revealed a higher abundance of N-cycling families involved in both nitrification and denitrification in the S10 soils, including genes for the anabolic and catabolic processing of organic N (i.e. *ure*, *nao* and *gdh*) (Fig. 4, Table S7).

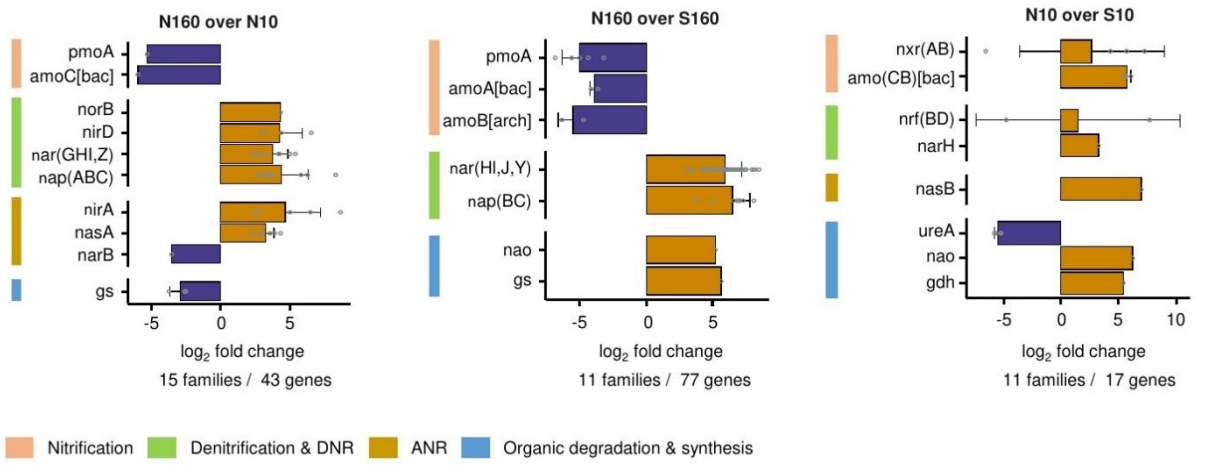

Figure 4. Differences in abundance of N-cycling families between the different soil habitats. Pairwise comparisons were conducted between north-facing permafrost and active-layer soils (N160 over N10), between north-facing permafrost and south-facing active-layer soils at a depth of 160 cm (N160 over S160), and between north-facing and south-facing active-layer soils at a depth of 10 cm (N10 over S10). The $\log_2$ fold change (lfc) value "N160 over N10" is the $\log_2$ of (gene abundance of N160 / gene abundance of N10). The same stands for "N160 over S160" and "N10 over S10". For each pairwise comparison, differentially abundant genes ($p < 0.05$) that were among the 80% most abundant genes assigned to N-cycling families were selected. The represented N-cycling families are those in which all selected genes were overrepresented (lfc > 0) or underrepresented (lfc < 0). Barplots depict the mean ± SD of the lfc values for the N-cycling families, whereas open dots represent the lfc values of the individual genes. Values below the bar graphs indicate the total number of N-cycling families and genes included in the representations. amo(ABC): ammonia monooxygenase, gdh: glutamate dehydrogenase, gs: glutamate synthase, nao: nitroalkane oxidase, nap(ABC): nitrate reductase, nar(GHIJYZ): nitrate reductase, nas(AB): assimilatory nitrate reductase, nir(AD): nitrite reductase, nrf(BD): nitrite reductase, nxr(AB): nitrate reductase, pmoA: particulate methane monooxygenase, ureA: urease. bac: Bacteria, arch: Archaea. A list of all selected genes with their relative abundance and their classification to N-cycling families and processes is provided in Table S7.

2.4.5. *Taxonomic analysis of the soil communities and functional assignment to taxa*

A total of 823 contigs, larger than 1 500 bp and with SSU rRNA (small subunit ribosomal ribonucleic acid) regions larger than 300 bp, were identified. Taxonomic annotation of these SSU rRNA harboring contigs revealed that the different soil habitats were dominated by Bacteria (Table 1). Archaea represented < 1% of the soil microbiota. Eukaryotic contigs were more abundant in the topsoils (S10 and N10), where abundances ranged from 5 to 12% of the total abundance of all contigs assigned to taxa (Table 1). Eukaryotes mostly consisted of fungi, but a large variety of sequences belonging to plants, protists and, to a lesser extent, invertebrates were also detected across the different soil habitats (Fig. S6).

The most abundant bacterial phyla were Proteobacteria, Chloroflexi, Acidobacteria, Actinobacteria, Verrucomicrobia, Gemmatimonadetes, Planctomycetes, Patescibacteria, Bacteroidetes and WPS-2 (i.e. Eremiobacterota), with abundances higher than 1% of the total abundance of all bacterial contigs (Table S8, Fig. S6). Contigs assigned to these phyla were found to contain CAZy genes coding for glycoside hydrolases (GHs) and carbohydrate-binding modules (CBMs), which govern the binding of the hydrolytic enzymes to their substrates (Fig. 5). Acidobacteria and WPS-2 contigs contained the highest proportion of CAZys. WPS-2 contigs also contained glutamine synthetase (GlnA) genes, involved in the metabolism of organic N (Fig. 5).

Binning of contigs produced 15 highly completed metagenome-assembled genomes (MAGs; > 90% completion, < 5% contamination). Most of these MAGs were phylogenetically classified to Acidobacteria and Proteobacteria (Table S9).

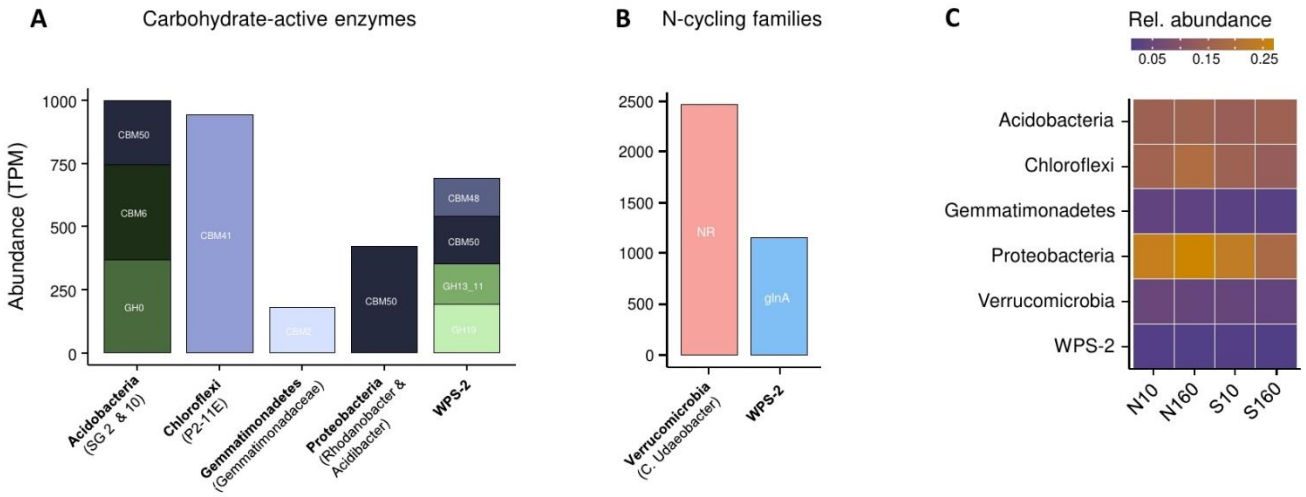

Figure 5. Bacterial phyla containing CAZys (**A**) and N-cycling families (**B**), and their abundances (**C**) across the different soil habitats. Contigs larger than 1500 bp were selected and bacterial taxa were identified by aligning 16S rRNA genomic regions (> 300 bp) against the SILVA database. Rel. abundance represents the mean proportion of the taxa in the different soil habitats relative to the total read depth of all bacterial contigs. TPM: transcripts-per-million. N: north-facing, S: south-facing, 160: at a depth of 160 cm, 10: at a depth of 10 cm.

2.5. Discussion

Functional profiling of permafrost microbial communities has largely focused on high-latitudinal soils, whereas the functional gene diversity of the oligotrophic, coarse-drained permafrost soils from mid-latitudinal alpine regions is poorly known. In this novel study, we applied shotgun DNA metagenomics to assess the metabolic potential of a temperate mountain permafrost microbiome from central Europe. Our study, conducted at the long-term permafrost monitoring site of Muot da Barba Peider (MBP) in the Swiss Alps, involved a functional gene comparison, not only between permafrost (160 cm depth) and the overlaying active layer (10 cm depth), but also between active-layer habitats with different expositions and therefore different mean annual temperatures. This latter comparison is not often possible in polar ecosystems.

In MBP, permafrost had the highest functional gene diversity among the soils considered, which corresponds to the high taxonomic diversity previously described at this site (Frey et al., 2016). In agreement with our first hypothesis, MBP permafrost (N160) showed a functional structure distinct from that of the south-facing active-layer soils collected from the same depth

(S160) and to a minor extent from the north-facing active layer (N10). Analysis of differentially abundant genes between the soil habitats revealed that, in line with our second hypothesis, permafrost was enriched in genes involved in stress responses, including cold-shock genes and chaperones, and those involved in cell defense, such as the antiviral CRISPRs proteins. Permafrost environments are dominated by the hostile-to-life conditions of constant freezing, desiccation and starvation (De Maayer et al., 2014). In line with findings from Arctic and Antarctic environments (Hultman et al., 2015; Koo et al., 2018; Tas et al., 2018; Zaikova et al., 2019), the higher potential of the MBP permafrost microorganisms to synthesize cold-shock proteins and chaperones could indicate their ability to survive prolonged freezing, as these proteins ensure the integrity of the cell components and the continuing functioning of the cells under environmental stress (Keto-Timonen et al., 2016).

In permafrost, microorganisms might thrive in small pockets of liquid water within the soil pores, which contain metabolic substrates (Coolen & Orsi, 2015; Jansson & Tas, 2014; Mackelprang et al., 2017; Tas et al., 2018). The cohabitation of the microbial cells in proximity would promote virulence (Coolen & Orsi, 2015), which, as underlined in previous permafrost investigations (Coolen & Orsi, 2015; De Maayer et al., 2014), could be related to the higher proportion of cell defense genes within the MBP permafrost. Microbial groups might compete to colonize the habitable liquid pockets in the permafrost and profit from the limited bioavailable C and nutrient resources (Mackelprang et al., 2017). As described for Arctic soils, enhanced microbial competition could be associated to the overrepresentation of antibiotic-related genes (e.g. β-lactamases) in MBP permafrost, as well as motility proteins and ABC transporters associated to the microbial search and uptake of simple C and nutrient sources from the surrounding environment (Bowman, 2017; Mackelprang et al., 2017).

Counterintuitively, relatively few sporulation genes were identified in the MBP soils. Instead, genes involved in chromatin remodeling, including DNA repair mechanisms, replication and biogenesis, characteristic of microorganisms in an active state (Ayala-del-Río et al., 2010; De

Maayer et al., 2014; Mykytczuk et al., 2013), were overrepresented in the permafrost. Similar observations have been reported in Arctic permafrost (Coolen & Orsi, 2015; Mackelprang et al., 2017; Xue et al., 2020), where bacterial growth at sub-zero temperatures has been demonstrated for isolated strains (Ayala-del-Río et al., 2010; Mykytczuk et al., 2013; Tuorto et al., 2014). As previously suggested (Burkert et al., 2019; Mackelprang et al., 2017; Xue et al., 2020), and despite the elevated energetic costs, permafrost microorganisms might retain activity because the risk of DNA degradation over time might select against spore formation as a long-term survival strategy (Burkert et al., 2019; Mackelprang et al., 2017; Xue et al., 2020). This is further supported by preliminary flow cytometry measurements in MBP soil samples, which indicate the existence of up to 40% living microbial cells in the permafrost (live-dead staining, unpublished data). This notwithstanding, the low abundance of sporulation genes in the MBP soils could be partly due to a limited recovery of DNA from spore-forming microorganisms during the DNA extractions. Spore lysis often require particularly strong mechanical (e.g. bead-beating at speeds > 4 m/s) and chemical treatments (Wunderlin et al., 2013) that were not included in our DNA extraction method.

The higher functional diversity observed in the MBP permafrost soils compared with the active-layer soils is surprising. Microbial communities in Arctic permafrost have been found to be highly diverse, both taxonomically (Hultman et al., 2015; Jansson & Tas, 2014; Mackelprang et al., 2016) and functionally (Ernakovich & Wallenstein, 2015; Hultman et al., 2015; Mackelprang et al., 2011; Morgalev et al., 2017; Tas et al., 2018; Woodcroft et al., 2018; Xue et al., 2020). However, taxonomic and functional diversity values reported from Arctic soils are often higher in the active layers than in the permafrost (Ernakovich & Wallenstein, 2015; Hultman et al., 2015; Morgalev et al., 2017; Mueller et al., 2018; Tas et al., 2018; Woodcroft et al., 2018), likely linked to the retention of fresher and more diverse organic substrates in shallow and aerated soil layers (Morgalev et al., 2017). The coarse-grained texture characteristic of alpine soils, such as the north-facing slopes of MPB, facilitates thermal conduction and the leaching of water and organic materials, as a result of enhanced

percolation (Chen et al., 2016; Gruber & Haeberli, 2007). The higher functional gene diversity in the MBP permafrost could be explained by the selective pressure imposed by freezing combined with the adaptation of the microorganisms inhabiting pockets of liquid water to different conditions of pH, redox and substrates (Tas et al., 2018; Xue et al., 2020). Alternatively, the higher diversity of genes detected in the permafrost might be attributed to the accumulation of genetic material over geological timescales, preserved by the sub-zero temperatures (Bellemain et al., 2013; Willerslev et al., 2004).

In support of our third hypothesis, permafrost samples contained a higher diversity of CAZy genes than the active layers, coding for multiple glycosyl hydrolases (GH), auxiliary enzymes and pectate lyases that together participate in the depolymerization of plant-derived recalcitrant (i.e. lignocellulosic and phenolic) compounds, labile polymers (i.e. starch) and microbial detritus (i.e. chitin). As in the Arctic, alpine permafrost microorganisms might preferentially utilize polymeric organic materials as primary sources of C, nutrients and energy (Mackelprang et al., 2017; Tveit et al., 2013; Woodcroft et al., 2018). Permafrost from Alaska (Leewis et al., 2020; Tas et al., 2018), Svalbard (Xue et al., 2020) and northern Sweden (Woodcroft et al., 2018) has been shown to be enriched in CAZy genes. Likewise, Biolog assays applied to Siberian soils (Ernakovich & Wallenstein, 2015; Morgalev et al., 2017) demonstrated the ability of the permafrost microorganisms to grow on complex biopolymers. In the mountain environments of the Tibetan Plateau, detailed characterization of the organic matter composition and microbial degradation patterns in permafrost and active layers revealed the existence of rich deposits of labile and recalcitrant C in the permafrost, both undergoing microbial degradation (Chen et al., 2016).

Interestingly, in MBP soils, CAZy genes coding for GH and carbohydrate-binding modules (CBM) were found to be associated with bacterial taxa, particularly Acidobacteria and WPS-2. This observation might suggest that these phyla are important contributors to C cycling in these soils (Woodcroft et al., 2018). Acidobacteria and WPS-2 are typically widespread in acidic soils,

including those from alpine, Arctic and Antarctic regions (Frey et al., 2016; Hu et al., 2015; Jansson & Tas, 2014; Lambrechts et al., 2019; Ward et al., 2019), and have been shown, in the multi-omic investigation of permafrost soils from Stordalen Mire (northern Sweden), to be dominant C degraders (Woodcroft et al., 2018). WPS-2 (i.e. *Candidatus* Eremiobacterota) (Ji et al., 2017) is an uncultured phylum, originally identified in Antarctic soil metagenomes (51). There are a few draft genomes available from this clade (Ji et al., 2017; Ward et al., 2019) where anoxygenic photosynthesis and chemosynthesis have been identified. Future analyses of the functional features of the highly completed MAGs recovered in the present study, which included numerous Acidobacteria, will facilitate insights into the ecological roles of alpine permafrost microorganisms and their metabolic interactions.

MBP permafrost also showed a higher abundance of fermentative and carbon-fixation genes than the active layers, indicating the potential use of simple sugars for carbon and energy gain, together with the use of carbon dioxide to support primary production. Furthermore, MBP permafrost was enriched in N-cycling genes involved in denitrification and anaerobic nitrate reduction, whereas genes involved in nitrification and organic N transformation were underrepresented in the permafrost compared with the active layers. GeoChip microarrays along altitudinal gradients (3200 to 3800 m a. s. l.) in the Tibetan plateau showed an increase in genes for carbon fixation and denitrification at a soil depth of 5 – 10 cm at higher altitudes, which was correlated with a decrease in organic C and N contents with increasing altitude (Guo et al., 2015; Yang et al., 2014). In Arctic permafrost, fermentative metabolism and denitrification (i.e. nitrate and nitrite reduction) have been observed often (Chauhan et al., 2014; Hultman et al., 2015; Mackelprang et al., 2016; Mueller et al., 2018; Woodcroft et al., 2018; Xue et al., 2020), although they have mostly been attributed to the anoxic niche conditions. Novel strains isolated from MBP have been reported to use a wide range of carbon sources and to assimilate nitrite and nitrate (Pontes et al., 2020). Further studies should include genome-guided insights into the *versatile metabolic* capabilities and process-based

measurements (e.g. respiration, N_2O) *in situ* or under controlled conditions to unveil the active members of the MBP permafrost microbiome.

Interestingly, the MBP permafrost showed a high proportion of genes involved on both aerobic and anaerobic respiratory metabolism (e.g. iron (III), sulfate reductases, and [NiFe]-hydrogenases). This could be linked to the well-drained coarse sediments that would enable aeration and thereby support the co-occurrence of aerobic and anaerobic microorganisms in the permafrost (Tas et al., 2018; Xue et al., 2020). The detection of [NiFe]-hydrogenases in the MBP permafrost is noteworthy. [NiFe]-hydrogenases are involved in the utilization of hydrogen for energy acquisition (Greening et al., 2016). Recent genomic studies indicate that hydrogen metabolism is widespread in prokaryotes (Greening et al., 2016), and might be predominant in oligotrophic Antarctic soils (Ji et al., 2017; Ortiz et al., 2020; Yang et al., 2019). The possibility that this energy-acquisition strategy is also prevalent in the temperate mountain permafrost microbiome is worthy of further investigation. Overall, more functional metagenomic studies in both Antarctic and alpine permafrost are needed, for comprehensive functional comparisons between the microbial communities of these desert soil ecosystems.

In agreement with our fourth hypothesis, the south-facing topsoils (S10) of MBP showed a higher functional gene diversity than the north-facing active layers (N10), including a greater variety of C metabolic pathways and genes involved in the processing of organic N. We also found a higher abundance of CAZy genes, potentially involved in the depolymerization of hemicellulose and starch, in the S10 soils. The S10 soils have higher annual mean soil temperature, moisture, and concentrations of C and N than the N10 soils, thereby representing a more favorable habitat for microbial life. The higher functional gene diversity of the MBP permafrost (N160) compared with the S160 soils might be linked to its particular habitat characteristics (i.e. frozen soils putatively seeded with liquid microniches of varying environmental conditions), and its high taxonomic diversity.

In the future, the environmental conditions of the north-facing soils may resemble the current conditions of south-facing soils to some extent, owing to the projected climate-change related temperature increases and denser vegetation cover (Hock et al., 2019; Steinbauer et al., 2018). Incubation of MBP permafrost (Adamczyk et al., 2021; Luláková et al., 2019) and permafrost-affected mineral soils (Adamczyk et al., 2020; Donhauser et al., 2020; Donhauser et al., 2021) at elevated temperatures indicate an increase in the abundance of metabolically versatile microbial taxa. These taxonomic changes could be coupled to the increase in microbial C decomposition and organic N cycling, as suggested in genomic surveys of Arctic soils undergoing warming (Coolen & Orsi, 2015; Feng et al., 2020; Johnston et al., 2019; Xue et al., 2016). Further research is needed to identify the active metabolisms of the MBP permafrost microbiota (e.g. through metatranscriptomics and metaproteomics) and its functional responses to warming.

2.6. Conclusions

Our study on the functional characteristics of the MBP metagenomes underline the remarkably high functional gene diversity of the temperate mountain permafrost microbiome, including a broad range of C- and N-cycling genes, and multiple survival and energetic metabolisms. Our findings indicate that permafrost in European alpine regions might be important genetic reservoirs, not only for the study of poorly characterized microbial metabolisms (e.g. H_2 metabolism) but also for proteins of pharmaceutical interest (e.g. antibiotics and CRISPRs); hence, our results underscore the need to extend investigations to other temperate mountain permafrost soils. Our findings represent a baseline for future investigations comparing the functional profiles of permafrost microbial communities at different latitudes, which in turn will widen our understanding of the global permafrost microbiome.

2.7. Data availability

Raw sequences of the 12 soil metagenomes analysed in the study are available in the NCBI Sequence Read Archive under the accession number PRJNA647119. The R scripts used for the statistical analyses are available in https://github.com/carlaperezmon/PerezMon_et_al_2020.

2.8. Author contributions

BF conceived the study and collected the samples. CP-M performed laboratory assays. CP-M and WQ analyzed the data. CP-M wrote the manuscript with the assistance of BF. All authors edited the manuscript and approved the final draft.

2.9. Funding information

This work was funded by the Swiss National Science Foundation (SNSF) under grant number IZLSZ2_170941.

2.10. Acknowledgements

We thank M. Phillips for access to the MBP long-term monitoring permafrost site, B. Stierli for field and laboratory assistance, and R. Köchli and the WSL Central Laboratory for completing soil analyses. We also thank M. Dawes for her valuable contribution to the editing of this article. We acknowledge the contribution of scientists at the Génome Québec Innovation Centre in Montreal, Canada, for performing the shotgun DNA sequencing.

2.11. Conflict of interest statement

The authors declare that there are no conflicts of interest.

2.12. Supplementary materials

2.12.1. *Supplementary figures*

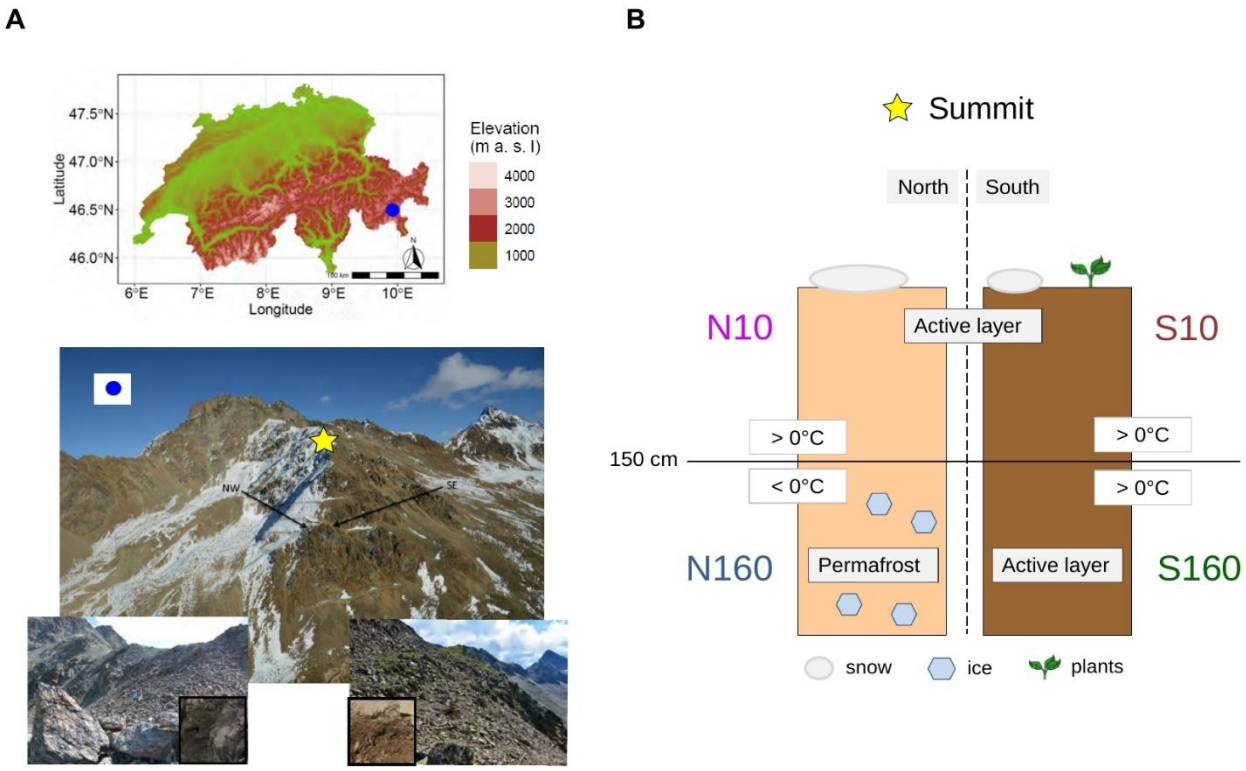

Figure S1. Geographic location of Muot da Barba Peider with an aerial view of the summit (**A**), and schematic representation of the soil sample collection (**B**). The blue fill dot represents the MBP mountain. The aerial photography of MBP was provided by Dr. Marcia Phillips. Pictures overlapping the aerial photography of MBP show the north-facing and south-facing sampling locations at the summit, accompanied with a close visualization of the topsoils. The solid line in (B) represents the permafrost table at a depth of 150 cm b.g.s. N: north-facing, S: south-facing, 10: at a depth of 10 cm, 160: at a depth of 160 cm.

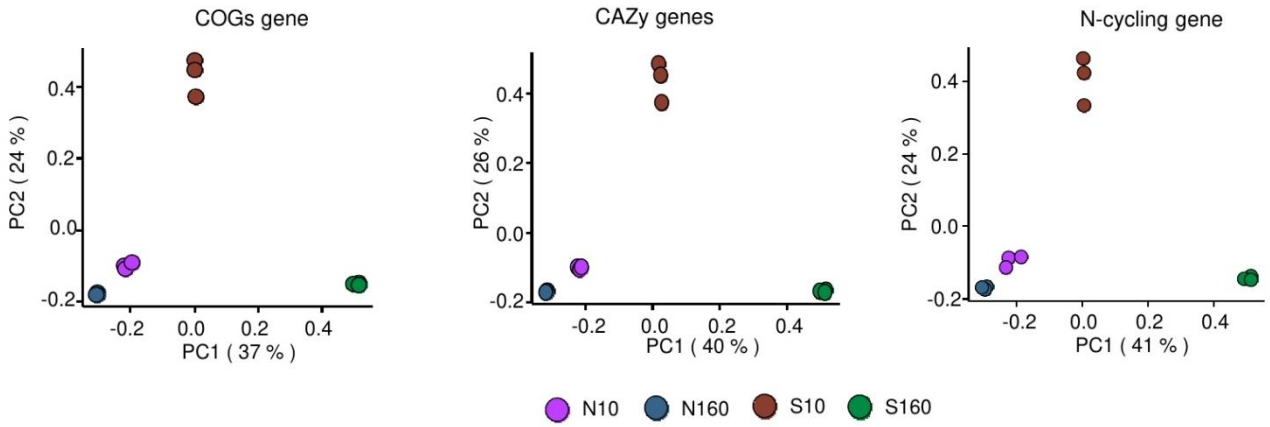

Figure S2. Functional structure of the different soil habitats for the genes assigned to functions. PCoAs computed on Bray-Curtis dissimilarities based on the abundance of selected genes for which the sum of the reads over all soil samples was ≥ 10. N: north-facing, S: south-facing, 10: at a depth of 10 cm, 160: at a depth of 160 cm.

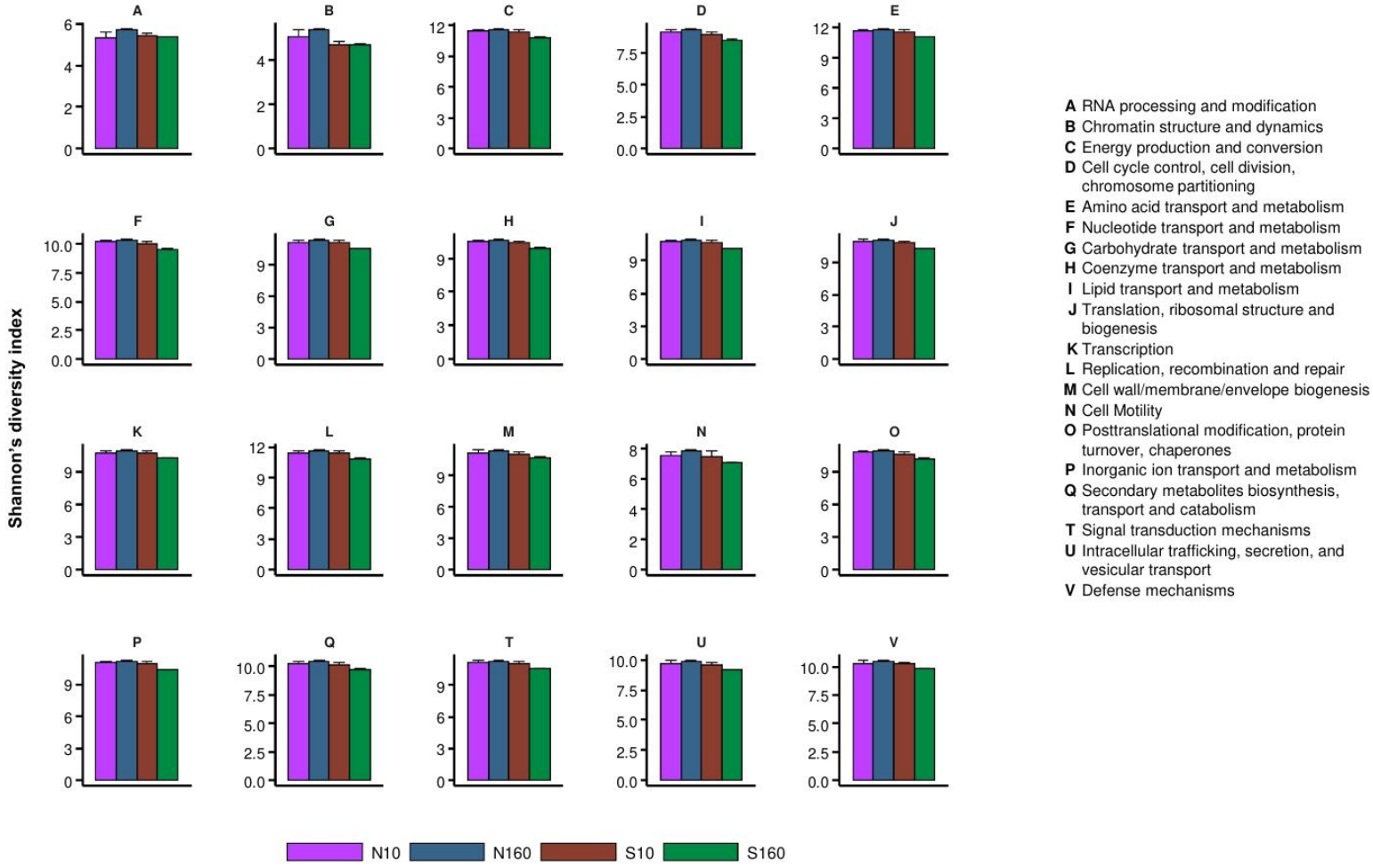

Figure S3. Shannon's diversity of COGs grouped into functional categories for the different soil habitats. Shannon's diversity indexes were calculated on read abundances normalized to transcripts-per-million (TPM). The represented genes are those for which the sum of the reads over all soil samples was ≥ 10. Mean ± SD (n=3). N: north-facing, S: south-facing, 160: at a depth of 160 cm, 10: at a depth of 10 cm.

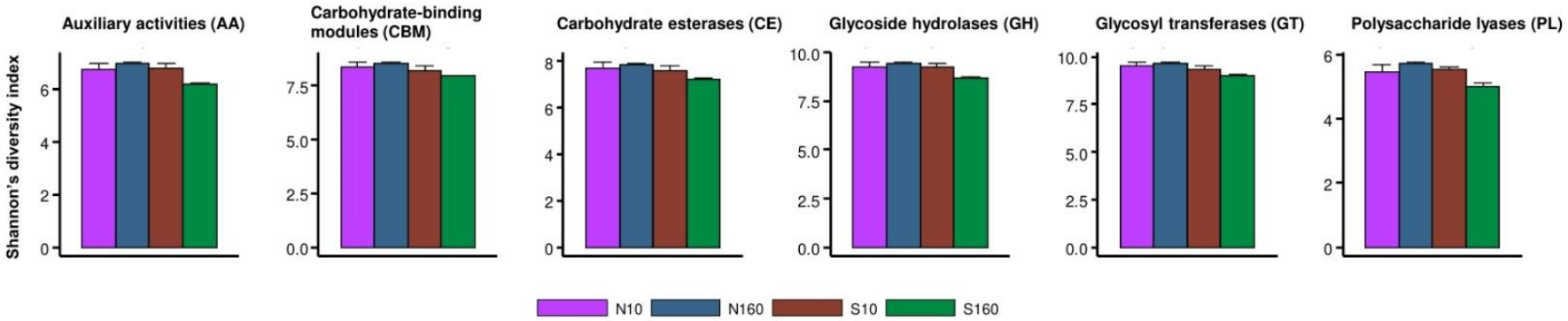

Figure S4. Shannon's diversity of CAZys classes for the different soil habitats. Shannon's diversity indexes were calculated on read abundances normalized to transcripts-per-million (TPM). The represented genes are those for which the sum of the reads over all soil samples was ≥ 10. Mean ± SD (n=3). N: north-facing, S: south-facing, 160: at a depth of 160 cm, 10: at a depth of 10 cm.

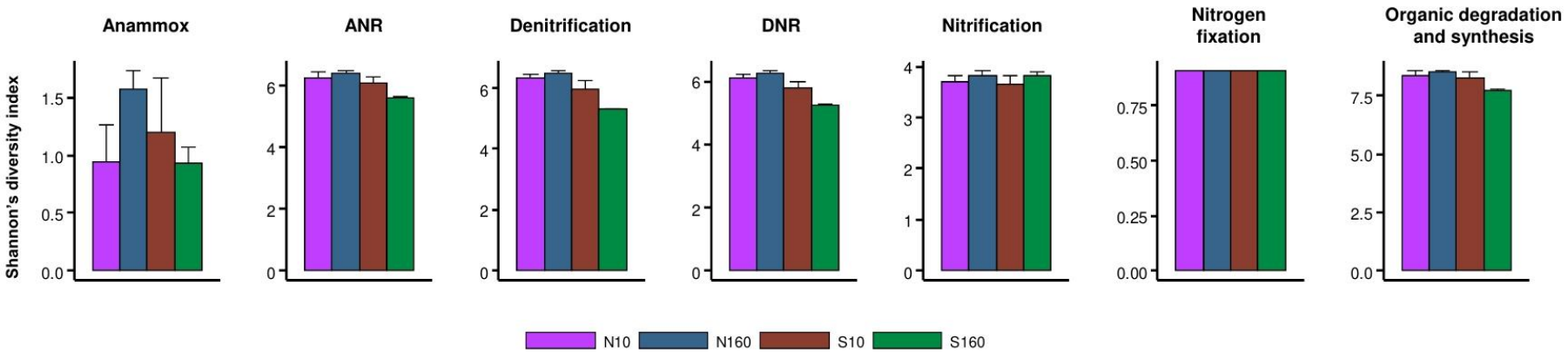

Figure S5. Shannon's diversity of N-cycling processes for the different soil habitats. Shannon's diversity indexes were calculated on read abundances normalized to transcripts-per-million (TPM). The represented genes are those for which the sum of the reads over all soil samples was ≥ 10. ANR: assimilatory nitrogen reduction, DNR: dissimilatory nitrogen reduction. Mean ± SD (n=3). N: north-facing, S: south-facing, 160: at a depth of 160 cm, 10: at a depth of 10 cm.

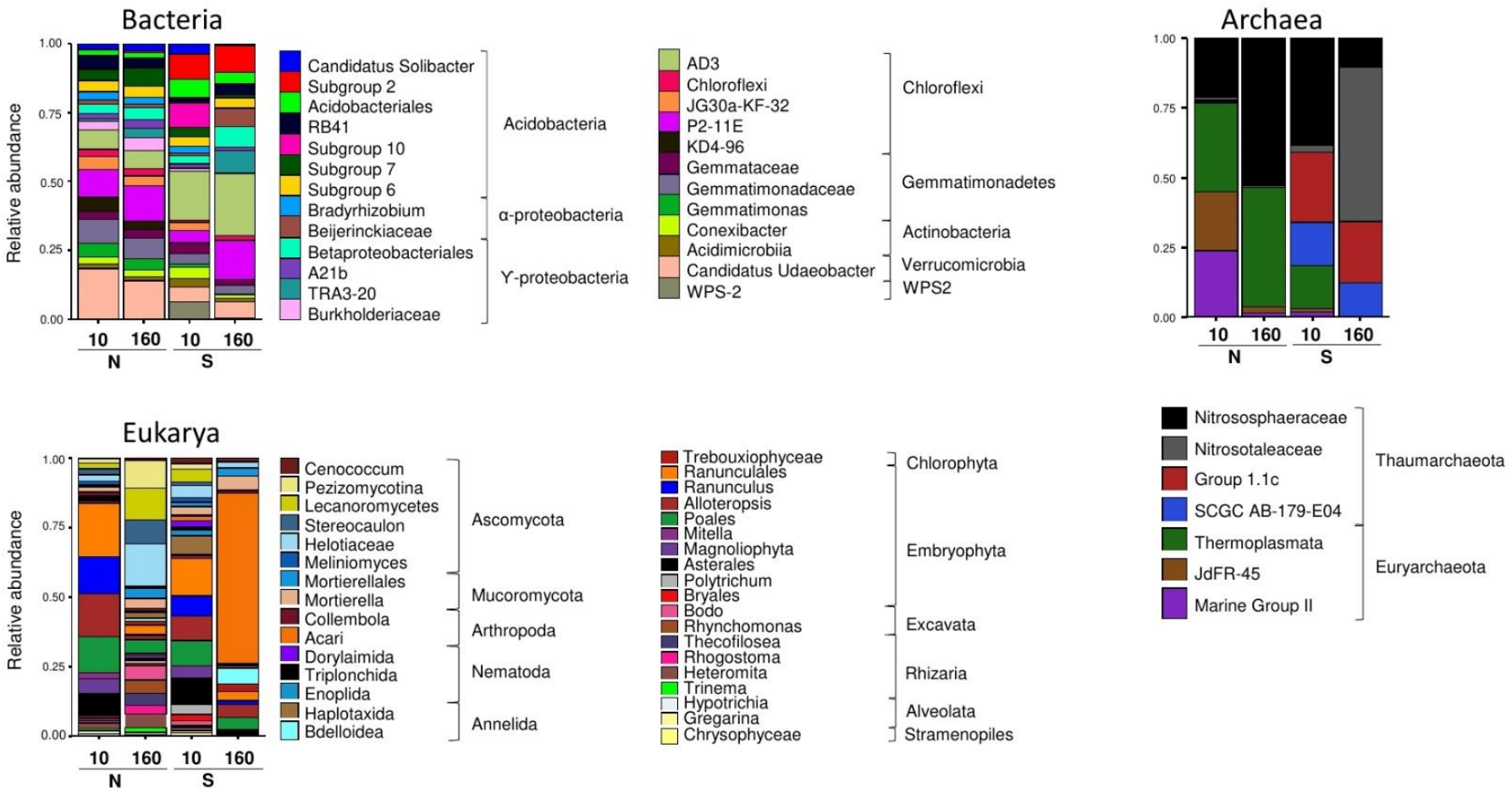

Figure S6. Prokaryotic and eukaryotic composition of the different soil habitats. Taxonomic classification was performed on the contigs larger than 1500 bps, in which SSU regions (> 300 bp) could be identified. Contigs were annotated against the SILVA database. The represented bacterial taxa are those for which the depth of coverage was ≥ 2% of the total depth of coverage over all bacterial contigs assigned to taxa beyond the kingdom level. Taxa were classified to the deepest taxonomic level possible. N: north-facing, S: south-facing, 160: at a depth of 160 cm, 10: at a depth of 10 cm.

2.12.2. *Supplementary tables*

Because of their large extension **tables S3**, **S5** and **S6** are provided electronically within an **excel file**, in the published version of this Chapter: https://www.microbiologyresearch.org/content/journal/mgen/10.1099/mgen.0.000558#supplementary_data

Table S1. Physico-chemical properties of the studied soils. Mean ± SD (n=3).

Properties	N10	N160	S10	S160
C (%)	0.1 ± 0	0.1 ± 0	0.9 ± 0	0.1 ± 0
N (%)	b.d.l.[2]	b.d.l.	0.1 ± 0	b.d.l.
OM[1] (%)	1.3 ± 0.1	1.1 ± 0.1	3.2 ± 0	1.1 ± 0
Al (mg kg^{-1} soil)	b.d.l.	b.d.l.	108 ± 2.3	59.2 ± 0.6
Ca (mg kg^{-1} soil)	675.8 ± 8.5	869.4 ± 57.7	5.6 ± 0.2	8.7 ± 0.1
Fe (mg kg^{-1} soil)	b.d.l.	b.d.l.	1.8 ± 0.3	b.d.l.
K (mg kg^{-1} soil)	44.3 ± 1.8	34.2 ± 4	b.d.l.	b.d.l.
Mg (mg kg^{-1} soil)	21.3 ± 0.5	44.2 ± 2.5	b.d.l.	b.d.l.
WHC (g H_2O g^{-1})[1]	0.2 ± 0	0.2 ± 0	0.3 ± 0	0.2 ± 0
pH [$CaCl_2$][1]	4.6 ± 0.1	5.8 ± 0	4.6 ± 0	4.8 ± 0
Sand (%)	80.5 ± 0.1	85.2 ± 0.2	83.8 ± 0.2	85.2 ± 0.1
Silt (%)	15.9 ± 0.2	11.2 ± 0.4	14 ± 0.3	13 ± 0.3
Clay (%)	3.6 ± 0.2	3.5 ± 0.2	2.2 ± 0.2	1.8 ± 0.2
Age [^{14}C dating](years)	12923 ± 149	12403 ± 69	4889 ± 76	12854 ± 79

[1]Measured in the present study. The rest of the data was reported in Frey et al. 2016. Measurements were normalized by dry weigth of soil. [2]b.d.l below detection limit (i.e. N < 0.015, Al < 0.1, Fe < 0.08, K < 1.6 and, Mg < 0.2). C: Total carbon, N: Total nitrogen, OM: organic matter, WHC: water holding capacity. N: north-facing, S: south-facing, 160: at a depth of 160 cm, 10: at a depth of 10 cm

Table S2. Differences in functional gene structure between the soil habitats.

	protein-coding genes		
Main test[1]	**F**	**P**	**ECV (%)**
	5.16	0	44.94
Pairwise tests	**t**	**P(MC)**	**BC (%)**
N10 vs N160	1.45	0.13	32.19
N10 vs S10	1.69	0.06	16.27
N160 vs S160	3.69	0	11.45
N10 vs N10			30.37
N160 vs N160			56.29
S10 vs S10			38.44
S160 vs S160			67.09

[1]Effects of soil origin as assessed by multivariate permutational ANOVA (PERMANOVA). F: pseudo-F ratio, t: univariate t-statistic, P(MC): Monte Carlo approximated level of significance, ECV: estimated components of variance for the main factor, BC: average similarity between groups. P-values from pairwise tests were adjusted for multiple comparisons with the Benjamini-Hochberg method. Tests were performed on Bray-Curtis dissimilarities matrices based on abundance of genes for which the sum of the reads over all soil samples was ≥ 10. N: north-facing, S: south-facing, 160: at a depth of 160 cm, 10: at a depth of 10 cm

Table S4. Differentially abundant genes assigned to functions obtained from the DESEq pairwise comparisons between soils of different origin.

	Total assigned genes[1]		N160 over N10		N160 over S160		N10 over S10	
Eggnog	4706835	incorporated[2]	3738153	79.4%[3]	3823476	81.20%	3949602	83.90%
		overrepresented[4]	93147	2.50%	1194040	31.00%	173071	4.40%
		underrepresented	39571	1.10%	571226	15.00%	292371	7.40%
CAZy	98331	incorporated	90586	92.10%	91110	92.70%	93932	95.50%
		overrepresented	3337	3.70%	36372	40.00%	8443	9.00%
		underrepresented	2102	2.30%	17142	19.00%	11555	12.00%
NCyc	14849	incorporated	14230	96%	14276	96%	14574	98%
		overrepresented	452	3%	5590	39%	1004	7%
		underrepresented	260	2%	2427	17%	1392	10%

[1]Total number of genes assigned to functions using the Eggnog, CAZy and NCyc dabatases. [2]Total number of genes incorporated in the DESEq pairwise comparisons. [3]Percentage of assigned genes incorporated in the DESEq pairwise comparisons. [4]Number and percentage of assigned genes incorporated in the DESEq pairwise comparisons with Log2 fold change > 0 (overrepresented) or Log2 fold change < 0 (underrepresented). Pairwise comparisons were conducted between permafrost and active layer (N160 over N10), permafrost and south-facing soils at a depth of 160 cm (N160 over S160) and between north-facing and south-facing soils at a depth of 10 cm (N10 over S10). The Log2 fold change value “N160 over N10” is the Log2 of (gene abundance of N160 / gene abundance of N10). The same stands for N160 over S160 and N10 over S10.

Table S7. Functional annotation, log2 fold change values and relative abundance of differentially abundant N-cycling families selected in the study.

Soils compared	Process	Family	n	Mean log2 fold change	SD	Rel. abundance[1]
N160 over N10	Nitrification	pmoA	1	-5.22	0.00	5.51E-05
N160 over N10	Nitrification	amoC_B	1	-5.94	0.00	1.10E-04
N160 over N10	Denitrification	norB	1	4.34	0.00	4.11E-04
N160 over N10	Dissimilatory nitrate reduction	nirD	4	4.26	1.61	4.48E-04
N160 over N10	Denitrification, Dissimilatory nitrate reduction	napB	1	5.78	0.00	6.08E-05
N160 over N10	Denitrification, Dissimilatory nitrate reduction	napA	6	4.50	2.24	5.82E-04
N160 over N10	Denitrification, Dissimilatory nitrate reduction	narG	4	4.27	1.29	3.63E-04
N160 over N10	Denitrification, Dissimilatory nitrate reduction	narH	3	3.58	1.04	3.15E-04
N160 over N10	Denitrification, Dissimilatory nitrate reduction	napC	2	3.42	0.62	1.90E-04
N160 over N10	Denitrification, Dissimilatory nitrate reduction	narI	1	3.17	0.00	1.68E-04
N160 over N10	Denitrification, Dissimilatory nitrate reduction	narZ	1	2.89	0.00	9.09E-05
N160 over N10	Assimilatory nitrate reduction	nirA	6	4.66	2.53	5.76E-04
N160 over N10	Assimilatory nitrate reduction	nasA	8	3.20	0.67	8.78E-04
N160 over N10	Assimilatory nitrate reduction	narB	1	-3.51	0.00	3.32E-04
N160 over N10	Organic degradation and synthesis	gs_K00284	3	-2.91	0.69	4.85E-04
N160 over S160	Nitrification	amoA_B	2	-3.87	0.34	1.46E-04
N160 over S160	Nitrification	pmoA	5	-4.96	1.34	1.00E-03
N160 over S160	Nitrification	amoB_A	2	-5.47	1.10	1.26E-04
N160 over S160	Denitrification, Dissimilatory nitrate reduction	napB	1	6.84	0.00	6.08E-05
N160 over S160	Denitrification, Dissimilatory nitrate reduction	napC	8	6.45	1.41	5.42E-04
N160 over S160	Denitrification, Dissimilatory nitrate reduction	narH	19	6.23	1.41	1.55E-03
N160 over S160	Denitrification, Dissimilatory nitrate reduction	narI	17	6.06	1.29	1.45E-03
N160 over S160	Denitrification, Dissimilatory nitrate reduction	narJ	6	5.64	0.76	4.60E-04
N160 over S160	Denitrification, Dissimilatory nitrate reduction	narY	15	5.45	0.94	1.20E-03
N160 over S160	Organic degradation and synthesis	gs_K00264	1	5.63	0.00	7.44E-05
N160 over S160	Organic degradation and synthesis	nao	1	5.19	0.00	1.42E-04
N10 over S10	Nitrification	amoC_B	2	5.78	0.46	2.09E-04
N10 over S10	Nitrification	nxrB	3	5.78	1.50	4.47E-04
N10 over S10	Nitrification	amoB_B	1	5.62	0.00	1.15E-04
N10 over S10	Nitrification	nxrA	1	-6.53	0.00	7.11E-05
N10 over S10	Dissimilatory nitrate reduction	nrfD	1	7.76	0.00	1.92E-04
N10 over S10	Dissimilatory nitrate reduction	nrfB	1	-4.78	0.00	1.25E-04
N10 over S10	Denitrification, Dissimilatory nitrate reduction	narH	1	3.28	0.00	1.28E-04
N10 over S10	Assimilatory nitrate reduction	nasB	1	7.02	0.00	1.42E-04

N10 over S10	Organic synthesis	degradation	and	nao	1	6.27	0.00	1.42E-04
N10 over S10	Organic synthesis	degradation	and	gdh_K00260	1	5.44	0.00	9.47E-05
N10 over S10	Organic synthesis	degradation	and	ureA	4	-5.48	0.31	4.12E-04

[1]Rel. abundance: sum of the abundance of the genes belonging to same N-cycling family relative to the total number of sequences in the pair of soils compared

Table S8. Relative abundance of identified bacterial phyla.

Phylum	Abundance (%)[1]	Richness
Proteobacteria	26	1627
Chloroflexi	22.4	1102
Acidobacteria	16.9	1029
Actinobacteria	9.5	800
Verrucomicrobia	6.3	287
Gemmatimonadetes	4.3	178
Planctomycetes	3.7	563
Patescibacteria	2.6	628
Bacteroidetes	2	238
WPS-2	1.1	84
Rokubacteria	0.7	24
Armatimonadetes	0.7	115
Nitrospirae	0.5	44
Elusimicrobia	0.4	84
Cyanobacteria	0.2	39
Chlamydiae	0.1	30
Dependentiae	0.1	34
FBP	0.1	13
Fibrobacteres	0	6
Latescibacteria	0	6
FCPU426	0	11
Omnitrophicaeota	0	5
Unclassified	2.2	193

[1]percentage of the total read depth of all bacterial contigs

Table S9. Metagenome-Assembled Genomes.

Genome Size (bp)	GC (%)	Coverage	unique markers (out of 43)	multi copy	Taxonomy (phylogenetic annotation)[1]
2824983	65	50	42	1	g__Novosphingobium
2770032	56	35	25	18	f__Verrucomicrobiaceae
4667137	60	28	41	2	p__Acidobacteria
3083626	68	19	42	1	p__Acidobacteria
4337313	69	29	42	1	k__Bacteria
2163302	58	136	43	0	c__Betaproteobacteria
3263296	66	106	42	0	k__Bacteria
3288972	65	27	22	0	k__Bacteria
4743197	66	10	23	1	f__Comamonadaceae
4066794	63	21	29	0	p__Acidobacteria
4306665	56	33	38	3	p__Acidobacteria
4155253	58	58	24	0	p__Acidobacteria
3380873	70	9	39	1	o__Actinomycetales
7122400	67	7	33	0	g__Burkholderia
6453707	64	7	40	2	g__Planctomyces

[1]The deepest taxonomic level assign is shown; k: kingdom, p: phylum, c: class, o: order, f: family, g: genus

3. CHAPTER 3. Functional and structural responses of arctic and alpine soil prokaryotic and fungal communities under freeze-thaw cycles of different frequencies

Authors: Carla Perez-Mon, Beat Frey and Aline Frossard*

Forest Soils and Biogeochemistry, Swiss Federal Institute for Forest, Snow and Landscape Research WSL, Birmensdorf, Switzerland

∗**Correspondence to:** Aline Frossard, Swiss Federal Research Institute WSL, Zürcherstrasse 111, CH-8903 Birmensdorf, Switzerland. Tel: +41-44-739-2807; E-mail: aline.frossard@wsl.ch

Keywords: alpine, arctic, freeze-thaw cycles, bacteria, fungi, climate change, global warming, snow scarcity

3.1. Abstract

Ongoing climate change involves increasing snow scarcity, which results in more frequent freeze-thaw cycles (FTCs) in polar and alpine soils. Although repeated FTCs have been shown to alter the structure and functions of soil microbial communities, a thorough understanding on the influence of FTCs frequency on polar and especially alpine soil microbiomes is still elusive. Here, we investigated the impact of repeated weekly vs. daily FTC frequencies on the structure and functions of prokaryotic and fungal communities from north- and south-facing soils from two mountain ridges, one in the Arctic and one in the High-Alps. FTCs affected prokaryotic communities more strongly than fungal communities, where mainly cold-tolerant and opportunistic fungi (e.g. *Mrakia*, *Mortierella*) were responsive. Prokaryotic communities were more affected by weekly FTCs than by daily FTCs. Daily FTCs favored fast-growing bacteria (e.g. *Arthrobacter*), while oligotrophic and largely uncultured taxa (e.g. Verrucomicrobia) benefited from weekly FTCs. FTCs negatively affected microbial respiration but had minor impacts on C-, N- and P-acquiring enzymatic activities. Plausible pre-adaptation of the microbial communities to naturally occurring frequent FTCs at their site of origin did not show a clear influence on the microbial responses to the tested FTCs. Altogether, our study provides an integrative overview on potential structural and functional changes of soil microbial

communities in polar and alpine regions in response to the projected increase in FTCs; therefore advancing our understanding on the impact of climate change in these rapidly changing ecosystems.

3.2. Introduction

Climate change scenarios predict an increase in air temperatures worldwide of up to 3.7°C by 2100, along with greater variation in air temperature and precipitation (IPCC, 2014). These climatological changes might have important consequences on soil ecosystems, where fluctuations in soil temperatures and moisture might alter microbial diversity (Balser et al., 2010), microbially-mediated ecological functions (Karhu et al., 2014; Steinweg et al., 2013) and, consequently, the above-ground growth of vegetation (Classen et al., 2015; Henry, 2013). Soil temperature oscillations around 0°C cause freeze-thaw cycles (FTCs), which are common in polar and alpine regions, especially during late fall and early spring when the absence of snow means a closer coupling between air and soil temperatures (Henry, 2013). As winters are becoming warmer and temperature oscillations and precipitation are becoming more erratic, the frequency of FTCs is predicted to increase, especially in polar and alpine regions, where the snow is being extensively replaced by rain (Henry, 2013; IPCC, 2014). Snow-covered soils remain at subzero temperatures for long periods, and they thaw gradually as air temperatures increase and snow melts (Freppaz et al., 2007). Snow-free soils, on the contrary, respond to hourly air temperature variations and undergo daily FTCs when night temperatures fall below 0°C (Freppaz et al., 2007).

Polar and alpine regions are both dominated by subzero temperatures, and they have landscape features in common, such as snow, permafrost and glaciers (Donhauser & Frey, 2018; Margesin, 2009). However, alpine regions have more precipitation and UV radiation, as well as larger seasonal and diurnal fluctuations in incoming solar radiation and temperature, than polar regions (Donhauser & Frey, 2018; Margesin, 2009). In addition, alpine regions exhibit strong altitudinal gradients, resulting in marked climatological heterogeneity at the local scale (Donhauser & Frey, 2018; Margesin, 2009). Soils from the south-facing slopes of mountains are warmer and experience more temperature variations and FTCs than soils from the north-facing slopes, where snow is present for longer periods (Donhauser & Frey, 2018).

In polar and alpine soils, FTCs have been shown to alter the structure of microbial communities (Eriksson et al., 2001; Han et al., 2018; Larsen et al., 2002; Mannisto et al., 2009; Ren et al., 2018; Yergeau & Kowalchuk, 2008), the patterns of microbial substrate utilization (Han et al., 2018; Schimel & Mikan, 2005), and soil ecosystem processes such as C and N mineralization (Han et al., 2018; Larsen et al., 2002; Schimel & Mikan, 2005; Stres et al., 2010). Freezing decreases soil water availability, increases osmotic pressure and causes severe physical damages to the microbial cells (Mazur, 1984; Panoff et al., 1998). This leads to the death of vulnerable microorganisms and, thereupon, to changes in the abundance and composition of the microbial communities (Eriksson et al., 2001; Han et al., 2018; Mannisto et al., 2009; Ren et al., 2018; Yergeau & Kowalchuk, 2008). Furthermore, the alternation between freezing and thawing causes the breaking of soil aggregates (Feng et al., 2007; Wang et al., 2012), which results in the release of labile carbon and nutrient sources in the soil (Feng et al., 2007). The preferential consumption of these newly available carbon and nutrients by survivor microorganisms to FTCs often translates to metabolic shifts at the community level, from the degradation of complex organic matter to the utilization of simpler carbon sources (Han et al., 2018; Schimel & Mikan, 2005; Stres et al., 2010). Likewise, FTCs might lead to decreases in the rates of soil respiration and N mineralization, likely because of the decrease in microbial abundance (Larsen et al., 2002; Stres et al., 2010) or alterations in microbial activities (Han et al., 2018; Schimel & Mikan, 2005).

Studies in polar regions and the Himalayas suggest that soil-related factors influence the resistance and resilience (tolerance) of microbial communities to FTCs (Bolter et al., 2005; Schimel & Mikan, 2005; Stres et al., 2010). A main influencing factor could be the FTC legacy of the soil (Stres et al., 2010; Yergeau & Kowalchuk, 2008). Soils subjected to frequent FTCs might harbor microbial communities better adapted to these variations in temperature and therefore more tolerant to FTCs (Stres et al., 2010; Yergeau & Kowalchuk, 2008). As alpine soils undergo greater temperature variation than polar soils, distinct responses of microbial communities to an increase in FTC frequency can be expected between alpine and polar soils. Moreover, differences might already be detectable at the local scale, between north- and south-facing soils, in alpine areas.

An increase in FTC frequency, such as more daily FTCs, could mean more frequent alterations in the polar and alpine soil ecosystems, resulting in considerable changes in soil microbial community structures and functions. The magnitude of the impact of this increase in FTC frequency could vary between the different microbial taxa. For instance, fungal communities have been found to be more tolerant to repeated FTCs than prokaryotes (Bacteria and Archaea) (Han et al., 2018; Schostag et al., 2019; Sharma et al., 2006). Further, the genomic study of Schostag et al. (2019) suggests that the ability of specific bacterial taxa to adjust to FTC temperature variations and associated changes in the soil environment might depend on their physiological traits (e.g. growth rate and metabolic versatility). However, detailed knowledge about the influence of repeated FTCs on polar and especially alpine soil microbiomes is still scarce. Moreover, fungal communities are often overlooked in FTC studies and we are not aware of interregional investigations that evaluate the effect of increasing FTC frequency on both polar and alpine soils. In the rapidly changing polar and alpine ecosystems, a comprehensive understanding on the changes in microbial composition in response to FTCs and their relation to potential alterations on soil microbially-mediated processes is much needed.

We conducted a microcosm experiment with north- (N) and south-facing (S) top soils from two mountain ridges, one in the Swedish Arctic and one in the High-Alps in Switzerland (soils of 4 different origin: Arctic-N and -S, Alps-N and -S) to evaluate the effects of repeated FTC of differing frequencies on both prokaryotic and fungal communities. The soils were incubated for 28 days under daily freeze-thaw cycles (D-FTC, alternations of 12 h at +5°C and 12 h at -5°C) and weekly freeze-thaw cycles (W-FTC, alternations of 7 days at +5°C and 7 days at -5°C), including controls (+5°C and -5°C) (Fig. S1). We hypothesized that: (1) repeated short and frequent FTCs cause larger alterations in the structure of soil microbial communities, (2) microbial compositional shifts are coupled to alterations in microbial metabolic functions, and (3) microbial communities from soils with a legacy of more frequent FTCs exhibit a higher tolerance to repeated shorter and more frequent FTCs.

3.3. Materials and methods

3.3.1. *Site description*

Study sites were located on north- and south-facing slopes near the summits of *Latnjachorru* in the Arctic (N 68°21.31500' E 018°31.16600', 1300 m a.s.l.) and *Muot de Barba Peider* in the Alps (N 46° 29.78040' E 009°55.88700', 2979 m a.s.l.). *Latnjachorru* is in Abisko, in the northernmost part of Sweden. Soil temperature measurements made on site at a depth of 5 cm for one year (iButtons; Maxim Integrated, San Jose, California, USA) showed a mean annual temperature (MAT) of -3°C (range -15°C to 20°C) for the north-facing slope and -1°C (range -12°C to 17°C) for the south-facing slope. Mean annual precipitation (MAP) in the region is 838 mm, most of which falls as snow from September to June (based on daily soil surface temperatures measured from 2006 to 2015 at Lantjajaure Field Station, 981 m a.s.l.). The bedrock is mainly composed of Cambro-Silurion mica-garnet schists (Beylich et al., 2004). Permafrost in the area is sporadic and may be found at 80 m depth at 1200 m a.s.l. (Beylich et al., 2006).

Muot de Barba Peider is situated in the upper Engadine valley, in the eastern part of Switzerland. Soil temperature measurements made at a depth of 5 cm at the summit during two consecutive years showed a MAT of -1.5°C (range -13°C to 23°C) for the north-facing slope and 2°C (range -5°C to 25°C) for the south-facing slope. MAP in the region is 1500 mm (Frey et al., 2016). Snow establishes from early in October to late in November and lasts until the end of April or as late as the end of June (Beniston et al., 2003; Rodder & Kneisel, 2012). The bedrock consists of gneiss from the upper Austroalpine Languard nappe, and permafrost is found at a depth of 1.5 to 2 m (Zenklusen Mutter et al., 2010).

Soil temperature measurements indicated larger temperature variations at the alpine site than at the arctic site (Fig. S2). Furthermore, oscillation of hourly temperatures around 0ºC suggested a mean value of 10 FTCs for the north- and south-slopes at the arctic sites, and mean values of 12 and 25 FTCs at the north- and south-slopes at the alpine site, respectively (one year measurements). Vegetation is scarce at both sites and is dominated by non-woody tundral species. The arctic site is populated by grass members of the genera *Agrostis*, *Calamagrostris*, *Festuca*, *Poa* and *Trisetum*, as well as bryophytes and lichens, such as *Cladonia* spp. and *Dicranum* spp. (Jagerbrand & Alatalo, 2015). Vegetation in the alpine site is scarcer than in the arctic site, with some occurrences of *Poa*, *Cerastium* and *Jacobea* spp. (Frey et al., 2016).

3.3.2. *Sample collection and experimental set-up*

Soil samples were collected in August 2017 at a depth of 5 cm in the north- and south-facing slopes of the arctic and alpine mountains. In each slope, subsamples were collected with shovels from five locations separated by 3 to 5 m. In the field, the five subsamples were pooled, mixed and sieved (4 mm mesh size). All steps were performed using sterilized materials. Four soil pooled samples were obtained: north-facing arctic soil (Arctic-N), south-facing arctic soil (Arctic-S), north-facing alpine soil (Alps-N) and south-facing alpine soil (Alps-S). Soil samples were stored at 5°C for one month. For each soil sample, 16 microcosms were prepared by adding 50 g of fresh soil to 150 ml Erlenmeyer flasks, which were then covered with gas-permeable lids made from cotton wool to allow for aeration (Luláková et al., 2019). The microcosms were divided into four groups (each with four replicates), which were subsequently incubated under different temperature regimes (Fig. S1): 1) daily freeze-thaw cycles (D-FTC) with alternations of 12 h at +5°C and 12 h at -5°C, 2) weekly freeze-thaw cycles (W-FTC) with alternations of 7 days at +5°C and 7 days at -5°C, 3) controls with constant +5°C (+5°C) and 4) controls with constant -5°C (-5°C). The incubations lasted 28 days. Water content (WC) of the soil's microcosms was determined at the start of the experiment by weighing soil samples before and after drying at 105°C. WC values for the soils of different origin corresponded in average to 50% of water holding capacity (WHC) for the north-facing and the south-facing arctic soils, 32% for the north-facing alpine soils and 40% for the south-facing alpine soils (Table S1). WC were maintained constant during the incubation by replacing the evaporated water with sterilized milliQ water. The experimental temperature oscillations (between +5°C and -5°C) were chosen in relation to the observed natural range of top soil temperature variations occurring at both the arctic and alpine sites during the months of September/October and April/May, when FTCs were observed (Fig. S2). Monitoring of temperatures in dummy soils via iButtons during the tested FTCs in the incubators indicated that soil temperatures changed from +5 to -5°C and *vice versa* in about two hours or less (freezing rates of -0.07± 0.003°C min^{-1} and thawing rates of 0.09 ± 0.005°C min^{-1}, n=2).

3.3.3. *Soil physico-chemical properties*

Soil texture was analyzed by the hydrometer method (Gee & Bauder, 1986). Water-holding capacity (WHC) was measured as the differences in weight between drained and dried soils

as described in Frossard et al. (2017). Soil organic matter (OM) content was determined by the weight loss-on-ignition method (Davies, 1974). pH was measured in 0.01 M $CaCl_2$ soil slurries (2:1 v/w). Total carbon (C) and nitrogen (N) were measured for dried (65°C) and fine-grained soil samples, using an elemental analyzer (NC-2500; CE Instruments, Wigan, UK). To measure labile C and nutrients, soil extracts were prepared in milliQ water (water:soil 10:1 v/w, shaken over night at room temperature) and filtered through DF 5895-150 ashless paper (Albert LabScience, Dassel, Germany). Labile organic C and total N were measured with a TOC/DTN analyzer (Sakalar Analytical B.V, Breda, The Netherlands) after acid digestion with 3 M HCl to remove carbonates. Ammonium was measured photometrically with an FIAS 300 flow injection system (Perkin-Elmer, Waltham, Massachusetts, USA).

3.3.4. *Basal respiration rates*

Soil basal respiration was measured once per week during the incubation period in the D-FTC, W-FTC and control +5°C microcosms. Measurements were performed at +5°C two hours after the onset of the thawing phase of the D-FTC samples (four measurements) and at the end of the thawing phase of the W-FTC microcosms (two measurements). The respiration measurements were performed 7 days after the start of the incubation, to avoid the potential artefacts on microbial activities created by the soil manipulation during experiment set-up. The microcosms were gas-tight sealed, and CO_2 concentrations accumulating in the flasks were measured at fixed intervals over a total time span of 8h using an infrared absorption CO_2 analyzer (EGM-4 Environmental Gas Monitor; PP systems, Amesbury, Massachusetts, USA) (Luláková et al., 2019). CO_2 rates were calculated as the slopes of fitted linear regressions of CO_2 concentrations over time. Regressions with $R^2 < 0.8$ were discarded. Before and after each respiration measuring period, microcosms we aeriated and covered with the gas-permeable lids.

3.3.5. *Enzymatic activity rates*

The potential activity of six extracellular enzymes, chosen based on their metabolic functions, was assessed: (1) β-glucosidases (BG), involved in the degradation of cellulose (C-acquiring enzyme); (2) β-xylosidases (XYL), involved in the degradation of hemicellulose (C-acquiring

enzyme); (3) N-acetyl-glucosaminidases (NAG), involved in the degradation of β-1,4 glucosamines (C- and N-acquiring enzyme); (4) Leucine aminopeptidases (LAP), involved in the degradation of peptides (N-acquiring enzyme); (5) Acid phosphatases (AP), involved in the degradation of phosphomonoesters (P-acquiring enzyme); and (6) Phenol peroxidases (PP), involved in polyphenol oxidation (lignin-degrading enzyme) (Sinsabaugh et al., 2008). Activity measurements were performed on soil slurries (buffer:soil 3:1 v/w, acetate buffer, pH = 4, autoclaved) as previously described (Frossard et al., 2012). The activity of the first five enzymes (BG, XYL, NAG, LAP and AP) were measured by fluorescence, using substrate analogues attached to fluorescent molecules 4-methylumbelliferone (MUB) or 7-amino-4-methylcoumarin (AMC). Phenol peroxidase activity (PP) was measured by colorimetry through the oxidative reaction of the substrate analogue 3-3,4-dihydroxyphenylalanine (L-DOPA) in the presence of H_2O_2. The substrate analogues were added to final concentrations of 40 µM, after determining that these concentrations saturated potential enzymatic activities in the tested soils. The extracellular enzymatic activities were measured at the end of the 28-day incubation period. The assays were performed at +5°C, and controls were included in the assays to correct for variations in fluorescence and absorbance backgrounds of the substrate solutions and the slurries.

3.3.6. *Microbial abundance*

Bacterial and fungal abundances were determined by quantitative PCR (qPCR) on a 7500 Fast Real-Time PCR System (Thermo Fisher Scientific, Waltham, Massachusetts, USA). qPCR reactions were prepared using the universal primers pairs 27F/519R amplifying the V1-V3 region of the 16S rRNA gene (prokaryotes) and ITS3/ITS4 amplifying the internal transcribed spacer region 2 (ITS2) of the eukaryotic ribosomal operon (fungi). qPCR programs were run as described by Hartmann et al. (2014).

3.3.7. *DNA extraction and high-throughput sequencing*

Total soil DNA was extracted with the DNeasy PowerSoil Kit (Quiagen, Hilden, Germany) and DNA concentrations were quantified with the PicoGreen dsDNA quantification kit (Thermo Fisher) according to the manufacturer's instructions. The 16S $rRNA_{V3\text{-}V4}$ genomic region

(prokaryotes) and the ITS2 region (fungi) were amplified by PCR using primer pairs 341F/806R and ITS3/ITS4, respectively, and 10 ng of extracted DNA, as previously described (Frey et al., 2016). A first amplification was performed in triplicate, and the pooled prokaryotic and eukaryotic amplicons were sent to the Génome Québec Innovation Center at McGill University (Montreal, Canada), where they were purified, quantified, barcoded and paired-end sequenced using the Illumina MiSeq v3 platform (Illumina Inc., San Diego, California, USA).

Prokaryotic and eukaryotic raw sequences were quality filtered, chimeras were removed, and high-quality reads were clustered into operational taxonomic units (OTUs) based on 97% identity threshold as described previously, using a customized pipeline largely based on UPARSE (Edgar, 2013; Edgar & Flyvbjerg, 2015) and implemented in USEARCH v.9.2 (Edgar, 2010). Singletons were removed. Taxonomic classification of the OTUs was performed by querying centroid sequences against reference databases using the naive Bayesian classifier (Wang et al., 2007), implemented in MOTHUR (Schloss et al., 2009), with a minimum bootstrap support of 60%. Prokaryotic sequences were queried against the SILVA database v.132 (Quast et al., 2013). Eukaryotic sequences were first curated using a custom-made ITS2 database retrieved from NCBI GenBank, and sequences assigned to fungi were classified to finer taxonomic levels using the UNITE database v.8.0 (Abarenkov et al., 2010).

3.3.8. *Data analyses*

Statistical analyses were completed, and graphs were generated using the open-source software R (version 3.6.0, R Core Team (2017)) with the *ggplot2* package, Wickham (2016)). A significance level of 0.05 was considered for all analyses. Overall effects of treatment (D-FTC, W-FTC, +5°C and -5°C), soil origin (Arctic-N, Arctic-S, Alps-N and Alps-S) and their interactions on the soil physico-chemical properties, basal respiration rates and enzymatic activity rates were tested with two-way ANOVAs. Normality of residuals and homoscedasticity of the response variables were checked, and transformations (normalization or log10) were applied when ANOVA conditions were not met. The effects of the FTC treatments (D-FTC and W-FTC) on the variables *basal respiration rate* and *enzymatic activity rate* were further tested with one-way ANOVAs and Tukey HSD post-hoc tests for each of the four different soils, separately. To ease the visualization and comparison of trends among the soils of different

origin, respiration and enzymatic activity rates were transformed into relative values by dividing the rates by the mean values of the +5°C controls within the four soil subsets. The relative rates of the enzymatic activities were further $\log_2$ transformed.

The α-diversity parameters richness, Pielou's evenness and Shannon diversity index were calculated on prokaryotic and fungal OTUs rarefied to the minimum number of reads (25936 for prokaryotes and 14324 for fungi), using an iterative approach (100 repetitions; *EcolUtils* package in R; Salazar 2019, accessed on January 2019). Differences in microbial *β*-diversity were assessed by computing Bray-Curtis dissimilarity matrices based on the relative abundance of the prokaryotic or fungi OTUs and visualized with Principal Coordinate Analyses (PCoAs) (*cmdscale* function and *vegan* package; Oksanen et al., 2019, accessed on January 2019). The statistical significance of observed differences was assessed with permutational analyses of variance (PERMANOVA, 10^5 permutations; Anderson 2001). Multivariate homogeneity of group dispersions was checked prior to the PERMANOVAs to ensure that detected significant differences were associated with the tested factors and not with differences in the within-group variabilities (Anderson & Walsh, 2013). Where dispersion among groups was significant, statistics were performed using Chord distance instead of Bray-Curtis matrices (Legendre & Gallagher, 2001).

Indicator analyses were performed on the OTU relative abundances using the *indicspecies* package in R (Cáceres & Legendre, 2009). Fungal OTUs indicators were functionally annotated with FungGuild v1.1 (Nguyen et al., 2016).

3.4. Results

3.4.1. *Soil physico-chemical properties*

Soil properties, determined at the beginning of the incubation experiment for the four soils of different origin, showed marked differences across the soils (Fig. S3). At the end of the 28 days of incubation, soil origin showed a stronger influence than FTC treatments on all measured soil physico-chemical and microbial parameters (two-way ANOVAs, Table 1). All soils were acidic (pH 4.0–4.6) and had a high sand content (67–90%) (Table S1). Water-holding capacity (WHC), OM, carbon (C) and nitrogen (N) were higher (≥ 2-fold) in the arctic

soils than in the alpine soils (Table S1). Similar trends were observed between the south-facing soils and the north-facing soils for both arctic and alpine sites, where soils from the south-facing slope consistently showed higher values for WHC, OM, C and N (Table S1). The FTC treatments had a significant effect on labile N (two-way ANOVAs, $F=16.87$, $p < 0.001$), labile ammonium ($F=3.71$, $p < 0.05$) and labile organic carbon ($F=3.22$, $p < 0.05$) concentrations (Table 1). However, effects were consistent across soils only partially for labile N, which was four times higher in the W-FTC treatment than in the +5°C control for both north- and south-facing alpine soils (Tables S2 and S3).

3.4.2. *Soil microbial activities*

FTCs had a strong influence on soil basal respiration (Table 1). Both the W-FTC and D-FTC treatments led to a decrease in the rates of basal respiration relative to the +5°C controls at the end of the incubation (day 28) in all but the south-facing arctic soils (Fig. 1, Tables S3 and S4). The decrease in basal respiration was greater for the W-FTCs (range 31–66% across all soils) than for the D-FTCs (18–44%). These differences between the W-FTC and the D-FTC treatments were significant in the north-facing soils of both Arctic and Alpine soils ($p < 0.05$, Fig. 1, Table S3).

Extracellular enzymatic activities were measured to evaluate changes in microbial acquisition of C-, N- and P-compounds. At the end of the incubation, extracellular enzymatic activities did not exhibit consistent response patterns across the four soils (Table 1, Fig. 1, Table S4). In the arctic soils, D-FTCs led to a general decrease in all enzymatic activities relative to the +5°C controls. The W-FTC treatment caused a significant increase in Leucine aminopeptidase activity in the north-facing arctic soil, while it drastically decreased in the south-facing soil. In the north-facing alpine soils, both FTC treatments led to an increase in all enzymatic activities relative to the +5°C controls. In contrast, in the south-facing alpine soils, all enzymatic activities decreased after the FTC treatments (Fig.1, Table S4).

Table 1. Effects of treatment, soil origin and their interaction on soil properties, microbial activities, microbial abundance and prokaryotic and fungal α-diversity.

	Variables	Treatment	Soil origin	Treatment x Soil origin
		$F_{3,48}$	$F_{3,48}$	$F_{9,48}$
Soil properties[1]	**pH**	2.79	**226.50*** **	1.11
	OM	2.29	**454.78*** **	0.99
	labile OC	**3.22***	**50.10*** **	**3.43****
	labile N	**16.87*** **	**368.69*** **	**7.53*** **
	Ammonium	**3.71***	**356.26*** **	**4.63*** **
Microbial activities[2]	**Respiration**[3]	**87.64*** **	**3.82***	**3.82****
	BG	1.03	1.94	0.65
	XYL	0.27	1.02	0.45
	AP	0.25	**4.72****	0.76
	NAG	0.51	2.50	0.79
	LAP	0.97	**8.22*** **	**3.65****
	PP	0.40	0.17	0.99
Microbial abundance	**DNA content**	1.42	**97.13*** **	1.33
	Prokaryotic abundance[4]	1.58	**1105.43*** **	1.64
	Fungal abundance[5]	2.11	**6.35****	1.10
Prokaryotic α-diversity	**Richness**	**6.61*** **	**96.37*** **	**3.85*** **
	Evenness	**5.29****	**238.80*** **	**8.76*** **
	Shannon	**9.62*** **	**297.33*** **	**9.51*** **
Fungal α-diversity	**Richness**	1.10	**191.10*** **	**4.02*** **
	Evenness	0.72	**10.51*** **	**2.23***
	Shannon	0.64	**19.90*** **	**2.46***

Significance of effects was assessed by two-way ANOVAs, with α=0.05.[1]Analyses were performed on normalized soil variables relevant to microbial life. OM: organic matter, Labile OC: water-extractable organic carbon, Labile N: water-extractable total nitrogen. [2]Analyses were performed on log-transformed variables. GLS: β-glucosidases, XYL: β-xylosidases, AP: Phosphatases, NAG: N-acetyl-glucosaminidase, LAP: Leucine aminopeptidases, PP: Peroxidases. [3]*Degrees of freedom* of F-values were lower for respiration because rates with $R^2 < 0.8$ were removed: Treatment $F_{2,34}$, Soil origin $F_{3,34}$, Treatment x Soil origin $F_{3,34}$. [4]Prokaryotic abundance: 16S gene copy number g^{-1} DW, [5]Fungal abundance: ITS gene copy number g^{-1} DW Numbers in bold and asterisks indicate significant differences between groups, with *** p<0.001, ** p<0.01, * p<0.05.

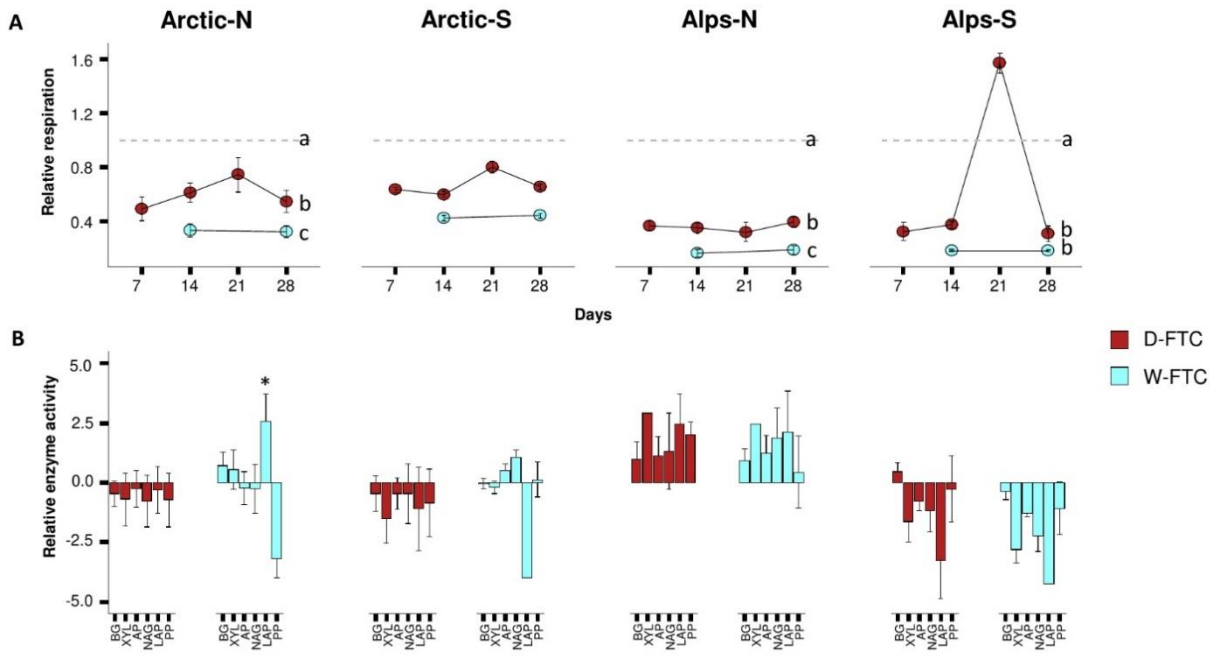

Figure 1. Microbial activities. **A**. Basal respiration. Values are given as the ratio of the daily freeze-thaw cycles (D-FTC; red) or weekly freeze-thaw cycles (W-FTC; blue) divided by the +5°C controls. Lower-case letters represent statistically different groups. **B**. Extracellular enzymatic activities. Relative activity is represented as the binary logarithm of the ratio of the daily freeze-thaw cycles (D-FTC) or the weekly freeze-thaw cycles (W-FTC) divided by the mean of the +5°C controls. Ratios were limited to the range of (-4, 4). BG: β-glucosidases, XYL: β-xylosidases, AP: Acid Phosphatase, NAG: N-acetyl-glucosaminidase, LAP: Leucine aminopeptidases, PP: Phenol Peroxidases. Mean ± SE (n=4). Arctic: arctic soils, Alps: alpine soils, -N: north-facing, -S: south-facing. * significant difference of LAP, W-FTC vs. control, $F_{1,3}=6.160$, $p=0.048$. Dotted line represents the intercept with the value 0 in the y axis.

3.4.3. *Microbial abundance*

Microbial abundance, measured by quantitative PCR of the 16S rRNA gene (prokaryotes) and the ITS2 (fungi) genomic regions, was not affected by the FTCs but by soil origin (Table 1). Arctic soils had a higher prokaryotic (ranging from 4×10^8 to 2×10^9 16S gene copies g^{-1} DW) and fungal (2×10^6 to 1×10^7 ITS gene copies g^{-1} DW) abundance than alpine soils (5×10^4 to 7×10^5 16S gene copies g^{-1} DW and 3×10^5 to 3×10^6 ITS gene copies g^{-1} DW; Fig. S4).

3.4.4. *Microbial community composition*

The composition of the soil prokaryotic and fungal communities was revealed by amplicon sequencing of the 16S rRNA and ITS2 genomic regions, respectively. A total of 2 965 563 (39 021 ± 4899 per sample) prokaryotic and 2 216 494 (29 165 ± 5901) eukaryotic high-quality

filtered reads were obtained, which clustered into 11 309 prokaryotic and 3976 eukaryotic OTUs. Prokaryotes mostly consisted of Bacteria (99.6% of prokaryotic reads, 11 270 OTUs), where most abundant phyla (> 1% of total reads) were Proteobacteria, Chloroflexi, Acidobacteria, Verrucomicrobia, Planctomycetes, Actinobacteria, Bacteroidetes, Gemmatimonadetes, WD272 and Parcubacteria (Table S5). Fungi (95% of eukaryotic reads, 3298 OTUs) mostly consisted of Ascomycota, Basidiomycota and Zygomycota (former classification, see Spatafora et al. (2016)) (Table S5).

Similar to the physico-chemical variables, the microbial composition of the four soils, assessed at the beginning and at the end of the incubation experiment, primarily differed according to their soil origin (Fig. S3). FTCs showed a significant influence on prokaryotic α-diversity at the end of the incubation period (OTUs richness, Pielou's evenness and Shannon's diversity; $p < 0.01$; Table 1). However, when analyzed independently, changes in α-diversity linked to the FTCs treatments were minor, and they varied depending on their origin (Fig. S5, Table S3). FTCs showed clear effects on prokaryotic β-diversity ($p < 0.001$, Table 2), where the structure of prokaryotic communities from the FTC treatments (D-FTC and W-FTC) and the controls (+5°C and -5°C) were significantly different ($p < 0.05$, Table 2, Fig. 2). Overall, dissimilarities in β-diversity were larger between the W-FTC and the +5°C controls than between the D-FTC and the +5°C controls (Figs 2 and S6).

In contrast, fungal communities were barely affected by the FTC treatments (Tables 1 and 2, Fig. 2). FTCs had no impact on fungal α-diversity (Fig. S5, Table S3), and significant differences in fungal β-diversity between D-FTCs, W-FTCs and controls were only detected for the south-facing arctic soils ($p < 0.05$, Table 2).

Table 2. Effects of treatment, soil origin and their interaction on microbial β-diversity.

	Prokaryotes						Fungi					
PERMANOVA												
	DF	**SS**	**MS**	**F[1]**	**R2**	***p***	**DF**	**SS**	**MS**	**F**	**R2**	***p***
Treatment	3	0.389	0.130	8.436	0.041	**< 0.001[2]**	3	0.574	0.191	2.047	0.026	**0.013**
Soil origin	3	7.891	2.630	171.151	0.838	**< 0.001**	3	15.723	5.241	56.101	0.706	**<0.001**
Treatment x Soil origin	9	0.395	0.044	2.853	0.042	**< 0.001**	9	1.475	0.164	1.754	0.066	**0.004**
Residuals	48	0.738	0.015		0.078		48	4.484	0.093		0.201	
Total	63	9.413			1		63	22.256			1	

Pairwise PERMANOVA

	Arctic				Alps				Arctic				Alps			
	N		**S**		**N[3]**		**S**		**N**		**S**		**N**		**S[3]**	
	F	***p***	**F**	***p***	**F**	***p***	**F**	***p***	**F**	***p***	**F**	***P***	**F**	***p***	**F**	***P***
D-FTC vs. +5°C	1.793	**0.028**	2.829	0.028	9.189	**0.029**	8.15	**0.029**	1.014	0.488	2.636	**0.028**	1.874	0.144	1.099	0.309
W-FTC vs. +5°C	1.900	**0.030**	3.571	**0.029**	8.543	**0.031**	6.53	**0.029**	2.176	0.027	3.442	**0.028**	2.188	0.166	2.242	0.06
D-FTC vs. -5°C	3.174	**0.028**	1.991	**0.028**	3.997	**0.03**	5.008	**0.027**	1.19	0.227	1.572	**0.03**	2.036	**0.032**	2.702	0.03
W-FTC vs. -5°C	1.590	0.055	2.851	**0.028**	3.689	**0.027**	2.989	**0.028**	0.952	0.518	1.818	**0.03**	1.266	0.14	1.728	0.059
D-FTC vs. W-FTC	2.971	**0.026**	1.573	0.057	3.325	**0.03**	4.044	**0.028**	1.207	0.258	1.23	0.201	1.098	0.262	2.776	**0.03**
+5°C vs. -5°C	3.078	**0.026**	1.717	**0.032**	10.413	**0.029**	9.175	**0.032**	1.466	0.03	1.002	0.482	4.755	**0.027**	2.365	**0.03**

General effects of treatment and soil origin on β-diversity were assessed by PERMANOVA tests. Differences among treatments within each four different soils were assessed by pairwise PERMANOVAs, with α=0.05. [1]F correspond to the pseudo-F ratio, [2]Numbers in bold indicate p < 0.05, [3]Based on Chord distances to meet the condition of homogeneity of dispersion between groups. DF: Degrees of freedom, SS: Sum of squares, MS: mean squares. D-FTC: daily freeze-thaw cycles, W-FTC: weekly freeze-thaw cycles, +5◦C: controls +5◦C, -5◦C: controls -5◦C, Arctic: arctic soils, Alps: alpine soils, -N: north-facing, -S: south-facing

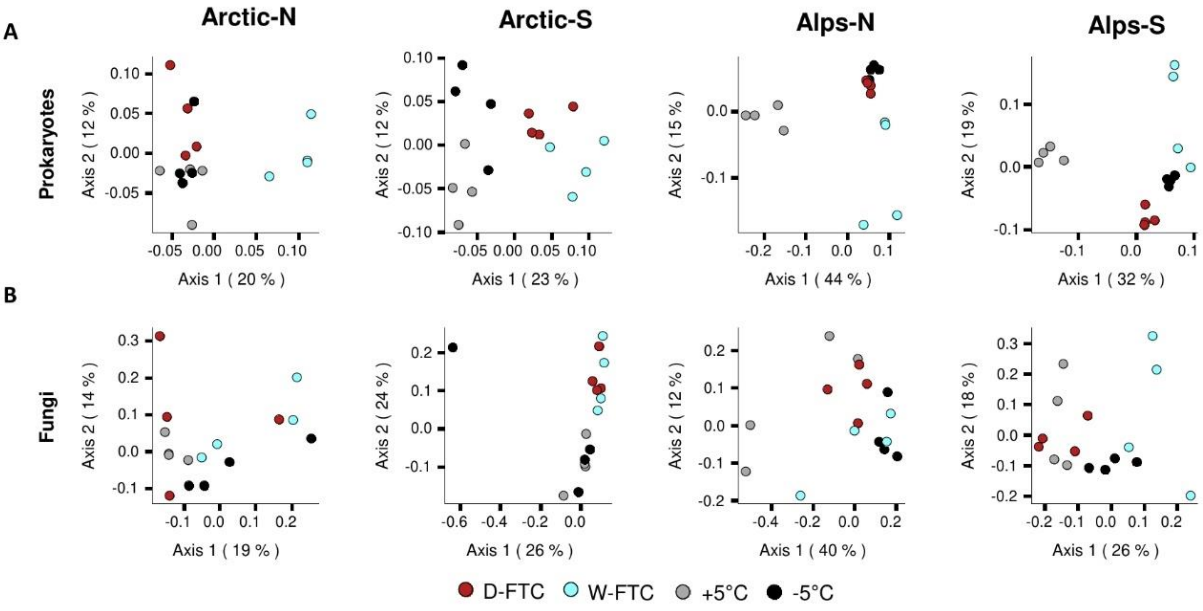

Figure 2. Microbial β-diversity of the incubated soils. PCoAs computed on Bray-Curtis dissimilarities based on OTU relative abundances of (**A**) Prokaryotes and (**B**) Fungi. Arctic: arctic soils, Alps: alpine soils, -N: north-facing, -S: south-facing. D-FTC: daily freeze-thaw cycles (red), W-FTC: weekly freeze-thaw cycles (blue), +5°C: controls +5°C (gray), -5°C: controls -5°C (black).

3.4.5. *Indicator taxa associated with FTCs*

Indicator species analyses were conducted for each soil independently to identify bacterial and fungal OTUs significantly associated with the D-FTC and W-FTC treatments at the end of the incubation. A total of 988 prokaryotic (8% of total prokaryotic OTUs) and 130 fungal OTU indicators (4% of total fungal OTUs) were significantly associated with the FTC treatments ($p < 0.05$). Only one bacterial indicator OTU (Fig. 3, OTU 31, *Arthrobacter*) was common to all four soils. D-FTC samples were enriched in bacterial indicator OTUs from Actinobacteria, a phylum with numerous members with copiotrophic lifestyles (Fig. 3, Table S6). Moreover, indicator OTUs from copiotrophic genera such as *Arthrobacter, Nocardioides* (Actinobacteria), *Noviherbaspirillum* (Proteobacteria), *Masillia, Burkholderia* (Proteobacteria) and *Rhodococcus* showed strong associations (≥ 0.75 indicator value index) with the D-FTCs and were negatively associated with the W-FTCs (Fig. 3). In contrast, W-FTC treatments were enriched in indicator OTUs from oligotrophic taxa, such as those in Verrucomicrobia (mainly DA101), Acidobacteria, Planctomycetes, Parcubacteria and WD272 phyla (Fig. 3, Table S6). Indicator OTUs from oligotrophic genera such as *Blastocatella, Bryobacter* (Acidobacteria) and *Gemmata* showed

strong associations (≥ 0.75) with the W-FTCs and were negatively associated with the D-FTCs (Fig. 3).

Fungal indicator OTUs were mostly composed of saprotrophic and pathogenic taxa (Fig. 4, Table S7). These included ubiquitous cold-tolerant and opportunistic genera such as *Mrakia*, *Geomyces, Mortierella, Dioszegia*, *Leucosporidium* and *Penicillium* (Fig. 4). Interestingly, several indicator OTUs associated with the FTC treatments were also associated with the -5°C controls, especially *Mortierella* and *Geomyces* in the alpine soils (Fig. 4). Complete information and statistics for all prokaryotic and fungal indicator OTUs at various taxonomical levels from phylum to genus are provided in Tables S8 and S9.

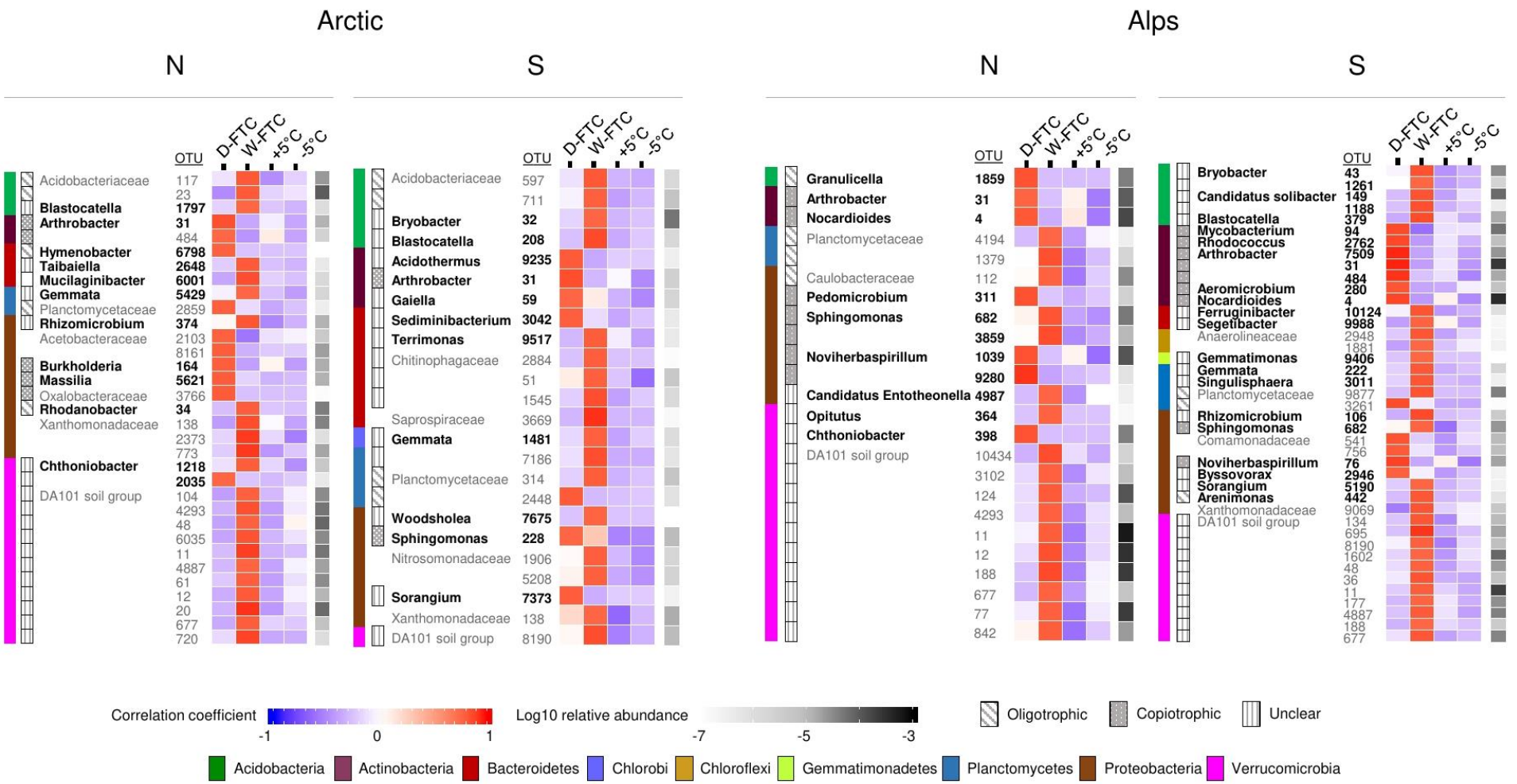

Figure 3. Bacterial indicators OTUs significantly associated to the daily freeze-thaw cycles (D-FTC) or the weekly freeze-thaw cycles (W-FTC) but not associated with the +5°C controls (+5°C) for the four different soils. Indicator taxa with and indicator value index to the W-FTC or the D-FTC greater than 0.75 and assigned beyond the family level are represented. Classification in oligotrophic and copiotrophic is based on the classifications in bacterial life strategies proposed by Fierer et al. (2007) and Ho et al. (2017), and on information about ecological and cultivation traits of bacterial groups compiled by Rosenberg et al. (2013). Unclear refers to taxa with insufficient information (taxa with fewer than 10 cultivated strains recorded in the NCBI database or candidate taxa) to be classified to a life strategy. Families containing both oligotrophic and copiotrophic taxa were not assigned a life strategy. Names in bold correspond to Genus taxonomic levels. -5°C: controls -5°C. Arctic: arctic soils, Alps: alpine soils, -N: north-facing, -S: south-facing.

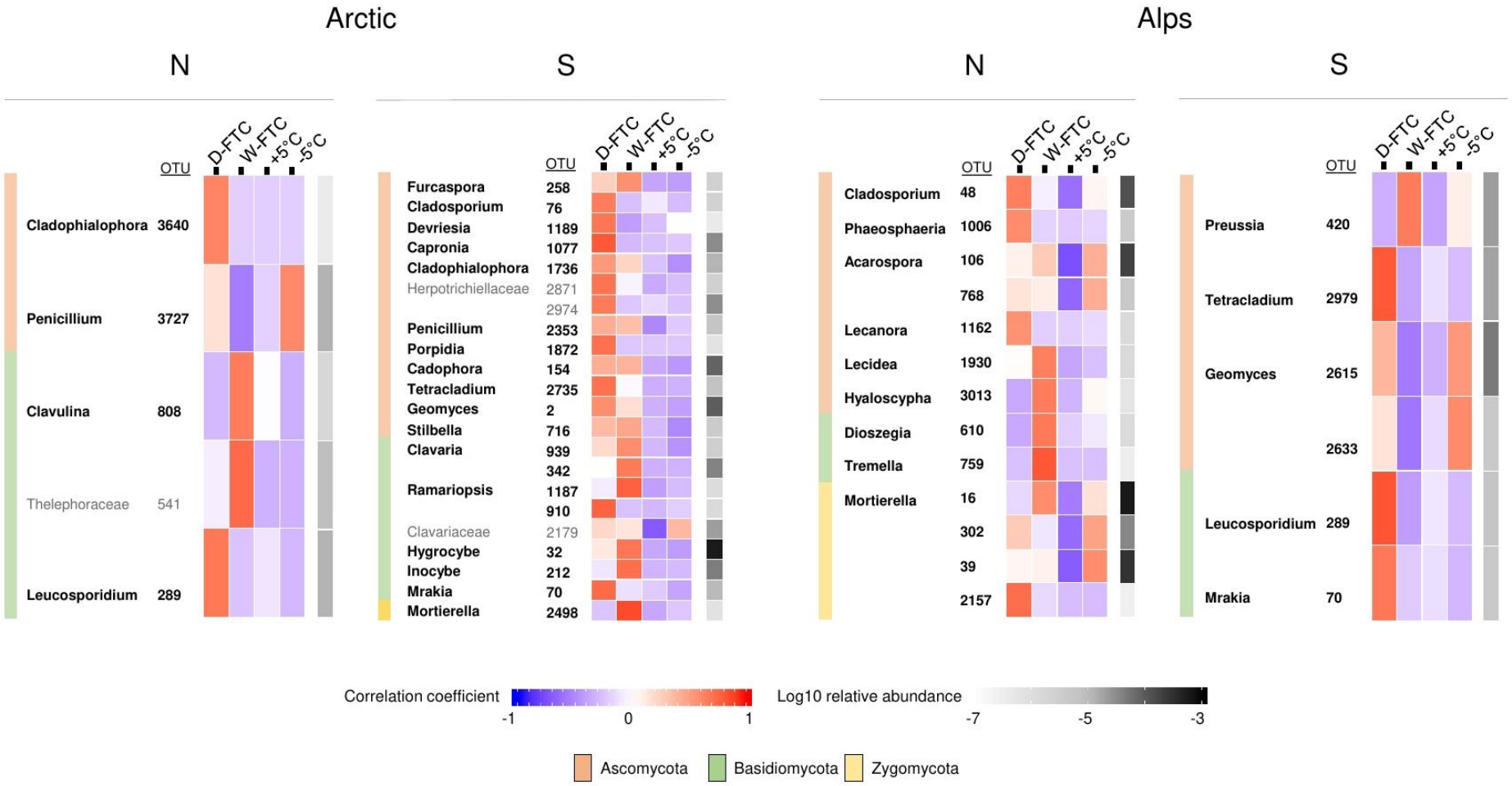

Figure 4. Fungal indicators OTUs significantly associated to the daily freeze-thaw cycles (D-FTC) or the weekly freeze-thaw cycles (W-FTC) but not associated with the +5°C controls (+5°C) for the four different soils. Indicators assigned beyond the family level are displayed. Names in bold correspond to Genus. -5°C: controls -5°C. Arctic: arctic soils, Alps: alpine soils, -N: north-facing, -S: south-facing.

3.5. Discussion

To our knowledge, this is the first experimental study comparing the effects of repeated FTCs between arctic and alpine soils, and in which changes on both taxonomical and functional components of the soil microbial communities are analyzed at fine-scale resolution. We acknowledge that our analyses of the microbial communities are based on DNA and thereby include both active and inactive microorganisms. Nevertheless, by comparing the highly frequent daily FTCs with the infrequent weekly FTCs and including compositional and functional data, we provide an integrative overview of potential dynamic responses that arctic and alpine soil microbiomes might undergo in the future, as snow becomes scarce and FTCs become more frequent.

Repeated FTCs have been shown to cause large alterations in the soil microbiota (Feng et al., 2007; Han et al., 2018; Schimel & Clein, 1996). We therefore hypothesized that shorter and more frequent FTCs (daily; D-FTCs) would cause larger compositional changes on the soil prokaryotic and fungal communities than longer and less frequent FTCs (weekly; W-FTCs). However, we observed the opposite: although both FTCs treatments led to significant shifts in β-diversity in the prokaryotic communities compared with the thaw controls, effects were larger for the W-FTCs than for the D-FTCs. Furthermore, we identified an apparent trait-based pattern of response of the prokaryotic communities to the tested FTC frequencies: D-FTCs stimulated copiotrophic and opportunistic bacteria over oligotrophic taxa while W-FTCs promoted oligotrophic bacteria over copiotrophs. We use the designation of “copiotrophs” for fast-growing and metabolically versatile microbial taxa, in opposition to “oligotroph”, which refers to slow-growing, stress-tolerant microorganisms that thrive on low nutrient concentrations (Koch, 2001). The categorization of microbial phylogenetic groups into copiotrophs or oligotrophs is however debatable (Ho et al., 2017), since physiological traits in microorganisms are context-dependent and they are highly variable, even at the deepest taxonomical level of species (Ho et al., 2017; Lauro et al., 2009; Morrissey et al., 2016). Nevertheless, we apply the categorization copiotroph-oligotroph in our study, since this categorization has been proven to be useful for describing general trends of association between microbial composition and function, and their ecological meaning in natural soil systems (Meisner et al., 2018; Schostag et al., 2019).

In the D-FTC treatment, the freezing phase was short (12 h) and freeze-thawing occurred daily. In each cycle, freeze-thawing causes the lysis of FTC-sensitive cells and the mobilization of labile carbon and nutrient sources from the physical disaggregation of soil organic materials (Feng et al., 2007; Wang et al., 2012). In this scenario, we propose that copiotrophic microorganisms outcompeted oligotrophs because they were able to withstand environmental changes and grow faster during the thawing phases by rapidly utilizing the newly labile substrates (Fierer et al., 2007; Koch, 2001). This could explain the increase in the number of indicator OTUs associated with the D-FTCs from fast-growing genera such as *Arthrobacter*, *Massilia* and *Rhodococcus. Arthrobacter* sp., which was observed in all four soils, exhibit a high diversity of cold-shock proteins and adjust quickly to temperature changes and cooling (Berger et al., 1996). *Arthrobacter* sp. and *Massilia* grow well in nutrient-amended media (Lee et al., 2004; Liu et al., 2018), and RISA fingerprinting has shown that *Rhodococcus* becomes dominant in arctic soils exposed to 24-hour FTCs (Eriksson et al., 2001).

In the longer W-FTC treatment, freeze-thawing occurred only twice, and the freezing phase lasted for 7 days, compared to 12 hours in the D-FTC treatment. Prolonged freezing leads to conditions of desiccation and starvation in the soil (Margesin, 2012; Panoff et al., 1998), and it triggers the activation of complex cell survival mechanisms (De Maayer et al., 2014; Koponen & Baath, 2016; Walker et al., 2006), including extensive synthesis of cold-shock proteins and cryoprotectants, which are energetically costly (De Maayer et al., 2014). Oligotrophs have lower growth rates than copiotrophs but they use nutritional resources more efficiently, thus requiring less energy to grow (Fierer et al., 2007; Koch, 2001). Therefore, oligotrophic microorganisms could have survived the freezing phases of the W-FTCs in better physiological conditions or in larger numbers than the copiotrophs, thus taking over during the thawing phase.

The higher tolerance of oligotrophic microorganisms to freezing compared to copiotrophic taxa could explain the higher proportion of indicator OTUs associated with the W-FTCs treatment from phyla such as Verrucomicrobia, Acidobacteria, Planctomycetes and Parcubacteria, which, based on current knowledge (Fierer et al., 2007; Ho et al., 2017), are enriched in oligotrophic members. Members belonging to Verrucomicrobia and Acidobacteria seem to thrive in nutrient-depleted media (Sangwan et al., 2005; Tanaka et al., 2017). In addition, Acidobacteria and Parcubacteria have been shown to be abundant in permafrost (Steven et al., 2007), where microbial activity has

been reported (Coolen & Orsi, 2015; Nikrad et al., 2016) despite the permanent freezing conditions. Furthermore, members from Acidobacteria phyla has been shown to increase in abundance in boreal wetland soils subjected to slow freeze-thawing (Ren et al., 2018). At finer taxonomical level, indicator OTUs associated with the W-FTCs mainly classified to uncultured genera (e.g. *Blastocatella* and *Gemmata*), which highlights the special growing requirements of these taxa and the vast microbial diversity still unknown in alpine and arctic soils.

In a future climate with less snow, the occurrence of shorter and more frequent FTCs might be disadvantageous for taxa with oligotrophic attributes in arctic and alpine soils, which, if failing to adapt, could be overtaken by copiotrophic groups. In addition, copiotrophic microorganisms would further benefit from the increase in soil temperatures, as observed in studies on permafrost affected soils (including the active layer) (Luláková et al., 2019; Schostag et al., 2015) and glacier forefields (Kim et al., 2017; Rime et al., 2015).

The weak response of the fungal communities to the FTC treatments is in line with previous studies (Han et al., 2018; Sharma et al., 2006) and might be attributed to the high tolerance of fungi to temperature fluctuations (Sharma et al., 2006) and their ability to endure freezing conditions (Lipson et al., 2002; Ozerskaya et al., 2009). In our study, we observed an accumulation of fungal indicator OTUs from cold-adapted, opportunistic genera, such as *Mortierella*, *Mrakia* and *Leucosporidium*, in association with both the D-FTC and W-FTC treatments. *Mortierella* sp. have been reported to grow at subzero temperatures (Schmidt et al., 2008b) and to be dominant in alpine and subalpine ecosystems (Adamczyk et al., 2019; Schmidt et al., 2012). The basidiomycetous yeasts *Mrakia* and *Leucosporidium* have been reported to be abundant in permafrost (Frey et al., 2016). Thus, alterations within arctic and alpine soil fungal communities subsequent to FTCs might only be relevant after years of ongoing variations in the soil environmental conditions linked to climate change (Rinnan et al., 2007; Xiong et al., 2014).

In agreement with our second hypothesis, the compositional shifts caused by the FTCs were accompanied by an overall decrease in the rates of soil basal respiration. However, this decrease in respiration was not associated with changes in microbial abundances, thereby suggesting a drop in microbial activity (Bolter et al., 2005; Grogan et al., 2004; Sharma et al., 2006; Stres et al., 2010), which could have resulted from the slowing down of metabolic processes of microbial

cells acclimatizing to freezing conditions. The stress that the prolonged freezing conditions pose to the microbial cells could be reflected in the higher levels of labile nitrogenous compounds detected in the alpine soils subjected to W-FTCs, associated to the increase in necromass (Han et al., 2018; Schimel & Clein, 1996). The lack of changes in microbial abundance together with the larger shifts in microbial composition in the W-FTCs treatments could indicate higher turnover rates, where the dying cells would be rapidly replaced by the microorganisms tolerant to freezing. Further experiments targeting specifically the active microbial populations (i.e. RNA based) and assessing growth rates would be necessary to test how turnover rates are associated with changes in microbial abundance and composition caused by FTCs.

FTCs provoked only weak changes in C-, N- and P-acquiring enzymatic activities, they did not affect the concentrations of soil OM, and they altered labile C only to a very limited extent. These results contrast with previously published findings that report an increase in labile organics in the soil along with a shift in OM microbial degradation processes subsequent to FTCs, from the utilization of complex substrates contained in the OM to the consumption of simple compounds (Han et al., 2018; Schimel & Mikan, 2005). The large differences in soil properties and microbial diversity among the different soils could explain the inconsistent changes in enzymatic activities observed across the FTC treatments. The influence of multiple soil factors on the synthesis of C-, N- and P-acquiring enzymatic activities could have overridden the possible effects of FTCs in the measured enzymatic activities. The synthesis of extracellular enzymes is regulated by the interplay of multiple factors, including the content and quality of the OM and the specific energetic and nutritional demands of the microbial community members (Burns, 2010; Kim, 2015; Mooshammer et al., 2017; Sinsabaugh et al., 2009; Steinweg et al., 2013). This notwithstanding, the decoupling of the changes in microbial structure associated with the FTCs from the shifts in C-, N- and P-acquiring enzymatic activities might additionally be due to functional redundancy (Frossard et al., 2012; Mooshammer et al., 2017).

In our third hypothesis, we predicted that soils with a legacy of more frequent FTCs harbor microbial communities more tolerant to the repeated shorter and more frequent FTCs (e.g. microbial communities from south-facing soils were expected to be better adapted to frequent FTCs than those from north-facing soils), as proposed previously (Stres et al., 2010; Yergeau & Kowalchuk, 2008). However, in the present study, soil FTC legacy did not show a clear influence

on the tolerance of the microbial communities to the tested FTCs of distinct frequencies. This observation could indicate that FTCs might be governed by common climatological factors between alpine and arctic soil ecosystems, such as the dominance of subzero temperatures and snow coverage, which are known to shape microbial adaptations to temperature variations (Koponen & Baath, 2016). Further investigations will be needed to identify such factors and understand their influence on the local and global microbial responses of arctic and alpine soils to FTCs in a changing world.

3.6. Conclusions

Overall, our integrative investigation of the impact of FTC frequency on the structure and functionality of microbial communities of arctic and alpine soils suggested a trait-based response of prokaryotic communities to FTC frequency, where repeated short and frequent FTCs seemed to benefit copiotrophic bacteria while longer and less frequent FTCs seemed to promote oligotrophic bacteria. Opportunistic, cold-adapted fungi were prevalent after FTCs. Compositional shifts were coupled with a decline in microbial respiration rates, which was larger in the soils exposed to longer and less frequent FTCs. Changes in specific metabolic responses (C-, N- and P-acquiring extracellular enzymes) to FTCs were heterogenous among the soils, and microbial tolerance to FTCs may be modulated by climatological factors common to arctic and alpine regions rather than by FTC soil legacies. Although limited to the comparison of only two sites, our findings indicate that future climate scenarios with projected snow-scarce winters in the Arctic and the Alps, and therefore more frequent FTCs, could lead to noticeable compositional and functional shifts in the soil microbiome from both ecosystems. In turn, this could result on potential changes in OM quality, soil C stocks and soil CO_2 fluxes at the ecosystem level.

3.7. Data availability

All raw sequencing data generated for this study have been deposited in the NCBI Sequence Read Archive under the BioProject accession identifier PRJNA535397.

3.8. Author contributions

CP-M, AF and BF designed the study. CP-M and BF participated in sample collection. CP-M performed the experiment and wrote the manuscript with the help of AF and BF.

3.9. Funding information

This study was funded by the Swiss National Science Foundation (SNSF) under the grant IZLSZ2_170941.

3.10. Acknowledgments

We thank M. Björkman for providing climatic data from Lantjajaure Field Station; J. Donhauser, B. Stierli, L. Zourek and K. Kleeb for field and laboratory assistance; and R. Köchli, N. Hajjar and the WSL Central Laboratory for completing soil analyses. We also thank M. Dawes for her valuable contribution to the editing of this article. We acknowledge the Genetic Diversity Centre (GDC) of the ETH Zürich and the contribution of scientists at the McGill University and Génome Québec Innovation Center in Montreal, Canada for performing Illumina MiSeq sequencing.

3.11. Conflict of interest statement

The authors declare that they have no conflict of interest.

3.12. Supplementary materials

3.12.1. *Supplementary figures*

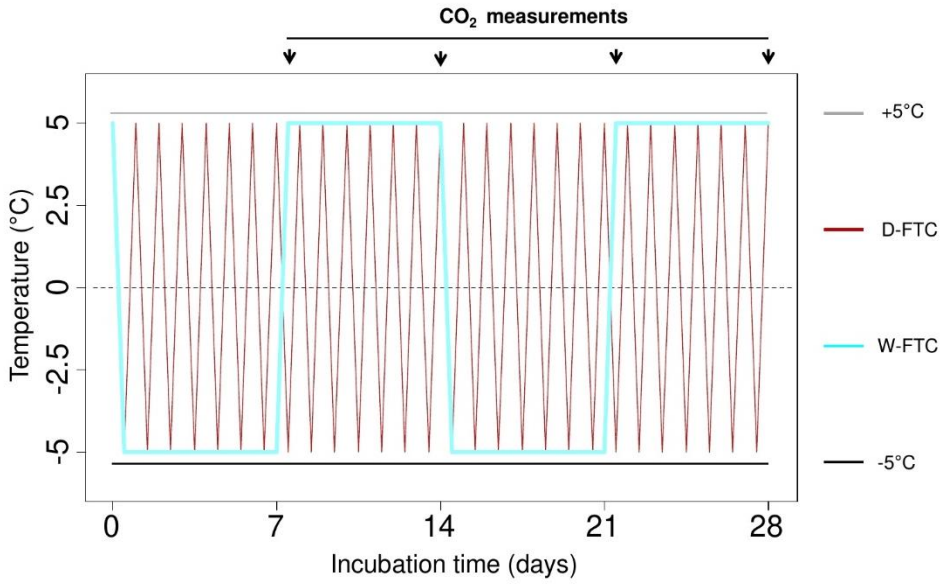

Figure S1. Scheme of the study design. Soil sample groups (each with four replicates) were subjected to (1) daily freeze-thaw cycles (D-FTC, 12h +5°C / 12h -5°C; red line); (2) weekly freeze-thaw cycles (W-FTC, 7 days +5°C / 7 days -5°C; blue line); (3) constant +5°C conditions (+5°C; gray line); or (4) constant -5°C conditions (-5°C; black line). Basal respiration (CO2) was measured once per week during the incubation period (28 days total).

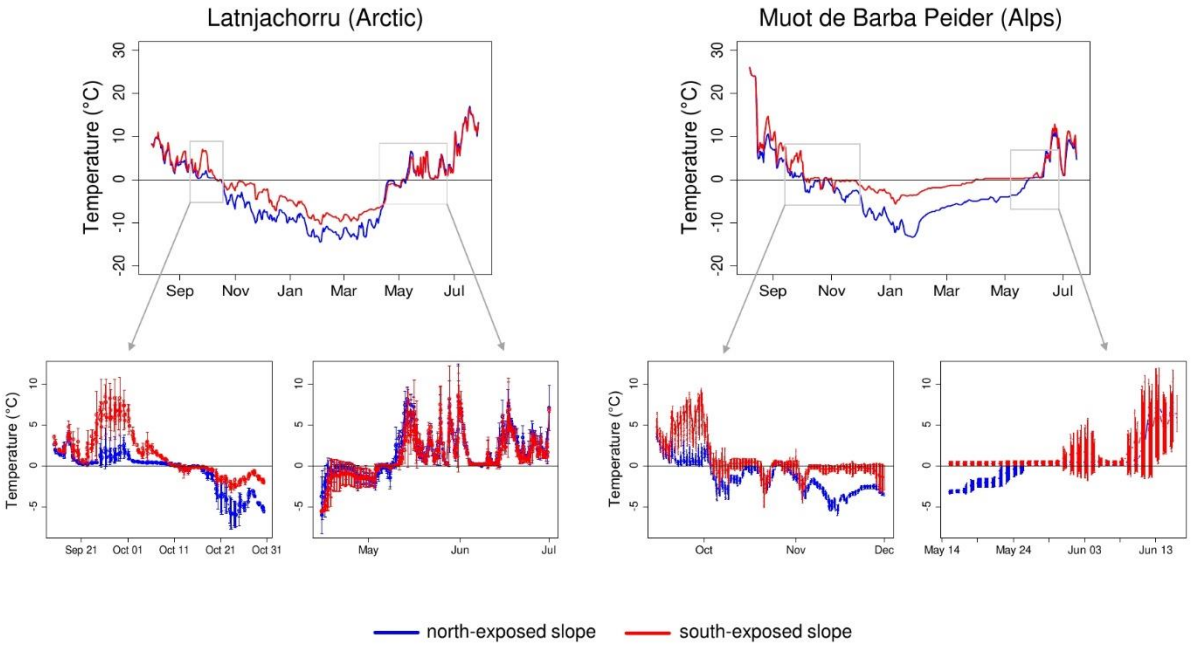

Figure S2. Yearly patterns of soil surface temperatures in the studied sites: Latnjachorru (Arctic) and Muot de Barba Peider (Alps). Values correspond to hourly temperature means; n=5 for the alpine soils and n=2 for the arctic soils. FTCs occur during the transitions from autumn to winter and spring to summer, as shown at higher time resolution in the lower part of the figure (Mean ± SD).

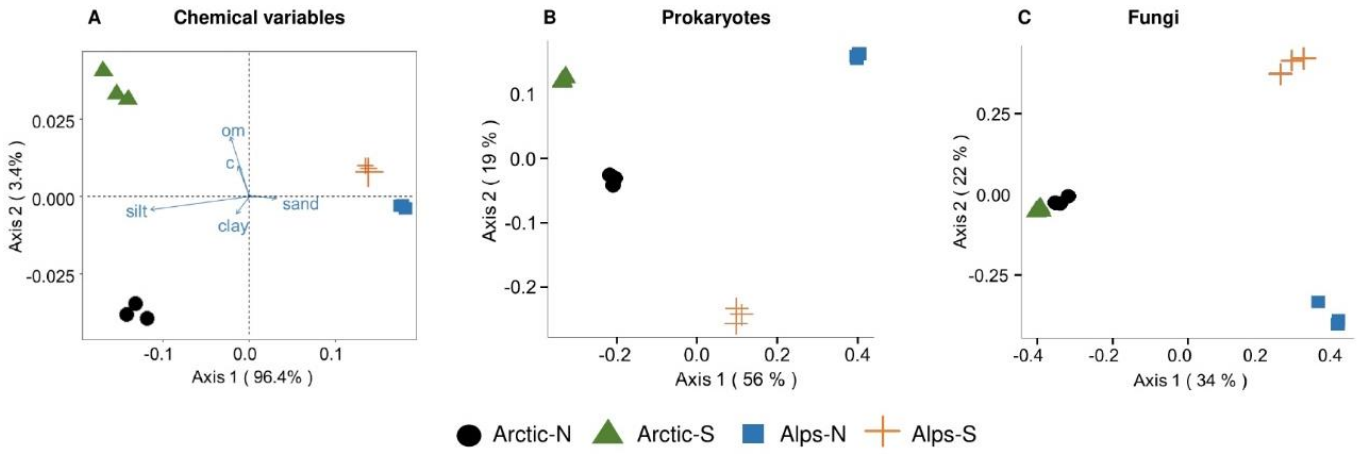

Figure S3. Differences among the four soils at the beginning of the experiment. **A**. PCA computed on normalized soil physico-chemical variables (Table S1). **B.** PCoA computed on Bray-Curtis dissimilarities based on prokaryotic OTU relative abundances. **C.** PCoA computed on Bray-Curtis dissimilarities based on fungal OTU relative abundances. Arctic: arctic soils, Alps: alpine soils, -N: north-facing, -S: south-facing.

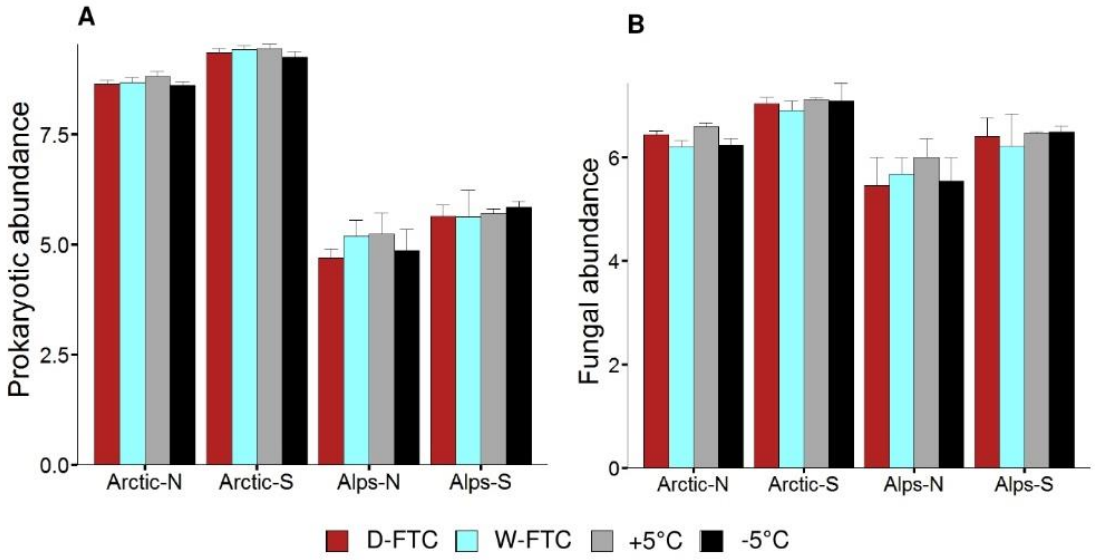

Figure S4. Prokaryotic (**A**) and Fungal (**B**) abundances. Abundance was measured as log10 of 16S gene copy number g^{-1} DW (prokaryotic abundance) and ITS gene copy number g^{-1} DW (fungal abundance). Mean ± SE (n=4). Arctic: arctic soils, Alps: alpine soils, -N: north-facing, -S: south-facing. D-FTC: daily freeze-thaw cycles (red), W-FTC: weekly freeze-thaw cycles (blue), +5°C: controls +5°C (gray), -5°C: controls -5°C (black).

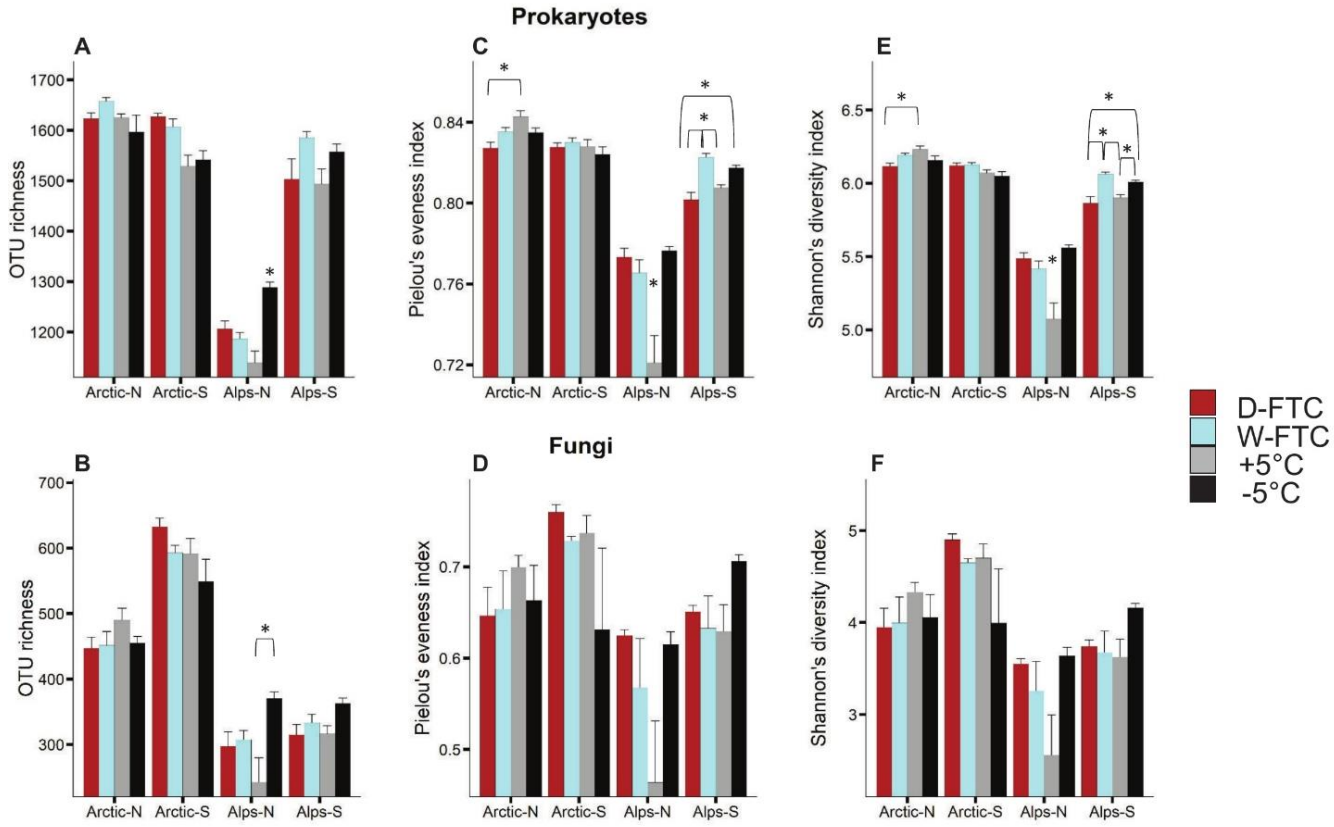

Figure S5. α-diversity of the prokaryotic and fungal communities for each treatments and soils. OTUs Richness (**A** and **B**), Pielou's evenness index (**C** and **D**) and Shannon diversity index (**E** and **F**). Asterisks over lines indicate statistically different groups ($p < 0.05$). Mean ± SE (n=4). Arctic: arctic soils, Alps: alpine soils, -N: north-facing, -S: south-facing. D-FTC: daily freeze-thaw cycles (red), W-FTC: weekly freeze-thaw cycles (blue), +5°C: controls +5°C (gray), -5°C: controls -5°C (black).

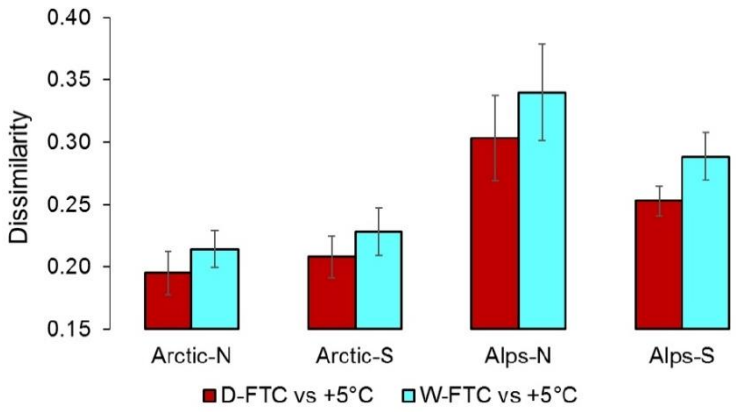

Figure S6. Dissimilarities between FTC treatments and controls. Bray-Curtis dissimilarity between daily freeze-thaw cycles (D-FTC) and controls +5°C (+5) and weekly freeze-thaw cycles and controls +5°C. Mean ± SD (n=4).

3.12.2. *Supplementary tables*

Because of their large extension **tables S8** and **S9** are provided electronically, in the published version of the Chapter:

https://www.frontiersin.org/articles/10.3389/fmicb.2020.00982/full#supplementary-material

Table S1. Physico-chemical properties of the studied soils. Mean ± SD (n=3).

	Arctic		Alps	
	N	**S**	**N**	**S**
Sand [%]	66.8 ± 0.14	66.8 ± 1.13	89.5 ± 0.00	86.3 ± 0.14
Silt [%]	27.30 ± 0.42	28.30 ± 0.99	7.00 ± 0.42	11.10 ± 0.28
Clay [%]	5.90 ± 0.28	4.90 ± 0.14	3.50 ± 0.42	2.60 ± 0.14
pH [$CaCl_2$]	4.24 ± 0.01	4.00 ± 0.05	4.59 ± 0.02	4.52 ± 0.01
WHC[1] [g H_2O g^{-1}]	0.46 ± 0.09	0.95 ± 0.21	0.22 ± 0.02	0.30 ± 0.01
WC [g H_2O g^{-1}]	0.25 ± 0.02	0.48 ± 0.01	0.07 ± 0.00	0.12 ± 0.01
C [%]	1.33 ± 0.02	4.05 ± 0.05	0.34 ± 0.00	0.82 ± 0.01
N [%]	0.08 ± 0.00	0.23 ± 0.00	0.03 ± 0.00	0.05 ± 0.00
OM [%]	2.43 ± 0.07	7.66 ± 0.55	1.13 ± 0.05	2.45 ± 0.18

[1]WHC: water holding capacity, WC: water content, OM: organic matter. Arctic: arctic soils, Alps: alpine soils, -N: north-facing, -S: south-facing

Table S2. Chemical properties in the soils at the end of the incubation for each FTCs treatment. Mean ± SD (n=4).

	Treatment	pH	OM[1]	labile OC	labile N	Ammonium	Nitrate[2]	Nitrite
Arctic-N	D-FTC	4.26 ± 0.01	2.23 ± 0.11	**57.744 ± 15.79^{ab}**	1.01 ± 0.53	0.71 ± 0.49	0.84 ± 0.56	b.d.l
	W-FTC	4.27 ± 0.02	2.33 ± 0.10	**44.91 ± 10.45^{b}**	1.11 ± 0.53	0.64 ± 0.25	3.35 ± 3.87	0.26 ± 0.00
	+5°C	4.22 ± 0.01	2.40 ± 0.06	**103.04 ± 31.82^{a}**	1.32 ± 0.39	0.63 ± 0.23	0.59 ± 0.12	b.d.l
	-5°C	4.28 ± 0.06	2.19 ± 0.17	**46.73 ± 11.10^{b}**	0.99 ± 0.28	0.69 ± 0.16	1.38 ± 0.74	0.16 ± 0.07
Arctic-S	D-FTC	4.15 ± 0.07	8.79 ± 0.32	156.42 ± 30.76	11.45 ± 1.89	**6.42 ± 1.45^{a}**	4.63 ± 1.32	0.35 ± 0.15
	W-FTC	4.18 ± 0.11	8.54 ± 0.21	134.97 ± 15.29	12.58 ± 0.84	**7.02 ± 0.87^{a}**	12.03 ± 0.72	0.2 ± 0.05
	+5°C	4.00 ± 0.03	7.38 ± 0.22	133.87 ± 28.58	9.26 ± 3.17	**3.63 ± 1.10^{ab}**	8.81 ± 6.48	0.67 ± 0.32
	-5°C	4.09 ± 0.08	7.71 ± 0.74	145.90 ± 22.88	12.28 ± 3.00	**5.85 ± 0.71^{b}**	4.14 ± 1.44	0.33 ± 0.12
Alps-N	D-FTC	4.57 ± 0.02	1.24 ± 0.05	42.20 ± 22.08	**0.62 ± 0.43^{c}**	0.63 ± 0.36	b.d.l	b.d.l
	W-FTC	4.57 ± 0.01	1.22 ± 0.04	43.60 ± 14.92	**2.73 ± 0.60^{b}**	0.48 ± 0.05	6.14 ± 3.81	0.32 ± 0.07
	+5°C	4.60 ± 0.02	1.25 ± 0.03	27.80 ± 7.50	**0.66 ± 0.29^{c}**	0.35 ± 0.08	b.d.l	b.d.l
	-5°C	4.57 ± 0.00	1.22 ± 0.05	30.54 ± 10.46	**3.96 ± 0.82^{a}**	0.73 ± 0.37	6.03 ± 2.73	0.33 ± 0.18
Alps-S	D-FTC	4.51 ± 0.01	2.27 ± 0.17	32.04 ± 10.62	**0.57 ± 0.46^{c}**	0.66 ± 0.26	b.d.l ±	b.d.l
	W-FTC	4.51 ± 0.01	2.33 ± 0.04	42.07 ± 43.13	**2.26 ± 0.59^{b}**	0.79 ± 0.14	4.03 ± 2.83	0.39 ± 0.26
	+5°C	4.48 ± 0.00	2.15 ± 0.05	32.04 ± 8.00	**0.55 ± 0.33^{c}**	0.62 ± 0.28	b.d.l ±	b.d.l
	-5°C	4.50 ± 0.01	2.22 ± 0.08	22.88 ± 7.91	**3.32 ± 0.21^{a}**	0.90 ± 0.17	5.16 ± 1.46	0.37 ± 0.09

Pair-wise statistical differences among treatments were assessed by Tukey HSD post-hoc tests in each subset of soils separately. Values in bold with different superscript letters represent groups in which differences were statistically significant ($p < 0.05$). [1]OM: organic matter, % DW, Labile OC: water-extractable organic carbon, Labile N: water-extractable total nitrogen, [2]Nitrate and Nitrite were measured for the soil water extracts with a Dionex Integrion high pressure chromatograph equipped with an AS9-HC 2*50 mm Viper Fitting pre-column coupled with an AS9-HC 2*250 mm Viper Fitting column (Thermo Fisher Scientific, Waltham, Massachusetts, USA). Labile OC, Labile N, Ammonium, Nitrate and Nitrite are measured in µg g^{-1} DW. Arctic: arctic soils, Alps: alpine soils, -N: north-facing, -S: south-facing, D-FTC: daily freeze-thaw cycles, W-FTC: weekly freeze-thaw cycles, +5°C: controls +5°C, -5°C: controls -5°C, b.d.l.: below detection limit.

Table S3. Tukey HSD post-hoc tests on differences among FTCs treatments for soil properties, microbial activities and microbial α-diversity parameters.

		Arctic-N				Arctic-S				Alps-N				Alps-S			
	Pairs	**diff[1]**	**lwr[2]**	**upr[3]**	***p***	**diff**	**lwr**	**upr**	**p.adj**	**diff**	**lwr**	**upr**	**p.adj**	**diff**	**lwr**	**upr**	***p***
Labile OC[4]	**D-FTC vs +5°C**	-0.57	-1.15	0.01	0.06												
	W-FTC vs +5°C	-0.81	-1.39	-0.23	**0.01**												
	D-FTC vs -5°C	0.20	-0.38	0.78	0.73												
	W-FTC vs -5°C	-0.04	-0.62	0.54	1.00												
	D-FTC vs W-FTC	-0.25	-0.83	0.33	0.60												
	+5°C vs -5°C	-0.77	-1.35	-0.19	**0.01**												
Labile N[5]	**D-FTC vs +5°C**									-0.04	-1.24	1.15	1.00	0.02	-0.87	0.91	1.00
	W-FTC vs +5°C									2.07	0.87	3.26	0.00	1.71	0.83	2.60	**0.00**
	D-FTC vs -5°C									-3.35	-4.54	-2.15	0.00	-2.75	-3.63	-1.86	**0.00**
	W-FTC vs -5°C									-1.24	-2.43	-0.04	0.04	-1.06	-1.94	-0.17	**0.02**
	D-FTC vs W-FTC									2.11	0.91	3.31	0.00	1.69	0.81	2.58	**0.00**
	+5°C vs -5°C									3.30	2.10	4.50	0.00	2.77	1.88	3.65	**0.00**
Ammonium	**D-FTC vs +5°C**					2.79	0.54	5.04	**0.01**								
	W-FTC vs +5°C					3.39	1.14	5.64	**0.00**								
	D-FTC vs -5°C					0.58	-1.67	2.82	0.87								
	W-FTC vs -5°C					1.18	-1.07	3.42	0.44								
	D-FTC vs W-FTC					0.60	-1.65	2.85	0.86								
	+5°C vs -5°C					2.21	-0.03	4.46	0.05								
Respiration	**W-FTC vs +5°C**	-1.56E-07	-2.25E-07	-8.65E-08	**5.21E-04**					-2.14E-07	-2.88E-07	-1.40E-07	**8.79E-05**	-2.40E-07	-2.94E-07	-1.86E-07	**1.52E-06**
	D-FTC vs +5°C	-2.32E-07	-2.96E-07	-1.68E-07	**1.71E-05**					-2.87E-07	-3.60E-07	-2.13E-07	**1.01E-05**	-2.85E-07	-3.38E-07	-2.31E-07	**3.56E-07**
	D-FTC vs W-FTC	-7.63E-08	-1.45E-07	-7.19E-09	**3.24E-02**					-7.27E-08	-1.41E-07	-4.40E-09	**3.82E-02**	-4.48E-08	-9.86E-08	8.98E-09	1.03E-01
Prokaryotic Richness	**D-FTC vs +5°C**									179.00	-4.55	362.55	0.06				
	W-FTC vs +5°C									170.75	-12.80	354.30	0.07				

	D-FTC vs -5°C					-297.50	-481.05	-113.95	**0.00**				
	W-FTC vs -5°C					-305.75	-489.30	-122.20	**0.00**				
	D-FTC vs W-FTC					-8.25	-191.80	175.30	1.00				
	+5°C vs -5°C					476.50	292.95	660.05	**0.00**				
Prokaryotic evenness	**D-FTC vs +5°C**	-0.02	-0.03	-0.01	**0.00**	0.04	0.01	0.08	**0.01**	-0.01	-0.01	0.00	0.10
	W-FTC vs +5°C	-0.01	-0.02	0.00	0.05	0.04	0.00	0.07	**0.02**	0.01	0.01	0.02	**0.00**
	D-FTC vs -5°C	-0.01	-0.02	0.00	0.14	0.00	-0.03	0.03	1.00	-0.02	-0.02	-0.01	**0.00**
	W-FTC vs -5°C	0.00	-0.01	0.01	0.98	-0.01	-0.04	0.02	0.77	0.00	0.00	0.01	0.38
	D-FTC vs W-FTC	0.01	0.00	0.02	0.26	-0.01	-0.04	0.02	0.87	0.02	0.01	0.03	**0.00**
	+5°C vs -5°C	-0.01	-0.02	0.00	0.09	0.05	0.02	0.08	**0.00**	0.01	0.00	0.02	**0.03**
Prokaryotic shannon	**D-FTC vs +5°C**	-0.15	-0.26	-0.03	**0.01**	0.40	0.12	0.69	**0.01**	-0.05	-0.18	0.09	0.71
	W-FTC vs +5°C	-0.06	-0.17	0.06	0.50	0.34	0.05	0.63	**0.02**	0.17	0.04	0.31	**0.01**
	D-FTC vs -5°C	-0.06	-0.17	0.06	0.52	-0.12	-0.41	0.17	0.60	-0.18	-0.31	-0.04	**0.01**
	W-FTC vs -5°C	0.03	-0.08	0.15	0.82	-0.19	-0.47	0.10	0.27	0.05	-0.09	0.18	0.73
	D-FTC vs W-FTC	0.09	-0.03	0.21	0.16	-0.06	-0.35	0.22	0.91	0.22	0.09	0.36	**0.00**
	+5°C vs -5°C	-0.09	-0.21	0.03	0.15	0.53	0.24	0.81	**0.00**	0.13	-0.01	0.26	0.07
Fungal richness	**D-FTC vs +5°C**					55.50	-42.42	153.42	0.37				
	W-FTC vs +5°C					64.50	-33.42	162.42	0.26				
	D-FTC vs -5°C					-70.75	-168.67	27.17	0.19				
	W-FTC vs -5°C					-61.75	-159.67	36.17	0.29				
	D-FTC vs W-FTC					9.00	-88.92	106.92	0.99				
	+5°C vs -5°C					126.25	28.33	224.17	**0.01**				

Tests were performed in each subset of soils separately. Only cases in which significant differences between pairs were detected are shown. α= 0.05. [1]diff: difference in observed means, [2]lwr: lower end point in the interval, [3]upr: upper end point in the interval, [4]Labile OC: water-extractable organic carbon, [5]Labile N: water-extractable total nitrogen. Arctic: arctic soils, Alps: alpine soils, -N: north-facing, -S: south-facing. D-FTC: daily freeze-thaw cycles, W-FTC: weekly freeze-thaw cycles, +5°C: controls +5°C, -5°C: controls -5°C. Numbers in bold indicate p-values < 0.05.

Table S4. Microbial activities in the soils at the end of the incubation for each FTCs treatment. Mean ± SD (n=4)

	Treatment	Respiration[1]			GLS[2]			XYL			AP			NAG			LAP			PP		
Arctic-N	D-FTC	4.11	±	1.12	72.43	±	36.64	11.54	±	8.32	204.3	±	135.11	19.21	±	13.68	17.62	±	17.1	1.21	±	0.99
	W-FTC	2.59	±	7.27	189.17	±	145.34	28.19	±	29.49	232.25	±	235.43	32.25	±	30.18	212.57	±	341.93	0.18	±	0.37
	+5◦C	8.22	±	0.50	92.49	±	46.44	12.45	±	4.67	194.26	±	73.5	22.25	±	11.3	13.25	±	22.43	1.22	±	1.21
Arctic-S	D-FTC	13.46	±	0.77	273.7	±	167.9	48.78	±	49.06	304.84	±	199.91	51.26	±	52.76	101.08	±	160.38	1.64	±	2.1
	W-FTC	8.80	±	0.52	274.1	±	80	69.89	±	25.16	471.05	±	159.69	76.36	±	30.63	0	±	0	1.71	±	1.96
	+5◦C	17.47	±	12.41	236.27	±	174.45	65.79	±	58.56	274.46	±	146.53	29.6	±	21.74	36.3	±	40.11	0.87	±	0.68
Alps-N	D-FTC	1.71	±	0.34	92.85	±	93.97	15.82	±	22.97	144.35	±	172.33	17.19	±	24.8	105.42	±	132.03	0.75	±	0.6
	W-FTC	0.80	±	0.30	74.6	±	54.91	13.11	±	15.4	138.71	±	126.21	16.68	±	19.3	149	±	206.9	0.45	±	0.36
	+5◦C	4.35	±	0.58	32.98	±	12.37	0.26	±	0.2	41.51	±	11.64	1.9	±	1.42	7.73	±	1.78	0.15	±	0.21
Alps-S	D-FTC	2.40	±	0.81	96.99	±	50.79	8.49	±	11.32	91.7	±	68.16	8.25	±	10.72	72.12	±	133.14	0.6	±	0.73
	W-FTC	1.46	±	0.13	54.45	±	23.12	2.5	±	2.63	56.57	±	10.76	2.57	±	2.1	20.08	±	32.2	0.29	±	0.35
	+5◦C	7.46	±	0.62	61	±	61.66	14.09	±	25.35	126.67	±	150.68	9.26	±	15.72	110.66	±	219.53	0.3	±	0.35

[1]Respiration is measured in nmol h^{-1} g DW, [2]GLS, XYL, AP, NAG and LAP are measured in µmol h^{-1} g DW, PP is measured in nmol h^{-1} g DW. GLS: β-glucosidases, XYL: β-xylosidases, AP: Phosphatases, NAG: N-acetyl-glucosaminidase, LAP: Leucine aminopeptidases, PP: Peroxidases. Arctic: arctic soils, Alps: alpine soils, -N: north-facing, -S: south-facing, D-FTC: daily freeze-thaw cycles, W-FTC: weekly freeze-thaw cycles, +5°C: controls +5°C, -5°C: controls -5°C

Table S5. Most common prokaryotes and fungal phyla across the treatments and soils of different origin at the end of the incubation.

	% reads[1]	# OTUs
PROKARYOTES		
Proteobacteria	21	2674
Chloroflexi	20	1203
Acidobacteria	17	892
Verrucomicrobia	12	800
Planctomycetes	10	1353
Actinobacteria	6	526
Bacteroidetes	4	614
Gemmatimonadetes	2	152
WD272	1.5	93
Parcubacteria	1	739
FUNGI		
Ascomycota	56	1790
Basidiomycota	14	832
Zygomycota	8	76

Prokaryotes phyla correspond to > 1% of the total prokaryotic reads. [1]% reads: number of reads assigned to the phyla divided by the total of prokaryotic reads (2 965 563) or fungal (2 110 838) reads, respectively.

Table S6. Prokaryotes and fungal phyla assign to OTU indicators associated with daily freeze-thaw cycles or weekly freeze-thaw cycles.

	Arctic-N		Arctic-S		Alps-N		Alps-S		Total OTUs	Mean seq	sd	Lifestyle	
	D-FTC	W-FTC	D-FTC	W-FTC	D-FTC	W-FTC	D-FTC	W-FTC					
PROKARYOTES													
Planctomycetes	18	20	17	24	17	18	25	45	184	12477	5149	o	
Acidobacteria	8	21	24	48	25	24	9	22	181	25565	9422	o	
Verrucomicrobia	4	35	16	29	6	23	2	33	148	37745	26545	o	***
Chloroflexi	10	11	25	19	18	14	13	22	132	27861	24126	o	
Actinobacteria	13		21	10	25	10	17	9	105	16349	13974	c (o)	*
Alphaproteobacteria	7	4	8	10	12	10	20	24	95	13446	9951	c (o)	
Betaproteobacteria	4	6	14	21	16	13	10	10	94	10750	6140	c	
Gammaproteobacteria	1	8	10	10	8	8	4	11	60	11020	4630	c (o)	
Deltaproteobacteria		1	6	2	5	5	10	10	39	706	638	o	
Bacteroidetes	2	6	11	20	2	1		14	56	2226	870	c (o)	
WD272	1	13	2	3	1	13	4	12	49	5522	2797	u$	*
Gemmatimonadetes		1	4	5	5	4	1	4	24	1179	1260	u	
Parcubacteria	1	2		5		1		5	14	60	49	u	*
Armatimonadetes		2	1	1	2	2		4	12	136	102	u	
Chlorobi		1					1	6	8	229	252		
Cyanobacteria	2	1		1		1	2	1	8	741	1438		
Nitrospirae	1	1	1	2		1	1	1	8	360	368	u	
Saccharibacteria		1	1	3	1				6	51	22	u	
Firmicutes			1	1			1	2	5	55	34	c (o)	
TA18	2	1					1	1	5	146	81	u$	
Microgenomates			2	2					4	180		u$	
SM2F11				1			0	3	4	432	586	u$	
Elusimicrobia	1			2					3	23	17	u	
SHA-109							1	1	2	26		u$	
Thermotogae							1	1	2	23			
TM6	1			1					2	18	19	u	
WCHB1-60				2					2	39		u	
Chlamydiae								1	1	6			
Deinococcus-Thermus					1				1	60			
Gracilibacteria				1					1	3		u$	

Hydrogenedentes				1					1	19		u$
unclassified	2		1	2	1	4	2		12	87	90	
TOTAL	**78**	**135**	**165**	**226**	**145**	**152**	**125**	**242**				
FUNGI												
Ascomycota	5	5	35	27	7	12	4	10	105	13538	13057	
Basidiomycota	2	3	7	8	0	3	2	1	26	5796	9804	
Zygomycota			0	1	3	2	0	1	7	10154	13684	
unclassified	1	2	7	6	3	5	3	2	29	2437	2577	
TOTAL	**8**	**10**	**49**	**42**	**13**	**22**	**9**	**14**				

ANOVAs were conducted to test differences in total OTU indicators assign to a same taxon between the daily freeze-thaw cycle (D-FTC) and weekly freeze-thaw cycle (W-FTC) treatments across the soils. Arctic: arctic soils, Alps: alpine soils, -N: north-facing, -S: south-facing, o: oligotrophic (yellow), c: copiotrophic (green), c(o): mostly copiotrophic but also association with oligotrophs, o(c): oligotrophic but also association with copiotrophs, u: unclear (blue); taxa with insufficient information (taxa with fewer than 10 cultivated strains recorded in the NCBI database or candidate taxa) to be classified to a life strategy, $ = candidate taxa, Grey color: higher number of OTUs. Mean seq and sd: mean number of reads across the samples classified to the specified taxa and 1 standard deviation. Grey: ***p<0.001, * p<0.05

Table S7. FunGuild functional assignments for fungal FTC-indicators.

Soil	OTUs	Taxon	Trophic.Mode	Guild	Growth morphology	Confidence ranking	D-FTC	W-FTC	+5°C	-5°C
Alps-N	OTUe_1006	Phaeosphaeria	saprotroph	undefined saprotroph	NA	probable	1	0	0	0
Alps-N	OTUe_106	Acarospora	symbiotroph	lichenized	thallus	highly probable	1	1	0	1
Alps-N	OTUe_1162	Lecanora	symbiotroph	lichenized	thallus	highly probable	1	0	0	0
Alps-N	OTUe_16	Mortierellaceae	saprotroph-symbiotroph	endophyte-litter saprotroph-soil saprotroph-undefined saprotroph	microfungus	possible	0	1	0	1
Alps-N	OTUe_1930	Lecidea	symbiotroph	lichenized	thallus	highly probable	0	1	0	0
Alps-N	OTUe_2000	Hypocreales	saprotroph	undefined saprotroph	microfungus	possible	1	1	0	0
Alps-N	OTUe_2157	Mortierellaceae	saprotroph-symbiotroph	endophyte-litter saprotroph-soil saprotroph-undefined saprotroph	microfungus	possible	1	0	0	0
Alps-N	OTUe_3013	Hyaloscypha	saprotroph	undefined saprotroph	NA	probable	0	1	0	0
Alps-N	OTUe_302	Mortierellaceae	saprotroph-symbiotroph	endophyte-litter saprotroph-soil saprotroph-undefined saprotroph	microfungus	possible	1	0	0	1
Alps-N	OTUe_39	Mortierellaceae	saprotroph-symbiotroph	endophyte-litter saprotroph-soil saprotroph-undefined saprotroph	microfungus	possible	1	1	0	1
Alps-N	OTUe_48	Cladosporium	pathotroph-saprotroph-symbiotroph	animal pathogen-endophyte-lichen parasite-plant pathogen-wood saprotroph	microfungus	possible	1	0	0	0
Alps-N	OTUe_610	Tremellales	pathotroph-saprotroph-symbiotroph	fungal parasite-undefined saprotroph	tremelloid-yeast	possible	0	1	0	0
Alps-N	OTUe_759	Tremella	pathotroph	fungal parasite-lichen parasite	facultative yeast-microfungus-tremelloid	probable	0	1	0	0
Alps-N	OTUe_768	Acarospora	symbiotroph	lichenized	thallus	highly probable	1	1	0	1
Alps-S	OTUe_2615	Geomyces	saprotroph	soil saprotroph	microfungus	probable	1	0	0	1
Alps-S	OTUe_2633	Geomyces	saprotroph	soil saprotroph	microfungus	probable	1	0	0	1
Alps-S	OTUe_2979	Tetracladium	saprotroph	undefined saprotroph	NA	probable	1	0	0	0
Alps-S	OTUe_420	Sporormiaceae	saprotroph	dung saprotroph-plant saprotroph	microfungus	probable	0	1	0	0
Arctic-N	OTUe_24	Tomentella	symbiotroph	ectomycorrhizal	corticioid	highly probable	0	1	0	0
Arctic-N	OTUe_3640	Cladophialophora	saprotroph	undefined saprotroph	facultative yeast	probable	1	0	0	0
Arctic-N	OTUe_3727	Eurotiales	saprotroph	undefined saprotroph	microfungus	possible	1	0	0	1
Arctic-N	OTUe_541	Thelephoraceae	saprotroph-symbiotroph	ectomycorrhizal-undefined saprotroph	clavarioid	probable	0	1	0	0
Arctic-N	OTUe_808	Clavulina	symbiotroph	ectomycorrhizal	clavarioid	highly probable	0	1	0	0
Arctic-S	OTUe_1077	Capronia	symbiotroph	endophyte	facultative yeast	highly probable	1	0	0	0
Arctic-S	OTUe_1187	Ramariopsis	saprotroph	undefined saprotroph	clavarioid	probable	0	1	0	0
Arctic-S	OTUe_1189	Devriesia	pathotroph	plant pathogen	NA	probable	1	0	0	0
Arctic-S	OTUe_154	Cadophora	symbiotroph	endophyte	microfungus	highly probable	1	1	0	0
Arctic-S	OTUe_1736	Cladophialophora	saprotroph	undefined saprotroph	facultative yeast	probable	1	1	0	0

Arctic-S	OTUe_1872	Porpidia	symbiotroph	lichenized	thallus		highly probable	1	0	0	0
Arctic-S	OTUe_2	Geomyces	saprotroph	soil saprotroph	microfungus		probable	1	1	0	0
Arctic-S	OTUe_212	Inocybaceae	symbiotroph	ectomycorrhizal	agaricoid		probable	0	1	0	0
Arctic-S	OTUe_2179	Clavariaceae	saprotroph-symbiotroph	lichenized-undefined saprotroph	clavarioid		probable	1	1	0	1
Arctic-S	OTUe_2353	Eurotiales	saprotroph	undefined saprotroph	microfungus		possible	1	1	0	0
Arctic-S	OTUe_2498	Mortierellaceae	saprotroph-symbiotroph	endophyte-litter saprotroph-soil saprotroph-undefined saprotroph	microfungus		possible	0	1	0	0
Arctic-S	OTUe_2735	Tetracladium	saprotroph	undefined saprotroph	NA		probable	1	0	0	0
Arctic-S	OTUe_2871	Herpotrichiellaceae	pathotroph-saprotroph	animal pathogen-fungal parasite-undefined saprotroph	facultative yeast-microfungus		probable	1	0	0	0
Arctic-S	OTUe_2974	Herpotrichiellaceae	pathotroph-saprotroph	animal pathogen-fungal parasite-undefined saprotroph	facultative yeast-microfungus		probable	1	0	0	0
Arctic-S	OTUe_3179	Sebacina	symbiotroph	ectomycorrhizal-orchid mycorrhizal-root associated biotroph	NA		possible	1	1	0	0
Arctic-S	OTUe_32	Hygrocybe	saprotroph-symbiotroph	undefined saprotroph-undefined biotroph	agaricoid		probable	1	1	0	0
Arctic-S	OTUe_342	Clavaria	saprotroph	undefined saprotroph	clavarioid		probable	0	1	0	0
Arctic-S	OTUe_473	Sebacina	symbiotroph	ectomycorrhizal-orchid mycorrhizal-root associated biotroph	NA		possible	1	1	0	0
Arctic-S	OTUe_716	Stilbella	saprotroph-symbiotroph	dung saprotroph-endophyte-wood saprotroph	NA		possible	1	1	0	0
Arctic-S	OTUe_76	Cladosporium	pathotroph-saprotroph-symbiotroph	animal pathogen-endophyte-lichen parasite-plant pathogen-wood saprotroph	microfungus		possible	1	0	0	0
Arctic-S	OTUe_910	Ramariopsis	saprotroph	undefined saprotroph	clavarioid		probable	1	0	0	0
Arctic-S	OTUe_939	Clavaria	saprotroph	undefined saprotroph	clavarioid		probable	1	1	0	0

1: significantly associated ($p < 0.05$), 0: non-significantly associated. pink: associated with the daily freeze-thaw cycles (D-FTC), yellow: associated with the weekly freeze-thaw cycles (W-FTC), blue: associated with both FTC treatments, green: highly probable and probable that the OTU truly belongs to the assigned taxon, NA: Not Assigned or unknown. Arctic: arctic soils, Alps: alpine soils, -N: north-facing, -S: south-facing, +5°C: controls +5°C, -5°C: controls -5°C.

4. CHAPTER 4. Fast and persistent responses of alpine permafrost microbial communities to in situ warming

Authors: **Carla Perez-Mon[1]**, Beat Stierli[1], Michael Plötze[2], Beat Frey[1]*

[1]Rhizosphere Processes Group, Swiss Federal Research Institute WSL, Birmensdorf, Switzerland

[2]Institute for Geotechnical Engineering, ETH Zurich, Zurich, Switzerland

∗**Correspondence to:** Beat Frey, Swiss Federal Research Institute WSL, Zuercherstrasse 111, CH-8903 Birmensdorf, Switzerland. Tel: +41-44-739-25-41; E-mail: beat.frey@wsl.ch.

Keywords: alpine, climate change, microbial community, permafrost, transplantation, warming

4.1. Abstract

Global warming in mid-latitude alpine regions results in permafrost thawing, together with greater availability of carbon and nutrients in soils and frequent freeze–thaw cycles. Yet it is unclear how these multifactorial changes will shape the 1m-deep permafrost microbiome in the future, and how this will in turn modulate microbially-mediated feedbacks between mountain soils and climate (e.g., soil CO_2 emissions). To unravel the responses of the alpine permafrost microbiome to in situ warming, we established a three-year experiment in a permafrost monitoring summit in the Alps. Specifically, we simulated conditions of warming by transplanting permafrost soils from a depth of 160 cm either to the active-layer topsoils in the north-facing slope or in the warmer south-facing slope, near the summit. qPCR-based and amplicon sequencing analyses indicated an augmented microbial abundance in the transplanted permafrost, driven by the increase in copiotrophic prokaryotic taxa (e.g. *Noviherbaspirillum* and *Massilia*) and metabolically versatile psychrotrophs (e.g. *Tundrisphaera* and *Granulicella*); which acclimatized to the changing environment and potentially benefited from substrates released upon thawing. Metabolically restricted Patescibacteria lineages vastly decreased with warming, as reflected in the loss of α-diversity

in the transplanted soils. Ascomycetous sapro-pathotrophs (e.g. *Tetracladium*) and a few lichenized fungi (e.g. *Aspicilia*) expanded in the transplanted permafrost, particularly in soils transplanted to the warmer south-facing slope, replacing basidiomycetous yeasts (e.g. *Glaciozyma*). The transplantation-induced loosening of microbial association networks in the permafrost could potentially indicate lesser cooperative interactions between neighboring microorganisms. Broader substrate-use microbial activities measured in the transplanted permafrost could relate to altered soil C dynamics. The three-year simulated warming did not, however, enhance heterotrophic respiration, which was limited by the carbon-depleted permafrost conditions. Collectively, our quantitative findings suggest the vulnerability of the alpine permafrost microbiome to warming, which might improve predictions on microbially-modulated transformations of mountain soil ecosystems under the future climate.

4.2. Introduction

Global warming is amplified in polar and mid-latitude alpine regions, with predicted increases in air temperature between 2 and 8°C by 2100 (Hock et al., 2019; IPCC, 2014). Permafrost, i.e. soil at subzero temperatures located under a seasonally frozen active layer, is a major component of polar and alpine cryoenvironments (Donhauser & Frey, 2018; Margesin, 2009). Elevated temperatures are causing extensive permafrost thawing, which results in increased soil water availability and the release of organic materials previously occluded in the frozen layers (Abbott et al., 2014; Chen et al., 2016; Gobiet et al., 2014). Reduced snowfall results in poorly insulated active layers, which therefore experience frequent freeze–thaw cycles (FTCs; Henry, 2008) . The warming-associated expansion of plants towards higher latitudes and altitudes (Elmendorf et al., 2012; Steinbauer et al., 2018) might translate into permafrost soils with augmented inputs of carbon (C) and nutrients (Hagedorn et al., 2019; Keuper et al., 2020). The warming-induced changes in soil temperature, moisture, C and nutrients impact the polar and alpine permafrost microbiome (i.e. prokaryotes and fungi), with direct consequences on microbially mediated soil processes (e.g. C mineralization) that might influence soil fertility (Fahad et al., 2021; Sönmez et al., 2021) and projected soil–climate feedbacks (e.g. soil CO_2 release) at latitudinal and global scales (Donhauser & Frey, 2018; Hock et al., 2019; Jansson & Hofmockel, 2020; Mackelprang et al., 2016; Nikrad et al., 2016).

The microbial responses of permafrost to warming have mainly been investigated in the polar regions, especially in the Arctic, whereas the alpine permafrost at lower latitudes is still poorly studied. Mid-latitude permafrost often occurs on poorly vegetated or barren steep slopes of mountains, above 2500 m a.s.l. (Donhauser & Frey, 2018; Margesin, 2009). In comparison with the permafrost soils at the polar regions, alpine permafrost is “warm” (0 to -2°C) and located at soil depths below 1 m. Similar to Antarctic soils and unlike Artic permafrost, alpine permafrost soils at lower latitudes are rocky, well-drained and depleted in organic carbon (i.e. global SOC stock of 66 Pg; Bockheim & Munroe, 2014).

Despite being C-poor, alpine permafrost soils harbor taxonomically and metabolically diverse prokaryotic (i.e. Bacteria and Archaea) and fungal communities (Frey et al., 2016; Hu et al., 2015; Margesin, 2012; Margesin & Collins, 2019; Perez-Mon et al., 2021) that are sensitive to the changing climate (Donhauser & Frey, 2018). Short-term (< 1 year) laboratory-controlled experiments conducted on Asian and European alpine permafrost soils have shown that conditions of elevated soil temperatures (Chen et al., 2021; Donhauser et al., 2020; Luláková et al., 2019), greater availability of soil C and nutrients (Adamczyk et al., 2021) or frequent FTCs (Perez-Mon et al., 2020) shift the structure of the soil prokaryotic communities. Fast-growing and metabolically versatile (i.e. *copiotrophic*) taxa respond quickly to the increased temperatures and substrates, outcompeting stress-tolerant and slow-growing (i.e. *oligotrophic*) taxa (Fierer et al., 2007; Ho et al., 2017), which abound in the energy-limited and freezing permafrost environments (De Maayer et al., 2014; Frey et al., 2016; Mackelprang et al., 2017). Furthermore, C and nutrient amendments in alpine permafrost and mineral Arctic soils have been shown to boost fungal growth, promoting the expansion of fungi over bacteria and compositional variations within the fungal communities (Adamczyk et al., 2020; Adamczyk et al., 2021; Deslippe et al., 2012). The enrichment in copiotrophs and fungi could translate into soils with broader substrate-use microbial activities (Llado & Baldrian, 2017), as indicated by Biolog assays applied to thawed alpine permafrost amended with labile C (Adamczyk et al., 2021) and Siberian soils incubated at increased temperatures (Ernakovich & Wallenstein, 2015). Greater soil microbial abundances and heterotrophic respiration rates have also been observed in alpine permafrost exposed to laboratory-induced warming (Adamczyk et al., 2021; Bao et al., 2016).

Soil transplantation field experiments conducted in the Tibetan mountains have made it possible to extrapolate the results from laboratory studies to natural scenarios, where the soil microbiota respond to multifactorial conditions of warming over the time span of years. Congruent with laboratory observations, downward transplantations of Tibetan grassland topsoils from > 3600 m a.s.l. to the warmer thermal regimes of vegetated land at < 3200 m a.s.l. led to an augmented microbial biomass in mineral layers (Gou et al., 2015) and long-lasting increases in copiotrophic bacterial groups (e.g. Actinomycetales; Rui et al., 2015; Ho et al., 2017) , as well as altered soil C and nitrogen (N) cycling functions and elevated rates of C mineralization (Yue et al., 2015; Zheng et al., 2014). In the alpine permafrost layers, where habitat conditions have remained stable for millennia, abrupt *in situ* temperature changes could affect the microbial communities more strongly than in the topsoils. Thawing might hamper long-term trophic or cooperative interactions between permafrost microorganisms, i.e. between neighbors failing to adapt to the changing environmental conditions. This could loosen microbial association networks in the permafrost, as observed for heavily disturbed agricultural soils (Banerjee et al., 2019), and it could potentially enhance the vulnerability of the alpine permafrost microbiome to warming. Existing quantitative data on the impacts of warming on the alpine soil microbiome under field conditions is, however, limited to shallow active layers (< 20 cm of depth). To the best of our knowledge, field-manipulation warming experiments outside the Tibetan regions and including both active and the 1m-deep permafrost layers are lacking.

We conducted a soil transplantation field experiment at the long-term permafrost monitoring site on *Muot da Barba Peider* (MBP) in eastern Switzerland (Frey et al., 2016; Haberkorn et al., 2021) for three years (2016 to 2019) to evaluate the *in situ* effects of climate warming on the diversity, community structure, association networks, abundances and activities of the alpine permafrost and active-layer microbiota. Similar to other mountain systems, permafrost in MBP is found near the summit, below a depth of 150 cm on the barren north-facing (N) slope. The south-facing (S) slope of MBP experiences a warmer climate than the N slope, featuring topsoils with 2–3°C higher soil temperatures, less snow and more vegetation, which results in greater soil C and nutrient contents. We simulated conditions of warming on MBP permafrost and overlaying active-layer topsoils by transplanting soils near the summit from the N to the S slope, where they were placed in the topsoil at a depth of 18 cm (Fig. 1). Permafrost

was also transplanted to the N topsoils. Reciprocally, we simulated conditions of cooling (colder climate) in the active layers by transplanting topsoils from the S to the N slope. Opposing microbial responses between the simulated warming and cooling helped us to identify climate-microbial links in the soils. We hypothesized that three years of *in situ* simulated warming would: (1) lead to augmented soil microbial abundance, associated with abundance increases of fungi and copiotrophic over oligotrophic prokaryotes and shifts in soil microbial diversity; (2) loosen microbial association networks in the soils; and (3) result in enhanced substrate-use microbial activities and soil CO_2 effluxes.

4.3. Materials and methods

4.3.1. *Site description*

Muot da Barba Peider (2979 m a.s.l., N 46°29.78040' E 009°55.88700') is located in the upper Engadine valley in eastern Switzerland. This site is part of the Swiss Permafrost Monitoring Network (PERMOS; http://www.permos.ch/). Hourly soil temperatures measured at a depth of 5 cm (M-Log5W-SIMPLE sensors; GeoPrecision GmbH, Ettlingen, Germany) during three consecutive years (2016 to 2019) had mean annual values of -2°C (ranging from -14°C to 21°C) in the north-facing (N) slope and 1°C (ranging from -8°C to 24°C) in the south-facing (S) slope. The N slope has permafrost below a depth of 150 cm (temperatures of 0 to -4°C measured at a depth of 1-2 m from August 2016 to August 2019, PERMOS borehole MBP_0196, 2946 m a.s.l., N 46°29.784' E 009°55.8645; http://www.permos.ch/data.html). The S slope is only seasonally frozen (Zenklusen Mutter et al., 2010). Mean annual precipitation in the region was 941 mm for the period of 2016-2019 (automatic meteorological station of Bernina, N 46°26.4656, E 009°59.2132, 2090 m a.s.l.; www.meteoswiss.admin.ch). Soils in the S slope experience more FTCs than in the N slope (Perez-Mon et al., 2020).

The soils around the MBP summit are mostly composed of gravel and sand materials, with low pH (< 6) and extremely low contents of water, C (< 1%) and N (≤ 0.1%), especially on the N slope (Table S1). The bedrock in MBP is gneiss from the upper Austroalpine Languard nappe. Quartz and feldspars are the dominant minerals. Vegetation mostly occurs in the S slope, with scattered occurrences of the taxa *Poa*, *Cerastium* and *Jacobea* spp. (Frey et al., 2016).

4.3.2. *Experiment set up*

The soil transplantation experiment in MBP was established during the summer of 2016 (Fig. 1). In the N (N 46.49634, E 9.93145) and the S (N 46.49587, E 9.93226; 2979 m a.s.l.) slope, 10 independent active-layer topsoil samples (approx. 200 g of fresh soil), separated by distances of 2–3 m, were collected using a soil corer (10 cm diameter x 10 cm height). A total of 20 topsoil samples were produced (10 samples × 2 slopes). Constrained by time and logistics, a maximum of three soil profiles of approx. 2 m^2 and separated by approx. 5 m were excavated with shovels on the N slope, down to a depth of 180 cm. Soils were collected at a depth of 160 cm from each profile using the corer, producing a total of 3 independent permafrost (P) samples. Two additional permafrost samples were produced by pooling soils from the three profiles. All collected samples were homogenized and transferred to 2L stainless-steel containers (12 cm diameter × 18 cm height, catalogue no. 301.317.16, IKEA, Älmhult, Sweden). Materials were sterilized with 70% ethanol between all steps of sample collection and processing.

The containers were divided in seven groups, each with five replicates: three groups of permafrost soils (P) and two groups each of N and S active-layer topsoils (N and S). For the transplantation, the containers filled with the soils were placed in the N slope (Nn, Pn and Sn containers) or the S slope (Ns, Ps and Ss containers). Climatic conditions of *warming* (i.e. warming treatments) were applied to the N and P soils. One group of N topsoils was transplanted to the S slope (Ns, active-layer warming) and the other to the N slope (Nn, disturbance control) (Fig. 1). Comparably, one group of P soils was transplanted to the topsoil in the N slope (Pn, permafrost warming 1) and a second group was transplanted to the S slope (Ps, permafrost warming 2; warmest climate). The third group of P samples were kept within the permafrost table (Pp). These containers will serve as long-term disturbance controls in future studies (e.g. resampling after ≥ 5 years) and were not sampled in the present study. Here, intact permafrost soils collected at the start of the transplantation experiment (t0, time zero) were used as controls. Climatic conditions of *cooling* (i.e. cooling treatments) were applied to the S soils: one group of S soils was transplanted to the N slope (Sn, active-layer cooling) and the other to the S slope (Ss, disturbance control).

In each slope the containers were buried (transplanted) at a depth of 18 cm, in a randomized arrangement. The containers were perforated at the sides and the bottom to prevent waterlogging and to allow the exchange of solutions between the soil and the surroundings (Zumsteg et al., 2013). The Pp long-term controls were produced by burying P soils at a depth of 180 cm, in one of the excavated profiles in the N slope. Profiles were sealed using the excavated soil.

The transplantation experiment started on 17 August 2016. The transplanted soils (i.e. transplants) were incubated in the field for three years. During the incubation, soil temperatures were measured continuously (via iButtons, Maxim Integrated, San Jose, California, USA) at a depth of 3 cm in five of the transplants incubated in each slope. Soil aliquots of all transplants were collected one (t1), two (t2) and three (t3) years after transplantation (summers of 2017, 2018 and 2019). In addition, N and S topsoils were collected every year around the experimental site to monitor temporal variations in the soil microbiota. Aliquots of intact P, N and S soils were also collected at t0. The collected soils were transported on ice from the field to the WSL laboratory facilities, where they were sieved with a 2 mm mesh and stored at -20°C (for genetic analyses) or 4°C (for microbial activity and soil chemical analyses). Intact permafrost samples at t0 were also stored at the *in situ* temperature of -1.5°C in a growth chamber at the Swiss Federal Research Institute WSL.

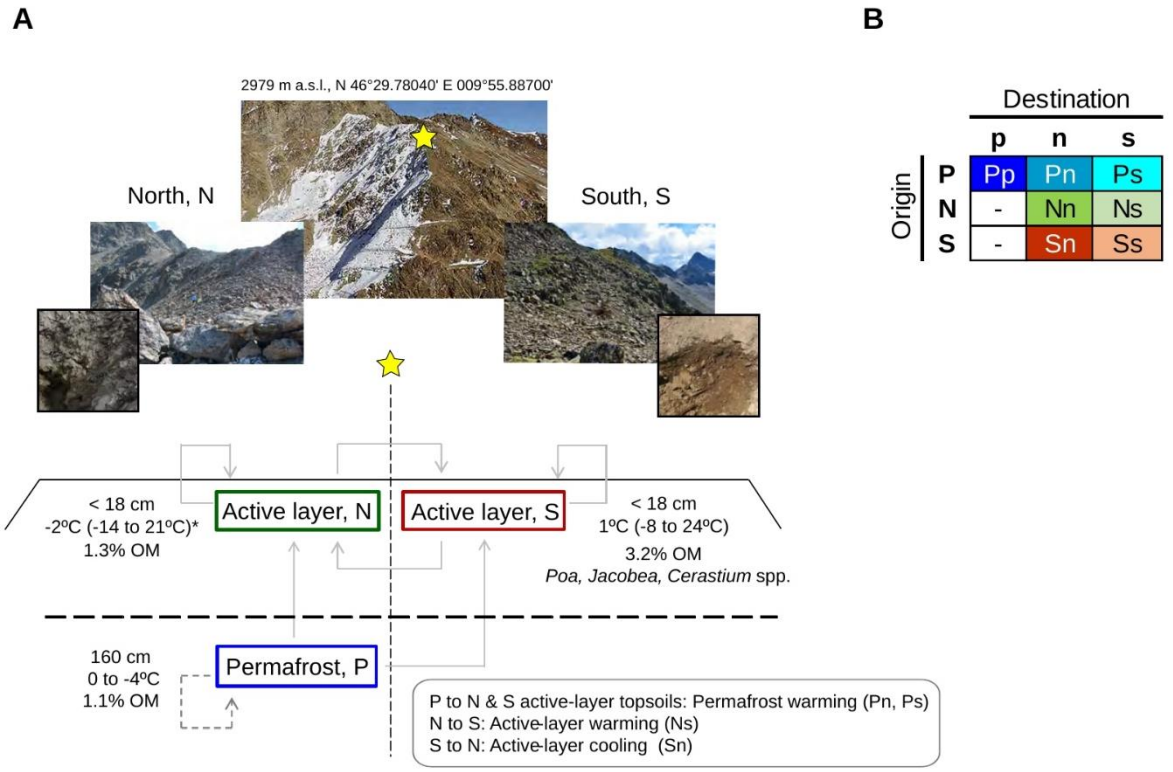

Figure 1. Visualization of Muot da Barba Peider (MBP) and scheme of the experimental set-up. **A.** The upper panel shows an aerial view of the MBP summit (yellow star), with overlapping images of the north-facing and south-facing sampling locations near the summit, and close-up photographs of the active layers. The lower panel shows the properties of the permafrost and north- and south-facing active-layer topsoils, accompanied by a representation of the transplantations using arrows. Permafrost (at 160 cm depth) and active-layer topsoils (at a depth of 10 cm) were collected in the north-and south-facing slopes near the summit of MBP. The collected soils were transplanted (solid-line arrows) to the north- and south-facing active-layer topsoils (at a depth of 18 cm). Permafrost soils were also transplanted within the permafrost table (dashed-line arrow). **B.** Tabular representation of the transplantation experiment. Capital letters represent the original soils: permafrost (P), north-facing active layer (N) and south-facing active layer (S), whereas lower-case letters represent the destination to which the soils were transplanted. Ns, Pn and Ps are warming treatments, whereas Sn represents cooling. Nn, Ss and Pp (to be used in future studies) are soil disturbance controls. *Average and range (in brackets) of topsoil temperatures measured during the three years of the experiment. Permafrost temperatures correspond to ground temperature measurements at a depth of 1-2 m (PERMOS borehole MBP_0196, 2946 m a.s.l., N 46°29.784' E 009°55.8645; http://www.permos.ch/data.html) for the entire period of August 2016 to August 2019. OM: organic matter. The aerial photograph of MBP was provided by Dr. Marcia Phillips.

4.3.3. *Amplicon sequencing, OTU clustering and taxonomic assignments*

DNA was extracted from each individual soil sample (1–2.5 g aliquots) using the DNeasy PowerSoil Kit (Quiagen, Hilden, Germany), and the DNA extracts were quantified with PicoGreen (Invitrogen, Carlsbad, CA, USA), following the manufacturer's instructions. To remove foreign DNA and prevent microbial contaminations, working bench surfaces and non-

autoclavable materials were cleaned with 5% sodium hypochlorite and 70% ethanol solutions prior to the DNA extractions. Triplicate PCR amplifications of the V3–V4 region of the 16S rRNA gene (prokaryotes) and of the ITS2 genomic region (fungi) were performed on 10 ng of the extracted DNA samples, using the primer pairs 341F/806R and ITS3/ITS4, and the conditions described in Frey et al. (2016). Negative controls for the DNA extractions (extraction buffer without soil) and PCR amplifications (high-purity water without DNA template) were included. The amplicon triplicates were pooled, purified (AMPure XP beads, Beckman Coulter, Beverly, MA, USA) and sent to the Génome Québec Innovation Centre at McGill University (Montreal, Canada), where the pools were paired-end sequenced using the Illumina MiSeq v3 platform (Illumina Inc., San Diego, CA, USA).

Quality filtering of the prokaryotic and eukaryotic sequences, clustering (at 97% identity) into operational taxonomic units (OTUs), and assignment of OTUs to taxa were accomplished as described previously (Frey et al., 2016), using a customized pipeline based on UPARSE (Edgar, 2013; Edgar & Flyvbjerg, 2015) and implemented in USEARCH v.9.2 (Edgar, 2010). OTUs were classified to taxa by querying centroid sequences against reference databases, using the naive Bayes classifier (Wang et al., 2007) implemented in MOTHUR (Schloss et al., 2009), with a minimum bootstrap support of 60%. Prokaryotic sequences were queried against the SILVA database v138 (Quast et al., 2013). Eukaryotic OTUs were first curated using a custom-made ITS2 database generated from NCBI GenBank. Centroid sequences assigned to fungi were classified to finer taxonomic levels with the UNITE database v8.2 (Nilsson et al., 2019). Singletons and chimeras were removed on-the-fly during OTU clustering. Prokaryotic or fungal taxa represented by less than 1% of all sequences were considered low-abundant (Shade et al., 2014; Zhao et al., 2019).

4.3.4. *Microbial abundance*

Bacterial and fungal abundance were estimated by quantitative PCR (qPCR) on a 7500 Fast Real-Time PCR System (Thermo Fisher Scientific, Waltham, MA, USA). qPCR reactions were prepared using 6.6 µl of the DNA extracts and the primer pairs 27F/519R and ITS3/ITS4, which amplify the V1–V3 region of the 16S rRNA gene in bacteria and the ITS2 genomic region in fungi, respectively. qPCR programs were performed as described by Hartmann et al. (2014)

and Frey et al. (2021). Three standard curves (correlations ≥ 0.99) per target region (16S or ITS2) were obtained using 10-fold serial dilutions (10^{-1} to 10^{9} copies per µl) of plasmids cloned with the targets.

4.3.5. *Substrate-use microbial activities*

The microbial utilization of 31 substrates (i.e. substrate-use activities) was investigated using 96-well EcoPlates™ (Biolog Inc., Hayward, CA) for the P, N and S soil transplants (five replicates) collected at t3, and for the P samples at t0, stored at -1.5°C (three replicates). Soils were pre-incubated for one week at 4°C, followed by one day of pre-incubation at 15°C. Soil suspensions were prepared by adding a 0.9% NaCl solution to the soils (10:1 v/w) and shaking the mix for 2 h at 15°C. To reduce the interference of soil materials in the colorimetric assays, soils were left to settle for 10 min and the clear supernatant was diluted 1:10 fold. The EcoPlate wells were inoculated with 125 µl of the dilutions and incubated at 15°C in dark growth chambers. Flasks containing water were added to the chambers to minimize evaporation. A soil temperature (at a depth of 5 cm) of 15°C was frequently measured at the MBP summit during summer (Fig. S1), and short-term incubations of Alpine soils at this temperature have only shown minor effects on the microbial communities (Adamczyk et al., 2021; Donhauser et al., 2020; Ruthi et al., 2020).

Absorbance (A) of the inocula was measured at 595 nm with an INFINITE F200 reader (TECAN, Männedorf, Switzerland) every 2–3 days. Measurements were collected until color saturation (A ≥ 2, exhaustion of the tetrazolium dye), which occurred between 1 (S soils) and 4 weeks (P soils). The absorbance values of the control wells (water) were subtracted from the values of the wells containing the substrates. Maximum rates (r, h^{-1}) of substrate-use microbial activities were calculated by fitting the time courses (hours, h) of absorbance (A) measurements to logistic growth models ($A_h = \frac{K}{1+\left(\frac{k-A0}{A0}\right)e^{-rh}}$), using the package *growthcurver* (Sprouffske & Wagner, 2016), implemented in R (R Core Team, 2020). Rates were set to 0 when A did not change over time or when the change in absorbance could not be fitted to the logistic growth model. The fitted curves were checked manually and outliers were removed where necessary to improve the fit, as recommended by Sprouffske (2016). We assumed that the soil microbial communities were not able to utilize a substrate when the substrate-use rates

were 0 in > 50% of the soil replicates from the same soil group (two out of three replicates for P', three out of five replicates for the soil transplants). Activity rates were normalized to g^{-1} DW. Substrates were grouped into classes according to Ernakovich & Wallenstein (2015).

4.3.6. *Heterotrophic respiration*

Cumulative CO_2 respiration and $\delta^{13}C$ were measured for the intact P soils (three replicates) and the Pn and Ps transplants at t3 (five replicates each). Aliquots of 0.5 g fresh soil were weighed into 12 ml glass vials. The vials were covered with air-permeable cotton lids and pre-incubated for one week at 4°C and for 5 days at 15°C, to minimize the potential influences of the soil manipulation and the sharp increase in temperature in the activity estimates. Soil moisture was equalized to 30–40% g^{-1} DW for all samples, by adding 0.1 ml of sterile milliQ water to the 0.5 g of soil. For the assays, the vials were gas-tight sealed and the concentrations of CO_2 (gas) accumulated in the headspace and $\delta^{13}C$ (gas) values were measured after 89 and 185 hours of dark incubation of the soils at 15°C, using a GasBench II system (Thermo Fisher Scientific). To avoid pseudoreplication, the measurements at 89 and 185 hours were performed in two independent aliquots (one for each time point) prepared for the same soil replicate (e.g. 2 time points × 5 replicates of Pn soils = 10 samples). CO_2 concentrations were normalized to g^{-1} DW. The increment (Δ) of respired CO_2 was calculated for each soil replicate, as $\Delta\ CO_2 = \frac{(CO_2 \text{ concentration at } 185\text{ h} - CO_2 \text{ concentration at } 89\text{ h})}{185\text{ h} - 89\text{ h}}$. $\Delta\ \delta^{13}C$ was calculated in a similar way.

4.3.7. *Chemical and mineralogical properties*

Chemical properties were measured for all soils collected in the different years, except for soil organic matter (OM), which was only measured in the t3 transplants. Total carbon (C) and nitrogen (N) were measured for dried (65°C) and fine-grained soil samples, using an elemental analyzer (NC-2500; CE Instruments, Wigan, UK). Dissolved organic C (DOC) and N (DN) were measured on carbonate-free soil extracts treated with 3 M HCl, using a TOC/DTN analyzer (Sakalar Analytical B.V., Breda, the Netherlands). The soil extracts were prepared in milliQ water (water:soil 10:1 v/w, shaken over night at room temperature) and filtered through DF 5895-150 ashless paper (Albert LabScience, Dassel, Germany). pH was measured in 0.01 M

$CaCl_2$ soil slurries (2:1 v/w). OM content was determined by the weight-loss-on-ignition method (Davies, 1974).

Mineralogy analyses were conducted on rocks (1–5 mm) recovered from the intact P, N and S soils at t0 and the Pn and Ps transplants at t3. The mineralogy of the rock materials was determined by X-ray powder diffraction, as described in Frey et al. (2010) and Kern et al. (2019).

4.3.8. *Data analyses*

Statistical analyses were completed using the open-source software R v4.0.2 with the RStudio v.1.3 environment (RStudio Team, 2020), and results were graphed with the R package *ggplot2* (Wickham, 2016). A significance level of 0.05 was considered for all statistical analyses.

Differences in prokaryotic and fungal β-diversity between soil transplantation treatments (Pn and Ps; permafrost warming, Ns; active-layer warming, Sn; active-layer cooling) and controls (intact P at t0; Nn and Ss, disturbance active-layer controls) were estimated from Bray-Curtis dissimilarity values based on OTU relative abundances (Legendre & Gallagher, 2001). Dissimilarities were visualized with principal coordinate analyses (PCoAs) and the statistical significance of observed differences between the soils was tested with permutational analyses of variance (PERMANOVAs, 10^5 permutations, function adonis in the *vegan* package; Anderson, 2001) . Multivariate homogeneity of group dispersions was checked prior to the PERMANOVAs to ensure that detected significant differences were associated with the transplantation treatments and not with distinct within-group variability of the soils (betadisper function; Anderson et al., 2013) . The microbial α-diversity parameters of richness (number of OTUs), and Shannon's and Pielou's evenness indices were calculated on OTU counts, rarefied to the lowest number of sequences per sample (12900 sequences for prokaryotes and 6170 sequences for fungi) through iteration (mean rarefied values from 100 rounds of rarefication, function rrarefy.perm, *EcolUtils* package; Salazar, 2019). To prevent underestimations of α-diversity indices (Cameron et al., 2021), one soil sample containing less than 5000 prokaryotic sequences was removed prior to rarefication.

Overall effects of the transplantation treatments, time and their interaction on the microbial α-diversity parameters were tested with two-way ANOVAs using trimmed means as robust estimators (function t2way, *WRS2* package; Mair et al., 2020), after verifying that the residuals of the data were normally distributed but that the response variables were heteroscedastic. The ANOVAs were applied on the separate subsets of permafrost, and north- and south-facing topsoils. Games-Howell pairwise tests were conducted afterwards to test for differences between soil transplants and controls in each of the years of the experiment. Similar statistics were used to determine the effects of transplantation and time on microbial abundance, microbial activities and the soil chemical properties. Welch tests were used instead of the two-way ANOVAs to evaluate the treatment effects on OM and microbial activities, because these variables were only measured at t3. To reduce heteroscedasticity, all variables were z-score transformed prior to testing, except for microbial abundance and microbial activities, which were $\log_{10}$ transformed. Bacterial cells containing multiple copies of the 16S gene in their genomes can cause overestimations of qPCR-based abundance measurements in soils (Angly et al., 2014). To minimize this bias and for each soil sample (e.g. Pn soil, replicate 1), bacterial abundance (16S rRNA gene copies g^{-1} DW) was divided by the weighted average of PICRUSt-predicted 16S copies per genome of the OTUs present in the soil ($\frac{\text{bacterial abundance of Pn soil, replicate 1}}{\sum_i^{total\ OTUs}(\text{relative abundance of OTU}i \times 16S\text{ copies of OTU}i)\text{ of Pn soil, replicate 1}}$). This calculation followed the rationale of Angly et al. (2014).

DESeq2 analyses were used to identify differentially abundant OTUs between the soil treatments and controls (i.e. responding OTUs). For each DESeq2 comparison of soil treatment vs. control, the $\log_2$-fold change (LFC) of each OTU was calculated as $\log_2$ ($\frac{\text{OTU abundance of treatment}}{\text{OTU abundance of control}}$). To account for differences in sequencing depth between samples, OTU abundances were normalized with the median of ratios method (Love et al., 2020). The statistical significance of the LFC was checked with Wald tests. *p* values were adjusted for multiple testing using the Benjamini–Hochberg (BH) method with a false discovery rate threshold of 5%. To lower the false discovery rate, the DESeq2 analyses only included OTUs for which the sum of the sequences over all soil samples was ≥ 10. The pairwise comparisons included all the soil transplants and controls collected in the different years (t0 to t3). The soil transplantation was implemented as the main factor in the DESeq2 tests, controlling for the additional factor of time (~ time + soil transplantation)(Love et al., 2020). For the graphical

representations, only highly (p < 0.01) differentially abundant OTUs among the 80% most abundant in the subsets of permafrost and north- and south-facing active-layer topsoils were selected. Selected OTUs were classified to the taxonomic levels of “phylum” and “genus”. Only the genera for which all assigned OTUs either increased (LFC > 0) or decreased (LFC < 0) in abundance in the soil treatments were included in the representations.

The 16S rRNA gene copy number per genome was predicted for the soil OTUs, by phylogenetically annotating the centroid sequences against fully sequenced genomes using the tool PICRUSt (Langille et al., 2013). The 16S rRNA gene copy number is an indicator of “copiotrophy”, because copiotrophs usually have > 1 copy of the 16S rRNA gene in their genomes (Lauro et al., 2009; Roller et al., 2016). Only OTUs with NSTI (Nearest Sequenced Taxon Index) scores < 2 were represented, as recommended in the PICRUSt documentation (https://github.com/picrust/picrust2/wiki/q2-picrust2-Tutorial).

To gain ecological information about the fungal taxa responding to the transplantation treatments, the tool FUNGuild (Nguyen et al., 2016) was applied to the differentially fungal OTUs detected in the Pn & Ps vs. P DESeq2 comparisons. The package FUNGuildR (https://rdrr.io/github/brendanf/FUNGuildR/) was used to apply the FUNGuild tool in the R environment.

4.3.9. *Co-abundance networks*

The co-abundance association patterns of the prokaryotic and fungal permafrost OTUs (p < 0.01, among the 80% most abundant) responding to warming were investigated. Correlation matrices were generated by calculating all pairwise Spearman’s rank correlations between the OTUs. Positively correlating OTUs (correlation coefficient > 0.6 and BH adjusted p < 0.05; Ju et al. 2014) were identified and the correlations were represented as networks using the *igraph* package (Csardi & Nepusz, 2006). In the network representations, OTUs were depicted as nodes and correlations as edges. To gain information about warming-associated alterations in the co-abundance association patterns of the microbial communities, network topological properties of modularity and average degree of connectivity between nodes were calculated, as described in Ju et al. (2014).

4.4. Results

4.4.1. *Changes in prokaryotic and fungal diversity*

Soil transplantation (Pn and Ps: permafrost warming, Ns: active-layer warming, and Sn: active-layer cooling) significantly altered microbial α- and β- diversity (PERMANOVAs, $p < 0.05$) in all soils (Tables 1 and 2). The soil prokaryotic communities experienced greater structural shifts (F=28, 68% of explained variation, EV) than the fungal communities (F=7, 39% EV, Table 2). These shifts were particularly pronounced between the transplanted permafrost (Pn and Ps) and the intact soils (P) (Table 2), where the alterations in prokaryotic β-diversity were coupled to a significant decrease in α-diversity (Fig. 2, Table S2). Diversity changes were stronger for the permafrost transplanted to the S (Ps) than to the N (Pn) topsoil, and mostly occurred during the first year of the experiment but persisted over time (Fig. 2, Tables 2 and S2).

Significant decreases in bacterial and fungal α-diversity were also observed for south-facing active-layer topsoils transplanted to the north-facing slope (active-layer cooling) (Tables 1 and S2). Differences in α- and β-diversity between the intact soils (N, S and P) and soils transplanted within the same habitats (Nn, Ss and P soils stored at -1.5°C) indicated influences of soil disturbance in the community assemblages (Table S3).

Table 1. Effects of the soil-transplantation treatments, time and their interaction on microbial α-diversity, microbial abundance and microbial activities, and soil chemical properties.

		Permafrost soils			North-facing soils			South-facing soils		
		Treatment	Time	Treatment × Time	Treatment	Time	Treatment × Time	Treatment	Time	Treatment × Time
Prokaryotic α-diversity	**Richness**	**273.94*** **	0.12	4.98	1.71	0.04	0.35	**8.81***	1.92	4.76
	Shannon index	**205.19*** **	**6.79**·	6.74	0.47	0.82	0.18	**10.60****	1.12	1.47
	Evenness	**133.59*** **	**16.08****	11.85	**4.07**·	1.39	0.42	**7.95***	1.09	0.56
Fungal α-diversity	**Richness**	4.08	**9.08**·	**18.15***	1.34	**15.30***	2.09	**14.70****	**50.96*** **	0.80
	Shannon index	3.42	0.13	0.88	0.28	**37.85*** **	5.31	3.22	5.21	4.40
	Evenness	3.77	0.23	0.47	0.40	**14.71***	1.40	0.54	2.89	2.68
Microbial abundance	**Bacteria**	**76.57*** **	**12.67***	**23.18***	0.00	**45.05*** **	0.01	1.96	4.55	3.51
	Fungi	**78.25*** **	5.35	6.11	0.26	**132.66*** **	0.00	0.21	**12.51***	3.75
	F:B ratio[1]	**7.14**·	**11.67***	**14.61**·	0.67	**25.1****	1.12	**4.12**·	1.50	0.01
Microbial activities[2]	**Substrate-use rates**[3]	**11.88*** **			**4.44***			0.41		
	Respiration	0.60								
Soil and microbial properties	**Total C**[4]	**25.24****	4.54	**115.82*** **	0.07	0.29	3.13	**8.76***	3.95	0.25
	Total N	**354.73*** **	**404.78*** **	**1392.81*** **	2.21	**10.78***	1.82	**8.68***	6.18	0.30
	DOC	**15.48***	0.02	8.20	0.05	0.44	0.20	**5.99***	2.56	0.67
	DN	**47.56*** **	**34.72****	**27.97***	0.03	**17.74***	5.92	1.91	1.20	2.87
	pH	**40.82*** **	**11.22***	**36.45****	0.02	1.24	0.21	**6.70***	0.15	1.42
	OM	**4.80**·			**8.07***			1.22		
	DNA content	**77.00*** **	4.94	15.17	0.83	**60.90*** **	0.98	**7.20***	**45.34*** **	4.18

Significance of effects were tested with two-way ANOVAs using trimmed means as robust estimators. α=0.05. The ANOVAs included the intact permafrost at the start of the experiment (2016; controls), and all permafrost and north-facing and south-facing transplanted soils from 2017, 2018 and 2019. Values in bold with superscript points and asterisks indicate marginally significant (· $p < 0.1$) and significant (* $p < 0.05$, ** $p < 0.01$, *** $p \leq 0.001$) differences between the soil groups for the tested factors. [1]F:B ratio: fungal-to-bacterial ratio. [2] Treatment effects on microbial activities and soil OM were evaluated with Welch tests because they were only measured in 2019. [3] Substrate-use rates include the rates of all the substrates used by the microbial communities across the different soils. Soil CO_2 respiration was only measured for the permafrost soils, where warming effects were the greatest. [4]Total C: total carbon, Total N: total nitrogen, DOC: dissolved organic carbon, DN: dissolved total nitrogen, OM: organic matter.

Table 2. Effects of the soil-transplantation treatments, time and their interaction on microbial β-diversity.

	Prokaryotes						Fungi					
Main PERMANOVA[1]												
	DF[2]	**SS**	**MS**	**F**	**EV [%]**	***p***	**DF**	**SS**	**MS**	**F**	**EV [%]**	***p***
Treatment	8	16.25	2.03	27.89	68	**< 0.001**	8	13.07	1.63	7.14	39	**< 0.001**
Time	2	0.81	0.40	5.53	3	**< 0.001**	2	0.89	0.44	1.94	3	**< 0.001**
Treatment × Time	10	1.16	0.12	1.59	5	**0.01**	10	2.00	0.20	0.87	6	0.93
Residuals	77	5.61	0.07		24		75	17.16	0.23		52	
Total	97	23.82					95	33.12				
Pairwise PERMANOVAs												
	t1		**t2**		**t3**		**t1**		**t2**		**t3**	
	F	***p***	**F**	***p***	**F**	***p***	**F**	***p***	**F**	***p***	**F**	***p***
Pn vs. P	9.71	**0.02**	27.46	**0.03**	15.17	**0.02**	4.37	**0.02**	5.44	**0.03**	4.94	**0.03**
Ps vs. P	21.25	**0.02**	24.16	**0.03**	20.78	**0.02**	6.93	**0.02**	4.97	**0.02**	4.82	**0.03**
Ps vs. Pn	3.70	**0.02**	4.74	**0.03**	3.82	**0.02**	2.55	**0.02**	2.35	**0.02**	1.87	**0.03**
Ns vs. Nn	1.99	**0.03**	1.75	0.06	2.73	**0.01**	1.16	0.29	1.36	0.12	1.84	**0.01**
Ss vs. Sn	2.05	0.09	2.46	0.06	2.76	**0.04**	1.61	**0.03**	1.38	0.06	1.85	**0.01**

General effects of treatment and time on β-diversity were assessed using PERMANOVA tests. Differences between pairs of soil treatments and controls were assessed using pairwise PERMANOVAs. α=0.05. Pn: permafrost incubated in the north-facing topsoil, Ps: permafrost incubated in the south-facing topsoil, Nn: north-facing active layer incubated in the north-facing topsoil, Ns: north-facing active-layer topsoil incubated in the south-facing topsoil, Ss: south-facing active-layer topsoil incubated in the south-facing topsoil, Sn south-facing active layer incubated in the north-facing topsoil.[1] Tests were performed on Bray-Curtis dissimilarity matrices based on the relative abundance of the prokaryotic or fungal OTUs. The main PERMANOVA tests included the permafrost (P), north-facing active-layer soils (N) and south-facing active-layer soils (S), sequenced at the start of the experiment (2016), and the sequences of all soil transplants (Pn, Ps, Nn, Ns, Ss, Sn) from 2017 (t1), 2018 (t2) and 2019 (t3). Controls correspond to P, Nn and Ss soils. [2]DF: degrees of freedom, SS: sum of squares, F: pseudo-F ratio, EV [%]: % of variation explained by the factors, MS: mean squares, *p: p* value. *p* values from pairwise tests were adjusted for multiple comparisons with the Benjamini-Hochberg method. EV = r-squared. Values in bold indicate significant differences between soil groups.

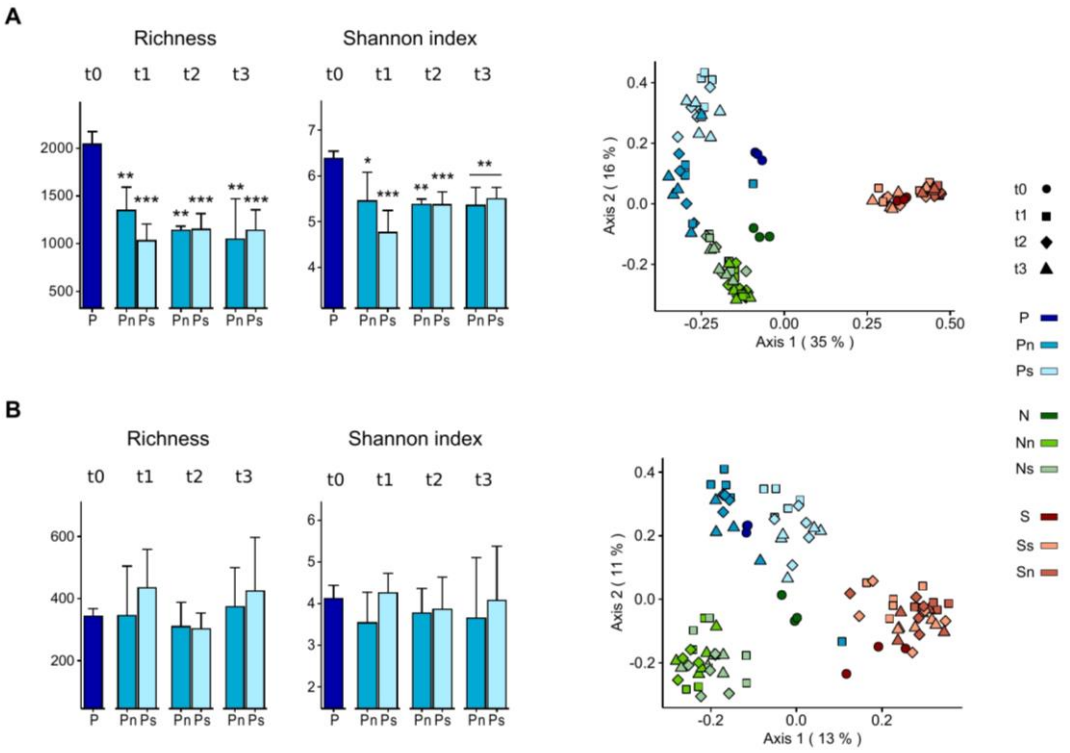

Figure 2. Prokaryotic (**A**) and fungal (**B**) diversity in transplanted soils and controls for the three years of the experiment. Bar plots represent the mean ± SD of the prokaryotic and fungal richness and Shannon index (α-diversity) in the permafrost (P) at the start of the experiment (t0, control) and in the soils transplanted to the north- and south-facing (Pn and Ps) active-layers topsoils after 1 (t1), 2 (t2) and 3 (t3) years. Symbols indicate marginally significant (· $p < 0.1$) and significant (* $p < 0.05$, ** $p < 0.001$, Games-Howell pairwise tests) differences between the soil groups Pn vs. P and Ps vs. P. Differences in β-diversity between soils are depicted with PCoAs computed on Bray-Curtis dissimilarities based on OTU relative abundances. Capital N and S letters represent the original north-facing (N) and south-facing (S) active layers, whereas lower-case letters represent the destination to which the soils were transplanted.

4.4.2. *Responses of prokaryotic taxa to transplantation*

Approximately 3000 prokaryotic OTUs were found to be differentially abundant (i.e. responding OTUs) between transplanted and intact (control) permafrost soils (Ps vs. P and Pn vs. P, DESeq2 tests $p < 0.05$), whereas fewer than 500 responding OTUs were detected for the Ns vs. Nn (active-layer warming vs. disturbance control) and Sn vs. Ss (active-layer cooling vs. disturbance control) comparisons (Table S4). Overall, more OTUs responded negatively (LFC < 0) than positively (LFC > 0) to transplantation (Pn vs. P, Ps vs. P, Ns vs. Nn and Ss vs. Sn). This trend, which persisted over time (Table S5), was particularly marked in the permafrost, where about 2200 prokaryotic OTUs decreased in abundance and only 600 OTUs increased in the transplanted (Pn and Ps) compared with the intact soils (P).

Taxonomic classification of the significantly ($p < 0.01$) responding OTUs, among the 80% most abundant in the separate subsets of permafrost and north- and south-facing active-layer soils, showed that, at the phylum level only, the low-abundant (< 1% total sequences; Table S6) bacterial phyla Deinococcota (genus *Deinococcus*), Firmicutes and Abditibacteriota, and the archaeal Crenarchaeota all increased with warming (LFC > 0, Pn vs. P, Ps vs. P and Ns vs. Nn; Fig. 3A, Table S7). The abundant phylum (> 1% of all sequences; Table S6) Patescibacteria decreased markedly with simulated warming conditions (704 responding OTUs within 28 uncultured lineages; Fig. 3A, Table S7), comprising groups (e.g. *Ca. Collierbacteria* and *Ca. Woesebacteria*) among the taxa with the strongest abundance reductions in the Pn and Ps soils (Fig. 3B). Numerous (~15) low-abundant (< 1% of all sequences) phyla also responded negatively to warming (LFC < 0, Pn vs. P, Ps vs. P and Ns vs. Nn; Fig. 3A, Table S7).

At the fine-resolution taxonomic level of genus, we observed that the abundant (3% of the total prokaryotic abundance) *Noviherbaspirillum* and *Massilia* (γ-Proteobacteria) were among the genera with the greatest increases in abundance in the transplanted permafrost soils (Pn vs. P and Ps vs. P; Fig. 3, Table S8). Other increasing genera included *Jatrophihabitants* and *Crosiella* (Actinobacteria), *Tundrisphaera* and *Ca. Nostocoida* (Planctomycetota), *Granulicella*, *Ca. Solibacter* and *Blastocatella* (Acidobacteria), and *Flavisolibacter* (Bacteroidota). These groups showed increased abundances in warmer vs. colder soil habitat comparisons (Ps vs. Pn, Ns vs. Nn) and, conversely, a lower abundance in the cooled S soils (Sn vs. Ss; Fig. 3, Table S8). The above-described patterns of taxa increasing and decreasing with warming did not change when differentially abundant OTUs between the intact permafrost at t0 and the soils stored at -1.5°C (soil disturbance controls, Table S5) were removed (data not shown). A list of all responding prokaryotic OTUs with their complete taxonomic classification and abundance information is provided in Table S9.

PICRUSt analyses suggested the *copiotrophic* features of the OTUs benefiting from warming. Collectively, the permafrost OTUs responding positively to warming (LFC > 0, Pn vs. P and Ps vs. P) had more 16S rRNA copies in their predicted genomes than the negatively responding OTUs (LFC > 0, Pn vs. P and Ps vs. P) (Fig. S2).

4.4.3. *Responses of fungal taxa to transplantation*

DESeq2 comparisons between the transplanted and intact (control) permafrost soils (Ps vs. P and Pn vs. P) showed a larger number (300–400) of differentially abundant fungal OTUs than in the Ns vs. Nn (active-layer warming vs. disturbance control) and Sn vs. Ss (active-layer cooling vs. disturbance control) comparisons (< 100; Table S4). Most of the fungal OTUs in the permafrost responded positively to simulated warming, especially for the permafrost transplanted to the S topsoils (Ps, warmest topsoil habitat), where the ratios of positively to negatively responding OTUs was 4:1 for Ps vs. P and ~ 340:1 for Ps vs. Pn. Similarly, most of the fungal OTUs in the N soils increased in abundance with transplantation from Nn to Ns (active-layer warming), whereas they decreased with transplantation from Ss to Sn (active-layer cooling) (Table S4).

The majority of the fungal OTUs responding ($p < 0.01$) positively to warming (among the 80% most abundant OTUs in the separate subsets of permafrost and north- and south-facing topsoils) belonged to the Ascomycota phylum (representing > 50% total fungal sequences; Table S6), together with *Chytridiomycota* (Fig. 4, Table S10). Mortierellomycota and Monoblepharomycota decreased with simulated warming, and Basidiomycota showed mixed responses (Fig. 4, Table S10). At the genus level, we observed that mainly ascomycetous sapro-pathotrophic taxa (e.g. *Extremus*, *Tetracladium* and *Protomyces*) were overrepresented (LFC > 0) in the transplanted warmer vs. colder soil habitat comparisons (Pn vs. P and Ps vs. P, Ps vs. Pn and Ns vs. Nn). Few lichenized genera (e.g. *Aspicilia* and *Lecanora*) were also abundant in warmer soils. Except for *Tausonia* and *Naganishia*, basidiomycetous yeasts responded negatively to warming. A list of all responsive fungal OTUs with their complete taxonomic classification and abundance information is provided in Table S11.

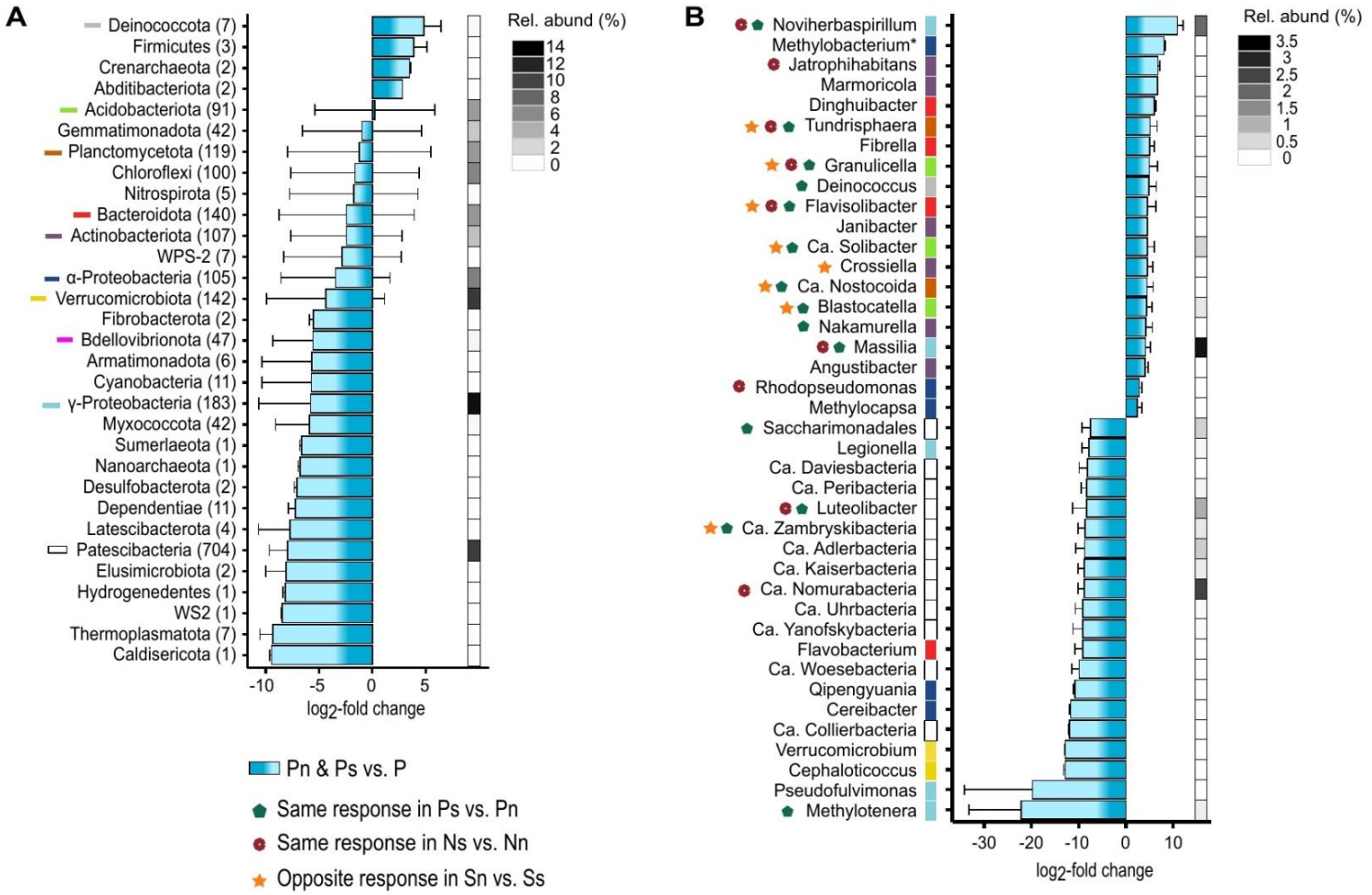

Figure. 3. Prokaryotic phyla (**A**) and genera (**B**) in the permafrost responding to warming. Highly (p < 0.01) differentially abundant OTUs (i.e. responding OTUs) from the DESeq2 comparisons between the north-facing (Pn) or south-facing (Ps) transplanted permafrost and controls (Pn vs. P, Ps vs. P), and among the 80% most abundant across the soils were assigned to phyla and genera. Barplots represent the mean ± SD of the log_2-fold change (LFC) values of the OTUs belonging to common taxa in Pn & Ps vs. P comparisons. Represented genera are those with the highest mean abundance increase (LFC > 0) or decrease (LFC < 0) in the transplanted soils, weighted by their representativeness in the permafrost (LFC × Rel. abund). The number of responding OTUs in each phylum is shown in brackets. Colors of genera in **B** correspond to the phyla in **A**. Rel. abund (%): sum of the abundance of the OTUs belonging to same taxa expressed as a percentage of the total sequences in the permafrost soils. Same response in Ps vs. Pn: the genera increased (or decreased) in abundance in all Pn vs. P, Ps vs. P and Ps vs. Pn comparisons. The same applies for "same response in Ns vs. Nn". Opposite response in Sn vs. Ss: the genera increased in abundance in Pn vs. P and Ps vs. P, and it decreased in Sn vs. Ss (cooling). Capital N and S letters represent the original north-facing (N) and south-facing (S) active layers, whereas lower-case letters represent the destination to which the soils were transplanted. Proteobacteria is represented at the level of *order*. Ca.: candidate, * Methylobacterium-Methylorubrum. Patescibacteria was classified to the taxonomic level of *order* instead of *genus*.

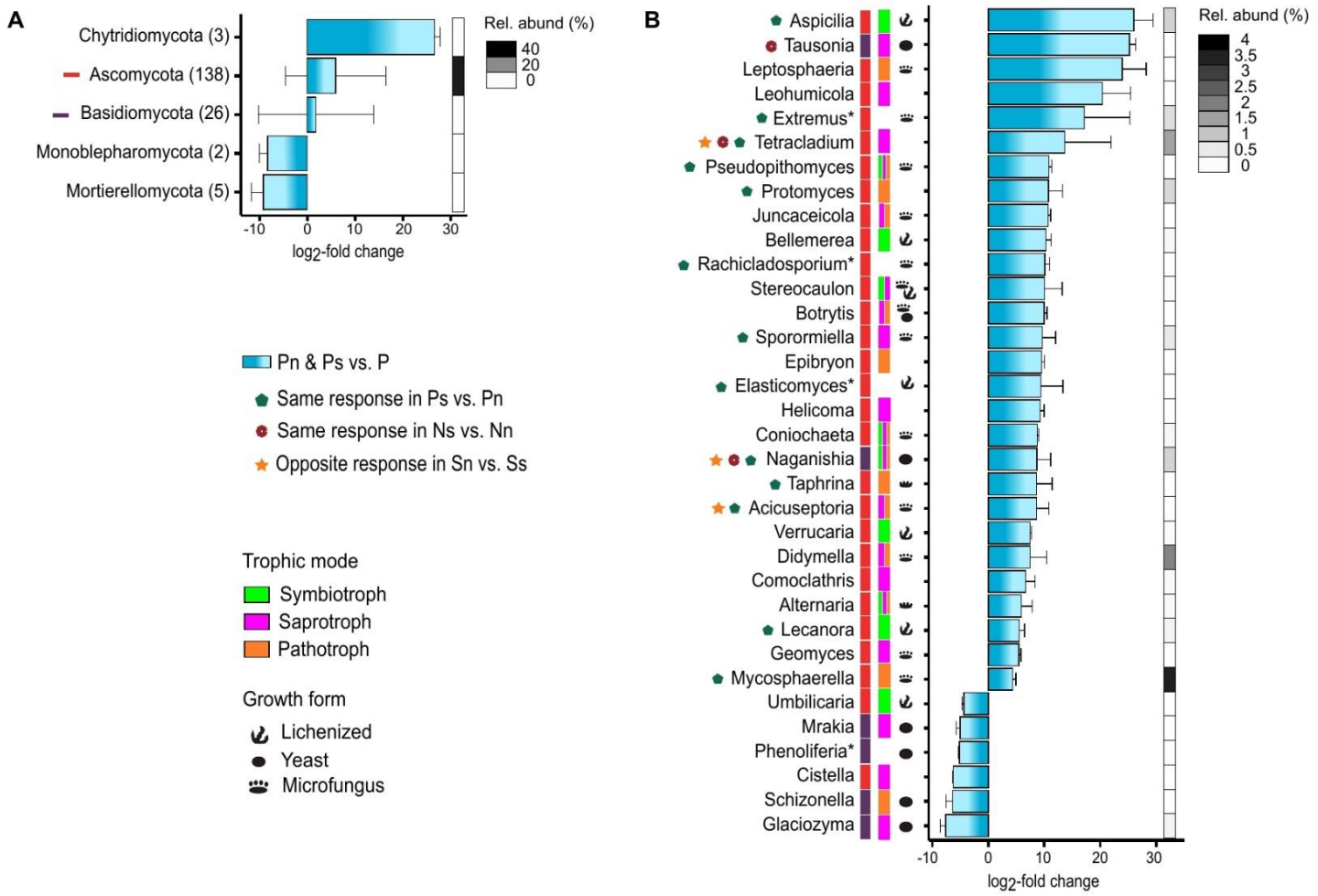

Figure 4. Fungal phyla (**A**) and genera (**B**) in the permafrost responding to warming. Highly ($p < 0.01$) differentially abundant OTUs (i.e. responding OTUs) from the DESeq2 comparisons between the north-facing (Pn) or south-facing (Ps) transplanted permafrost and controls (Pn vs. P, Ps vs. P), and among the 80% most abundant across the soils were assigned to phyla and genera. Barplots represent the mean ± SD of the log2-fold change (LFC) values of the OTUs belonging to common taxa in Pn & Ps vs. P comparisons. Red and purple colors of genera in B correspond to the phyla in A. Secondary bar colors and symbols provide ecological information about the fungal genera retrieved from the FUNGuild (http://www.funguild.org/) and www.fungalgenera.org (*) databases. Rel. abund (%): sum of the abundance of the OTUs belonging to same taxa expressed as a percentage of the total sequences in the permafrost soils. Same response in Ps vs. Pn: the genera increased (or decreased) in abundance in all Pn vs. P, Ps vs. P and Ps vs. Pn. The same applies for “same response in Ns vs. Nn”. Opposite response in Sn vs. Ss: the genera increased in abundance in Pn vs. P and Ps vs. P, and it decreased in Sn vs. Ss (cooling). Capital N and S letters represent the original north-facing (N) and south-facing (S) active layers, whereas lower-case letters represent the destination to which the soils were transplanted.

4.4.4. *Changes in microbial networks*

Co-abundance networks of the positively correlating prokaryotic and fungal OTUs responding to warming (DESeq2 tests $p < 0.01$, 80% most abundant in the permafrost soils) were less complex for the transplanted (Ps and Pn) compared with the intact permafrost (P) at the start of the experiment (Fig. 5). Specially for the OTUs responding negatively to warming (LFC < 0, Pn vs. P and Ps vs. P), networks became increasingly more disconnected between the P, Pn and Ps soils, showing a steep increase in modularity (m) and a decrease in the average degree (ad) of connectivity between the nodes (m=0.02, 0.34 and 0.92, and ad=906, 23 and 5 in P, Pn and Ps, respectively; Fig. 5). Associations between taxa were not phylogenetically conserved.

4.4.5. *Changes in microbial abundance*

Permafrost transplantation led to an increase in bacterial and fungal abundance, which occurred during the first year of the experiment and persisted over time (Fig. 6, Table S12). Increasing fungal-to-bacteria (F:B) ratios in the transplanted permafrost, particularly in the soils transplanted in the south-facing slope (Ps, warmest climate) indicated a trend of more rapid increase in abundance for fungi than for bacteria. Microbial abundance was not significantly affected in the transplanted N topsoils (active-layer warming) and only weakly in the transplanted S topsoils (active-layer cooling), being influenced by time and soil disturbance (Table S12).

4.4.6. *Changes in substrate-use activities and heterotrophic respiration*

Biolog assays (at 15°C) showed that the permafrost transplanted to the N (Pn) and S (Ps) topsoils harbored microbiota capable of growing on a wider range of substrates than the intact permafrost (soils stored at -1.5°C), and at greater rates (Fig. 7). Particularly, the Pn and Ps microbiota metabolized a larger number of amino acids and, to a lesser extent, carboxylate compounds (Fig. 7). Additional assays did not show a significant influence of incubation temperature (4 vs. 15°C) and initial inoculum (undiluted vs. 1:10 dilution) in the maximum rates of substrate-use activities for the permafrost (data not shown). Substrate-use activities of the N and S active-layer topsoils were only minimally affected by the transplantation (N to S, active-

layer warming and S to N, active-layer cooling; Fig. S3). Basal respiration (respired CO_2 and $\delta^{13}C$ values at 15°C) was similar between the three-year transplanted soils (Pn and Ps) and the one-week thawed intact permafrost (P) (Fig. S4). $\delta^{13}C$ values (approx. -28) measured in the solid phase were also similar for all permafrost soils.

4.4.7. *Changes in soil properties*

Permafrost transplantation to the N and S topsoils was associated with a significant ($p < 0.05$) increment of up to 54% in total C (Tables 1 and S13), although overall values remained low (≤ 0.17% C). Total N became measurable in the transplanted permafrost soils (~0.01% N). Dissolved N (DN) significantly increased 6-fold in the transplanted permafrost soils, whereas dissolved organic carbon (DOC) decreased between 10 and 30% (Table S13). Significant differences were also detected for pH and OM content between transplanted and intact permafrost soils (Pn vs. P and Ps vs. P) and between transplanted N active-layer topsoils and disturbance controls (Ns vs. Nn), but values differed minimally between the soil groups (pH ~ 6, OM ranging from 0.9 to 1%).

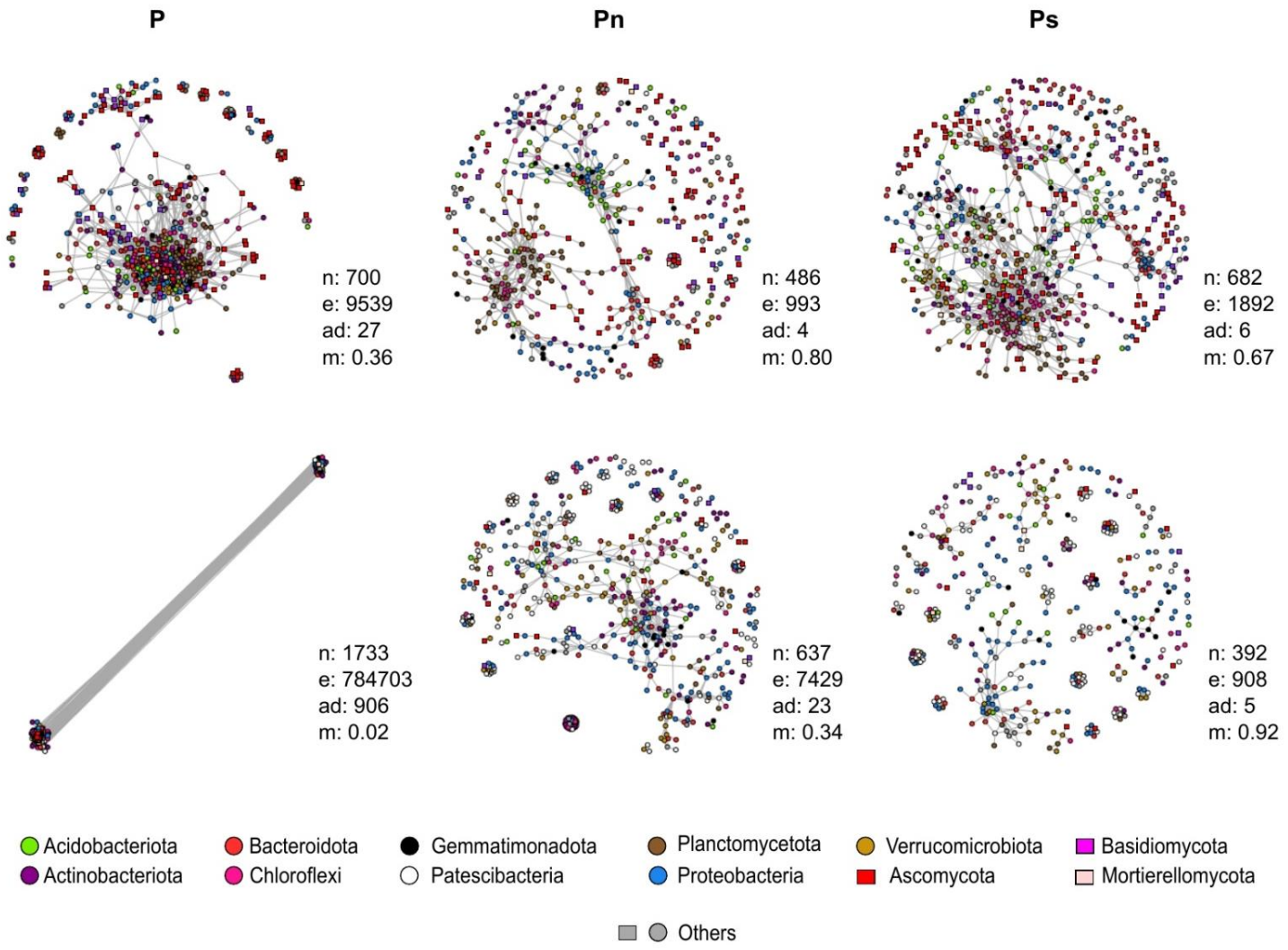

Figure 5. Co-abundance networks of the prokaryotic (circles) and fungal (squares) permafrost OTUs responding to warming. Highly (p < 0.01) differentially abundant OTUs (i.e. responding OTUs), among the 80% most abundant in the permafrost, were identified in the DESeq2 comparisons between the permafrost transplanted to the north- or south-facing active-layer topsoils (Pn and Ps, warming treatments) and the intact soils (P, control). The responding OTUs were grouped into OTUs responding positively (log_2-fold change, LFC > 0, **upper panel**) and negatively (LFC < 0, **lower panel**) to warming. Significant positive correlations between the abundances of the grouped OTUs were identified for the P, Pn and Ps soils, separately. Co-abundant OTUs are represented as networks, where nodes (n) depict the OTUs and edges (e) depict the correlations. Nodes are colored according to the phyla assigned to the OTUs. ad: average degree of connectivity between the nodes, m: modularity.

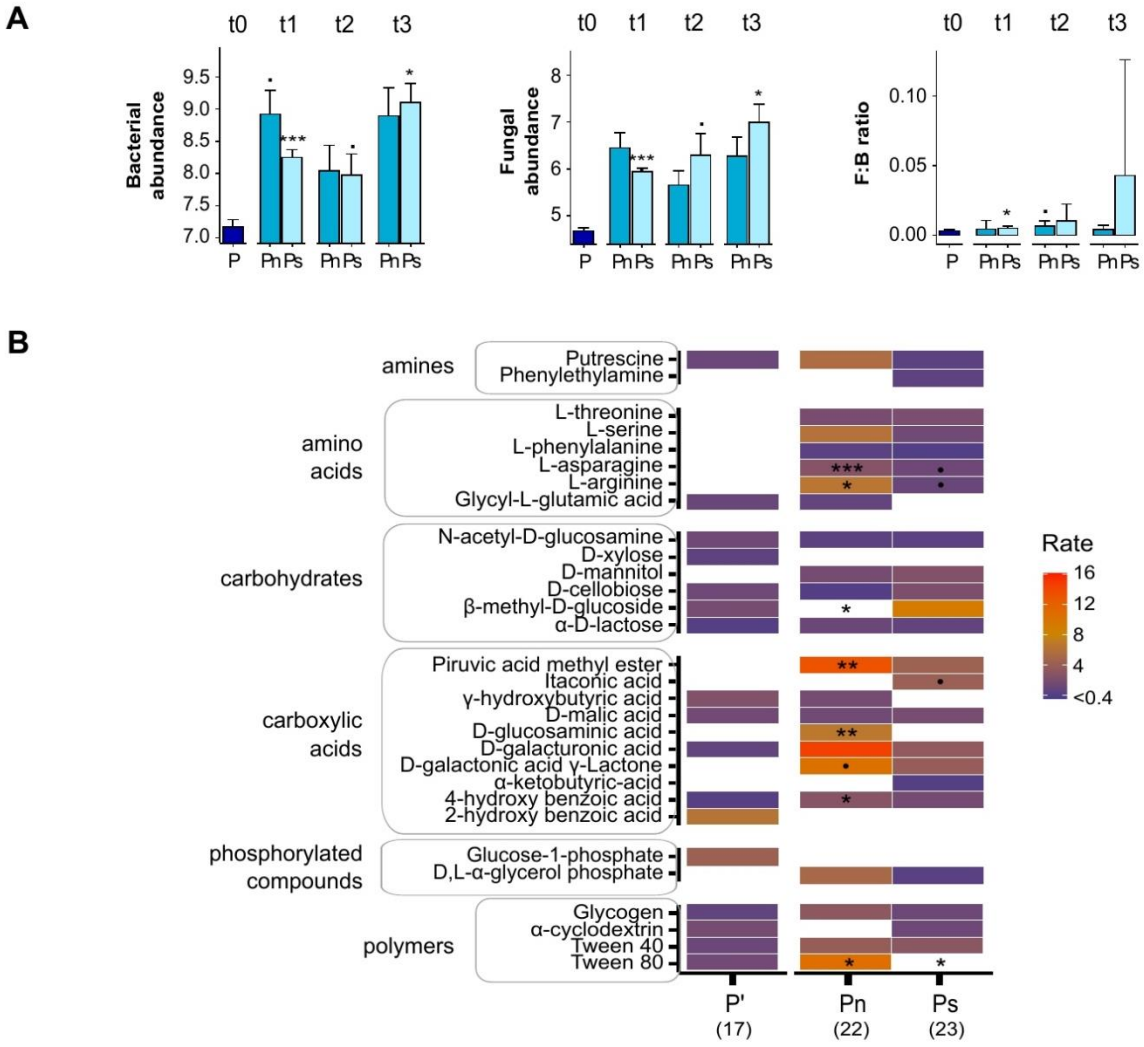

Figure 6. Bacterial and fungal abundances, fungal-to-bacteria ratio (F:B) **(A)** and substrate-use microbial activities **(B)** in the transplanted permafrost and controls. Soil bacterial (16s rRNA gene) and fungal (ITS gene) abundances are measured as the $\log_{10}$ (gene copies g^{-1} DW). Measurements were performed in the intact permafrost at the start of the experiment (t0, control) and in the permafrost transplanted to the north- and south-facing active-layer topsoils (Pn and Ps) after 1 (t1), 2 (t2) and 3 years (t3; mean ± SD). Substrate-use activity assays were performed at 15°C in the Pn and Ps soils at t3, and in intact permafrost samples previously stored at -1.5°C (P', controls). Rates (*r*) represent the maximum increase in substrate-use activities over time, expressed as Absorbance $hours^{-1}$ g^{-1} DW. Cells in the heatmap represent mean *r* values for the P', Pn and Ps soils. Blank cells represent substrates that were not utilized by the microbial communities. The total number of substrates used by the communities in the P, Pn and Ps soils are shown in parentheses. Symbols indicate marginally significant (· $p < 0.1$) and significant (* $p < 0.05$, ** $p < 0.01$, *** $p < 0.001$, Games-Howell pairwise tests) differences between the soil groups Pn vs. P and Ps vs. P.

4.5. Discussion

4.5.1. *Simulated warming promotes the abundance increase of copiotrophic and metabolically versatile prokaryotic taxa*

In agreement with our first hypothesis, the transplantation treatments simulating warming led to augmented microbial abundance in the MBP permafrost soils, and shifted the structure of the microbial communities, particularly the prokaryotic communities, in both the permafrost soil transplanted into the active-layer topsoils and, to a lesser extent, the north-facing active layers transplanted into south-facing active-layer topsoils. As expected, prokaryotic taxa increasing in abundance with simulated warming in the permafrost and active layers, or conversely decreasing with simulated cooling (S to N topsoil transplantation) included abundant bacterial genera with copiotrophic attributes, such as *Noviherbaspirillum* and *Massilia*. These genera have been shown to be fast-growing (i.e. forming colonies in less than 7 days of incubation at 25°C) and they are easily culturable in nutrient-rich artificial media (Baldani et al., 2014; Lin et al., 2013; Ofek et al., 2012). Genera within Actinobacteria and Bacteroidota, which increased in the MBP soils with simulated warming, might behave copiotrophically at elevated concentrations of C and nutrients (Ho et al., 2017; Senechkin et al., 2010). The warming-induced increase in *copiotrophy* of the MBP soils was further indicated by the greater number of OTUs in the permafrost transplants, which contained multiple 16S rRNA gene copies in their genomes (Donhauser et al., 2020; Lauro et al., 2009).

An increased abundance of copiotrophic prokaryotic taxa, including *Noviherbaspirillum* and *Massilia*, has previously been observed in laboratory incubations of MBP soils at elevated temperatures (Donhauser et al., 2020; Luláková et al., 2019) and receiving inputs of root-exudates (Adamczyk et al., 2021), as well as in nutrient-enriched Arctic soils undergoing thawing (Adamczyk et al., 2020; Schostag et al., 2019). Likewise, transplantation of Tibetan topsoils from 3800 to 3200 m a.s.l. showed an increase in Actinobacterial strains in the transplants under the warmer climate of the lower altitudes (Rui et al., 2015). The thawing temperatures experienced by the MBP permafrost soil transplanted into topsoils would have activated the permafrost microbiota surviving the freezing conditions, here reflected in the increased abundance of spore-forming Firmicutes upon soil transplantation (Coolen & Orsi, 2015; Schostag et al., 2019). The availability of liquid water following thawing and the release of C and nutrients from the previously frozen layers (Abbott et al., 2014; Chen et al., 2016) in

the permafrost transplants could have particularly benefited copiotrophic prokaryotic taxa, which adjust quickly to temperature changes and grow faster than other groups with the available nutritional resources (Ho et al., 2017).

The frequent FTCs occurring in the topsoils might have additionally favored copiotrophs in the transplanted permafrost, concurring with previous findings from MBP soil incubations with an increased FTC frequency (Perez-Mon et al., 2020). *Crosiella* and *Deinococcus* genera, which are adapted to environments of highly fluctuating temperature (Villa & Cappitelli, 2019), might have also benefited from the FTCs. Particularly the 3°C warmer climate of the south-facing slope of MBP, with less snow, could have facilitated the expansion of copiotrophic microorganisms in the permafrost, and active layers incubated in the south-facing slope.

In disagreement with our first hypothesis, simulated conditions of warming in the permafrost and overlying active layers led to an abundance increase of under-characterized soil bacterial taxa within Acidobacteriota and Planctomycetota, that *a priori* would be considered oligotrophic (Fierer et al., 2007; Ho et al., 2017). These included genera such as *Tundrisphaera*, *Granulicella* which contain strains that require nutrient-poor artificial media and several weeks to grow (Kulicheyskaya et al., 2017; Rawat et al., 2012). *Tundrisphaera* and *Granulicella* have been described as important litter degraders in Arctic soils (Dedysh & Ivanova, 2019; Klarenberg et al., 2020; Kulicheyskaya et al., 2017; Rawat et al., 2012), encoding for a wide variety of hydrolytic enzymes that enable them to utilize lignocellulosic polysaccharides (Dedysh & Ivanova, 2019; Rawat et al., 2012).

Metagenomic assessments of MBP soils in a previous study indicated the presence of plant cell debris (e.g. from Poales) in the permafrost layers, and the enhanced functional genetic potential of the permafrost microbiota to degrade polymeric substrates (Perez-Mon et al., 2021). We theorize that the release of preserved biopolymers upon permafrost thawing could have stimulated the growth of the polymer-degrading *Tundrisphaera* and *Granulicella*, explaining their abundance increase in the transplanted MBP permafrost. Our reasoning is in line with GeoChip gene profiling of Tibetan permafrost soils laboratory-incubated at 5°C for five months (Chen et al., 2021), where an overrepresentation of C-degrading genes suggested the microbial mobilization of biopolymers in the thawed soils. A greater content of plant-derived

detritus in the south-facing topsoils of MBP (Perez-Mon et al., 2021) could potentially have contributed to the increased abundance of metabolically versatile prokaryotes capable of utilizing complex polymers in the active layers transplanted in the south-facing slope, through the exchange of material with the surrounding soils.

4.5.2. *Metabolically restricted oligotrophic bacterial taxa are vulnerable to simulated warming*

In contrast to the increase in copiotrophs, conditions of warming in the MBP permafrost led to a severe decrease mainly of OTUs belonging to the uncultured Patescibacteria superphylum, as reflected in the loss of prokaryotic α-diversity after transplantation into topsoils. A previous metabarcoding study conducted in the MBP soils showed the overrepresentation of Patescibacteria lineages in the permafrost (Frey et al., 2016). Patescibacteria members feature ultra-small cell sizes (< 0.1 μm) and streamlined genomes (~ 1 Mbp) of reduced metabolic capabilities, likely related to syntrophic lifestyles (Brown et al., 2015; Ortiz et al., 2020; Rinke et al., 2013; Tian et al., 2020; Vigneron et al., 2020). Genome simplicity might be advantageous for the Patescibacterial cells in the oligotrophic permafrost habitats, as these cells would require little energy to grow and divide (Ortiz et al., 2020; Tian et al., 2020). The metabolic restrictions of Patescibacteria would, however, limit their growth upon thawing. Under a warmer mountain climate, alpine permafrost soils might lose their unique prokaryotic populations (Chen et al., 2021), which could be replaced by the copiotrophic and metabolically versatile strains in the soils studied here.

4.5.3. *Permafrost fungi benefited overall from simulated warming*

MBP fungal communities profited overall from the simulated warming in the permafrost transplanted into the active-layer topsoils and, to a lesser extent, in the north-facing active layers transplanted into south-facing active layers. The trend of increasing fungal-to-bacterial (ITS:16S) ratios over time, measured in the transplanted permafrost, could be explained by fungi using the increased soil C and nutrients more efficiently than bacteria (Kallenbach et al., 2016). Mainly sapro-pathotrophs, and a few cold-adapted lichenized genera (e.g. *Aspicilia* and *Lecanora*; Singh et al., 2015; Nimis et al., 2018; Coleine et al., 2021) increased in abundance

with the changing environment. Elevated soil temperatures could have promoted the growth of the sapro-pathotrophs in the transplanted soils, as they are highly adaptable to environmental changes (Schmidt et al., 2012; Selbmann et al., 2013). Further, the exposure to sunlight in the topsoil, which is intensified in the south-facing slopes, could have enabled the hyphal growth of the lichenized fungi together with their algal partners. In contrast, psychrophilic basidiomycetous yeasts (e.g. *Glaciozyma*, *Schizonella* and *Mrakia*) inhabiting the permafrost decreased with warming. The thick cell walls of basidiomycetous yeasts and their ability to form cryoprotective exo-polymeric capsules might explain their prevalence in the frozen permafrost environments (Coleine et al., 2021), but our results suggest that they will be poor competitors against other fungal groups in the future warmer climate.

4.5.4. *Simulated warming loosened the microbial association networks in the permafrost*

In agreement with our second hypothesis, the diversity loss and compositional shifts within the permafrost microbial communities transplanted into topsoils resulted in more disconnected microbial networks, with fewer positive associations between the fungal and prokaryotic members. In line with the reasoning of Banerjee et al. (2019) and Morrien et al. (2017), the simpler microbial networks in the MBP transplanted permafrost could potentially reflect a loss of cooperative or trophic interactions between neighboring microorganisms (e.g. syntrophic Patescibacteria obtaining nutrients from their partners), and thereby result in soil microbial communities that are overall more vulnerable to environmental perturbations. This notwithstanding, microbial association networks based on correlations should be interpreted with care, because microbial taxa that do not interact could co-occur in the soils owing to shared habitat preferences. Microbial structural alterations in the transplanted soils, persisting over time after the first year of our experiment, suggest long-lasting effects of the changing soil conditions on the microbiome. Monitoring of the experimental samples in the future is, however, necessary to reveal the longer-term (≥ 5 years) dynamics of the fungal and bacterial populations. Taxonomic shifts within fungal communities, particularly, might occur over longer periods of time than for prokaryotes, owing to lower growth rates of fungi compared with prokaryotic taxa (Rousk & Baath, 2011).

4.5.5. *Three years of simulated warming altered microbial substrate utilization but did not enhance soil respiration*

In partial agreement with our third hypothesis, the topsoil-transplanted permafrost microbiota, enriched in fungi and copiotrophic prokaryotes, grew on a broader range of substrates and at enhanced rates in Biolog assays. These observations corroborate the recent findings from GeoChip-based studies in Tibetan permafrost (Chen et al., 2021) and metagenomic profiling of permafrost-affected topsoils in the Swiss Alps (Donhauser et al., 2021), where soil microbial communities at elevated temperatures exhibited greater C-degrading genetic capabilities. Broader microbial activities, particularly for the recycling of N compounds (e.g. microbial necromass, Donhauser et al., 2021) , might improve the nutritional status of alpine soils (Metrak et al., 2020), thereby contributing to the ongoing advancement of mountain vegetation towards higher altitudes (Adamczyk et al., 2019; Steinbauer et al., 2018).

In discrepancy with our third hypothesis, soil CO_2 emissions rates were similar between three-year thawed permafrost and one-week thawed controls. The MBP permafrost microbiota transplanted into topsoils might feed on necromass or detritus-derived organics in the soils, and it could even benefit from inputs of C and N from the atmosphere (Brankatschk et al., 2011) and the surrounding topsoils. These nutritional sources might support microbial growth after thawing but they might not be enough to sustain high rates of cell metabolic activity. The MBP microbiota might require both elevated temperatures and high C inputs to boost soil respiration (Adamczyk et al., 2021). This reasoning is in line with the findings from a nine-year field experiment in which Tibetan grasslands were exposed to 1.6°C higher soil temperatures (at a depth of 5 cm), where the authors proposed that the observed steady increase in heterotrophic respiration over time was promoted by labile C inputs into the soils from the warming-enhanced vegetation (Peng et al., 2020). Metagenomic analyses of the transplanted MBP soils in the future, complemented with *in situ* measurements of soil microbial processes (e.g. CO_2 fluxes), even if challenging because of the coarse soil texture, will enable a better examination of the functional changes in the soil microbiota and its potential feedbacks to the atmosphere.

4.6. Conclusions

Here we demonstrate the fast acclimation of a temperate permafrost microbiota to three-year field-simulated conditions of warming, confirming the indications from short-term laboratory-controlled studies. Our findings suggest that the future warmer climate in mid-latitude mountains lead to the growth of copiotrophic and metabolically versatile bacteria, as well as sapro-pathotrophic fungi within the permafrost, superseding metabolically restricted oligotrophic bacteria (e.g. Patescibacteria) and basidiomycetous yeasts. A warming-induced loosening of microbial association networks could result in permafrost microbial communities being more vulnerable to the changing climate, whereas the growth of microbiota that use a broader range of substrates could alter the C pools in the soil. Three years of simulated warming did not result in greater CO2 effluxes in the here transplanted permafrost, but the soil microbiota needs high inputs of C and nutrients for their heterotrophic activities to increase substantially. Collectively, our findings provide first insights on the structural and functional acclimations of both the alpine permafrost and active layer microbiomes to *in situ* warming, which help to improve the prediction of the responses of the mountain soils to the future warmer climate.

4.7. Data availability

All raw sequencing data generated for this study have been deposited in the NCBI Sequence Read Archive under the BioProject accession identifier PRJNA726951.

4.8. Author contributions

B.F. designed the study. B.F. and B.S. set up the field experiment. B.F., B.S. and C.P-M. collected the samples in the field. B.S., C.P-M. and M.P. performed laboratory assays. C.P-M performed data analyses and wrote the manuscript with the contribution of B.F. All authors helped to edit and complete the manuscript.

4.9. Funding information

This study was funded by the Swiss National Science Foundation (SNSF) under the grant IZLSZ2_170941.

4.10. Acknowledgements

We thank M. Phillips for access to the MBP long-term monitoring permafrost site, M. Cerbera for his support in the excavation of the soil profiles at MBP, J. Rüthi for laboratory assistance, and R. Köchli, N. Hajjar and the WSL Central Laboratory for completing soil analyses. We also thank M. Dawes for her valuable contribution to the editing of this article. We acknowledge the Genetic Diversity Centre (GDC) of the ETH Zürich and the contribution of scientists at the McGill University and Génome Québec Innovation Centre in Montreal, Canada for performing Illumina MiSeq sequencing.

4.11. Conflict of interest statement

The authors declare that they have no known competing financial interests or personal relationships that could have appeared to influence the work reported in this paper.

4.12. Supplementary information

4.12.1. *Supplementary figures*

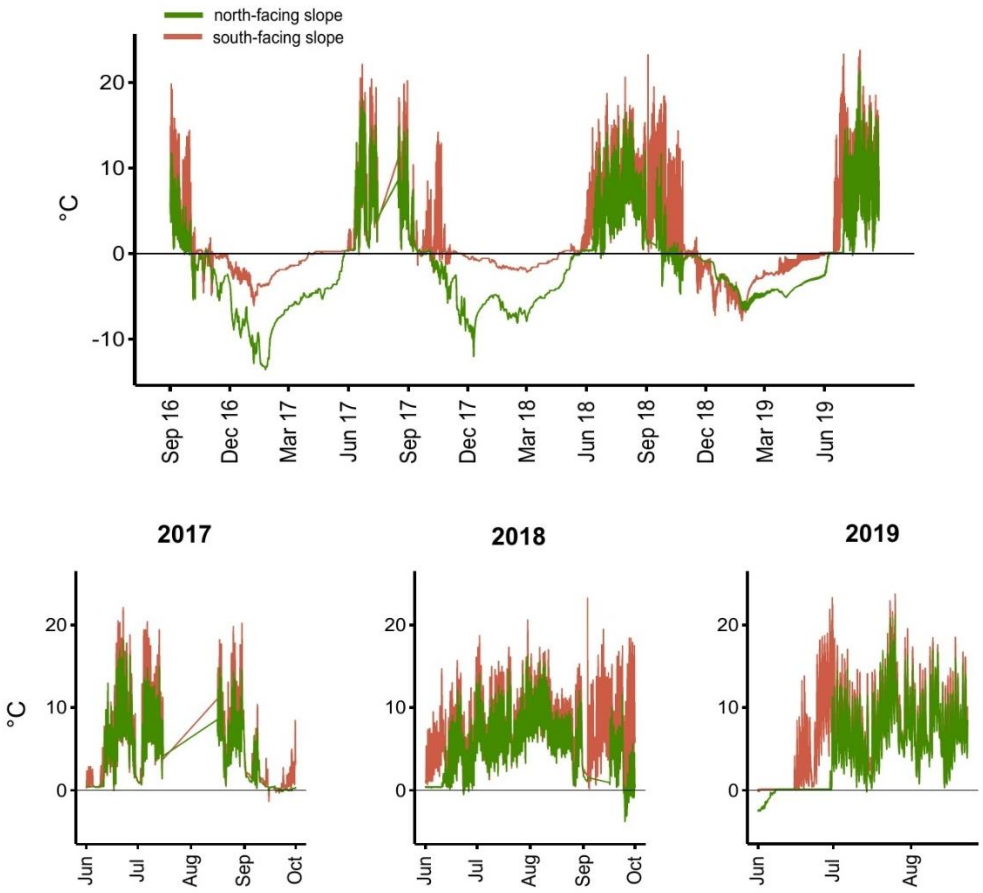

Figure S1. Top panel: temperatures of the soils transplanted to the north-facing (green line) and the south-facing (red line) active-layer topsoils, measured at a depth of 3 cm inside the transplanted soils (via iButtons, n=5 in each slope) and in the surrounding topsoil (via M-Log5W-SIMPLE sensors, n=2 in each slope) during the three years of the experiment. The lower panel shows closer views of the temperatures during the summers of 2017, 2018 and 2019, corresponding to 1, 2 and 3 years after soil transplantation. Temperature measurements for 2019 are shown only until the 30th of September. Values are hourly temperature means, n=7 in each slope.

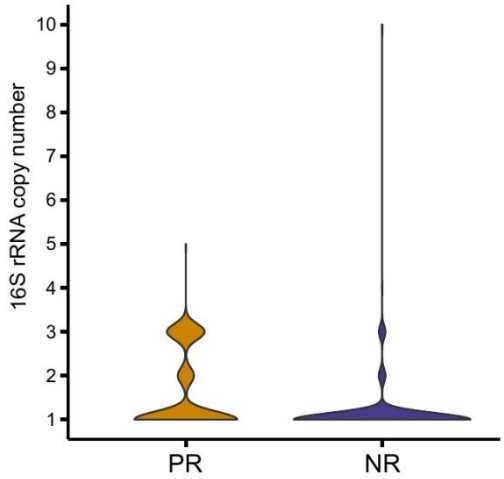

Figure S2. PICRUST-predicted 16S rRNA gene copies per genome of the permafrost OTUs responding to warming. Responding OTUs correspond to the highly (p < 0.01) differentially abundant OTUs identified in the DESeq2 comparisons between the permafrost transplanted to the north-facing (Pn) and the south-facing (Ps) topsoils and the intact soils (P). Only responding OTUs among the 80% most abundant in the permafrost are included. OTUs were grouped into positively responding (PR, LFC > 0) and negatively responding (NR, LFC < 0) to warming.

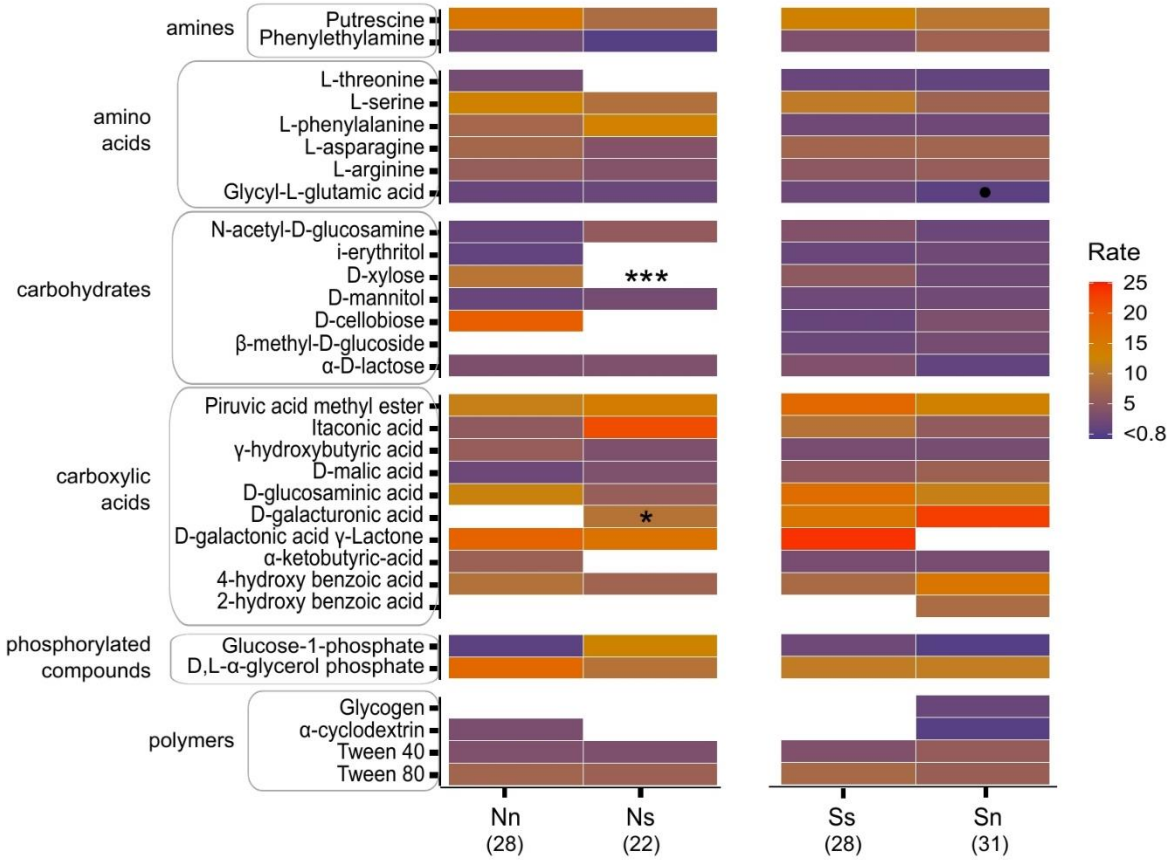

Figure S3. Substrate-use microbial activities measured in the north-facing (N) and south-facing (S) active-layer topsoils transplanted (lower-case letters) to their original and opposite slopes. Activity assays were performed at 15°C in the soils three years after transplantation. Rates (*r*) represent the maximum increase in substrate-use activities over time, expressed as Absorbance hours^{-1} g^{-1} DW. Cells in the heatmap represent mean *r* values for the soil groups. Blank cells represent substrates that were not utilized by the microbial communities. The total number of substrates used by the communities in the soils are shown in parentheses. Symbols indicate marginally significant (· $p < 0.1$) and significant (* $p < 0.05$, *** $p < 0.001$, Games-Howell pairwise tests) differences between the soil groups Ns vs. Nn and Sn vs. Ss (treatment vs. control).

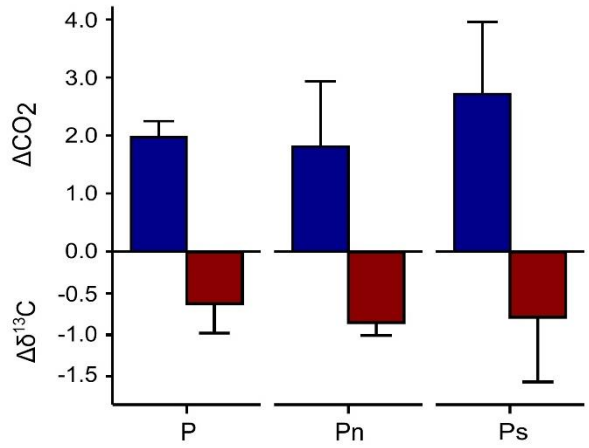

Figure S4. Increment (Δ) in respired CO_2 concentrations and $\delta^{13}C$ in the native permafrost (P) and in the soils transplanted to the north-facing (Pn) and south-facing (Ps) topsoils. Respiration assays were performed in the Pn and Ps soils three years after transplantation, and in the permafrost stored *in-vitro* at -1.5°C. Soils were incubated at 15°C and respired CO_2 concentrations (ppm) and $\delta^{13}C$ were measured after 89 and 185 hours (h). ΔCO_2 and $\delta^{13}C$ correspond to the differences in the measurements between the two time points, expressed as (ppm) h^{-1} g^{-1} DW. CO_2 concentrations at 89 h were 2039 ± 54, 1784 ± 45 and 2060 ± 140 ppm for the P (three replicates), and Pn and Ps soils (five replicates).

4.12.2. *Supplementary tables*

Because of their large extension **tables S7, S8, S9, S10** and **S11** are provided electronically, in the published version of the Chapter::

https://www.sciencedirect.com/science/article/pii/S0048969721057983#s0145

Table S1. Physico-chemical properties of the studied soils. Mean ± SD (n=3).

	P	N	S
C [%]	0.1 ± 0	0.1 ± 0	0.9 ± 0
N [%]	b.d.l.[1]	b.d.l.	0.1 ± 0
OM [%]	1.1 ± 0.1	1.3 ± 0.1	3.2 ± 0
WHC [g H_2O g^{-1}]	0.2 ± 0	0.2 ± 0	0.3 ± 0
pH [$CaCl_2$]	5.8 ± 0	4.6 ± 0.1	4.6 ± 0
Sand [%]	85.2 ± 0.2	80.5 ± 0.1	83.8 ± 0.2
Silt [%]	11.2 ± 0.4	15.9 ± 0.2	14 ± 0.3
Clay [%]	3.5 ± 0.2	3.6 ± 0.2	2.2 ± 0.2
Quartz[2]	34 ± 3	39 ± 7	42 ± 5
K-Feldspar	10 ± 1	7 ± 2	8 ± 2
Na-Plagioclase	24 ± 0	21 ± 0	24 ± 3
Illite+Muscovite	15 ± 2	17 ± 3	12 ± 3
Chlorite	17 ± 0	16 ± 3	14 ± 0
Age [^{14}C dating]	12403 ± 69	12923 ± 149	4889 ± 76

[1]b.d.l. below detection limit (N < 0.015), [2]The minerological composition was measured in the present study. The rest of the data was reported in Frey et al. (2016) and Perez-Mon et al. (2021). C: total carbon, N: total nitrogen, OM: organic matter, WHC: water holding capacity. P: permafrost, N: north-facing active-layer topsoil, S: south-facing active-layer topsoil.

Table S2. Microbial α-diversity calculated in the soils during the three years of the transplantation experiment.

			Permafrost soils			North-facing soils			South-facing soils		
			P	Pn	Ps	N	Nn	Ns	S	Ss	Sn
Bacteria	**Richness**	**t0**[1]	2043 ± 132			1176 ± 29			539 ± 27		
		t1									
		t2	1263 ± 308	**1347 ± 247****	**1032 ± 175*****	1451 ± 291	1601 ± 248	1433 ± 166	1698 ± 494	1255 ± 202	**1009 ± 86**·
		t3	1346 ± 0	**1141 ± 44****	**1151 ± 164*****	1718 ± 114	1645 ± 323	1452 ± 143	1330 ± 176	1313 ± 183	1174 ± 86
			903 ± 0	**1049 ± 421****	**1140 ± 217*****	1584 ± 181	1632 ± 318	1409 ± 119	1088 ± 199	1255 ± 140	1147 ± 65
	Shannon index	**t0**									
		t1	6.38 ± 0.16			5.52 ± 0.09			4.16 ± 0.12		
		t2									
		t3	4.78 ± 0.62	**5.45 ± 0.63***	**4.76 ± 0.48*****	5.51 ± 0.14	5.70 ± 0.39	5.74 ± 0.27	5.95 ± 0.61	5.69 ± 0.26	**5.20 ± 0.31***
			4.84 ± 0.00	**5.38 ± 0.11****	**5.37 ± 0.28*****	5.86 ± 0.15	5.77 ± 0.47	5.76 ± 0.20	5.55 ± 0.38	5.68 ± 0.19	5.41 ± 0.27
	Eveness	**t0**	3.90 ± 0.00	**5.36 ± 0.39****	**5.50 ± 0.25****	5.63 ± 0.25	5.69 ± 0.44	5.60 ± 0.26	5.39 ± 0.30	5.70 ± 0.12	**5.48 ± 0.18**·
		t1									
		t2	0.84 ± 0.01			0.78 ± 0.01			0.66 ± 0.02		
		t3									
			0.67 ± 0.07	**0.76 ± 0.07**·	**0.69 ± 0.05****	0.76 ± 0.01	0.77 ± 0.04	0.79 ± 0.03	0.80 ± 0.06	0.80 ± 0.02	**0.75 ± 0.04***
Fungi	**Richness**	**t0**	0.67 ± 0.00	**0.76 ± 0.01****	**0.76 ± 0.025****	0.79 ± 0.01	0.78 ± 0.04	0.79 ± 0.02	0.77 ± 0.04	0.79 ± 0.01	0.77 ± 0.03
		t1	0.57 ± 0.00	**0.78 ± 0.02****	**0.78 ± 0.02****	0.76 ± 0.02	0.77 ± 0.04	0.77 ± 0.03	0.77 ± 0.03	0.80 ± 0.01	**0.78 ± 0.02**·
		t2									
		t3	344 ± 24			183 ± 87			95 ± 31		
	Shannon index	**t0**	218 ± 54	345 ± 160	434 ± 124	349 ± 70	286 ± 71	342 ± 98	318 ± 66	346 ± 52	**266 ± 49***
		t1	154 ± 0	310 ± 78	303 ± 50	270 ± 67	238 ± 77	246 ± 39	213 ± 60	290 ± 76	226 ± 32
		t2	86 ± 0	374 ± 126	425 ± 172	259 ± 87	323 ± 16	328 ± 66	222 ± 147	367 ± 46	**296 ± 29***
		t3									
			4.12 ± 0.31			2.13 ± 1.23			2.26 ± 0.18		
	Eveness	**t0**									
		t1	2.95 ± 0.55	3.54 ± 0.73	4.26 ± 0.46	4.00 ± 0.42	3.52 ± 0.28	3.56 ± 0.54	3.84 ± 0.43	4.02 ± 0.58	4.01 ± 0.26
		t2	2.76 ± 0.00	3.78 ± 0.59	3.86 ± 0.78	3.19 ± 0.72	3.59 ± 0.34	3.54 ± 0.48	3.08 ± 0.80	4.05 ± 0.32	3.53 ± 0.49
		t3	1.82 ± 0.00	3.65 ± 1.45	4.07 ± 1.30	2.98 ± 0.94	4.09 ± 0.08	3.75 ± 0.70	3.13 ± 0.87	4.10 ± 0.37	3.98 ± 0.17

[1]Measurements were performed on aliquots of the soil pools prepared at the start of the experiment (summer 2016, t0) and on aliquots of soils collected during the summers of 2017 (t1), 2018 (t2) and 2019 (t3). Mean ± SD (n=3 for t0 soils and n=5 for t1, t2 and t3 soils). Values in bold with superscript points and asterisks indicate marginally significant (· $p < 0.1$) and significant (* $p < 0.05$, ** $p < 0.01$) differences between the soil groups Pn vs. P, Ps vs. P, Ns vs Nn and Sn vs. Ss. Significance was calculated with Games-howell pairwise tests applied to the subsets of soils separated by year. P: permafrost at the start of the experiment, N: north-facing active layer at the start of the experiment, S: south-facing active layer at the start of the experiment, Pn: permafrost transplanted to the north-facing topsoil, Ps: permafrost transplanted to the south-facing topsoil, Nn: north-facing active-layer topsoil transplanted to the north-facing topsoil, Ns: north-facing active-layer topsoil transplanted to the south-facing topsoil, Ss: south-facing active-layer topsoil transplanted to the south-facing topsoil, Sn south-facing active-layer topsoil transplanted to the north-facing topsoil.

Table S3. Differences in microbial β-diversity between transplanted and intact soils collected during the different years of the experiment. Differences were evaluated with pairwise PERMANOVAs. α=0.05.

	Prokaryotes[1]						Fungi					
	t1		t2		t3		t1		t2		t3	
	F[2]	*p*	F	*p*	F	*p*	F	*p*	F	*p*	F	*p*
P vs. P'[3]	25.98	**0.01**					10.39	**0.01**				
N vs. N'[4]	8.10	0.12	10.72	**0.03**	9.53	0.12	2.37	0.13	2.71	**0.04**	1.95	0.13
N vs. Nn	12.54	**0.03**	13.47	**0.03**	15.54	**0.03**	2.97	0.05	3.18	**0.04**	3.99	**0.04**
N vs. Ns	12.14	**0.03**	13.7	**0.03**	15.84	**0.03**	2.93	**0.04**	3.32	**0.04**	3.32	**0.04**
S vs. S'	5.54	0.12	5.42	**0.04**	4.68	0.12	5.88	0.12	6.17	**0.03**	2.95	0.12
S vs. Ss	7.01	**0.04**	8.78	**0.04**	10.58	**0.04**	4.39	**0.03**	4.58	**0.03**	4.82	**0.03**
S vs. Sn	7.8	**0.04**	12.03	**0.04**	16.71	**0.04**	5.57	**0.03**	4.13	**0.03**	6.04	**0.03**

Differences were evaluated with pairwise PERMANOVAs. α=0.05. [1]Pairwise PERMANOVA tests were performed on Bray-Curtis dissimilarity matrices based on the relative abundance of the prokaryotic or fungal OTUs, [2]F: pseudo-F ratio, *p*: p-value. *p* values from pairwise tests were adjusted for multiple comparisons with the Benjamini-Hochberg method, [3]P vs P': comparison between permafrost soils collected in the field (P) at the start of the experiment (2016) and aliquots (collected during the period from 2017 to 2019) of permafrost soils stored at -1°C in dark conditions, [4]N vs N': comparison between intact north-facing active-layer soil collected at 10 cm depth at the start of the experiment (N) and intact north-facing active-layer soil collected at 10 cm depth in the field in 2017 (t1), 2018 (t2) and 2019 (t3). The same holds for the south-facing active-layer soils (S vs S'). Values in bold indicate significant differences between soil groups. Nn: north-facing active-layer topsoil transplanted to the north-facing topsoil, Ns: north-facing active-layer topsoil transplanted to the south-facing topsoil, Ss: south-facing active-layer topsoil transplanted to the south-facing topsoil, Sn south-facing active-layer topsoil transplanted to the north-facing topsoil.

Table S4. Number of differentially abundant OTUs in DESeq2 comparisons between transplanted soils and controls.

	Prokaryotes						Fungi					
	Increased			Decreased			Increased			Decreased		
	OTUs[1]		Rel. abund[2]	OTUs		Rel. abund	OTUs		Rel. abund	OTUs		Rel. abund
Pn vs. P	557	8%	45%	2218	31%	35%	171	7%	22%	120	5%	38%
Ps vs. P	633	9%	50%	2240	31%	34%	354	14%	29%	84	3%	37%
Ps vs. Pn	430	8%	30%	327	6%	22%	345	15%	47%	1	0%	1%
Ns vs. Nn	208	4%	12%	282	5%	20%	75	4%	24%	18	1%	6%
Sn vs. Ss	151	4%	27%	323	7%	16%	19	1%	9%	42	2%	7%

[1]Number of OTUs that increased (log2 fold change, LFC > 0) and decreased (LFC < 0) in the treatments, and the percentage of the total OTUs they represent in the soils, separated by their origin: permafrost (7113 prokaryotic and 2588 fungal OTUs), north-facing active layer (5702 prokaryotic and 1825 fungal OTUs), and south-facing active layer (4354 prokaryotic and 1769 fungal OTUs). [2]Rel. abund: abundance of the responsive OTUs as a percentage of the total OTU abundance in the subsets of permafrost (P, Pn and Ps), north-facing active-layer (Nn and Ns) and south-facing active-layer (Sn, Ss) soils. Full DESeq2 results and taxonomic classification of differentially abundant prokaryotic and eukaryotic OTUs are provided in Tables S9 and S11, respectively. P: permafrost at the start of the experiment, Pn: permafrost transplanted to the north-facing topsoil, Ps: permafrost transplanted to the south-facing topsoil, Ns: north-facing active-layer topsoil transplanted to the south-facing topsoil, Nn: north-facing active-layer topsoil transplanted to the north-facing topsoil, Sn south-facing active-layer topsoil transplanted to the north-facing topsoil, Ss: south-facing active-layer topsoil transplanted to the south-facing topsoil.

Table S5. Number of differentially abundant OTUs between aliquots of the same transplanted soils collected in different years (time influence), and between transplanted and intact permafrost.

		Prokaryotes						Fungi					
		Increased[1]			Decreased			Increased			Decreased		
Pn	**2018 vs 2017**	4	0%		9	0%		0	0%		0	0%	
	2019 vs 2018	24	1%		0	0%		0	0%		0	0%	
Ps	**2018 vs 2017**	76	1%		54	1%		0	0%		2	0%	
	2019 vs 2018	65	1%		16	0%		0	0%		0	0%	
Nn	**2018 vs 2017**	0	0%		0	0%		0	0%		0	0%	
	2019 vs 2018	25	0%		14	0%		1	0%		0	0%	
Ns	**2018 vs 2017**	0	0%		0	0%		1	0%		1	0%	
	2019 vs 2018	1	0%		0	0%		0	0%		0	0%	
Ss	**2018 vs 2017**	0	0%		1	0%		0	0%		0	0%	
	2019 vs 2018	0	0%		0	0%		0	0%		0	0%	
Sn	**2018 vs 2017**	1	0%		1	0%		0	0%		1	0%	
	2019 vs 2018	90	2%		64	1%		1	0%		0	0%	
P vs. P'[2]		406	6%	(49%)	1573	22%	(40%)	71	3%	(28%)	138	5%	(37%)

[1]Number of OTUs that increased (log2 fold change, LFC > 0) and decreased (LFC < 0) in the soil transplants over time, and the percentage of the total OTUs they represent in the soils, separated by their origin: permafrost (7113 prokaryotic and 2588 fungal OTUs), north-facing active layer (5702 prokaryotic and 1825 fungal OTUs) and south-facing active layer (4354 prokaryotic and 1769 fungal OTUs). [2]P vs P': comparison between permafrost soils collected in the field (P) at the start of the experiment (2016) and aliquots (collected during the period from 2017 to 2019) of permafrost soils stored at -1.5°C and under dark conditions (*in situ* conditions) (P'). These soils comprised a total of 5342 prokaryotic and 1141 fungal OTUs. Numbers in parentheses represent the abundance of the responsive OTUs as a percentage of the total OTU abundance in the subset of P and P' soils. P: permafrost at the start of the experiment, Pn: permafrost transplanted to the north-facing topsoil, Ps: permafrost transplanted to the south-facing topsoil, Ns: north-facing active-layer topsoil transplanted to the south-facing topsoil, Nn: north-facing active-layer topsoil transplanted to the north-facing topsoil, Sn south-facing active-layer topsoil transplanted to the north-facing topsoil, Ss: south-facing active-layer topsoil transplanted to the south-facing topsoil.

Table S6. Overall abundance of prokaryotic and fungal phyla.

Bacteria			Fungi		
Phyla	**Rel. abund (%)[1]**	**# OTUs[2]**	**Phyla**	**Rel. abund (%)**	**# OTUs**
Chloroflexi	20.08	1225	Ascomycota	62.22	2602
Verrucomicrobiota	16.86	1040	Basidiomycota	10.78	1167
Proteobacteria	15.65	1999	Mortierellomycota	7.07	58
Acidobacteriota	11.54	714	Chytridiomycota	0.96	97
Planctomycetota	11.01	1545	Mucoromycota	0.31	28
Actinobacteriota	6.09	790	Monoblepharomycota	0.09	7
Bacteroidota	5.29	838	Rozellomycota	0.08	21
Patescibacteria	3.50	2809	Glomeromycota	0.06	11
Gemmatimonadota	3.35	246	Calcarisporiellomycota	0.03	2
Myxococcota	0.87	544	Neocallimastigomycota	0.03	4
WPS-2	0.87	52	Olpidiomycota	0.01	2
Firmicutes	0.63	137	Entorrhizomycota	1.45×10^{-3}	1
Bdellovibrionota	0.41	567	Zoopagomycota	3.97×10^{-4}	1
Cyanobacteria	0.35	149	Basidiobolomycota	1.98×10^{-4}	1
Crenarchaeota	0.34	26			
Nitrospirota	0.26	14			
Deinococcota	0.20	33			
Armatimonadota	0.16	123			
Elusimicrobiota	0.10	121			
Abditibacteriota	0.08	58			
RCP2-54	0.08	16			
Methylomirabilota	0.07	9			
Thermoplasmatota	0.04	14			
Sumerlaeota	0.03	27			
Dependentiae	0.03	151			
Desulfobacterota	0.02	24			
Latescibacterota	0.02	19			
FCPU426	0.02	16			
GAL15	0.01	2			
Fibrobacterota	0.01	6			
SAR324_clade	4.87×10^{-3}	18			
Hydrogenedentes	4.42×10^{-3}	7			
Nanoarchaeota	3.21×10^{-3}	9			
WS2	3.11×10^{-3}	4			
Caldisericota	1.60×10^{-3}	1			
MBNT15	1.25×10^{-3}	7			
Entotheonellaeota	6.82×10^{-4}	1			
NB1-j	4.82×10^{-4}	2			
Margulisbacteria	3.6×10^{-4}	3			
Unclassified	1.39	1068		18.36	1122

[1]Rel. abund (%): abundance of all OTUs belonging to the same phylum, expressed as a percentage of the total OTU counts across all soils. [2] #OTUs: total number of OTUs within the phylum.

Table S12. Microbial abundance measured in the soils during the three years of the transplantation experiment.

		Permafrost soils			North-facing soils			South-facing soils		
		P	Pn	Ps	N	Nn	Ns	S	Ss	Sn
Bacterial abundance[1]	**t0[2]**	$1.5x10^7 \pm 4.5x10^6$			$5.1x10^8 \pm 1.0x10^8$			$3.8x10^9 \pm 1.4x10^9$		
	t1	$1.4x10^8 \pm 8.5x10^7$	**$8.4x10^8 \pm 1.1x10^9$**	**$1.8x10^8 \pm 5.5x10^{7***}$**	$1.2x10^9 \pm 8.0x10^8$	$8.6x10^8 \pm 6.1x10^8$	$9.6x10^8 \pm 7.8x10^8$	$2.1x10^9 \pm 2.5x10^9$	$1.2x10^9 \pm 3.4x10^8$	**$2.3x10^9 \pm 6.5x10^{8**}$**
	t2	$5.8x10^5 \pm 2.1x10^4$	$1.1x10^8 \pm 1.6x10^8$	**$9.5x10^7 \pm 1.1x10^{8\cdot}$**	$7.7x10^8 \pm 7.1x10^8$	$2.7x10^8 \pm 3.3x10^7$	$2.8x10^8 \pm 2.0x10^7$	$9.3x10^8 \pm 3.6x10^8$	$1.1x10^9 \pm 6.2x10^8$	$9.4x10^8 \pm 3.4x10^8$
	t3	$4.7x10^7 \pm 2.2x10^7$	$7.8x10^8 \pm 1.4x10^9$	**$1.3x10^9 \pm 1.2x10^{9*}$**	$1.0x10^9 \pm 1.2x10^8$	$1.5x10^9 \pm 7.3x10^8$	$1.9x10^9 \pm 1.4x10^9$	$3.2x10^9 \pm 2.8x10^9$	$1.4x10^9 \pm 1.1x10^9$	$1.9x10^9 \pm 1.1x10^9$
Fungal abundance	**t0**	$4.7x10^4 \pm 7.3x10^3$			$7.6x10^6 \pm 6.5x10^6$			$1.6x10^8 \pm 1.9x10^7$		
	t1	$4.2x10^5 \pm 2.4x10^5$	$2.8x10^6 \pm 3.1x10^6$	**$8.8x10^5 \pm 1.5x10^{5***}$**	$1.2x10^7 \pm 1.0x10^7$	$5.7x10^6 \pm 2.7x10^6$	$5.2x10^6 \pm 4.9x10^6$	$5.9x10^7 \pm 8.7x10^7$	$4.3x10^6 \pm 2.4x10^6$	$3.6x10^6 \pm 1.8x10^6$
	t2	b.d.l	$4.5x10^5 \pm 4.7x10^5$	**$1.9x10^6 \pm 3.7x10^{6\cdot}$**	$1.3x10^6 \pm 2.0x10^6$	$1.9x10^5 \pm 1.3x10^5$	$5.1x10^5 \pm 7.2x10^5$	$2.4x10^7 \pm 1.9x10^7$	$4.5x10^6 \pm 4.9x10^6$	$1.7x10^6 \pm 5.2x10^5$
	t3	$9.2x10^5 \pm 3.1x10^5$	$1.9x10^6 \pm 2.9x10^6$	**$9.8x10^6 \pm 1.4x10^{7*}$**	$2.0x10^6 \pm 1.9x10^6$	$4.6x10^6 \pm 2.9x10^6$	$3.6x10^6 \pm 2.2x10^6$	$1.2x10^7 \pm 4.7x10^6$	$9.8x10^6 \pm 1.5x10^7$	$4.1x10^6 \pm 1.5x10^6$
F:B ratio[3]	**t0**	0.003 ± 0.001			0.014 ± 0.009			0.047 ± 0.013		
	t1	0.003 ± 0	0.004 ± 0.006	**0.005 ± 0.001***	0.011 ± 0.005	0.012 ± 0.009	0.007 ± 0.006	0.025 ± 0.014	0.004 ± 0.003	**0.002 ± 0.001·**
	t2	0 ± 0	**0.007 ± 0.003.**	0.01 ± 0.012	0.002 ± 0.003	0.001 ± 0	0.002 ± 0.002	0.025 ± 0.014	0.004 ± 0.003	0.002 ± 0
	t3	0.02 ± 0.003	0.004 ± 0.003	0.043 ± 0.083	0.002 ± 0.002	0.003 ± 0.001	0.003 ± 0.002	0.005 ± 0.004	0.006 ± 0.004	**0.002 ± 0.001·**
DNA content	**t0**	0.001 ± 0			0.615 ± 0.081			6.723 ± 1.007		
	t1	0.007 ± 0.003	**0.051 ± 0.036***	**0.009 ± 0.000****	3.504 ± 1.613	1.1 ± 0.627	0.731 ± 0.273	3.721 ± 4.351	2.266 ± 0.753	**3.824 ± 1.719·**
	t2	0.001 ± 0	**0.012 ± 0.013·**	**0.015 ± 0.014****	0.198 ± 0.098	0.139 ± 0.091	0.188 ± 0.132	1.229 ± 0.285	1.324 ± 0.551	1.312 ± 0.197
	t3	0.002 ± 0	0.038 ± 0.057	**0.063 ± 0.069***	0.79 ± 0.131	1.269 ± 0.702	1.064 ± 0.588	5.214 ± 5.087	2.367 ± 1.316	3.431 ± 1.581

[1]Abundance is measured as 16S gene copies g^{-1} DW (bacterial abundance) and ITS gene copies g^{-1} DW (fungal abundance). DNA content is measured as µg of DNA g^{-1} DW. [2]Measurements were performed on aliquots of the soil pools prepared at the start of the experiment (summer 2016, t0) and in aliquots of soils collected during the summers of 2017 (t1), 2018 (t2) and 2019 (t3). Mean ± SD (n=3 for t0 soils and n=5 for t1,t2 and t3 soils). [3]Fungal-to-bacterial ratio. Values in bold with points and asterisks indicate marginally significant (. $p < 0.1$) and significant (* $p < 0.05$, ** $p < 0.01$, *** $p < 0.001$) differences between the soil groups Pn vs. P, Ps vs. P, Ns vs Nn and Sn vs. Ss. Significance was calculated with Games-howell pairwise tests applied to the subsets of soils separated by year. P: permafrost at the start of the experiment, N: north-facing active layer at the start of the experiment, S: south-facing active layer at the start of the experiment, Pn: permafrost transplanted to the north-facing topsoil, Ps: permafrost transplanted to the south-facing topsoil, Nn: north-facing active-layer topsoil transplanted to the north-facing topsoil, Ns: north-facing active-layer topsoil transplanted to the south-facing topsoil, Ss: south-facing active-layer topsoil transplanted to the south-facing topsoil, Sn south-facing active-layer topsoil transplanted to the north-facing topsoil.

Table S13. Chemical properties in the transplanted soils and controls during the three years of the transplantation experiment.

		Permafrost soils			North-facing soils			South-facing soils		
		P	Pn	Ps	N	Nn	Ns	S	Ss	Sn
C [% DW]	t0[1]	0.11 ± 0.00			0.16 ± 0.01			1.25 ± 0.02		
	t1		**0.16 ± 0.01****	0.15 ± 0.05	0.41 0.09	0.61 ± 0.05	0.58 ± 0.04	0.77 0.58	1.35 ± 0.55	2.54 ± 0.87
	t2		0.11 ± 0.03	0.14 ± 0.04	0.58 0.03	0.67 ± 0.10	0.58 ± 0.13	1.28 0.80	1.90 ± 0.88	2.65 ± 0.88
	t3	0.11 ± 0.00	0.13 ± 0.02	**0.17 ± 0.03***	0.42 ± 0.08	0.50 ± 0.04	**0.67 ± 0.15**·	1.75 ± 1.50	1.25 ± 0.62	1.91 ± 0.69
N [% DW]	t0	b. d. l			0.01 ± 0.00			0.08 ± 0.00		
	t1		**0.01 ± 0.00*****	**0.01 ± 0.00***	0.04 0.01	0.02 ± 0.01	0.02 ± 0.00	0.06 0.04	0.09 ± 0.04	0.16 ± 0.05
	t2		**0.01 ± 0.00***	**0.01 ± 0.00*****	0.02 0.00	0.03 ± 0.01	0.02 ± 0.01	0.08 0.05	0.13 ± 0.05	0.17 ± 0.05
	t3	b. d. l	b. d. l	0.00 ± 0.01	0.02 ± 0.00	0.02 ± 0.01	0.02 ± 0.00	0.12 ± 0.10	0.09 ± 0.04	0.12 ± 0.04
DOC [µg g^{-1} DW][2]	t0	115.37 ± 19.90			93.10 ± 16.63			164.50 ± 5.76		
	t1		97.52 ± 1.02	**78.04 ± 13.50**·	173.33 12.77	116.37 ± 19.61	108.05 ± 6.50	178.08 111.06	194.06 ± 43.95	258.58 ± 90.81
	t2		86.72 ± 22.99	127.33 ± 102.12	133.37 15.07	120.99 ± 29.05	110.69 ± 25.22	152.09 51.71	153.48 ± 60.48	**251.70 ± 69.33***
	t3	115.37 ± 19.90	81.24 ± 40.70	102.87 ± 39.74	124.00 ± 6.66	142.57 ± 59.44	138.63 ± 68.39	189.31 ± 80.93	147.63 ± 42.95	210.90 ± 95.72
DN [µg g-1 DW]	t0	0.62 ± 0.37			1.63 ± 0.11			7.26 ± 0.43		
	t1		**1.45 ± 0.50**·	0.54 ± 0.14	8.04 1.64	4.59 ± 2.23	2.51 ± 0.32	8.74 6.64	9.76 ± 3.23	14.24 ± 3.85
	t2		**3.18 ± 0.83****	6.63 ± 7.04	8.53 1.47	6.59 ± 2.30	5.74 ± 1.09	11.38 5.87	10.92 ± 3.73	**15.85 ± 3.65**·
	t3	0.62 ± 0.37	**3.96 ± 2.22***	**4.36 ± 2.74***	1.98 ± 0.36	3.76 ± 2.55	6.90 ± 2.88	13.10 ± 9.70	11.47 ± 4.99	9.90 ± 4.05
pH	t0	5.80 ± 0.00			6.67 ± 0.06			4.60 ± 0.00		
	t1		5.73 ± 0.15	5.67 ± 0.15	4.60 0.00	4.83 ± 0.25	4.77 ± 0.12	4.50 0.00	4.50 ± 0.00	4.40 ± 0.00
	t2		5.76 ± 0.17	**5.68 ± 0.11**·	4.67 0.15	4.72 ± 0.19	4.68 ± 0.11	4.63 0.25	4.50 ± 0.10	**4.38 ± 0.08**·
	t3	5.80 ± 0.00	**5.66 ± 0.11**·	**5.44 ± 0.11****	4.53 ± 0.06	4.66 ± 0.19	4.76 ± 0.17	4.33 ± 0.35	4.44 ± 0.09	4.43 ± 0.05
OM [% DW]	t0	1.07 ± 0.19			1.27 ± 0.12			3.23 ± 0.06		
	t1									
	t2									
	t3	1.07 ± 0.06	**0.92 ± 0.08***	1.08 ± 0.11	1.10 ± 0.17	1.12 ± 0.15	**1.34 ± 0.09***	4.30 ± 3.12	3.48 ± 1.58	4.50 ± 1.32

[1]Measurements were performed on the permafrost (P), north-facing active layer (N) and south-facing active layer at the start of the experiment (t0) and in the soils incubated for 1 (t1), 2 (t2) and 3 (t3) years in the north-facing (Pn, Nn, Sn) and south-facing (Ps, Ns, Ss) topsoils. Mean ± SD (n=3 for t0 soils and n=5 for t1, t2 and t3 soils). [2]DOC: dissolved organic carbon, DN: dissolved total nitrogen. DOC and DN were measured in soil water extracts. Values in bold with superscript points or asterisks indicate marginally significant (· $p < 0.1$) and significant (* $p < 0.05$, ** $p < 0.01$, *** $p < 0.001$) differences between the soil groups Pn vs. P, Ps vs. P, Ns vs Nn and Sn vs. Ss. Significance was calculated with Games-howell pairwise tests applied to the subsets of soils separated by year. P: permafrost at the start of the experiment, N: north-facing active layer at the start of the experiment, S: south-facing active layer at the start of the experiment, Pn: permafrost transplanted to the north-facing topsoil, Ps: permafrost transplanted to the south-facing topsoil, , Nn: north-facing active-layer topsoil transplanted to the north-facing topsoil, Ns: north-facing active-layer topsoil transplanted to the south-facing topsoil, Ss: south-facing active-layer topsoil transplanted to the south-facing topsoil, Sn south-facing active-layer topsoil transplanted to the north-facing topsoil.

5. CHAPTER 5. General Discussion

5.1. The alpine permafrost microbiome of Muot da Barba Peider in the present

In alpine permafrost ecosystems, taxonomic and functional comparisons between permafrost and active layers are largely missing. This precludes an ecological understanding of the niche partitioning of microbial taxa, and how these microbial taxa drive biogeochemical processes within these mountain soils. In the mountain summit of Muot da Barba Peider (MBP), a first amplicon sequencing study in the MBP soils revealed an unexpectedly high soil microbial diversity in the permafrost, which was enriched in potentially novel taxa of unknown physiologies (Frey et al., 2016). The metagenomic study presented in Chapter 2 of this Dissertation complements the observations of Frey et al. (2016), and, together with this previous work, serves as a first baseline to compare permafrost microbiota from alpine and polar soils, and better understand the diversity and functional features of the global permafrost microbiome.

A first important indication of my research in **Chapter 2** was that at least part of the microbiota inhabiting the MBP permafrost is active (Fig. 1), which challenges the historic assumption that microbial life within permafrost is mostly quiescent. Similar to previous investigations in Arctic permafrost (Burkert et al., 2019; Coolen & Orsi, 2015; Mackelprang et al., 2017), the MBP permafrost metagenomes contained few sporulation genes and, comparatively, had a high proportion of cold-stress genes **(hypothesis 2.1)** and active-cell related genes involved in transcription, and DNA remodeling and biomolecule repair.

A second observation, relevant in the framework of global warming, was the overrepresentation of C-cycling genes in the MBP permafrost metagenomes, which drives CO_2 exchanges between the soil and the atmosphere. More specifically, I detected a higher diversity of microbial genes coding for enzymes involved in the hydrolysis of plant-, fungal-, and animal-derived polymeric substrates (e.g. lignocellulose and chitin) in the permafrost compared with the active layers, together with genes associated with fermentation and CO_2-fixation processes **(hypothesis 2.2)**. Contrary to well-studied, waterlogged sub-Arctic soils, both aerobic and anaerobic C mineralization might occur within the permafrost of less stratified alpine soils, whose coarse texture facilitates oxygenation and the percolation of materials along the soil depth gradient (Chen et al., 2016). Trapping of plant and animal detritus in

permafrost was further supported by the detection of metagenomic reads from both kingdoms. The existence of microbial communities with versatile organic C degrading catabolic potential in the permafrost links to the **hypothesis 4.2** (Chapter 4), in which I hypothesized that field-simulated warming of permafrost enhances the turnover of carbon substrates, potentially liberated from the soil upon thawing.

5.2. The alpine permafrost microbiome of Muot da Barba Peider in the future

In alpine permafrost areas it is still not clear to what extent changes in soil owing to climate warming impact the taxonomic compositions of soil prokaryotic and fungal communities, and how these compositional shifts relate to alterations in microbial activities (e.g. heterotrophic respiration) that influence model-predicted feedbacks of mountain soils to the climate (e.g. enhanced soil CO_2 emissions). Short-term (1- 3 month) responses of MBP soil microbiomes to warming-induced conditions of (1) elevated soil temperature (Luláková et al., 2019) and (2) increased availability of plant-derived C and nutrients (Adamczyk et al., 2021) have been studied. The microcosm experiment using MBP soils which I presented in **Chapter 3** expand on these aforementioned studies, in that I tested effects of (3) warming-related increases in FTC frequency (daily vs. weekly FTCs) in the MBP active layers.

All tested warming-related changes shifted the structure of the soil prokaryotic communities, whereas fungal communities might mostly respond to greater C and nutrients in the future warmer climate (Adamczyk et al., 2021). At first, my results in Chapter 3 indicate that, contrary to the effects of elevated temperature (Luláková et al., 2019) and greater soil C and nutrient availability (Adamczyk et al., 2021), more FTCs in the future could diminish soil heterotrophic respiration. However, I observed that the drop in heterotrophic respiration rates was greater for weekly FTCs (7 days of freezing) than for daily FTCs (12 h of freezing, **hypothesis 3.1** and **3.2**). This suggest that shorter periods of freezing during warmer winters may promote soil CO_2 releases in the future, which could offset the decrease in respiration driven by daily freeze-thawing. Importantly, my results also suggest common microbial responses to increased FTC frequency between alpine and Artic soils, despite their distinct environmental legacies (**hypothesis 3.3**).

The field experiment that I presented in **Chapter 4** of this Dissertation extrapolates results from laboratory incubations conducted on the MBP soils to natural scenarios. There, the permafrost (transplanted into the topsoils) and north-facing active layer (transplanted into the south-facing topsoil) microbiomes responded, over a time span of three years, to co-occurring warming-associated soil conditions of (1) increased temperatures, (2) a greater availability of C and nutrients and (3) (more) frequent FTCs.

One of the most relevant implication of the findings in **Chapter 4** in MBP**,** is that alpine permafrost microbiomes might acclimate fast (within one year) to the projected warmer climate, wherein changes in microbial diversity and community structure might persist over time. Coinciding with the laboratory observations of Luláková et al. (2019), Adamczyk et al. (2021) and my results from Chapter 3, field-simulated warming favored the expansion of copiotrophic prokaryotic taxa (e.g. *Noviherbaspirillum* and *Massilia*) in the topsoil-transplanted MBP permafrost and, to a lesser extent, the south-transplanted active layer, whereas metabolically restricted taxa (mainly Patescibacteria) decreased with warming (Fig. 1, **hypothesis 4.1**). The warming-associated increases of *Noviherbaspirillum* and *Massilia* in Arctic soils (Adamczyk et al., 2020) suggest common microbial indicators of the changing climate across differing latitudes.

In line with the findings of Adamczyk et al. (2021), field-warming also promoted ascomycetous patho-saprotrophic fungal taxa in the transplanted permafrost, but it lead to the decrease in Basidiomycetous yeasts. Importantly, the warming-induced alterations in the MBP fungal communities were less pronounced than in the prokaryotic communities. This supports the view that soil fungi may be overall less sensitive than soil prokaryotes to the changing climate (De Vries et al., 2018; Feng et al., 2020; Sharma et al., 2006; Xiong et al., 2014), or that shifts between soil fungal taxa in the future might be slower than for prokaryotic taxa, owing to lower growth rates of fungi compared with prokaryotes (Classen et al., 2015; Rousk & Baath, 2011).

A second relevant observation in Chapter 4 was that field-warming did not enhance heterotrophic respiration in the permafrost (**hypothesis 4.2**). As in the laboratory (Adamczyk et al., 2021; Luláková et al., 2019), the transplantation of the permafrost into the topsoils led to thawing, and thereby to the solubilization of autochthonous C-substrates within the soil.

Furthermore, I posited that in the field, the permafrost soil microbiota receives allochthonous C and nutrient sources, e.g. from atmospheric deposition, autotrophic activities (Rime et al., 2016; Schmidt et al., 2008a), or materials from the surrounding soils. The total autochthonous and allochthonous C resources in the transplanted permafrost could have been enough to support a substantial growth of the soil microbiota (Adamczyk et al., 2021). This explains the increase in microbial abundance in the soil, where the microbiota was able to grow on a broader range of C-substrates. The C resources might, however, have been insufficient to support high rates of cell activity. In the absence of vegetation, my current observations indicate that C-depleted soils, such as MBP, will not become CO_2 sources in the future (Fig. 1).

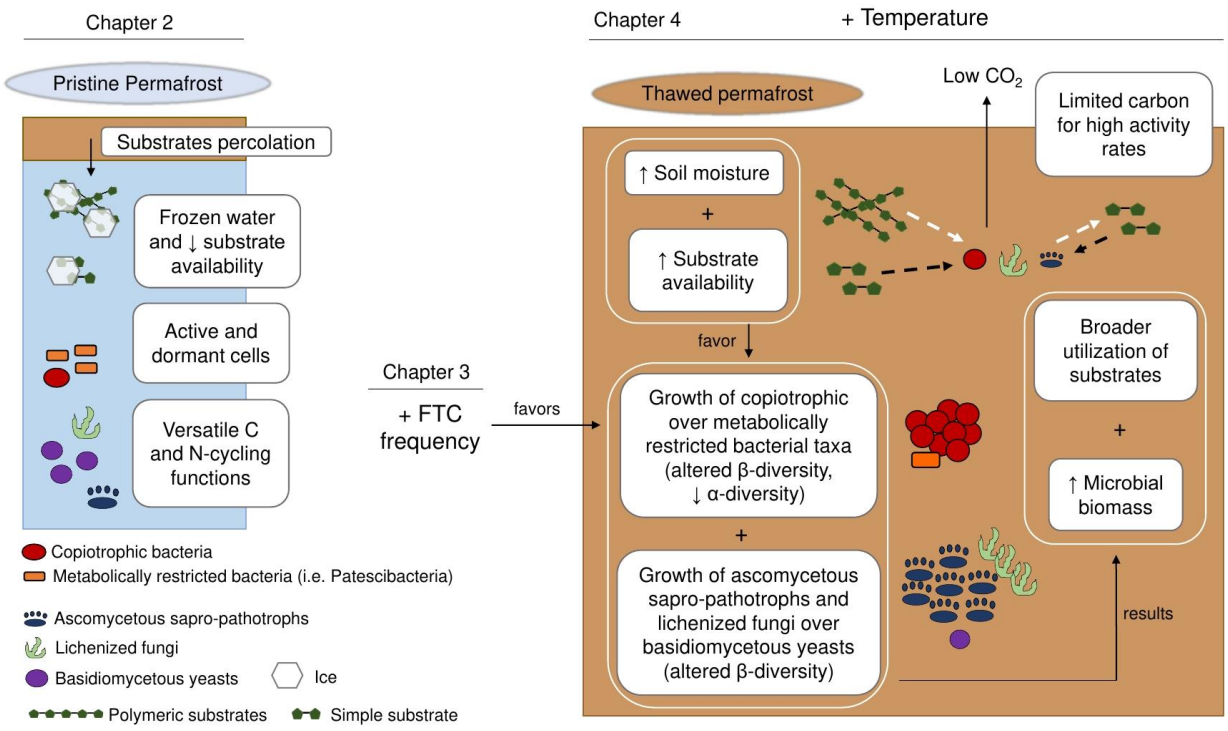

Figure 1. Summary of the main findings from the studies conducted in Muot da Barba Peider (MBP), and presented in Chapters 2, 3 and 4. In Chapter 2, I conducted metagenomic analyses of the MBP permafrost and active layer soils. These analyses indicate that the MBP permafrost contain active microbial communities of versatile C and N-cycling functions. In Chapter 3 I evaluated *in vitro* the effects of increased (+) freeze-thaw cycle (FTC) frequency on the MBP active layers. In Chapter 4 I evaluated the effects of *in situ* conditions of warming during three years on the diversity and activities of the MBP permafrost and active layer microbiomes. Field-simulated conditions of warming implied the co-occurrence of increased soil temperatures, greater availability of C and N, and FTCs in the soils. All these factors could have contributed to shifts in the structure and substrate-use capabilities of the permafrost microbiome. Although *in situ* warming promoted the growth of the microbiota in the MBP permafrost, it did not enhance heterotrophic respiration, likely constrained by the limited C content of the soil.

5.3. Beyond the ecological findings of this Dissertation

5.3.1. *Approaches to complement and extent the metagenomic analyses of the MBP soils*

In Chapter 2 of this Dissertation I successfully used metagenomic approaches to provide insights into the high functional gene diversity of poorly characterized alpine permafrost microbiomes. Although metagenomic approaches provide a holistic overview on potential metabolic capabilities and adaptative strategies of soil microbiota, they do not inform about active microbial metabolisms in soils. The Rhizosphere Processes (RPR) team is making a great effort to culture the microorganisms inhabiting the MBP soils. Up to date, the team has isolated > 1000 prokaryotic and fungal taxa from the MBP permafrost and active layers, including novel groups (e.g. Cryolevonia; Pontes et al., 2020). The ability to culture these microorganisms in the laboratory will enable to 1) verify physiological features of MBP soil taxa indicated by their metagenomes, and 2) quantify the growth and active metabolic functions of microbial cells under different habitat conditions. To complement the metagenomic and culture-based investigations of the MBP soil microbiota, it would be valuable to conduct metatranscriptomic analyses on MBP soils. Metatranscriptomic approaches largely follow the same steps as metagenomics, but inform about the active functions of the culturable and yet-to-culture soil microbiome (Shakya et al., 2019). The optimization of soil RNA extraction protocols to generate higher RNA yields will enable metatranscriptomics screenings on these soils in the future.

Besides the need of combining distinct methodologies (e.g. metagenomics, culture-based and metatranscriptomics approaches), it is crucial to determine whether the microbial findings described for MBP soils are representative of other mountain permafrost environments. During the time period of my PhD, I, together with other members of the RPR team, collected permafrost and active layers from other sites in Switzerland. Furthermore, the RPR team has collected permafrost-like topsoils from other mountain summits (> 2500 m a.s.l) in the Alps, and has used these in other projects (e.g. in Adamczyk et al., 2019 and Donhauser et al., 2020) . An immediate step to test the representativeness of my findings at MBP would be to conduct amplicon and metagenomic sequencing comparisons between MBP and these other soils from the Alps. For instance, the identification of prokaryotic and fungal taxa, and functional genes that occur across all soils, could help pinpoint microorganisms which are endemic to

these cold-dominated environments, and provide ecological insights into their physiological adaptations to alpine soil habitats (e.g. in a similar way as in Ortiz et al., 2020). Extending metagenomic studies to other alpine soils would also enable a better exploration of soil archaeal communities. Archaea are scarce in MBP (≤0.5% abundance), yet studies indicate active populations of methanogenic archaea together with methanotrophs in dry and C-depleted soils in the Alps (Hofmann et al., 2016). As a minor project, it would be interesting to compare the abundances of genes encoding key methanogenic (e.g. Methyl coenzyme M reductase gene) and methane oxidation enzymes (e.g. particulate methane monooxygenase) across alpine permafrost metagenomes, to gain insights into potential exchanges of the greenhouse gas CH_4 between these soils and the atmosphere.

It is important to highlight the significance of metagenomic surveys for the scientific community. The metagenomic data that I generated for the MBP soils, as for other metagenomic investigations, has been stored for a lifetime in the NCBI GenBank public repository. Scientists around the globe can access this data and use it to address scientific questions, which are different to the ones that I investigated here. For instance, one of the projects of the RPR team aim to unravel the role of cold soil microorganisms in degrading plastic, which is a widespread pollutant of global environmental concern (Ruthi et al., 2020). The MBP metagenomes are used in this project to identify microorganisms that harbor plastic-degrading enzymes.

5.3.2. *Future experiments to refine the links between variations in the soil microbiome and the climate*

In Chapter 3 and 4 of this Dissertation I provided an overview on potential responses of the MBP permafrost and active layer microbiota to changes in soil conditions associated with warming. However, future work is needed to better discriminate the climatic drivers that shape the microbial communities in the warmer soils. For instance, warming is associated with higher fluctuations in precipitation (IPCC, 2014, 2019). This might lead to drying and rewetting events that could affect the diversity and activities of the alpine permafrost microbiome (Meisner et al., 2021). It would be valuable to evaluate the impacts of drying and rewetting events on MBP soils microbiota, e.g. by exposing the soils to drying-rewetting cycles, in a similar microcosm incubation approach as in Chapter 3 of this Dissertation. Understanding the influence of soil

moisture on the MBP soil microbiome would improve the interpretation of FTC experiments conducted in Chapter 3, because freeze thawing implies the drying and the regaining of water in the soil matrix (Meisner et al., 2021). Drying-rewetting experiments could also enable to infer the possible influences of soil moisture on the permafrost and active layer microbial responses to *in situ* warming, that I identified in the field-warming experiment in MBP (Chapter 4).

Concerning the field experiment in Chapter 4, it is important to underline that the microbial responses to simulated warming that I identified for the MBP permafrost and active layers correspond to the first three years after soil transplantation. Future monitoring of the transplanted soils by the RPR team could reveal an evolution of microbial responses to warming. For instance, as observed in decadal field-warming studies in Arctic soils (Deslippe et al., 2012; Monteux et al., 2018), oligotrophic taxa inhabiting the warmed MBP permafrost could replace copiotrophic taxa in the long-term because of a gradual enrichment in recalcitrant compounds as soil microorganisms more rapidly deplete more energy-rich, labile carbon sources (Li et al., 2021). Fungi and oligotrophic prokaryotes generally assimilate carbon compounds more efficiently than copiotrophs, thereby producing less CO_2 per unit of substrate (Ho et al., 2017; Kallenbach et al., 2016). If oligotrophs and fungi eventually expand over copiotrophic prokaryotic taxa in the MBP soils undergoing warming, these soils could decrease their (already low) CO_2 emissions. The warmer thermal regimes could also select for soil microbial communities with higher optimal growth temperatures (Donhauser et al., 2020; Li et al., 2021).

Importantly, soil copiotrophic taxa might also switch to oligotrophic lifestyles in warmer future soils, slowing down their growth rates and adjusting their metabolic profiles to less energy-rich substrates (Senechkin et al., 2010), or even evolving (Chase et al., 2021). As discussed in Senechkin et al. (2010), “true” oligotrophs, therein understood as microorganisms only capable of growing in low C (10 µg C ml^{-1} in agar medium) may be rare. Taxonomic information provides insights about potential functional traits of soil prokaryotic community members, but these traits must be quantified for certainty (Morrissey et al., 2016). In the future, experiments could be performed to better discriminate the copiotrophic or oligotrophic prokaryotes in the MBP soils, which could in turn help linking variations in functional microbial groups with ecosystem-level activities (e.g. soil CO_2 production). For instance, aliquots of the MBP soils

exposed to field-warming could be amended with ^{13}C-labelled labile (e.g. glucose), preferably consumed by the copiotrophs, or (more) recalcitrant (e.g. cellulose) substrates, promoting the oligotrophs. Measurements of the substrates consumption and CO_2 production rates by tracing the ^{13}C, combined with sequencing and microbial abundance or biomass estimates, could indicate whether the soils are enriched in taxa of copiotrophic (i.e. high CO_2 production per unit of C or biomass), or oligotrophic attributes (Geyer et al., 2019; Naylor et al., 2020).

5.3.3. *Incorporation of metagenomic analyses to better understand functional changes in the soil microbiome owing to warming*

An open question is whether the MBP soils could become CO_2 sinks in the future, and thereby offset warming. In the conceptual model developed by Donhauser & Frey (2018) (Fig. 4 of the review), the authors theorized that in C-deficient alpine soils, warming-stimulated CO_2-fixation activities, first by microorganisms and, in the long-term, through potential colonization by upward migrating plants, could outweigh heterotrophic respiration. An immediate step to better understand the warming-associated alterations in C-cycling functions in the MBP soils would be to perform metagenomic analyses of the topsoil-transplanted permafrost and south-transplanted active layers. The metagenomic data would enable to quantify key genes involved in CO_2-fixation (e.g. genes coding for the enzyme ribulose-1,5-bisphosphate carboxylase) and C-degrading microbial activities (e.g. carbohydrate-active enzyme genes) in the soils. In a similar way as I did for the amplicon data, functional genes increasing or decreasing with warming could be identified by comparing gene abundances between: (1) the topsoil-transplanted permafrost (thawed) with intact permafrost collected at the beginning of the field experiment, and (2) north-facing active layers transplanted to the south-facing slope of MBP with north-facing active layers transplanted within the north-facing slope. In a further step the MBP soil metagenomes could be used to reconstruct MAGs, which would enable to better identify the microbial taxa potentially driving the recycling of C and nutrients in the soils (e.g. as in Woodcroft et al., 2018). Prokaryotic MAGs could also reveal genetic signatures that indicate copiotrophic (e.g. large genomes and many 16S rRNA copies) or oligotrophic lifestyles (Lauro et al., 2009; Okie et al., 2020).

Besides unveiling potential warming-induced changes in soil C processing, the metagenomic data obtained from the transplanted MBP soils could enable to investigate alterations in N-cycling genes associated with warming. The metagenomic profiling of the MBP soils (Chapter 3) showed that the soils contained abundant genes coding for key enzymes involved in all N-cycling processes, despite the extremely low N content of the soils. The mobilization of substrates and the warming-induce increase in microbial abundance could explain the increase of N in the transplanted MBP permafrost (Chapter 4). Lower C:N contents favors fungal over prokaryotic growth (Soares & Rousk, 2019). The fungal and prokaryotic-mediated liberation of nutrients in the soils, including nitrate and ammonium, could stimulate vegetation growth in the future (Naylor et al., 2020). In turn, plant-derived C and N inputs in the soils could amplify the growth and C- and N-cycling activities of the MBP soil microorganisms (Adamczyk et al., 2021). Recent reviews point that in poorly vegetated alpine soils, N sequestration processes (e.g. through complete denitrification and N fixation) could outweigh N losses (e.g. through incomplete denitrification) and that these soils could become N sinks in the long-term, thereby mitigating warming (Voigt et al., 2020). N-cycling studies in alpine soils will enable to verify this prediction.

5.3.4. *Further analyses and field experiments to better understand the alpine permafrost ecosystem and its global microbial responses to warming*

Ideally, the genetic findings from MBP would need to be complemented with measurements of microbial activities in the field, including *in situ* rates of soil CO_2 fixation and respiration, and N_2O fluxes. Future monitoring of the field experiment in MBP would greatly benefit from the development of a gas-tight system that would enable to obtain reliable estimates of soil gas fluxes in these rocky soils. Furthermore, it would be valuable to characterize the organic pools within the MBP soils (e.g. fractions of lignin and hemicellulose components, indicated in the metagenomic reads; Chapter 2) to reveal the *in situ* C and N-substrates which are available for the soil microbiota. Studies point that deep soils (> 1 m b.g.s), including alpine permafrost, contain highly diverse labile and recalcitrant C pools of old age which could be mobilized under climate warming (e.g. Chen et al., 2016; Van der Voort et al., 2019). Characterizations of these pools are, however, remarkably scarce and, overall, the biogeochemical processes involved in the transformations of organic materials and minerals in these soils are largely unknown.

Last but not least, it would be necessary to investigate whether the microbial responses to warming observed in MBP are universal to other permafrost environments. In parallel with the field experiment established in MBP, additional transplantation experiments were set up in other summits in the Alps by Donhauser and RPR coworkers (Donhauser, 2021). In these experiments topsoils were transplanted 1) from the north to the south slope in each of the summits to simulate warming, and 2) from the summits at higher elevations (2800- 3000 m a.s.l.) to the warmer thermal regimes of the summit at 2400 m a.s.l. It would be possible to combine the microbial data collected from the field experiment in MBP with microbial data obtained from these other transplantations in the Alps. The observation of common taxa increasing in abundance with the simulated warming across all the summits could help identifying microbial groups at the regional scale, which will benefit from the warmer mountain climate in the future. Additionally, to better understand the effects of the projected increase in vegetation on the soil microbiota, these transplantation experiments could be supplemented with plant-related treatments. For instance, new or already transplanted soil replicates in MBP or the other summits could be amended with litter (or root exudates) to evaluate the *in situ* effects of augmented plant-derived C and nutrient inputs on the alpine soil microbiomes (e.g. as in Adamczyk et al., 2020) .

5.4. Global perspectives and concluding remarks

My investigations build up on previous microbial studies in Tibetan permafrost soils and together with this previous work underline the sensitivity of the alpine permafrost microbiome to warming and its influences to the climate. Organic Arctic permafrost soils are expected to release substantial C upon thawing, whereas part of the CO_2 could be eventually sequestered by C-depleted alpine soils (Donhauser & Frey, 2018; Nikrad et al., 2016). Future studies identifying the functional permafrost microbial groups (e.g. copiotrophs / oligotrophs) responding to warming across the different latitudes will enable to verify these predictions. Furthermore, refined global taxonomic and functional characterizations of the permafrost microbiota would advance our understanding about the C and nutrient cycling processes in these soil ecosystems, and their behavior in the future.

6. Bibliography

Abarenkov K., Henrik Nilsson R., Larsson K.H., Alexander I.J., Eberhardt U., Erland S., Hoiland K., Kjoller R., Larsson E., Pennanen T., Sen R., Taylor A.F., Tedersoo L., Ursing B.M., Vralstad T., Liimatainen K., Peintner U. & Koljalg U. (2010). The UNITE database for molecular identification of fungi--recent updates and future perspectives. New Phytologist 186(2), 281-5. doi:10.1111/j.1469-8137.2009.03160.x

Abbott B.W., Larouche J.R., Jones J.B., Bowden W.B. & Balser A.W. (2014). Elevated dissolved organic carbon biodegradability from thawing and collapsing permafrost. Journal of Geophysical Research-Biogeosciences 119(10), 2049-2063. doi:10.1002/2014jg002678

Abrams Z.B., Johnson T.S., Huang K., Payne P.R.O. & Coombes K. (2019). A protocol to evaluate RNA sequencing normalization methods. BMC Bioinformatics 20(Suppl 24), 679-679. doi:10.1186/s12859-019-3247-x

Adamczyk M., Hagedorn F., Wipf S., Donhauser J., Vittoz P., Rixen C., Frossard A., Theurillat J.P. & Frey B. (2019). The soil microbiome of GLORIA mountain summits in the Swiss Alps. Frontiers in Microbiology 10, 1080. doi:10.3389/fmicb.2019.01080

Adamczyk M., Perez-Mon C., Gunz S. & Frey B. (2020). Strong shifts in microbial community structure are associated with increased litter input rather than temperature in High Arctic soils. Soil Biology and Biochemistry 151, 108054. doi:10.1016/j.soilbio.2020.108054

Adamczyk M., Ruthi J. & Frey B. (2021). Root exudates increase soil respiration and alter microbial community structure in alpine permafrost and active layer soils. Environmental Microbiology 23(4), 2152-2168. doi:10.1111/1462-2920.15383

Anderson M.J. (2001). A new method for non-parametric multivariate analysis of variance. Austral Ecology 26(1), 32-46. doi:10.1111/j.1442-9993.2001.01070.pp.x

Anderson M.J. & Walsh D.C.I. (2013). PERMANOVA, ANOSIM, and the Mantel test in the face of heterogeneous dispersions: what null hypothesis are you testing? Ecological Monographs 83(4), 557-574. doi:10.1890/12-2010.1

Angly F.E., Dennis P.G., Skarshewski A., Vanwonterghem I., Hugenholtz P. & Tyson G.W. (2014). CopyRighter: a rapid tool for improving the accuracy of microbial community profiles through lineage-specific gene copy number correction. Microbiome 2(11). doi:10.1186/2049-2618-2-11

Anwar M.Z., Lanzen A., Bang-Andreasen T. & Jacobsen C.S. (2019). To assemble or not to resemble-a validated Comparative Metatranscriptomics Workflow (CoMW). Gigascience 8(8). doi:10.1093/gigascience/giz096

Aszalos J.M., Szabo A., Megyes M., Anda D., Nagy B. & Borsodi A.K. (2020). Bacterial Diversity of a High-Altitude Permafrost Thaw Pond Located on Ojos del Salado (Dry Andes, Altiplano-Atacama Region). Astrobiology 20(6), 754-765. doi:10.1089/ast.2018.2012

Ayala-del-Río H.L., Chain P.S., Grzymski J.J., Ponder M.A., Ivanova N., Bergholz P.W., Di Bartolo G., Hauser L., Land M., Bakermans C., Rodrigues D., Klappenbach J., Zarka D., Larimer F., Richardson P., Murray A., Thomashow M. & Tiedje J.M. (2010). The genome sequence of *Psychrobacter arcticus* 273-4, a psychroactive Siberian permafrost bacterium, reveals

mechanisms for adaptation to low-temperature growth. Applied and environmental microbiology 76(7), 2304-2312. doi:10.1128/AEM.02101-09

Bakermans C., Bergholz P.W., Rodrigues D.F., Vishnivetskaya T.A., Ayala-del-Río H.L. & Tiedje J.M. (2012). Genomic and expression analyses of cold-adapted microorganisms. In: Miller RV, Whyte LG, editors. Polar microbiology: life in a deep freeze. American Society of Microbiology, United States, pp. 126-155.

Baldani J.I., Rouws L., Cruz L.M., Olivares F.L., Schmid M. & Hartmann A. (2014). The family *Oxalobacteraceae*. In: Rosenberg E, DeLong EF, Lory S, Stackebrandt E, Thompson F, editors. The Prokaryotes: Alphaproteobacteria and Betaproteobacteria. Springer, Berlin, Heidelberg, pp. 919-974.

Balser T.C., Gutknecht J.L.M. & Liang C. (2010). How will climate change impact soil microbial communities? In: Dixon GR, Tilston EL, editors. Soil microbiology and sustainable crop production. Springer Netherlands, Dordrecht, pp. 373-397.

Banerjee S., Walder F., Buchi L., Meyer M., Held A.Y., Gattinger A., Keller T., Charles R. & van der Heijden M.G.A. (2019). Agricultural intensification reduces microbial network complexity and the abundance of keystone taxa in roots. ISME Journal 13(7), 1722-1736. doi:10.1038/s41396-019-0383-2

Bao X., Zhu X., Chang X., Wang S., Xu B., Luo C., Zhang Z., Wang Q., Rui Y. & Cui X. (2016). Effects of soil temperature and moisture on soil respiration on the Tibetan Plateau. Plos One 11(10), e0165212. doi:10.1371/journal.pone.0165212

Barry R.G. (2008). Geographical controls of mountain meteorological elements. In: Barry RG, editor. Mountain weather and climate. Cambridge University Press, Cambridge, pp. 24-124.

Bellemain E., Davey M.L., Kauserud H., Epp L.S., Boessenkool S., Coissac E., Geml J., Edwards M., Willerslev E., Gussarova G., Taberlet P., Haile J. & Brochmann C. (2013). Fungal palaeodiversity revealed using high-throughput metabarcoding of ancient DNA from arctic permafrost. Environmental Microbiology 15(4), 1176-89. doi:10.1111/1462-2920.12020

Beniston M., Keller F. & Goyette S. (2003). Snow pack in the Swiss Alps under changing climatic conditions: an empirical approach for climate impacts studies. Theoretical and Applied Climatology 74(1-2), 19-31. doi:10.1007/s00704-002-0709-1

Berger F., Morellet N., Menu F. & Potier P. (1996). Cold shock and cold acclimation proteins in the psychrotrophic bacterium *Arthrobacter globiformis* SI55. Journal of Bacteriology 178(11), 2999-3007. doi:10.1128/jb.178.11.2999-3007.1996

Beylich A.A., Kolstrup E., Thyrsted T., Linde N., Pedersen L.B. & Dynesius L. (2004). Chemical denudation in arctic-alpine Latnjavagge (Swedish Lapland) in relation to regolith as assessed by radio magnetotelluric-geophysical profiles. Geomorphology 57(3-4), 303-319. doi:10.1016/S0169-555x(03)00162-4

Beylich A.A., Sandberg O., Molau U. & Wache S. (2006). Intensity and spatio-temporal variability of fluvial sediment transfers in an Arctic-oceanic periglacial environment in northernmost Swedish Lapland (Latnjavagge catchment). Geomorphology 80(1-2), 114-130. doi:10.1016/j.geomorph.2005.09.014

Biskaborn B.K., Smith S.L., Noetzli J., Matthes H., Vieira G., Streletskiy D.A., Schoeneich P., Romanovsky V.E., Lewkowicz A.G., Abramov A., Allard M., Boike J., Cable W.L., Christiansen H.H., Delaloye R., Diekmann B., Drozdov D., Etzelmüller B., Grosse G., Guglielmin M., Ingeman-Nielsen T., Isaksen K., Ishikawa M., Johansson M., Johannsson H., Joo A., Kaverin D., Kholodov A., Konstantinov P., Kröger T., Lambiel C., Lanckman J.-P., Luo D., Malkova G., Meiklejohn I., Moskalenko N., Oliva M., Phillips M., Ramos M., Sannel A.B.K., Sergeev D., Seybold C., Skryabin P., Vasiliev A., Wu Q., Yoshikawa K., Zheleznyak M. & Lantuit H. (2019). Permafrost is warming at a global scale. Nature Communications 10(1), 264. doi:10.1038/s41467-018-08240-4

Bockheim J.G. & Munroe J.S. (2014). Organic carbon pools and genesis of alpine soils with permafrost: A review. Arctic, Antarctic, and Alpine Research 46(4), 987-1006. doi:10.1657/1938-4246-46.4.987

Böckli L. (2013). Characterizing permafrost in the entire European Alps: spatial distribution and ice content. Doctoral dissertation, Zurich University, Zurich. Retrieved from: https://www.zora.uzh.ch/id/eprint/89504/

Bolger A.M., Lohse M. & Usadel B. (2014). Trimmomatic: a flexible trimmer for Illumina sequence data. Bioinformatics 30(15), 2114-20. doi:10.1093/bioinformatics/btu170

Bolter M., Soethe N., Horn R. & Uhlig C. (2005). Seasonal development of microbial activity in soils of northern Norway. Pedosphere 15(6), 716-727. url:<Go to ISI>://WOS:000233780600004

Bowers R.M., Kyrpides N.C., Stepanauskas R., Harmon-Smith M., Doud D., Reddy T.B.K., Schulz F., Jarett J., Rivers A.R., Eloe-Fadrosh E.A., Tringe S.G., Ivanova N.N., Copeland A., Clum A., Becraft E.D., Malmstrom R.R., Birren B., Podar M., Bork P., Weinstock G.M., Garrity G.M., Dodsworth J.A., Yooseph S., Sutton G., Glockner F.O., Gilbert J.A., Nelson W.C., Hallam S.J., Jungbluth S.P., Ettema T.J.G., Tighe S., Konstantinidis K.T., Liu W.T., Baker B.J., Rattei T., Eisen J.A., Hedlund B., McMahon K.D., Fierer N., Knight R., Finn R., Cochrane G., Karsch-Mizrachi I., Tyson G.W., Rinke C., Lapidus A., Meyer F., Yilmaz P., Parks D.H., Eren A.M., Schriml L., Banfield J.F., Hugenholtz P., Woyke T. & Consortium G.S. (2017). Minimum information about a single amplified genome (MISAG) and a metagenome-assembled genome (MIMAG) of bacteria and archaea. Nature Biotechnology 35(8), 725-731. doi:10.1038/nbt.3893

Bowman J.P. (2017). Genomics of psychrophilic Bacteria and Archaea. In: Margesin R, editor. Psychrophiles: from biodiversity to biotechnology. Springer International Publishing, Cham, pp. 345-387.

Brankatschk R., Towe S., Kleineidam K., Schloter M. & Zeyer J. (2011). Abundances and potential activities of nitrogen cycling microbial communities along a chronosequence of a glacier forefield. ISME Journal 5(6), 1025-1037. doi:10.1038/ismej.2010.184

Breitwieser F.P., Lu J. & Salzberg S.L. (2019). A review of methods and databases for metagenomic classification and assembly. Briefings in Bioinformatics 20(4), 1125-1139. doi:10.1093/bib/bbx120

Brown C.T., Hug L.A., Thomas B.C., Sharon I., Castelle C.J., Singh A., Wilkins M.J., Wrighton K.C., Williams K.H. & Banfield J.F. (2015). Unusual biology across a group comprising more than 15% of domain Bacteria. Nature 523(7559), 208-211. doi:10.1038/nature14486

Burkert A., Douglas T.A., Waldrop M.P. & Mackelprang R. (2019). Changes in the active, dead, and dormant microbial community structure across a Pleistocene permafrost chronosequence. Applied and Environmental Microbiology 85(7). doi:10.1128/AEM.02646-18

Burns R.G. (2010). How do microbial extracellular enzymes locate and degrade natural and synthetic polymers in soil. In: Xu J, Huang PM, editors. Molecular environmental soil Science at the interfaces in the Earth's Critical Zone. Springer Berlin Heidelberg, Berlin, Heidelberg, pp. 294-297.

Cáceres M.D. & Legendre P. (2009). Associations between species and groups of sites: indices and statistical inference. Ecology 90(12), 3566-3574. doi:10.1890/08-1823.1

Cameron E.S., Schmidt P.J., Tremblay B.J.M., Emelko M.B. & Müller K.M. (2021). To rarefy or not to rarefy: enhancing microbial community analysis through next-generation sequencing. bioRxiv. doi:10.1101/2020.09.09.290049

Cantarel B.L., Coutinho P.M., Rancurel C., Bernard T., Lombard V. & Henrissat B. (2009). The Carbohydrate-Active EnZymes database (CAZy): an expert resource for Glycogenomics. Nucleic Acids Research 37(Database issue), D233-8. doi:10.1093/nar/gkn663

Cao Y.F., Ke X., Guo X.W., Cao G.M. & Du Y.O. (2018). Nitrous oxide emission rates over 10 years in an alpine meadow on the Tibetan Plateau. Polish Journal of Environmental Studies 27(3), 1353-1358. doi:10.15244/pjoes/76795

Chase A.B., Weihe C. & Martiny J.B.H. (2021). Adaptive differentiation and rapid evolution of a soil bacterium along a climate gradient. Proceedings of the National Academy of Sciences 118(18), e2101254118. doi:10.1073/pnas.2101254118

Chauhan A., Layton A.C., Vishnivetskaya T.A., Williams D., Pfiffner S.M., Rekepalli B., Stackhouse B., Lau M.C., Phelps T.J., Mykytczuk N., Ronholm J., Whyte L., Onstott T.C. & Sayler G.S. (2014). Metagenomes from thawing low-soil-organic-carbon mineral cryosols and permafrost of the Canadian High Arctic. Genome Announcements 2(6). doi:10.1128/genomeA.01217-14

Chen L.Y., Liang J.Y., Qin S.Q., Liu L., Fang K., Xu Y.P., Ding J.Z., Li F., Luo Y.Q. & Yang Y.H. (2016). Determinants of carbon release from the active layer and permafrost deposits on the Tibetan Plateau. Nature Communications 7, 13046. doi:10.1038/ncomms13046

Chen Y., Liu F., Kang L., Zhang D., Kou D., Mao C., Qin S., Zhang Q. & Yang Y. (2021). Large-scale evidence for microbial response and associated carbon release after permafrost thaw. Global Change Biology, 00: 1–12. doi:10.1111/gcb.15487

Claridge G.G.C., Campbell I.B. & Sheppard D.S. (2000). Carbon pools in Antarctica and their significance for global climate change. In: Kimble JM, editor. Global Climate Change and Cold Regions Ecosystems. CRC Press, Boca Raton, USA, pp. 59-78.

Clarke K.R. & Gorley R.N. (2015). PRIMER v7: User manual/tutorial. Retrieved from: http://updates.primer-e.com/primer7/manuals/User_manual_v7a.pdf. Access date: 2017

Classen A.T., Sundqvist M.K., Henning J.A., Newman G.S., Moore J.A.M., Cregger M.A., Moorhead L.C. & Patterson C.M. (2015). Direct and indirect effects of climate change on soil microbial and soil microbial-plant interactions: what lies ahead? Ecosphere 6(8), 1-21. doi:10.1890/es15-00217.1

Coleine C., Stajich J.E., de los Rios A. & Selbmann L. (2021). Beyond the extremes: rocks as ultimate refuge for fungi in drylands. Mycologia 113(1), 108-133. doi:10.1080/00275514.2020.1816761

Coolen M.J. & Orsi W.D. (2015). The transcriptional response of microbial communities in thawing Alaskan permafrost soils. Frontiers in Microbiology 6(MAR), 197. doi:10.3389/fmicb.2015.00197

Csardi G. & Nepusz T. (2006). The igraph software package for complex network research. InterJournal Complex Systems, 1695. url:http://igraph.org

Davies B.E. (1974). Loss-on-ignition as an estimate of soil organic-matter. Soil Science Society of America Journal 38(1), 150-151. doi:10.2136/sssaj1974.03615995003800010046x

De Maayer P., Anderson D., Cary C. & Cowan D.A. (2014). Some like it cold: understanding the survival strategies of psychrophiles. EMBO Reports 15(5), 508-17. doi:10.1002/embr.201338170

De Vries F.T., Griffiths R.I., Bailey M., Craig H., Girlanda M., Gweon H.S., Hallin S., Kaisermann A., Keith A.M., Kretzschmar M., Lemanceau P., Lumini E., Mason K.E., Oliver A., Ostle N., Prosser J.I., Thion C., Thomson B. & Bardgett R.D. (2018). Soil bacterial networks are less stable under drought than fungal networks. Nature Communications 9, 3033. doi:10.1038/s41467-018-05516-7

Dedysh S.N. & Ivanova A.A. (2019). Planctomycetes in boreal and subarctic wetlands: diversity patterns and potential ecological functions. FEMS Microbiology Ecology 95(2), fiy227. doi:10.1093/femsec/fiy227

Deslippe J.R., Hartmann M., Simard S.W. & Mohn W.W. (2012). Long-term warming alters the composition of Arctic soil microbial communities. FEMS Microbiology Ecology 82(2), 303-315. doi:10.1111/j.1574-6941.2012.01350.x

Ding J.Z., Chen L.Y., Zhang B.B., Liu L., Yang G.B., Fang K., Chen Y.L., Li F., Kou D., Ji C.J., Luo Y.Q. & Yang Y.H. (2016). Linking temperature sensitivity of soil CO_2 release to substrate, environmental, and microbial properties across alpine ecosystems. Global Biogeochemical Cycles 30(9), 1310-1323. doi:10.1002/2015gb005333

Donhauser J. (2021). Structural and functional characterization of climate change impacts on the microbiome in Arctic and alpine terrestrial cryoenvironments. Doctoral Dissertation, Swiss Federal Institute of Technology in Zürich, Zurich. Retrieved from: https://www.research-collection.ethz.ch/handle/20.500.11850/470200?show=full

Donhauser J. & Frey B. (2018). Alpine soil microbial ecology in a changing world. FEMS Microbiology Ecology 94(9), fiy099. doi:10.1093/femsec/fiy099

Donhauser J., Niklaus P.A., Rousk J., Larose C. & Frey B. (2020). Temperatures beyond the community optimum promote the dominance of heat-adapted, fast growing and stress resistant bacteria in alpine soils. Soil Biology and Biochemistry 148, 107873. doi:10.1016/j.soilbio.2020.107873

Donhauser J., Qi W., Bergk-Pinto B. & Frey B. (2021). High temperatures enhance the microbial genetic potential to recycle C and N from necromass in high-mountain soils. Global Change Biology 27(7), 1365-1386. doi:10.1111/gcb.15492

Edgar R.C. (2010). Search and clustering orders of magnitude faster than BLAST. Bioinformatics 26(19), 2460-1. doi:10.1093/bioinformatics/btq461

Edgar R.C. (2013). UPARSE: highly accurate OTU sequences from microbial amplicon reads. Nature Methods 10(10), 996-8. doi:10.1038/nmeth.2604

Edgar R.C. & Flyvbjerg H. (2015). Error filtering, pair assembly and error correction for next-generation sequencing reads. Bioinformatics 31(21), 3476-82. doi:10.1093/bioinformatics/btv401

Elmendorf S.C., Henry G.H.R., Hollister R.D., Bjork R.G., Bjorkman A.D., Callaghan T.V., Collier L.S., Cooper E.J., Cornelissen J.H.C., Day T.A., Fosaa A.M., Gould W.A., Gretarsdottir J., Harte J., Hermanutz L., Hik D.S., Hofgaard A., Jarrad F., Jonsdottir I.S., Keuper F., Klanderud K., Klein J.A., Koh S., Kudo G., Lang S.I., Loewen V., May J.L., Mercado J., Michelsen A., Molau U., Myers-Smith I.H., Oberbauer S.F., Pieper S., Post E., Rixen C., Robinson C.H., Schmidt N.M., Shaver G.R., Stenstrom A., Tolvanen A., Totland O., Troxler T., Wahren C.H., Webber P.J., Welker J.M. & Wookey P.A. (2012). Global assessment of experimental climate warming on tundra vegetation: heterogeneity over space and time. Ecology Letters 15(2), 164-175. doi:10.1111/j.1461-0248.2011.01716.x

Eriksson M., Ka J.O. & Mohn W.W. (2001). Effects of low temperature and freeze-thaw cycles on hydrocarbon biodegradation in Arctic tundra soil. Applied and Environmental Microbiology 67(11), 5107-12. doi:10.1128/AEM.67.11.5107-5112.2001

Ernakovich J.G. & Wallenstein M.D. (2015). Permafrost microbial community traits and functional diversity indicate low activity at in situ thaw temperatures. Soil Biology and Biochemistry 87, 78-89. doi:10.1016/j.soilbio.2015.04.009

Fahad S., Sönmez O., Saud S., Wang D., Wu C., Adnan M. & Turan V. (2021). Sustainable soil and land management and climate change. CRC Press, Boca Raton

Feng J.J., Wang C., Lei J.S., Yang Y.F., Yan Q.Y., Zhou X.S., Tao X.Y., Ning D.L., Yuan M.T.M., Qin Y.J., Shi Z.J., Guo X., He Z.L., Van Nostrand J.D., Wu L.Y., Bracho-Garillo R.G., Penton C.R., Cole J.R., Konstantinidis K.T., Luo Y.Q., Schuur E.A.G., Tiedje J.M. & Zhou J.Z. (2020). Warming-induced permafrost thaw exacerbates tundra soil carbon decomposition mediated by microbial community. Microbiome 8(1). doi:10.1186/s40168-019-0778-3

Feng X.J., Nielsen L.L. & Simpson M.J. (2007). Responses of soil organic matter and microorganisms to freeze-thaw cycles. Soil Biology and Biochemistry 39(8), 2027-2037. doi:10.1016/j.soilbio.2007.03.003

Fierer N., Bradford M.A. & Jackson R.B. (2007). Toward an ecological classification of soil bacteria. Ecology 88(6), 1354-64. doi:10.1890/05-1839

Fontaine S., Barot S., Barre P., Bdioui N., Mary B. & Rumpel C. (2007). Stability of organic carbon in deep soil layers controlled by fresh carbon supply. Nature 450(7167), 277-80. doi:10.1038/nature06275

Freppaz M., Williams B.L., Edwards A.C., Scalenghe R. & Zanini E. (2007). Simulating soil freeze/thaw cycles typical of winter alpine conditions: implications for N and P availability. Applied Soil Ecology 35(1), 247-255. doi:10.1016/j.apsoil.2006.03.012

Frey B., Rieder S.R., Brunner I., Plotze M., Koetzsch S., Lapanje A., Brandl H. & Furrer G. (2010). Weathering-associated bacteria from the Damma glacier forefield: physiological capabilities and impact on granite dissolution. Applied and Environmental Microbiology 76(14), 4788-96. doi:10.1128/AEM.00657-10

Frey B., Rime T., Phillips M., Stierli B., Hajdas I., Widmer F. & Hartmann M. (2016). Microbial diversity in European alpine permafrost and active layers. FEMS Microbiology Ecology 92(3), fiw018. doi:10.1093/femsec/fiw018

Frey B., Walthert L., Perez-Mon C., Stierli B., Köchli R., Dharmarajah A. & Brunner I. (2021). Deep soil layers of drought-exposed forests harbor poorly known bacterial and fungal communities. Frontiers in Microbiology 12, 1061. doi:10.3389/fmicb.2021.674160

Frossard A., Gerull L., Mutz M. & Gessner M.O. (2012). Disconnect of microbial structure and function: enzyme activities and bacterial communities in nascent stream corridors. ISME Journal 6(3), 680-91. doi:10.1038/ismej.2011.134

Frossard A., Hartmann M. & Frey B. (2017). Tolerance of the forest soil microbiome to increasing mercury concentrations. Soil Biology and Biochemistry 105, 162-176. doi:10.1016/j.soilbio.2016.11.016

Gee G. & Bauder J. (1986). Particle-size analysis. In: Klute A, editor. Methods of soil analysis.Physical and mineralogical methods.Agronomy Monograph. 9. Soil Science Society of America, Madison, WI, USA.

Genxu W., Yuanshou L., Yibo W. & Qingbo W. (2008). Effects of permafrost thawing on vegetation and soil carbon pool losses on the Qinghai–Tibet Plateau, China. Geoderma 143(1-2), 143-152. doi:10.1016/j.geoderma.2007.10.023

Germino M.J. (2013). Plants in alpine environments. In: Monson RK, editor. Ecology and the Environment. Springer New York, New York, NY, pp. 1-30.

Geyer K.M., Dijkstra P., Sinsabaugh R. & Frey S.D. (2019). Clarifying the interpretation of carbon use efficiency in soil through methods comparison. Soil Biology and Biochemistry 128, 79-88. doi:10.1016/j.soilbio.2018.09.036

Gobiet A., Kotlarski S., Beniston M., Heinrich G., Rajczak J. & Stoffel M. (2014). 21st century climate change in the European Alps--a review. Science of the Total Environment 493, 1138-51. doi:10.1016/j.scitotenv.2013.07.050

Gou X.L., Tan B., Wu F.Z., Yang W.Q., Xu Z.F., Li Z.P. & Zhang X.T. (2015). Seasonal dynamics of soil microbial biomass C and N along an elevational gradient on the eastern Tibetan Plateau, China. Plos One 10(7), e0132443. doi:10.1371/journal.pone.0132443

Greening C., Biswas A., Carere C.R., Jackson C.J., Taylor M.C., Stott M.B., Cook G.M. & Morales S.E. (2016). Genomic and metagenomic surveys of hydrogenase distribution indicate H_2 is a widely utilised energy source for microbial growth and survival. ISME Journal 10(3), 761-777. doi:10.1038/ismej.2015.153

Grogan P., Michelsen A., Ambus P. & Jonasson S. (2004). Freeze-thaw regime effects on carbon and nitrogen dynamics in sub-arctic heath tundra mesocosms. Soil Biology and Biochemistry 36(4), 641-654. doi:10.1016/j.soilbio.2003.12.007

Gruber S. & Haeberli W. (2007). Permafrost in steep bedrock slopes and its temperature-related destabilization following climate change. Journal of Geophysical Research-Earth Surface 112(F2). doi:10.1029/2006jf000547

Guo G.X., Kong W.D., Liu J.B., Zhao J.X., Du H.D., Zhang X.Z. & Xia P.H. (2015). Diversity and distribution of autotrophic microbial community along environmental gradients in grassland soils

on the Tibetan Plateau. Applied Microbiology and Biotechnology 99(20), 8765-8776. doi:10.1007/s00253-015-6723-x

Haberkorn A., Kenner R., Noetzli J. & Phillips M. (2021). Changes in ground temperature and dynamics in mountain permafrost in the Swiss Alps. Frontiers in Earth Science 9, 234. doi:10.3389/feart.2021.626686

Haeberli W. & Gruber S. (2009). Global warming and mountain permafrost. In: Margesin R, editor. Permafrost soils. Springer Berlin Heidelberg, Berlin, Heidelberg, pp. 205-218.

Hagedorn F., Gavazov K. & Alexander J.M. (2019). Above- and belowground linkages shape responses of mountain vegetation to climate change. Science 365(6458), 1119-+. doi:10.1126/science.aax4737

Han C.L., Gu Y.J., Kong M., Hu L.W., Jia Y., Li F.M., Sun G.J. & Siddique K.H.M. (2018). Responses of soil microorganisms, carbon and nitrogen to freeze thaw cycles in diverse land-use types. Applied Soil Ecology 124, 211-217. doi:10.1016/j.apsoil.2017.11.012

Hartmann M., Niklaus P.A., Zimmermann S., Schmutz S., Kremer J., Abarenkov K., Luscher P., Widmer F. & Frey B. (2014). Resistance and resilience of the forest soil microbiome to logging-associated compaction. ISME Journal 8(1), 226-44. doi:10.1038/ismej.2013.141

Hassan N., Rafiq M., Hayat M., Shah A.A. & Hasan F. (2016). Psychrophilic and psychrotrophic fungi: a comprehensive review. Reviews in Environmental Science and Bio-Technology 15(2), 147-172. doi:10.1007/s11157-016-9395-9

Henry H.A.L. (2008). Climate change and soil freezing dynamics: historical trends and projected changes. Climatic Change 87(3-4), 421-434. doi:10.1007/s10584-007-9322-8

Henry H.A.L. (2013). Soil freezing dynamics in a changing climate: implications for agriculture. In: Imai R, Yoshida M, Matsumoto N, editors. Plant and microbe adaptations to cold in a changing world. Springer New York, New York, NY, pp. 17-27.

Ho A., Di Lonardo D.P. & Bodelier P.L. (2017). Revisiting life strategy concepts in environmental microbial ecology. FEMS Microbiology Ecology 93(3), fix006. doi:10.1093/femsec/fix006

Hock R., Rasul G., Adler C., Cáceres B., Gruber S., Hirabayashi Y., Jackson M., Kääb A., Kang S., Kutuzov S., Milner A., Molau U., Morin S., Orlove B. & Steltzer H. (2019). High Mountain areas. In: Pörtner H-O, Roberts DC, Masson-Delmotte V, Zhai P, Tignor M, Poloczanska E, et al., editors. IPCC special report on the Ocean and Cryosphere in a changing climate pp. 131-202.

Hofmann K., Pauli H., Praeg N., Wagner A.O. & Illmer P. (2016). Methane-cycling microorganisms in soils of a high-alpine altitudinal gradient. FEMS Microbiology Ecology 92(3). doi:10.1093/femsec/fiw009

Hu W., Zhang Q., Tian T., Cheng G., An L. & Feng H. (2015). The microbial diversity, distribution, and ecology of permafrost in China: a review. Extremophiles 19(4), 693-705. doi:10.1007/s00792-015-0749-y

Huerta-Cepas J., Forslund K., Coelho L.P., Szklarczyk D., Jensen L.J., von Mering C. & Bork P. (2017). Fast genome-wide functional annotation through orthology assignment by eggNOG-mapper. Molecular Biology and Evolution 34(8), 2115-2122. doi:10.1093/molbev/msx148

Huerta-Cepas J., Szklarczyk D., Forslund K., Cook H., Heller D., Walter M.C., Rattei T., Mende D.R., Sunagawa S., Kuhn M., Jensen L.J., von Mering C. & Bork P. (2016). eggNOG 4.5: a

hierarchical orthology framework with improved functional annotations for eukaryotic, prokaryotic and viral sequences. Nucleic Acids Research 44(D1), D286-93. doi:10.1093/nar/gkv1248

Hultman J., Waldrop M.P., Mackelprang R., David M.M., McFarland J., Blazewicz S.J., Harden J., Turetsky M.R., McGuire A.D., Shah M.B., VerBerkmoes N.C., Lee L.H., Mavrommatis K. & Jansson J.K. (2015). Multi-omics of permafrost, active layer and thermokarst bog soil microbiomes. Nature 521(7551), 208-12. doi:10.1038/nature14238

IPCC. (2014). Climate change 2014: synthesis report. Contribution of working groups I, II and III to the fifth assessment report of the Intergovernmental Panel on Climate Change. IPCC, Geneva, Switzerland

IPCC. (2019). Summary for policymakers. In: Pörtner H-O, Roberts DC, Masson-Delmotte V, Zhai P, Tignor M, Poloczanska E, et al., editors. IPCC special report on the Ocean and Cryosphere in a changing climate.

Jacoby R., Peukert M., Succurro A., Koprivova A. & Kopriva S. (2017). The role of soil microorganisms in plant mineral nutrition: current knowledge and future directions. Frontiers in Plant Science 8. doi:10.3389/fpls.2017.01617

Jagerbrand A.K. & Alatalo J.M. (2015). Effects of human trampling on abundance and diversity of vascular plants, bryophytes and lichens in alpine heath vegetation, Northern Sweden. Springerplus 4(1), 95. doi:10.1186/s40064-015-0876-z

Jansson J.K. & Hofmockel K.S. (2020). Soil microbiomes and climate change. Nature Reviews Microbiology 18(1), 35-46. doi:10.1038/s41579-019-0265-7

Jansson J.K. & Tas N. (2014). The microbial ecology of permafrost. Nature Reviews Microbiology 12(6), 414-25. doi:10.1038/nrmicro3262

Ji M., Greening C., Vanwonterghem I., Carere C.R., Bay S.K., Steen J.A., Montgomery K., Lines T., Beardall J., van Dorst J., Snape I., Stott M.B., Hugenholtz P. & Ferrari B.C. (2017). Atmospheric trace gases support primary production in Antarctic desert surface soil. Nature 552(7685), 400-+. doi:10.1038/nature25014

Johnston E.R., Hatt J.K., He Z.L., Wu L.Y., Guo X., Luo Y.Q., Schuur E.A.G., Tiedje J.M., Zhou J.Z. & Konstantinidis K.T. (2019). Responses of tundra soil microbial communities to half a decade of experimental warming at two critical depths. Proceedings of the National Academy of Sciences of the United States of America 116(30), 15096-15105. doi:10.1073/pnas.1901307116

Ju F., Xia Y., Guo F., Wang Z.P. & Zhang T. (2014). Taxonomic relatedness shapes bacterial assembly in activated sludge of globally distributed wastewater treatment plants. Environmental Microbiology 16(8), 2421-2432. doi:10.1111/1462-2920.12355

Kallenbach C.M., Frey S.D. & Grandy A.S. (2016). Direct evidence for microbial-derived soil organic matter formation and its ecophysiological controls. Nature Communications 7, 13630. doi:10.1038/ncomms13630

Kang D.W.D., Froula J., Egan R. & Wang Z. (2015). MetaBAT, an efficient tool for accurately reconstructing single genomes from complex microbial communities. Peerj 3. doi:10.7717/peerj.1165

Karhu K., Auffret M.D., Dungait J.A.J., Hopkins D.W., Prosser J.I., Singh B.K., Subke J.A., Wookey P.A., Agren G.I., Sebastia M.T., Gouriveau F., Bergkvist G., Meir P., Nottingham A.T., Salinas N. & Hartley I.P. (2014). Temperature sensitivity of soil respiration rates enhanced by microbial community response. Nature 513(7516), 81-+. doi:10.1038/nature13604

Kern R., Hotter V., Frossard A., Albrecht M., Baum C., Tytgat B., De Maeyer L., Velazquez D., Seppey C., Frey B., Plotze M., Verleyen E., Quesada A., Svenning M.M., Glaser K. & Karsten U. (2019). Comparative vegetation survey with focus on cryptogamic covers in the High Arctic along two differing catenas. Polar Biology 42(11), 2131-2145. doi:10.1007/s00300-019-02588-z

Keto-Timonen R., Hietala N., Palonen E., Hakakorpi A., Lindstrm M. & Korkeala H. (2016). Cold shock proteins: a minireview with special emphasis on csp-family of enteropathogenic *Yersinia*. Frontiers in Microbiology 7. doi:10.3389/fmicb.2016.01151

Keuper F., Wild B., Kummu M., Beer C., Blume-Werry G., Fontaine S., Gavazov K., Gentsch N., Guggenberger G., Hugelius G., Jalava M., Koven C., Krab E.J., Kuhry P., Monteux S., Richter A., Shahzad T., Weedon J.T. & Dorrepaal E. (2020). Carbon loss from northern circumpolar permafrost soils amplified by rhizosphere priming. Nature Geoscience 13(8), 560-+. doi:10.1038/s41561-020-0607-0

Kim H. (2015). A review of factors that regulate extracellular enzyme activity in wetland soils. The Korean Journal of Microbiology 51(2), 97-107. doi:10.7845/kjm.2015.4087

Kim M., Jung J.Y., Laffly D., Kwon H.Y. & Lee Y.K. (2017). Shifts in bacterial community structure during succession in a glacier foreland of the High Arctic. FEMS Microbiology Ecology 93(1), fiw213. doi:10.1093/femsec/fiw213

Klarenberg I.J., Keuschnig C., Warshan D., Jónsdóttir I.S. & Vilhelmsson O. (2020). The total and active bacterial community of the chlorolichen *Cetraria islandica* and its response to long-term warming in sub-Arctic tundra. Frontiers in Microbiology 11, 3299. doi:10.3389/fmicb.2020.540404

Knowles J.F., Blanken P.D., Lawrence C.R. & Williams M.W. (2019). Evidence for non-steady-state carbon emissions from snow-scoured alpine tundra. Nature Communications 10, 1306. doi:10.1038/s41467-019-09149-2

Koch A.L. (2001). Oligotrophs versus copiotrophs. Bioessays 23(7), 657-61. doi:10.1002/bies.1091

Koo H., Hakim J.A., Morrow C.D., Crowley M.R., Andersen D.T. & Bej A.K. (2018). Metagenomic analysis of microbial community compositions and cold-responsive stress genes in selected Antarctic lacustrine and soil ecosystems. Life 8(3). doi:10.3390/life8030029

Koponen H.T. & Baath E. (2016). Soil bacterial growth after a freezing/thawing event. Soil Biology and Biochemistry 100, 229-232. doi:10.1016/j.soilbio.2016.06.029

Kulicheyskaya I.S., Ivanova A.A., Detkova E.N., Rijpstra W.I.C., Damste J.S.S. & Dedysh S.N. (2017). *Tundrisphaera lichenicola* gen. nov., sp nov., a psychrotolerant representative of the family *Isosphaeraceae* from lichen-dominated tundra soils. International Journal of Systematic and Evolutionary Microbiology 67(9), 3583-3589. doi:10.1099/ijsem.0.002172

Lambrechts S., Willems A. & Tahon G. (2019). Uncovering the uncultivated majority in Antarctic soils: toward a synergistic approach. Frontiers Microbiology 10, 242. doi:10.3389/fmicb.2019.00242

Langille M.G.I., Zaneveld J., Caporaso J.G., McDonald D., Knights D., Reyes J.A., Clemente J.C., Burkepile D.E., Thurber R.L.V., Knight R., Beiko R.G. & Huttenhower C. (2013). Predictive

functional profiling of microbial communities using 16S rRNA marker gene sequences. Nature Biotechnology 31(9), 814-+. doi:10.1038/nbt.2676

Larsen K.S., Jonasson S. & Michelsen A. (2002). Repeated freeze-thaw cycles and their effects on biological processes in two arctic ecosystem types. Applied Soil Ecology 21(3), 187-195. doi:10.1016/S0929-1393(02)00093-8

Lauro F.M., McDougald D., Thomas T., Williams T.J., Egan S., Rice S., DeMaere M.Z., Ting L., Ertan H., Johnson J., Ferriera S., Lapidus A., Anderson I., Kyrpides N., Munk A.C., Detter C., Han C.S., Brown M.V., Robb F.T., Kjelleberg S. & Cavicchioli R. (2009). The genomic basis of trophic strategy in marine bacteria. Proceedings of the National Academy of Sciences of the United States of America 106(37), 15527-15533. doi:10.1073/pnas.0903507106

Lee Y.-K., Kim H.-W., Cho K.-H., Kang S.-H., Lee H.-K. & Kim Y.-D. (2004). Phylogenetic analysis of culturable arctic bacteria. Ocean and Polar Research 26(1), 51-58. doi:10.4217/opr.2004.26.1.051

Leewis M.-C., Berlemont R., Podgorski D.C., Srinivas A., Zito P., Spencer R.G.M., McFarland J., Douglas T.A., Conaway C.H., Waldrop M. & Mackelprang R. (2020). Life at the frozen limit: microbial carbon metabolism across a late pleistocene permafrost chronosequence. Frontiers in Microbiology 11(1753). doi:10.3389/fmicb.2020.01753

Legendre P. & Gallagher E.D. (2001). Ecologically meaningful transformations for ordination of species data. Oecologia 129(2), 271-280. doi:10.1007/s004420100716

Li D.H., Liu C.M., Luo R.B., Sadakane K. & Lam T.W. (2015). MEGAHIT: an ultra-fast single-node solution for large and complex metagenomics assembly via succinct de Bruijn graph. Bioinformatics 31(10), 1674-1676. doi:10.1093/bioinformatics/btv033

Li H. (2013). Aligning sequence reads, clone sequences and assembly contigs with BWA-MEM. bioRxiv. doi:arXiv:1303.3997v2

Li H., Yang S., Semenov M.V., Yao F., Ye J., Bu R.C., Ma R., Lin J.J., Kurganova I., Wang X.G., Deng Y., Kravchenko I., Jiang Y. & Kuzyakov Y. (2021). Temperature sensitivity of SOM decomposition is linked with a K-selected microbial community. Global Change Biology 27(12), 2763-2779. doi:10.1111/gcb.15593

Liang Y., Jiang Y., Wang F., Wen C., Deng Y., Xue K., Qin Y., Yang Y., Wu L., Zhou J. & Sun B. (2015). Long-term soil transplant simulating climate change with latitude significantly alters microbial temporal turnover. ISME Journal 9(12), 2561-72. doi:10.1038/ismej.2015.78

Liao Y., Smyth G.K. & Shi W. (2014). featureCounts: an efficient general purpose program for assigning sequence reads to genomic features. Bioinformatics 30(7), 923-30. doi:10.1093/bioinformatics/btt656

Lin S.Y., Hameed A., Arun A.B., Liu Y.C., Hsu Y.H., Lai W.A., Rekha P.D. & Young C.C. (2013). Description of *Noviherbaspirillum malthae* gen. nov., sp. nov., isolated from an oil-contaminated soil, and proposal to reclassify *Herbaspirillum soli*, *Herbaspirillum aurantiacum*, *Herbaspirillum canariense* and *Herbaspirillum psychrotolerans* as *Noviherbaspirillum soli* comb. nov., *Noviherbaspirillum aurantiacum* comb. nov., *Noviherbaspirillum canariense* comb. nov. and *Noviherbaspirillum psychrotolerans* comb. nov. based on polyphasic analysis. International

Journal of Systematic and Evolutionary Microbiology 63(Pt 11), 4100-7. doi:10.1099/ijs.0.048231-0

Lipson D.A., Schadt C.W. & Schmidt S.K. (2002). Changes in soil microbial community structure and function in an alpine dry meadow following spring snow melt. Microbial Ecology 43(3), 307-14. doi:10.1007/s00248-001-1057-x

Liu Y., Priscu J.C., Yao T., Vick-Majors T.J., Michaud A.B. & Sheng L. (2018). Culturable bacteria isolated from seven high-altitude ice cores on the Tibetan Plateau. Journal of Glaciology 65(249), 29-38. doi:10.1017/jog.2018.86

Llado S. & Baldrian P. (2017). Community-level physiological profiling analyses show potential to identify the copiotrophic bacteria present in soil environments. Plos One 12(2), e0171638. doi:10.1371/journal.pone.0171638

Love M.I., Anders S. & Huber W. (2020). Analyzing RNA-seq data with DESeq2. Retrieved from: https://www.bioconductor.org/packages/devel/bioc/vignettes/DESeq2/inst/doc/DESeq2.html. Access date: September 2020

Love M.I., Huber W. & Anders S. (2014). Moderated estimation of fold change and dispersion for RNA-seq data with DESeq2. Genome Biology 15(12). doi:10.1186/s13059-014-0550-8

Luláková P., Perez-Mon C., Šantrůčková H., Ruethi J. & Frey B. (2019). High-alpine permafrost and active-layer soil microbiomes differ in their response to elevated temperatures. Frontiers in Microbiology 10, 668. doi:10.3389/fmicb.2019.00668

Mackelprang R., Burkert A., Haw M., Mahendrarajah T., Conaway C.H., Douglas T.A. & Waldrop M.P. (2017). Microbial survival strategies in ancient permafrost: insights from metagenomics. ISME Journal 11(10), 2305-2318. doi:10.1038/ismej.2017.93

Mackelprang R., Saleska S.R., Jacobsen C.S., Jansson J.K. & Tas N. (2016). Permafrost Meta-omics and climate change. Annual Review of Earth and Planetary Sciences 44(1), 439-+. doi:10.1146/annurev-earth-060614-105126

Mackelprang R., Waldrop M.P., DeAngelis K.M., David M.M., Chavarria K.L., Blazewicz S.J., Rubin E.M. & Jansson J.K. (2011). Metagenomic analysis of a permafrost microbial community reveals a rapid response to thaw. Nature 480(7377), 368-U120. doi:10.1038/nature10576

Magnin F., Josnin J.Y., Ravanel L., Pergaud J., Pohl B. & Deline P. (2017). Modelling rock wall permafrost degradation in the Mont Blanc massif from the LIA to the end of the 21st century. Cryosphere 11(4), 1813-1834. doi:10.5194/tc-11-1813-2017

Mair P. & Wilcox R. (2020). Robust statistical methods in R using the WRS2 package. Behavior Research Methods 52(2), 464-488. doi:10.3758/s13428-019-01246-w

Mannisto M.K., Tiirola M. & Haggblom M.M. (2009). Effect of freeze-thaw cycles on bacterial communities of arctic tundra soil. Microbial Ecology 58(3), 621-31. doi:10.1007/s00248-009-9516-x

Margesin R. (2009). Permafrost soils. Springer, Berlin

Margesin R. (2012). Psychrophilic microorganisms in alpine soils. In: Lütz C, editor. Plants in alpine regions: cell physiology of adaption and survival strategies. Springer, Vienna, pp. 187-198.

Margesin R. & Collins T. (2019). Microbial ecology of the cryosphere (glacial and permafrost habitats): current knowledge. Applied Microbiology and Biotechnology 103(6), 2537-2549. doi:10.1007/s00253-019-09631-3

Mazur P. (1984). Freezing of living cells: mechanisms and implications. American Journal of Physiology 247(3 Pt 1), C125-42. doi:10.1152/ajpcell.1984.247.3.C125

Meisner A., Jacquiod S., Snoek B.L., Ten Hooven F.C. & van der Putten W.H. (2018). Drought legacy effects on the composition of soil fungal and prokaryote communities. Frontiers in Microbiology 9, 294. doi:10.3389/fmicb.2018.00294

Meisner A., Snoek B.L., Nesme J., Dent E., Jacquiod S., Classen A.T. & Prieme A. (2021). Soil microbial legacies differ following drying-rewetting and freezing-thawing cycles. ISME Journal 15(4), 1207-1221. doi:10.1038/s41396-020-00844-3

Meredith M., Sommerkorn M., Cassotta S., Derksen C., Ekaykin A., Hollowed A., Kofinas G., Mackintosh A., Melbourne-Thomas J.M., M.M.C. , Ottersen G., Pritchard H. & E.A.G. S. (2019). Polar regions. In: Pörtner H-O, Roberts DC, Masson-Delmotte V, Zhai P, Tignor M, Poloczanska E, et al., editors. IPCC special report on the Ocean and Cryosphere in a changing climate pp. 203-320.

Metrak M., Pokarowski P., Sulwinski M., Gantumur A. & Suska-Malawska M. (2020). Plant response to N availability in permafrost-affected alpine wetlands in arid and semi-arid climate zones. Science of the Total Environment 721, 137791. doi:10.1016/j.scitotenv.2020.137791

Mishra U., Hugelius G., Shelef E., Yang Y.H., Strauss J., Lupachev A., Harden J.W., Jastrow J.D., Ping C.L., Riley W.J., Schuur E.A.G., Matamala R., Siewert M., Nave L.E., Koven C.D., Fuchs M., Palmtag J., Kuhry P., Treat C.C., Zubrzycki S., Hoffman F.M., Elberling B., Camill P., Veremeeva A. & Orr A. (2021). Spatial heterogeneity and environmental predictors of permafrost region soil organic carbon stocks. Science Advances 7(9). doi:10.1126/sciadv.aaz5236

Monteux S., Weedon J.T., Blume-Werry G., Gavazov K., Jassey V.E.J., Johansson M., Keuper F., Olid C. & Dorrepaal E. (2018). Long-term in situ permafrost thaw effects on bacterial communities and potential aerobic respiration. ISME Journal 12(9), 2129-2141. doi:10.1038/s41396-018-0176-z

Mooshammer M., Hofhansl F., Frank A.H., Wanek W., Hammerle I., Leitner S., Schnecker J., Wild B., Watzka M., Keiblinger K.M., Zechmeister-Boltenstern S. & Richter A. (2017). Decoupling of microbial carbon, nitrogen, and phosphorus cycling in response to extreme temperature events. Science Advances 3(5), e1602781. doi:10.1126/sciadv.1602781

Morgalev Y.N., Lushchaeva I.V., Morgaleva T.G., Kolesnichenko L.G., Loiko S.V., Krickov I.V., Lim A., Raudina T.V., Volkova I.I., Shirokova L.S., Morgalev S.Y., Vorobyev S.N., Kirpotin S.N. & Pokrovsky O.S. (2017). Bacteria primarily metabolize at the active layer/permafrost border in the peat core from a permafrost region in western Siberia. Polar Biology 40(8), 1645-1659. doi:10.1007/s00300-017-2088-1

Morrien E., Hannula S.E., Snoek L.B., Helmsing N.R., Zweers H., de Hollander M., Soto R.L., Bouffaud M.L., Buee M., Dimmers W., Duyts H., Geisen S., Girlanda M., Griffiths R.I., Jorgensen H.B., Jensen J., Plassart P., Redecker D., Schmelz R.M., Schmidt O., Thomson B.C., Tisserant E.,

Uroz S., Winding A., Bailey M.J., Bonkowski M., Faber J.H., Martin F., Lemanceau P., de Boer W., van Veen J.A. & van der Putten W.H. (2017). Soil networks become more connected and take up more carbon as nature restoration progresses. Nature Communications 8, 14349. doi:10.1038/ncomms14349

Morrissey E.M., Mau R.L., Schwartz E., Caporaso J.G., Dijkstra P., van Gestel N., Koch B.J., Liu C.M., Hayer M., McHugh T.A., Marks J.C., Price L.B. & Hungate B.A. (2016). Phylogenetic organization of bacterial activity. ISME Journal 10(9), 2336-40. doi:10.1038/ismej.2016.28

Mueller O., Bang-Andreasen T., White R.A., Elberling B., Tas N., Kneafsey T., Jansson J.K. & Ovreas L. (2018). Disentangling the complexity of permafrost soil by using high resolution profiling of microbial community composition, key functions and respiration rates. Environmental Microbiology 20(12), 4328-4342. doi:10.1111/1462-2920.14348

Mykytczuk N.C.S., Foote S.J., Omelon C.R., Southam G., Greer C.W. & Whyte L.G. (2013). Bacterial growth at -15 degrees C; molecular insights from the permafrost bacterium *Planococcus halocryophilus* Or1. ISME Journal 7(6), 1211-1226. doi:10.1038/ismej.2013.8

Naylor D., Sadler N., Bhattacharjee A., Graham E.B., Anderton C.R., McClure R., Lipton M., Hofmockel K.S. & Jansson J.K. (2020). Soil microbiomes under climate change and implications for carbon cycling. Annual Review of Environment and Resources 45, 29-59. doi:10.1146/annurev-environ-012320-082720

Nguyen N.H., Song Z.W., Bates S.T., Branco S., Tedersoo L., Menke J., Schilling J.S. & Kennedy P.G. (2016). FUNGuild: an open annotation tool for parsing fungal community datasets by ecological guild. Fungal Ecology 20, 241-248. doi:10.1016/j.funeco.2015.06.006

Nikrad M.P., Kerkhof L.J. & Haggblom M.M. (2016). The subzero microbiome: microbial activity in frozen and thawing soils. FEMS Microbiology Ecology 92(6), fiw081. doi:10.1093/femsec/fiw081

Nilsson R.H., Larsson K.H., Taylor A.F.S., Bengtsson-Palme J., Jeppesen T.S., Schigel D., Kennedy P., Picard K., Glockner F.O., Tedersoo L., Saar I., Koljalg U. & Abarenkov K. (2019). The UNITE database for molecular identification of fungi: handling dark taxa and parallel taxonomic classifications. Nucleic Acids Research 47(D1), D259-D264. doi:10.1093/nar/gky1022

Nimis P.L., Hafellner J., Roux C., Clerc P., Mayrhofer H., Martellos S. & Bilovitz P.O. (2018). The lichens of the Alps - an annotated checklist. Mycokeys(31), 1-634. doi:10.3897/mycokeys.31.23658

Noetzli J., Hoelzle M. & Haeberli W. (2003). Mountain permafrost and recent Alpine rock-fall events: a GIS-based approach to determine critical factors. Permafrost, Vols 1 and 2, 827-832. url:<Go to ISI>://WOS:000185049300145

Obu J., Westermann S., Vieira G., Abramov A., Balks M.R., Bartsch A., Hrbacek F., Kaab A. & Ramos M. (2020). Pan-Antarctic map of near-surface permafrost temperatures at 1 km(2) scale. Cryosphere 14(2), 497-519. doi:10.5194/tc-14-497-2020

Ofek M., Hadar Y. & Minz D. (2012). Ecology of root colonizing *Massilia* (*Oxalobacteraceae*). Plos One 7(7), e40117. doi:10.1371/journal.pone.0040117

Okie J.G., Poret-Peterson A.T., Lee Z.M.P., Richter A., Alcaraz L.D., Eguiarte L.E., Siefert J.L., Souza V., Dupont C.L. & Elser J.J. (2020). Genomic adaptations in information processing underpin trophic strategy in a whole-ecosystem nutrient enrichment experiment. eLife 9, e49816. doi:10.7554/eLife.49816

Oksanen J., Blanchet G.F., Friendly M., Kindt R., Legendre P., McGlinn D., Minchin P.R., O'Hara R.B., Simpson G.L., Solymos P., Henry H., Stevens H., Szoecs E. & Wagner H. (2019). vegan: Community Ecology Package. R package version 2.5-5.

Ortiz M., Leung P.M., Shelley G., Van Goethem M.W., Bay S.K., Jordaan K., Vikram S., Hogg I.D., Makhalanyane T.P., Chown S.L., Grinter R., Cowan D.A. & Greening C. (2020). A genome compendium reveals diverse metabolic adaptations of Antarctic soil microorganisms. bioRxiv. doi:10.1101/2020.08.06.239558

Overland J., Dunlea E., Box J.E., Corell R., Forsius M., Kattsov V., Olseng M.S., Pawlak J., Reiersen L.O. & Wang M.Y. (2019). The urgency of Arctic change. Polar Science 21, 6-13. doi:10.1016/j.polar.2018.11.008

Ozerskaya S., Kochkina G., Ivanushkina N. & Gilichinsky D.A. (2009). Fungi in permafrost. In: Margesin R, editor. Permafrost soils. Springer Berlin Heidelberg, Berlin, Heidelberg, pp. 85-95.

Panoff J.M., Thammavongs B., Gueguen M. & Boutibonnes P. (1998). Cold stress responses in mesophilic bacteria. Cryobiology 36(2), 75-83. doi:10.1006/cryo.1997.2069

Parks D.H., Imelfort M., Skennerton C.T., Hugenholtz P. & Tyson G.W. (2015). CheckM: assessing the quality of microbial genomes recovered from isolates, single cells, and metagenomes. Genome Research 25(7), 1043-1055. doi:10.1101/gr.186072.114

Pei Z., Ouyang H., Zhou C. & Xu X. (2003). Fluxes of CO_2, CH_4 and N_2O from alpine grassland in the Tibetan Plateau. Journal of Geographical Sciences 13(1), 27-34. doi:10.1007/BF02873144

Pei Z.Y., Ouyang H., Zhou C.P. & Xu X.L. (2004). N_2O exchange within a soil and atmosphere profile in alpine grasslands on the Qinghai-Xizang Plateau. Acta Botanica Sinica 46(1), 20-28. url:<Go to ISI>://WOS:000189278000003

Peng F., Zhang W.J., Li C.Y., Lai C.M., Zhou J., Xue X. & Tsunekawa A. (2020). Sustained increase in soil respiration after nine years of warming in an alpine meadow on the Tibetan Plateau. Geoderma 379, 114641. doi:10.1016/j.geoderma.2020.114641

Peng X.Q., Zhang T.J., Frauenfeld O.W., Wang K., Luo D.L., Cao B., Su H., Jin H.J. & Wu Q.B. (2018). Spatiotemporal changes in active layer thickness under contemporary and projected climate in the Northern Hemisphere. Journal of Climate 31(1), 251-266. doi:10.1175/Jcli-D-16-0721.1

Perez-Mon C., Frey B. & Frossard A. (2020). Functional and structural responses of Arctic and alpine soil prokaryotic and fungal communities under freeze-thaw cycles of different frequencies. Frontiers in Microbiology 11, 982. doi:10.3389/fmicb.2020.00982

Perez-Mon C., Qi W., Vikram S., Frossard A., Makhalanyane T.P., Cowan D.A. & Frey B. (2021). Shotgun metagenomics reveals distinct functional diversity and metabolic capabilities between 12 000-year-old permafrost and active layers on Muot da Barba Peider (Swiss Alps). Microbial Genomics 7(4). doi:10.1099/mgen.0.000558

PERMOS. (2016). Permafrost in Switzerland 2010/2011 to 2013/2014. In: Noetzli J, Luethi R, Staub B, editors. Glaciological report permafrost No. 12–15 Cryospheric Commission of the Swiss Academy of Sciences, Fribourg, pp. 85.

Pontes A., Ruethi J., Frey B., Aires A., Thomas A., Overy D., Halti B., Kerr R. & Sampaio J.P. (2020). *Cryolevonia* gen. nov. and *Cryolevonia schafbergensis* sp. nov., a cryophilic yeast from ancient

permafrost and melted sea ice. International Journal of Systematic and Evolutionary Microbiology 70(4), 2334-2338. doi:10.1099/ijsem.0.004040

Pruesse E., Peplies J. & Glockner F.O. (2012). SINA: Accurate high-throughput multiple sequence alignment of ribosomal RNA genes. Bioinformatics 28(14), 1823-1829. doi:10.1093/bioinformatics/bts252

Quast C., Pruesse E., Yilmaz P., Gerken J., Schweer T., Yarza P., Peplies J. & Glockner F.O. (2013). The SILVA ribosomal RNA gene database project: improved data processing and web-based tools. Nucleic Acids Research 41(D1), D590-D596. doi:10.1093/nar/gks1219

R Core Team. (2017). R: A language and environment for statistical computing. R Foundation for Statistical Computing, Vienna, Austria

R Core Team. (2020). R: A language and environment for statistical computing. R Foundation for Statistical Computing., Vienna, Austria

Rawat S.R., Mannisto M.K., Bromberg Y. & Haggblom M.M. (2012). Comparative genomic and physiological analysis provides insights into the role of Acidobacteria in organic carbon utilization in Arctic tundra soils. FEMS Microbiology Ecology 82(2), 341-355. doi:10.1111/j.1574-6941.2012.01381.x

Ren J., Song C., Hou A., Song Y., Zhu X. & Cagle G.A. (2018). Shifts in soil bacterial and archaeal communities during freeze-thaw cycles in a seasonal frozen marsh, Northeast China. Science of the Total Environment 625, 782-791. doi:10.1016/j.scitotenv.2017.12.309

Reyes F.R. & Lougheed V.L. (2015). Rapid nutrient release from permafrost thaw in arctic aquatic ecosystems. Arctic Antarctic and Alpine Research 47(1), 35-48. doi:10.1657/Aaar0013-099

Rime T., Hartmann M., Brunner I., Widmer F., Zeyer J. & Frey B. (2015). Vertical distribution of the soil microbiota along a successional gradient in a glacier forefield. Molecular Ecology 24(5), 1091-108. doi:10.1111/mec.13051

Rime T., Hartmann M. & Frey B. (2016). Potential sources of microbial colonizers in an initial soil ecosystem after retreat of an alpine glacier. ISME Journal 10(7), 1625-1641. doi:10.1038/ismej.2015.238

Rinke C., Schwientek P., Sczyrba A., Ivanova N.N., Anderson I.J., Cheng J.-F., Darling A., Malfatti S., Swan B.K., Gies E.A., Dodsworth J.A., Hedlund B.P., Tsiamis G., Sievert S.M., Liu W.-T., Eisen J.A., Hallam S.J., Kyrpides N.C., Stepanauskas R., Rubin E.M., Hugenholtz P. & Woyke T. (2013). Insights into the phylogeny and coding potential of microbial dark matter. Nature 499(7459), 431-437. doi:10.1038/nature12352

Rinnan R., Michelsen A., Baath E. & Jonasson S. (2007). Fifteen years of climate change manipulations alter soil microbial communities in a subarctic heath ecosystem. Global Change Biology 13(1), 28-39. doi:10.1111/j.1365-2486.2006.01263.x

Rodder T. & Kneisel C. (2012). Influence of snow cover and grain size on the ground thermal regime in the discontinuous permafrost zone, Swiss Alps. Geomorphology 175, 176-189. doi:10.1016/j.geomorph.2012.07.008

Roller B.R., Stoddard S.F. & Schmidt T.M. (2016). Exploiting rRNA operon copy number to investigate bacterial reproductive strategies. Nature Microbiology 1(11), 16160. doi:10.1038/nmicrobiol.2016.160

Rousk J. & Baath E. (2011). Growth of saprotrophic fungi and bacteria in soil. FEMS Microbiology Ecology 78(1), 17-30. doi:10.1111/j.1574-6941.2011.01106.x

RStudio Team. (2020). RStudio: Integrated Development Environment for R. RStudio, Inc., Boston, MA

Rui J., Li J., Wang S., An J., Liu W.T., Lin Q., Yang Y., He Z. & Li X. (2015). Responses of bacterial communities to simulated climate changes in alpine meadow soil of the Qinghai-Tibet Plateau. Applied and Environmental Microbiology 81(17), 6070-7. doi:10.1128/AEM.00557-15

Ruthi J., Bolsterli D., Pardi-Comensoli L., Brunner I. & Frey B. (2020). The "Plastisphere" of biodegradable plastics is characterized by specific microbial taxa of alpine and Arctic Soils. Frontiers in Environmental Science 8, 173. doi:10.3389/fenvs.2020.562263

Salazar G. (2019). EcolUtils: utilities for community ecology analysis. R package version 0.1.

Sangwan P., Kovac S., Davis K.E., Sait M. & Janssen P.H. (2005). Detection and cultivation of soil Verrucomicrobia. Applied and Environmental Microbiology 71(12), 8402-10. doi:10.1128/AEM.71.12.8402-8410.2005

Scapozza C., Deluigi N., Bulgheroni M., Ibarguren S.P., Pozzoni M., Colombo L. & Lepori F. (2020). Assessing the impact of ground ice degradation on high mountain lake environments (Lago Nero catchment, Swiss Alps). Aquatic Sciences 82(1), 5. doi:10.1007/s00027-019-0675-7

Schimel J.P. & Clein J.S. (1996). Microbial response to freeze-thaw cycles in tundra and taiga soils. Soil Biology and Biochemistry 28(8), 1061-1066. doi:Doi 10.1016/0038-0717(96)00083-1

Schimel J.P. & Mikan C. (2005). Changing microbial substrate use in Arctic tundra soils through a freeze-thaw cycle. Soil Biology and Biochemistry 37(8), 1411-1418. doi:10.1016/j.soilbio.2004.12.011

Schloss P.D., Westcott S.L., Ryabin T., Hall J.R., Hartmann M., Hollister E.B., Lesniewski R.A., Oakley B.B., Parks D.H., Robinson C.J., Sahl J.W., Stres B., Thallinger G.G., Van Horn D.J. & Weber C.F. (2009). Introducing mothur: open-source, platform-independent, community-supported software for describing and comparing microbial communities. Applied and Environmental Microbiology 75(23), 7537-41. doi:10.1128/AEM.01541-09

Schmidt S.K., Naff C.S. & Lynch R.C. (2012). Fungal communities at the edge: ecological lessons from high alpine fungi. Fungal Ecology 5(4), 443-452. doi:10.1016/j.funeco.2011.10.005

Schmidt S.K., Reed S.C., Nemergut D.R., Grandy A.S., Cleveland C.C., Weintraub M.N., Hill A.W., Costello E.K., Meyer A.F., Neff J.C. & Martin A.M. (2008a). The earliest stages of ecosystem succession in high-elevation (5000 metres above sea level), recently deglaciated soils. Proceedings of the Royal Society B-Biological Sciences 275(1653), 2793-2802. doi:10.1098/rspb.2008.0808

Schmidt S.K., Wilson K.L., Monson R.K. & Lipson D.A. (2008b). Exponential growth of “snow molds” at sub-zero temperatures: an explanation for high beneath-snow respiration rates and Q 10 values. Biogeochemistry 95(1), 13-21. doi:10.1007/s10533-008-9247-y

Schostag M., Prieme A., Jacquiod S., Russel J., Ekelund F. & Jacobsen C.S. (2019). Bacterial and protozoan dynamics upon thawing and freezing of an active layer permafrost soil. ISME Journal 13(5), 1345-1359. doi:10.1038/s41396-019-0351-x

Schostag M., Stibal M., Jacobsen C.S., Baelum J., Tas N., Elberling B., Jansson J.K., Semenchuk P. & Prieme A. (2015). Distinct summer and winter bacterial communities in the active layer of

Svalbard permafrost revealed by DNA- and RNA-based analyses. Frontiers in Microbiology 6, 399. doi:10.3389/fmicb.2015.00399

Schuster P.F., Schaefer K.M., Aiken G.R., Antweiler R.C., Dewild J.F., Gryziec J.D., Gusmeroli A., Hugelius G., Jafarov E., Krabbenhoft D.P., Liu L., Herman-Mercer N., Mu C.C., Roth D.A., Schaefer T., Striegl R.G., Wickland K.P. & Zhang T.J. (2018). Permafrost stores a globally significant amount of mercury. Geophysical Research Letters 45(3), 1463-1471. doi:10.1002/2017gl075571

Schuur E.A.G., Bockheim J., Canadell J.G., Euskirchen E., Field C.B., Goryachkin S.V., Hagemann S., Kuhry P., Lafleur P.M., Lee H., Mazhitova G., Nelson F.E., Rinke A., Romanovsky V.E., Shiklomanov N., Tarnocai C., Venevsky S., Vogel J.G. & Zimov S.A. (2008). Vulnerability of permafrost carbon to climate change: implications for the global carbon cycle. Bioscience 58(8), 701-714. doi:10.1641/B580807

Selbmann L., Egidi E., Isola D., Onofri S., Zucconi L., de Hoog G.S., Chinaglia S., Testa L., Tosi S., Balestrazzi A., Lantieri A., Compagno R., Tigini V. & Varese G.C. (2013). Biodiversity, evolution and adaptation of fungi in extreme environments. Plant Biosystems 147(1), 237-246. doi:10.1080/11263504.2012.753134

Senechkin I.V., Speksnijder A.G., Semenov A.M., van Bruggen A.H. & van Overbeek L.S. (2010). Isolation and partial characterization of bacterial strains on low organic carbon medium from soils fertilized with different organic amendments. Microbial Ecology 60(4), 829-39. doi:10.1007/s00248-010-9670-1

Shade A., Jones S.E., Caporaso J.G., Handelsman J., Knight R., Fierer N. & Gilbert J.A. (2014). Conditionally rare taxa disproportionately contribute to temporal changes in microbial diversity. mBio 5(4), e01371-14. doi:10.1128/mBio.01371-14

Shakya M., Lo C.C. & Chain P.S.G. (2019). Advances and challenges in metatranscriptomic analysis. Frontiers in Genetics 10, 904. doi:10.3389/fgene.2019.00904

Sharma S., Szele Z., Schilling R., Munch J.C. & Schloter M. (2006). Influence of freeze-thaw stress on the structure and function of microbial communities and denitrifying populations in soil. Applied and Environmental Microbiology 72(3), 2148-54. doi:10.1128/AEM.72.3.2148-2154.2006

Singh S.M., Olech M., Cannone N. & Convey P. (2015). Contrasting patterns in lichen diversity in the continental and maritime Antarctic. Polar Science 9(3), 311-318. doi:10.1016/j.polar.2015.07.001

Sinsabaugh R.L., Hill B.H. & Follstad Shah J.J. (2009). Ecoenzymatic stoichiometry of microbial organic nutrient acquisition in soil and sediment. Nature 462(7274), 795-8. doi:10.1038/nature08632

Sinsabaugh R.L., Lauber C.L., Weintraub M.N., Ahmed B., Allison S.D., Crenshaw C., Contosta A.R., Cusack D., Frey S., Gallo M.E., Gartner T.B., Hobbie S.E., Holland K., Keeler B.L., Powers J.S., Stursova M., Takacs-Vesbach C., Waldrop M.P., Wallenstein M.D., Zak D.R. & Zeglin L.H. (2008). Stoichiometry of soil enzyme activity at global scale. Ecology Letters 11(11), 1252-1264. doi:10.1111/j.1461-0248.2008.01245.x

Soares M. & Rousk J. (2019). Microbial growth and carbon use efficiency in soil: links to fungal-bacterial dominance, SOC-quality and stoichiometry. Soil Biology and Biochemistry 131, 195-205. doi:10.1016/j.soilbio.2019.01.010

Song H.K., Song W., Kim M., Tripathi B.M., Kim H., Jablonski P. & Adams J.M. (2017). Bacterial strategies along nutrient and time gradients, revealed by metagenomic analysis of laboratory microcosms. FEMS Microbiology Ecology 93(10), fix114. doi:10.1093/femsec/fix114

Sönmez O., Saud S., Wang D., Wu C., Adnan M. & Turan V. (2021). Developing climate-resilient crops: improving global food security and safety. CRC Press, Boca Raton

Spatafora J.W., Chang Y., Benny G.L., Lazarus K., Smith M.E., Berbee M.L., Bonito G., Corradi N., Grigoriev I., Gryganskyi A., James T.Y., O'Donnell K., Roberson R.W., Taylor T.N., Uehling J., Vilgalys R., White M.M. & Stajich J.E. (2016). A phylum-level phylogenetic classification of zygomycete fungi based on genome-scale data. Mycologia 108(5), 1028-1046. doi:10.3852/16-042

Sprouffske K. (2016). Growthcurver: Simple metrics to summarize growth curves. Retrieved from: https://cran.microsoft.com/snapshot/2016-03-14/web/packages/growthcurver/vignettes/Growthcurver-vignette.html. Access date: August 2020

Sprouffske K. & Wagner A. (2016). Growthcurver: an R package for obtaining interpretable metrics from microbial growth curves. BMC Bioinformatics 17, 172. doi:10.1186/s12859-016-1016-7

Steinbauer M.J., Grytnes J.A., Jurasinski G., Kulonen A., Lenoir J., Pauli H., Rixen C., Winkler M., Bardy-Durchhalter M., Barni E., Bjorkman A.D., Breiner F.T., Burg S., Czortek P., Dawes M.A., Delimat A., Dullinger S., Erschbamer B., Felde V.A., Fernandez-Arberas O., Fossheim K.F., Gomez-Garcia D., Georges D., Grindrud E.T., Haider S., Haugum S.V., Henriksen H., Herreros M.J., Jaroszewicz B., Jaroszynska F., Kanka R., Kapfer J., Klanderud K., Kuhn I., Lamprecht A., Matteodo M., di Cella U.M., Normand S., Odland A., Olsen S.L., Palacio S., Petey M., Piscova V., Sedlakova B., Steinbauer K., Stockli V., Svenning J.C., Teppa G., Theurillat J.P., Vittoz P., Woodin S.J., Zimmermann N.E. & Wipf S. (2018). Accelerated increase in plant species richness on mountain summits is linked to warming. Nature 556(7700), 231-+. doi:10.1038/s41586-018-0005-6

Steingruber S.M., Bernasconi S.M. & Valenti G. (2020). Climate change-induced changes in the chemistry of a high-altitude mountain lake in the Central Alps. Aquatic Geochemistry. doi:10.1007/s10498-020-09388-6

Steinweg J.M., Dukes J.S., Paul E.A. & Wallenstein M.D. (2013). Microbial responses to multi-factor climate change: effects on soil enzymes. Frontiers in Microbiology 4, 146. doi:10.3389/fmicb.2013.00146

Steven B., Briggs G., McKay C.P., Pollard W.H., Greer C.W. & Whyte L.G. (2007). Characterization of the microbial diversity in a permafrost sample from the Canadian High Arctic using culture-dependent and culture-independent methods. FEMS Microbiology Ecology 59(2), 513-23. doi:10.1111/j.1574-6941.2006.00247.x

Stres B., Philippot L., Faganeli J. & Tiedje J.M. (2010). Frequent freeze-thaw cycles yield diminished yet resistant and responsive microbial communities in two temperate soils: a laboratory experiment. FEMS Microbiology Ecology 74(2), 323-35. doi:10.1111/j.1574-6941.2010.00951.x

Tanaka Y., Matsuzawa H., Tamaki H., Tagawa M., Toyama T., Kamagata Y. & Mori K. (2017). Isolation of novel bacteria including rarely cultivated phyla, Acidobacteria and Verrucomicrobia, from the

roots of emergent plants by simple culturing method. Microbes and Environments 32(3), 288-292. doi:10.1264/jsme2.ME17027

Tas N., Prestat E., Wang S., Wu Y., Ulrich C., Kneafsey T., Tringe S.G., Torn M.S., Hubbard S.S. & Jansson J.K. (2018). Landscape topography structures the soil microbiome in arctic polygonal tundra. Nature Communications 9(1), 777. doi:10.1038/s41467-018-03089-z

Tian R., Ning D., He Z., Zhang P., Spencer S.J., Gao S., Shi W., Wu L., Zhang Y., Yang Y., Adams B.G., Rocha A.M., Detienne B.L., Lowe K.A., Joyner D.C., Klingeman D.M., Arkin A.P., Fields M.W., Hazen T.C., Stahl D.A., Alm E.J. & Zhou J. (2020). Small and mighty: adaptation of superphylum Patescibacteria to groundwater environment drives their genome simplicity. Microbiome 8(1), 51. doi:10.1186/s40168-020-00825-w

Tu Q., Lin L., Cheng L., Deng Y. & He Z. (2019). NCycDB: a curated integrative database for fast and accurate metagenomic profiling of nitrogen cycling genes. Bioinformatics 35(6), 1040-1048. doi:10.1093/bioinformatics/bty741

Tuorto S.J., Darias P., McGuinness L.R., Panikov N., Zhang T.J., Haggblom M.M. & Kerkhof L.J. (2014). Bacterial genome replication at subzero temperatures in permafrost. ISME Journal 8(1), 139-149. doi:10.1038/ismej.2013.140

Tveit A., Schwacke R., Svenning M.M. & Urich T. (2013). Organic carbon transformations in High-Arctic peat soils: key functions and microorganisms. ISME Journal 7(2), 299-311. doi:10.1038/ismej.2012.99

Van der Voort T.S., Mannu U., Hagedorn F., McIntyre C., Walthert L., Schleppi P., Haghipour N. & Eglinton T.I. (2019). Dynamics of deep soil carbon – insights from ^{14}C time series across a climatic gradient. Biogeosciences 16(16), 3233-3246. doi:10.5194/bg-16-3233-2019

Van Goethem M.W., Pierneef R., Bezuidt O.K.I., Van De Peer Y., Cowan D.A. & Makhalanyane T.P. (2018). A reservoir of 'historical' antibiotic resistance genes in remote pristine Antarctic soils. Microbiome 6(1), 40. doi:10.1186/s40168-018-0424-5

Vaser R., Pavlovic D. & Sikic M. (2016). SWORD-a highly efficient protein database search. Bioinformatics 32(17), i680-i684. doi:10.1093/bioinformatics/btw445

Vigneron A., Cruaud P., Langlois V., Lovejoy C., Culley A.I. & Vincent W.F. (2020). Ultra-small and abundant: candidate phyla radiation bacteria are potential catalysts of carbon transformation in a thermokarst lake ecosystem. Limnology and Oceanography Letters 5(2), 212-220. doi:10.1002/lol2.10132

Villa F. & Cappitelli F. (2019). The ecology of subaerial biofilms in dry and inhospitable terrestrial environments. Microorganisms 7(10), 380. doi:10.3390/microorganisms7100380

Voigt C., Marushchak M.E., Abbott B.W., Biasi C., Elberling B., Siciliano S.D., Sonnentag O., Stewart K.J., Yang Y. & Martikainen P.J. (2020). Nitrous oxide emissions from permafrost-affected soils. Nature Reviews Earth and Environment 1(8), 420-434. doi:10.1038/s43017-020-0063-9

Walker V.K., Palmer G.R. & Voordouw G. (2006). Freeze-thaw tolerance and clues to the winter survival of a soil community. Applied and Environmental Microbiology 72(3), 1784-92. doi:10.1128/AEM.72.3.1784-1792.2006

Wang E.H., Cruse R.M., Chen X.W. & Daigh A. (2012). Effects of moisture condition and freeze/thaw cycles on surface soil aggregate size distribution and stability. Canadian Journal of Soil Science 92(3), 529-536. doi:10.4141/Cjss2010-044

Wang J.F., Wu Q.B., Yuan Z.Q. & Kang H. (2020). Soil respiration of alpine meadow is controlled by freeze-thaw processes of active layer in the permafrost region of the Qinghai-Tibet Plateau. Cryosphere 14(9), 2835-2848. doi:10.5194/tc-14-2835-2020

Wang Q., Garrity G.M., Tiedje J.M. & Cole J.R. (2007). Naive Bayesian classifier for rapid assignment of rRNA sequences into the new bacterial taxonomy. Applied and Environmental Microbiology 73(16), 5261-7. doi:10.1128/AEM.00062-07

Ward L.M., Cardona T. & Holland-Moritz H. (2019). Evolutionary implications of anoxygenic phototrophy in the bacterial phylum *Candidatus* Eremiobacterota (WPS-2). Frontiers in Microbiology 10. doi:10.3389/fmicb.2019.01658

Wickham H. (2016). ggplot2: Elegant Graphics for Data Analysis. Springer, New York

Wilke A., Harrison T., Wilkening J., Field D., Glass E.M., Kyrpides N., Mavrommatis K. & Meyer F. (2012). The M5nr: a novel non-redundant database containing protein sequences and annotations from multiple sources and associated tools. BMC Bioinformatics 13. doi:10.1186/1471-2105-13-141

Willerslev E., Hansen A.J., Ronn R., Brand T.B., Barnes I., Wiuf C., Gilichinsky D., Mitchell D. & Cooper A. (2004). Long-term persistence of bacterial DNA. Current Biology 14(1), R9-R10. doi:10.1016/j.cub.2003.12.012

Woodcroft B.J., Singleton C.M., Boyd J.A., Evans P.N., Emerson J.B., Zayed A.A.F., Hoelzle R.D., Lamberton T.O., McCalley C.K., Hodgkins S.B., Wilson R.M., Purvine S.O., Nicora C.D., Li C., Frolking S., Chanton J.P., Crill P.M., Saleska S.R., Rich V.I. & Tyson G.W. (2018). Genome-centric view of carbon processing in thawing permafrost. Nature 560(7716), 49-54. doi:10.1038/s41586-018-0338-1

Wunderlin T., Junier T., Roussel-Delif L., Jeanneret N. & Junier P. (2013). Stage 0 sporulation gene A as a molecular marker to study diversity of endospore-forming Firmicutes. Environmental Microbiology Reports 5(6), 911-924. doi:10.1111/1758-2229.12094

Xiong J., Chu H., Sun H., Xue X., Peng F. & Zhang H. (2014). Divergent responses of soil fungi functional groups to short-term warming. Microbial Ecology 68(4), 708-15. doi:10.1007/s00248-014-0385-6

Xue K., Yuan M.M., Shi Z.J., Qin Y.J., Deng Y., Cheng L., Wu L.Y., He Z.L., Van Nostrand J.D., Bracho R., Natali S., Schuur E.A.G., Luo C.W., Konstantinidis K.T., Wang Q., Cole J.R., Tiedje J.M., Luo Y.Q. & Zhou J.Z. (2016). Tundra soil carbon is vulnerable to rapid microbial decomposition under climate warming. Nature Climate Change 6(6), 595-+. doi:10.1038/Nclimate2940

Xue Y., Jonassen I., Øvreås L. & Taş N. (2020). Metagenome-assembled genome distribution and key functionality highlight importance of aerobic metabolism in Svalbard permafrost. FEMS Microbiology Ecology 96(5). doi:10.1093/femsec/fiaa057

Yang Y.F., Gao Y., Wang S.P., Xu D.P., Yu H., Wu L.W., Lin Q.Y., Hu Y.G., Li X.Z., He Z.L., Deng Y. & Zhou J.Z. (2014). The microbial gene diversity along an elevation gradient of the Tibetan grassland. ISME Journal 8(2), 430-440. doi:10.1038/ismej.2013.146

Yang Z.F., Zhang Y., Lv Y.X., Yan W.K., Xiao X., Sun B. & Ma H.M. (2019). H_2 metabolism revealed by metagenomic analysis of subglacial sediment from East Antarctica. Journal of Microbiology 57(12), 1095-1104. doi:10.1007/s12275-019-9366-2

Yergeau E. & Kowalchuk G.A. (2008). Responses of Antarctic soil microbial communities and associated functions to temperature and freeze-thaw cycle frequency. Environmental Microbiology 10(9), 2223-35. doi:10.1111/j.1462-2920.2008.01644.x

Yue H., Wang M., Wang S., Gilbert J.A., Sun X., Wu L., Lin Q., Hu Y., Li X., He Z., Zhou J. & Yang Y. (2015). The microbe-mediated mechanisms affecting topsoil carbon stock in Tibetan grasslands. ISME Journal 9(9), 2012-20. doi:10.1038/ismej.2015.19

Zaikova E., Goerlitz D.S., Tighe S.W., Wagner N.Y., Bai Y., Hall B.L., Bevilacqua J.G., Weng M.M., Samuels-Fair M.D. & Johnson S.S. (2019). Antarctic relic microbial mat community revealed by metagenomics and metatranscriptomics. Frontiers in Ecology and Evolution 7. doi:10.3389/fevo.2019.00001

Zenklusen Mutter E., Blanchet J. & Phillips M. (2010). Analysis of ground temperature trends in alpine permafrost using generalized least squares. Journal of Geophysical Research 115(F4), F04009. doi:10.1029/2009jf001648

Zhang S.H., Yang G.L., Hou S.G., Zhang T.J., Li Z.G. & Liang F. (2018). Distribution of ARGs and MGEs among glacial soil, permafrost, and sediment using metagenomic analysis. Environmental Pollution 234, 339-346. doi:10.1016/j.envpol.2017.11.031

Zhao R.X., Feng J., Liu J., Fu W.J., Li X.Y. & Li B. (2019). Deciphering of microbial community and antibiotic resistance genes in activated sludge reactors under high selective pressure of different antibiotics. Water Research 151, 388-402. doi:10.1016/j.watres.2018.12.034

Zheng Y., Yang W., Hu H.W., Kim Y.C., Duan J.C., Luo C.Y., Wang S.P. & Guo L.D. (2014). Ammonia oxidizers and denitrifiers in response to reciprocal elevation translocation in an alpine meadow on the Tibetan Plateau. Journal of Soils and Sediments 14(6), 1189-1199. doi:10.1007/s11368-014-0867-7

Zhu W.H., Lomsadze A. & Borodovsky M. (2010). Ab initio gene identification in metagenomic sequences. Nucleic Acids Research 38(12), e132. doi:10.1093/nar/gkq275

Zumsteg A., Baath E., Stierli B., Zeyer J. & Frey B. (2013). Bacterial and fungal community responses to reciprocal soil transfer along a temperature and soil moisture gradient in a glacier forefield. Soil Biology and Biochemistry 61, 121-132. doi:10.1016/j.soilbio.2013.02.017

7. Acknowledgements

When I say "I", I mean "We"

First, I would like to thank Beat Frey and Aline Frossard for giving me the opportunity to pursuit this fascinating PhD project. Thank you Beat and Aline for teaching me how to conduct rigorous research and how to write scientific papers. I am heartily thankful for your support during all the years of my PhD and for the fruitful discussions about our research work together. I would also like to thank my PhD advisors in ETH, Mark Lever and Martin Schroth, for their constant support and helpful suggestions to improve my investigations.

Second, I would like to thank my co-workers in the RPR team. Beat Stierli, thank you for your tutoring in the laboratory, and thank you for your help in the field and in conducting laboratory analyses. Johanna Donhauser and Magdalene Adamczyk, many thanks for our scientific discussions in the office and your technical support with the R codes. Together we could find those annoying R-coding errors! Magda, I wish that little Zoe keeps growing as healthy and happy as until now. Johanna, I would never forget the fun days doing field work together, especially in Lapland, eating Swedish polar bread compulsively and fighting the mosquitoes. Joel Ruethi, thank you for your mentoring in culturing soil microorganisms in the lab, and for solving my questions about microbial isolates. It really helped for the interpretations of my sequencing analyses. I also thank the many interns that helped me in the laboratory, in the field, or with *in silico* analyses, including Leo, Damian, Simon, Kevin and Samuel.

Third, I would like to extent my gratitude to my colleagues at WSL. In the Forest Soils and Biogeochemistry (BOWISS) research unit, I would like to thank Roger Koechli, Noureddine Hajjar and Alois Zuercher for their support in performing soil physico-chemical analyses. I would also like to thank Frank Hagedorn, for his useful perspectives about soil C cycling and Joerg Luster, who helped me interpreting measurements of micronutrients in my permafrost soils. Ivano Brunner, many thanks for helping me to interpret my soil fungal data. To the BOWISS team members, thank you for your helpful insights about my investigations that I presented in the Science club and BOWISS meetings. Also, thank you all for the fun excursions and Christmas dinners of the research unit. Special thanks to Jasmin, Maggie, Fabian,

Margaux, Luisa, Sonia, Mathias, Claudia and Koko for the chilling socializing moments during lunch, aperos and coffee breaks. Such moments brought lightness to the research tasks. Thank you, Mathias (and Frank), for those impossible climbs. You guys are real pros! Outside the BOWISS research unit, I would like to thank specially the Central lab for their support in conducting soil C and nutrient analyses. I would also like to thank my other PhD and postdoc peers at WSL, specially Joan, with whom I have shared precious experiences in the mountains and the city. I extent my gratitude to the members of the Environmental Microbiology group in the D-USYS department at ETH. Our scientific discussions in the group's Journal Club broadened my microbial knowledge beyond the field of Soil Science.

Fourth, I would like to thank my research collaborators in the Microbial Ecology and Genomic research group at the University of Pretoria in South Africa. Don Cowan and Thulani Makhalanyane, many thanks for welcoming me in the group and advising me about the soil metagenomic analyses. Surendra Vikram, a million thanks for teaching me how to analyze metagenomic data. Max, Carlos and Pedro, I am really grateful for your help during the training and for showing me around Pretoria. I wish we see each other again in the future!

Fifth, I would like to thank the military crew and scientific crew of the Station Nord and the Villum Research Station in Greenland, for their assistance during the field campaigns in the region. Although my investigations about the high Artic permafrost are not included in this Dissertation, they were a substantial part of my research work during the period of my PhD. Special thanks to Jørgen Skafte for his assistance in arranging transportation in and out Greenland, and providing logistic support during the campaigns.

Sixth, I thank my friends in Lausanne and Zurich for all their moral support during my PhD. To my friends in Lausanne, particularly to Miguel, many thanks for your unconditional support during the difficult times there and for encouraging me to pursuit my PhD in Zurich. To my friends in Zurich, particularly to my partner Ale, thank you for your caring love and encouragement during the PhD period. I also extent my gratitude to Rebecca Gugerli, with whom I represented the Association of Polar Early Career Scientists (APECS) in Switzerland during the PhD years. Rebecca, I really enjoyed organizing APECS activities with you and I

enjoyed our scientific exchanges with other polar early careers and mentors during the APECS's events.

Last but not least, I would like to thank my family and friends in Spain, Cuba and around the world overall, for supporting me during the whole period of my academic education. Particularly to my parents, grandparents and my aunt: I do not have words to describe how fortunate I am for having you as my family. You always supported me in my career path and helped me, morally and economically, to reach my professional goals. My academic achievements are as yours as they are mine. I will always love you.

Last paragraph translation / Traducción del último párrafo:

Quiero agradecer a mi familia y amigos en España, Cuba y en el mundo, en general, por su apoyo durante toda mi educación académica. En especial a mis padres, mis abuelos y mi tía: no tengo palabras para describir lo afortunada que soy de tenerlos a ustedes como mi familia. Han sido un apoyo esencial durante toda mi trayectoria profesional y siempre me han ayudado, moral y económicamente, a lograr mis objetivos profesionales. Mis logros son tan suyos como míos. Los quiero y querré siempre.